Development of a Genetic Algorithm Optimisation Tool for the Early Stage Design of Low and Net-Zero Energy Solar Homes

Rémi Charron

A Thesis

in

The Department

of

Building, Civil, and Environmental Engineering

Presented in Partial Fulfillment of the Requirements
for Ph.D. (Building Engineering) at
Concordia University
Montreal, Quebec, Canada

December 20th, 2007

Your file Votre référence
ISBN: 978-0-494-37737-6
Our file Notre référence
ISBN: 978-0-494-37737-6

Abstract

Development of a Genetic Algorithm Optimisation Tool for the Early Stage Design of Low and Net-Zero Energy Solar Homes

Rémi Charron, Ph.D.
Concordia University, 2007

Homes that utilise solar thermal and solar photovoltaic (PV) technologies to generate as much energy as they consume in a year, are referred to as net-Zero Energy Solar Homes (ZESH). This thesis presents the methodology used to develop a Genetic Algorithm (GA) Optimisation Tool that finds optimal configurations of low and net-zero energy solar homes taking into consideration effects from the use of different technologies, local climate, economics, and other factors. The tool links a low energy solar home model developed in TRNSYS with a GA optimisation program that automates the search for cost-effective building designs. The tool varies a predefined set of parameters including building width to length ratio, heating system type, solar thermal collector type and size, and more.

The results from the TRNSYS model are compared with monitored data of an energy efficient house to verify that the model was correctly implemented. A total of 40 test cases were evaluated with the tool in order to verify the effects of climate, energy consumption target, control strategy, utility price structures, and other factors, to examine their impact on the resulting optimal design configurations. The GA program was capable of finding designs that were on average within 0.5% of the best known solution with the evaluation of only 0.00012% of the solution space. Results indicated that homes could be built with near equivalent monthly costs of conventional homes, while reducing the annual net-energy consumption by an order of magnitude. A reduction in PV system

costs or the introduction of appropriate feed-in-tariffs had significant impacts on the overall cost-effectiveness of ZESH.

The thesis clearly demonstrated the extent to which local climate, economic factors, and specific design constraints can have a major impact on the optimal design configuration, which limits the usefulness of generic design guidelines. The methodology developed was also a novel way of using TRNSYS for the optimisation of whole building design through the use in updated input and parameter files. The development of building design optimisation tools will lead to various applications ranging from policy development work where the benefits of different incentive mechanisms are quantified, to design assistance, and building code development work.

Acknowledgements

This Ph.D. thesis, although lengthy, covers only a part of the journey that I took in trying to find an optimal design strategy for net-zero energy solar homes (ZESH). After completing my Master's research on the modelling of ventilated façades with integrated photovoltaics (PV) (Charron, 2004), I started working in industry as an energy consultant. Over the years I had begun to develop an interest in the concept of building houses that combined energy efficiency and renewable energy technologies, such that they would generate as much energy as they consume. If building such houses in Canada was feasible, then it could go a long way in helping reduce our energy consumption, helping address human induced global warming. Therefore, when my Master's thesis supervisor, Dr. Athienitis, came to me with a proposed joint project with the CANMET Energy Technology Centre (CETC) in Varennes that would involve finding optimal combinations of energy efficiency with PV in houses, it was an offer I could not refuse.

Special thanks and appreciation go to my wife Carrie for her patience, understanding, encouragement, moral support, and for leaving her job to move back to Montreal with me. I would also like to thank my thesis supervisor, Dr. Andreas Athienitis, and my supervisor at CETC-Varennes, Dr. Lisa Dignard-Bailey, for their guidance, encouragement, and support during my graduate studies. Thank you to Robert Dumont of the Saskatchewan Research Council for monitoring his house's energy consumption.

Financial support for this research project was provided in part by Natural Resources Canada through the Technology and Innovation Program and from the Natural Sciences and Engineering Research Council of Canada through a scholarship and the Solar Buildings Research Network.

Table of Contents

List of Figures

List of Tables

Nomenclature

Acronyms

ach	air change per hour
ASHRAE	American Society of Heating, Refrigerating and Air-Conditioning Engineers
CANMET	Canada Centre for Mineral and Energy Technology
CDD	cooling degree-days
CEPHEUS	Cost Efficient Passive Houses as European Standards
CETC	CANMET Energy Technology Centre
CF	cost function
CFD	computational fluid dynamics
CFL	compact fluorescent lights
cfm	cubic feet per minutes
CMHC	Canadian Mortgage and Housing Corporation
COP	coefficient of performance
CS	cooling season
DHW	domestic hot water
DOE	United-States Department of Energy
EPS	extruded polystyrene
ET	evacuated tube solar collector
FP	flat plate solar collector
GA	genetic algorithms
GSHP	ground source heat pumps

HDD	heating degree-days
HP	heat pump
HPWH	heat pump water heater
HRV	heat recovery ventilator
HS	heating season
HVAC	heating, ventilation, and air conditioning
IAM	incidence angle modifier
IAQ	indoor air quality
ICF	insulated concrete forms
IDP	integrated design process
IEA	International Energy Agency
kWp	size of photovoltaic system in kilowatt peak
LED	light emitting diode
MRT	mean radiant temperature
NREL	United-States National Renewable Energy Laboratory
NV	natural ventilation
OA	outdoor air
OECD	Organisation for Economic Co-operation and Development
OH	overhang
OSB	oriented strand board
O&M	operation and maintenance
P, PI, PID	combinations of Proportional, Integral and Differential control
PMV	predicted mean vote index for thermal comfort

PPD	predicted percent dissatisfied related to thermal comfort
PV	photovoltaic
PVPS	photovoltaic and power systems
RAM	random access memory
RSI	thermal resistance value using International System of Units
SEER	seasonal energy efficiency ratio
SHGC	solar heat gain coefficient
SIP	structural insulated panels
TESS	Thermal Energy System Specialists
TF	transfer function
TFM	transfer function method
UEC	unit energy consumption
VAV	variable air volume
wg	water gage pressure
ZESH	net-zero energy solar homes

Equation Variables

α	solar absorptance
$\Delta 1c$	cooling called for in CS when $T_Z = H95_c - \Delta 1c$
$\Delta 1h$	heating turns on in HS when $T_Z = L95_h + \Delta 1h$
$\Delta 2c$	OA introduced in zone in CS when $T_Z = H95_c - \Delta 2c$
$\Delta 2h$	OA introduced in zone in HS when $T_Z = H95_h - \Delta 2h$
$\Delta 3c$	on/off heating temperature setpoint in CS: $T_{H,on/off} = L95_c + \Delta 3c$
Δt	simulation time-step

η	efficiency
θ	solar incidence angle
ρ_{OA}	outdoor air density
σ	Stephen-Boltzmann constant ($5.67 \cdot 10^{-8}$ W/m^{2}K^4)
τ_b	transmittance of incident beam radiation
τ_{blind}	blind transmissivity
a0, a1, a2	solar collector efficiency constant empirical coefficients
A_i	total area of surface i
b	TF coefficient for current and previous sol-air temperature
b0, b1	constant empirical coefficients used to calculate IAM
c	TF coefficient for current and previous equivalent zone air temperature
Cap	effective capacitance of room air plus any mass not considered with transfer functions
d	TF coefficient for current and previous heat flux to zone
$db_{h,c}$	deadband for either heating (h) or cooling (c) season
$F_{i,j}$	view factor between surfaces i and j for radiation exchange
$H95_{h,c}$	temperature that zone temperature must remain below for 95% of heating (h) or cooling (c) season
$h_{c,i}$	convection coefficient at inside surface i
$h_{c,o}$	outdoor convection heat transfer coefficient
$h_{r,ij}$	linearised radiative coefficient between surface i and j
i	interest rate for mortgage financing

I_{bT}	beam solar radiation incident on window
I_T	total incident solar radiation
K1,2 and 3	constant empirical coefficients used in infiltration calculations
kL	extinction coefficient times individual window pane thickness
$L95_{h,c}$	temperature that zone temperature must remain above for 95% of heating (h) or cooling (c) season
$\dot{m}_{AS\_62}$	amount of OA required to meet ASHRAE 62 standard
$\dot{m}_{infil}$	amount of air infiltrating into the zone
$\dot{m}_{NV}$	amount of OA introduced by NV for cooling purposes
$\dot{m}_{OA}$	total amount of OA including infiltration, NV, and $\dot{m}_{AS\_62}$
n	duration of mortgage in years
$\dot{Q}_{b,blind}$	rate of beam radiation after passing through blind
$\dot{Q}_i$	total heat transfer coming from surface i
$\dot{Q}_{infil}$	rate of energy gain to zone from infiltration
$\dot{Q}_{int}$	rate of energy transfer to zone due to internal gains other than people or lights
$\dot{Q}_n$	net rate of energy transfer across window
$\dot{Q}_s$	rate of energy gain through window
$\dot{Q}_{s,blind}$	rate of energy gain through window with blind
$\dot{Q}_{s,people}$	sensible load to room from zone occupants
$\dot{Q}_t$	rate of thermal energy transfer across window

$\dot{Q}_V$	rate of energy gain to zone from ventilation flow stream
$\dot{Q}_Z$	rate of energy gain to zone due to convection from attached zones
s	sum of radiative energy absorbed at an inside surface due to solar, lights, and people
$T_{C,\,off}$	temperature at which cooling turns off in CS: $T_{C,off} = T_{C,on} - db_c$
$T_{C,on}$	temperature at which cooling turns on in CS: $T_{C,on} = H95_c - \Delta 1c$
T_{eq}	equivalent zone air temperature
$T_{H,off}$	temperature at which heating turns off in HS: $T_{H,off} = T_{H,on} + db_h$
$T_{H,on}$	temperature at which heating turns on in HS: $T_{H,on} = L95_h + \Delta 1h$
$T_{H,on/off}$	on/off heating temperature setpoint in CS: $T_{H,on/off} = L95_c + \Delta 3c$
$T_{high,\,mix\,or\,low}$	two-zone model control using either highest temperature (high), mixed temperature (mix) or low temperature (low)
T_{in}	temperature of fluid going into solar collector
T_o	outdoor temperature
T_s	vector containing all the surface temperatures
T_{sa}	solar-air temperature
T_Z	zone temperature
UA	heat exchanger overall heat transfer coefficient
V_w	wind velocity
V_{zone}	zone volume
$\dot{W}$	power consumption of fan introducing higher level for NV
X	time varying inputs vector affecting surface and zone temperatures

Z	time independent factors matrix affecting surface and zone temperatures

1. INTRODUCTION

In recent years there have been a growing number of projects and initiatives to promote the development and market introduction of low and net-zero energy solar homes (ZESH). The Japanese manufactured housing industry, having successfully partnered with the Japanese Photovoltaic (PV) industry, has been in the forefront of commercialisation of factory-built homes equipped with PV systems. Japanese PV companies manufactured 60% (or 400 MW) of global PV modules in 2003, and 55% of it was destined for the local market (Charron, 2005). Of the local market, the residential sector had the greatest share at 85%. This means that in 2003 alone, approximately 204 MW of PV was installed in the residential sector in Japan. In contrast, the vast majority of PV systems installed in Canada are currently in off-grid applications and the cumulative PV power capacity was below 12 MW in 2003.

The United-States Department of Energy (US DOE) published the US Zero Net Energy Buildings Outreach and Action Plan in January 2000 (US DOE, 2000). The action plan called for over 100,000 affordable ZESH to be built in the US by 2020. Since 2000, two significant efforts have been launched in order to reach this goal. The first was the creation of six ZESH homebuilder teams to design, build, and monitor marketable ZESH prototypes and subdivisions. The second initiative was the launch of the Solar Decathlon competition, which had the first of its biannual competitions in September 2003 (Solar Decathlon, 2005).

In Europe, the Cost Efficient Passive Houses as European Standards (CEPHEUS) project consisted of constructing 250 housing units to the Passive House standard

(Passive House, 2004) in five European countries, with the objective of accomplishing the following three goals:

1. Demonstrate that strict energy performance standards could be applied to a variety of buildings in different European locations at low additional cost;
2. To test the feasibility of implementing the Passive House quality standard; and,
3. To create the preconditions for broad market introduction of cost-efficient Passive Houses.

The International Energy Agency (IEA) has also been involved in studying and promoting low energy buildings. Most of the tasks from the IEA Solar Heating and Cooling (SHC) Programme relate in some way to the advancement of low energy buildings, with the most relevant tasks being:

TASK 8: Passive and Hybrid Solar Low Energy Buildings;

TASK 12: Building Energy Analysis and Design Tools for Solar Applications;

TASK 13: Advanced Solar Low Energy Buildings;

TASK 22: Building Energy Analysis Tools; and

TASK 28: Solar Sustainable Housing.

In Canada, Natural Resources Canada (NRCan) launched the Advanced Houses Program in the early nineties to help develop and test innovative methods of reducing energy consumption, provide better indoor environments, and to reduce the environmental impact of houses (NRCan, 2005a). In all, ten different advanced houses were built across Canada as a result of this program. A similar method of establishing technical requirements as the R2000 standard was established (NRCan, 2005c); however, it went beyond R2000 requirements which deal only with space and water heating, to also

include total purchased energy. The goal was to use half the energy of a typical R2000 home, or one quarter of the energy and half the water of conventional Canadian homes.

More recently, the Canada Mortgage and Housing Corporation (CMHC) launched the EQuilibrium Housing competition that will see 12 low and net-zero energy houses built across Canada in 2007 (CMHC, 2007). This initiative followed a holistic approach that incorporated principles of occupant health and comfort, affordability, resource conservation and reduced environmental impact. In general, the houses are projected to consume approximately half the energy compared to the Advanced House Standard and will use onsite renewable energy technologies to generate an equivalent amount of energy to achieve the net-zero energy target.

The CANMET Energy Technology Centre (CETC) in Varennes started a three-year project in 2005 that aimed to build on past projects, consider all existing and emerging technologies, and support the development of simulation and optimisation software. This R&D project was done in collaboration with Concordia University to provide in-depth analyses to Canadian stakeholders on the optimisation of low and net-zero energy homes for Canadian climatic conditions. This Ph.D. thesis was initiated as a result of this collaborative work with an aim to develop a design methodology that would help designers develop optimal ZESH.

Given that the term optimal is focused on throughout this thesis and that it could have a different meaning to different people, the interpretation of the term used for this thesis is described in the following three sentences. A design was considered optimal if it had the lowest average net-monthly energy and financing costs of energy efficiency and renewable energy upgrades. Other factors such as daylighting and environmental

footprint were not considered. However, the resulting design tool methodology that was developed is generic enough that the user could change the objective function to develop designs that would be optimal for a different set of criteria.

The use of design guidelines is one way that designers try to optimise building performance. There are various books and articles that give specific guidelines on how to design energy efficient houses following passive solar techniques: (Chiras, 2002, CMHC, 1998, Athienitis and Santamouris, 2002) to list a few. The difficulty of using design guidelines is that they are generally dependent on the climate where they were developed and the specific technologies that were used in their development. For example, if we use window area design guidelines developed using double-glazed windows, for triple glazed and other advanced window systems, the resulting area would likely not be optimal. Another drawback of using guidelines is that they are generally developed assuming ideal conditions. There may be situations where a solar house is built on a property that is not directly facing south or that is partially shaded, where existing design guidelines would fail. Basically, general guidelines provide a range of possible solutions that have been known to work well; however, they are not necessarily the most optimal values to use for a particular design.

Only detailed simulation can help determine situation specific optimal values. For example, Chiras (2002) suggests using a thickness of 10-15 cm (4-6 in) of concrete for thermal mass. However, the optimal mass thickness will change depending on wall composition and material properties. In order to verify the validity of this rule of thumb, the magnitude and phase angle of a wall's important transfer functions such as the self-admittance (Ys) and transfer admittance (Yt) needs to be examined (Athienitis and

Santamouris 2002). The self-admittance relates the effect that a heat source acting on a surface has on that surface's temperature, whereas the transfer admittance relates the effect of the exterior sol-air temperature variation to the resulting heat flow at the inside surface.

Figures 1.1a-d show the magnitude of the self-admittance for different concrete thicknesses using a fundamental frequency of one cycle per day, representing a dominant diurnal harmonic such as outdoor temperature and solar radiation, which are important in passive solar design. The wall is composed of an interior massive layer of concrete, and an exterior insulating layer of negligible thermal capacity (RSI 4). Different concrete mixes generate different material properties. Figures 1.1a-d show the results using four different concrete properties as summarised in Table 1.1. The maximum admittance occurs at thicknesses ranging from 13 cm to 24 cm (5.1-9.4 in), which corresponds to the thickness that would reduce the room temperature fluctuations the most. Varying the RSI value (R-value) of the exterior insulation does not make an appreciable difference in the optimal thickness. However, varying the specific heat of the concrete from the assumed value of 840 J/kg·°C (0.2 Btu/lb·°F) does have an impact. Other factors also come into play when determining what thickness of concrete to use in a house. For example, using 24 cm (9.4 in) of concrete for the floor of a wood-framed house would result in serious structural challenges. This one example shows that design guidelines are not necessarily the most optimal.

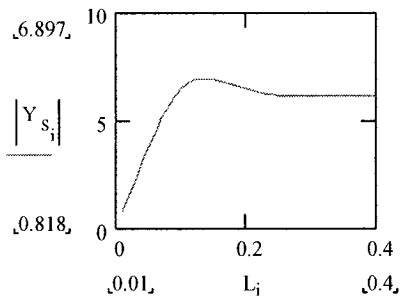

Figure 1.1a: Peak Y_s at 13 cm

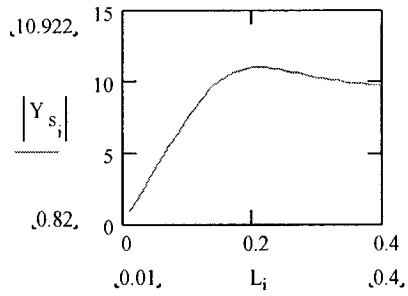

Figure 1.1b: Peak Y_s at 21 cm

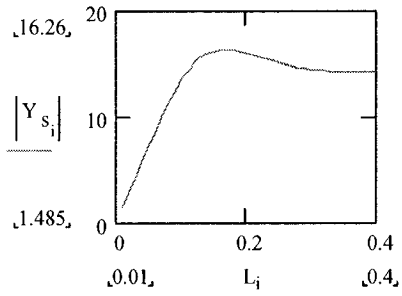

Figure 1.1c: Peak Y_s at 17 cm

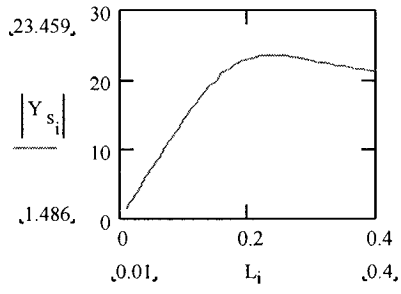

Figure 1.1d: Peak Y_s at 24 cm

Table 1.1: Various properties of concrete used in Figures 1.1a-d (McQuiston et al. 2005)

Figure	Density (kg/m^3) [lb/ft^3]	Thermal conductivity (W/m·°C) [Btu/hr·ft·°F]	Specific heat (J/kg·°C) [Btu/lb·°F]
1.1a	1280 [80]	0.48 [0.28]	840 [0.2]
1.1b	1280 [80]	1.19 [0.69]	
1.1c	2400 [150]	1.4 [0.81]	
1.1d	2400 [150]	2.9 [1.68]	

Design guidelines that aim to help improve cost effectiveness are also very dependent on the costs of energy and relevant technologies. Projected decreases in the price of PV technologies in the next couple of decades (Hoffmann, 2006) will result in changes to the configuration of optimal designs. If it becomes less expensive in the future to install larger PV systems as opposed to certain energy efficiency measures, it will likely change the recommended designs.

As the research progressed, it became apparent that developing new design guidelines for low and net-zero energy solar homes would not be the ideal design optimisation strategy to develop for this thesis. A more useful tool that is needed and that is not yet available would assist designers to find optimal configurations while taking into account changes in technologies, local climate, economics, and specific design constraints that do not allow for the direct application of guidelines. This thesis presents a design optimisation methodology that links a formal optimisation algorithm with an energy simulation tool that models the house and its associated systems along with the necessary renewable energy technologies. The methodology was demonstrated by developing an early stage Genetic Algorithm (GA) Optimisation Tool for low and net-zero energy solar homes that links a GA program with a TRNSYS (Klein, et al., 2000) energy simulation model. The objective of the thesis was to develop a design methodology that would assist designers in finding optimal configurations of low and net-zero energy solar homes. The resulting methodology takes into consideration effects from changes in technologies, local climate, economics, and other design constraints and is adaptable such that it could work with different optimisation algorithms and building energy simulation software. The focus was not on the specific optimisation algorithm or the building simulation software that was used, but on the methodology that was taken to develop the demonstration tool.

The thesis begins with a brief literature review that starts with an overview of the current situation in Canada related to building energy consumption to provide an assessment on what needs to be changed to achieve the net-zero energy consumption target. The literature then discusses the reasoning behind the selection of TRNSYS for

the demonstration tool, reviews optimisation for building system design, and concludes with an overview of the selection of genetic algorithms for this study. Section 3 discusses the methodology used for the development of the demonstration GA Optimisation Tool, from developing the low energy house model in TRNSYS to implementing the GA program and the interaction between these two programs. Section 4 focuses on verifying that the one-zone low energy model was implemented correctly, and also briefly demonstrates that the GA program performs as expected on a given mathematical problem to make sure it was correctly implemented. Section 5 analyses the performance of the GA Optimisation Tool and how it was refined to improve its performance. It also reviews the selection of the design parameters optimised in the tool and it examines how the various modelling assumptions affect the optimisation process. Section 6 analyses the results, focusing on the different optimal design configurations that are found by varying the initial design conditions. Section 7 covers the contributions of this research along with future work that is still needed. Finally, the last section reviews the basic conclusions that can be drawn from this research.

2. LITERATURE REVIEW

2.1 Residential Energy Consumption

In order to determine what to strive for in terms of an energy balance target for a ZESH, it is beneficial to examine what the current and best practices are. The Government of Canada periodically publishes the Energy Use Data Handbook (NRCan, 2005b), which has a section on residential energy use, where it presents aggregated data for the whole sector. Table 2.1 summarises the data by dividing the aggregated data by the total number of residences, and then the result by the average size of residences. The table provides an average of the data published between 1990 and 2002. Note that this does not give exact numbers and is more for comparative purposes, as the data includes all types of residential buildings from apartments to detached homes for the whole building stock, new and old. An example of this limitation is the average energy use for cooling. The amount is averaged over all residences, which reduces the actual consumption for houses that have cooling, since not all houses are actively cooled.

Table 2.1: Average yearly energy consumption of residential dwellings in Canada between 1990 and 2002 based on aggregated energy data (NRCan, 2005b)

	Average Energy Use (kWh)	Average Energy Use (kWh/m^2)
Space heating	20,596	166.0
Water heating	7,163	57.7
Major appliances	3,082	24.8
Other appliances	1,408	11.3
Lighting	1,418	11.4
Space cooling	296	2.4
TOTAL	33,963	273.7

In the early nineties, NRCan launched an Advanced House program that had the objective of building 10 houses in Canada that would consume half the energy of R2000 houses. More analysis on the energy consumption of the resulting 10 houses can be found in (Charron, 2005). In this section, we will look at an 11^{th} house that was built in Saskatoon, by Robert Dumont, a participant in the Advanced House program who decided to build his family's residence using the advanced house standard. The yearly energy consumption of this house is on average ~15,000 kWh (~46 kWh/m^2), which is in the mid to low range of the consumption compared to the other advanced houses and less than half of the consumption of the average residence shown in Table 2.1. The house actually consumes less than half of the actual consumption of the official Saskatoon Advanced House (predicted 20,514 kWh, actual 31,322 kWh) (Charron, 2005). Table 2.2 provides a breakdown of the average yearly energy consumption of the Dumont house. Note that the consumption is further broken down in Table 4.1 in Section 4.1. On a per square metre basis, the house does not consume a significant amount of energy; however, the house is large (326.3 m^2 floor area) and has some rooms which are often unused and unheated. A smaller house would present a more efficient use of energy. The Swedish terrace houses (Table 2.3) have roughly the same energy intensity (46.6 kWh/m^2), but consume about a third of the total energy (for a third of the floor area). Based on the data presented in (NRCan, 2005b), the average Canadian residence, including apartments, is only 124 m^2, although this average is lower than what would be expected of single detached houses, which have been increasing in size over the last century. However, some experts expect the trend to slow or reverse as Canada's baby boomers downsize their homes after their children leave home (Turner, 2002).

Table 2.2: Total yearly energy consumption breakdown of Dumont residence

	Electricity (kWh)	Electricity (kWh/m^2)	Avg. Canadian (kWh/m^2)
Heating	8,349	25.6	166.0
Cooling	0	0	2.4
Domestic Hot Water (DHW)	1,114	3.4	57.7
Heat recovery ventilator	482	1.5	n/a
Major Appliances	3,183*	9.8	24.8
Lighting , minor appliances (incl. electronics), other misc. loads	2,113	6.5	22.7
Monitoring equipment	1,086	3.3	
Solar Heat for DHW	Undetermined**	Undetermined**	
TOTAL	16,327	50.0	273.7

* Load does not include hot water component for dishwasher and washing machine

**The house has a 15.6 m^2 solar thermal collector that is not monitored.

Table 2.3: Yearly energy consumption of Swedish terrace homes demonstration project (IEA SHC, 2004)

	Yearly (kWh)	Yearly (kWh/m^2)
Appliances and lights	2,900	25.0
Hot water*	1,500	12.9
Electrical services (fans, pumps)	1,000	8.6
TOTAL	5,400	46.6

*50% of 3,000 kWh load supplied by 5 m^2 solar collector

Coupling a low energy house with sufficient thermal and PV solar collectors and passive solar design can lead to a ZESH. The Maine Solar House utilises a 35.7 m^2, 4.2 kW PV system, and 44.6 m^2 of solar thermal collectors (Solar House, 2005). In 1998, the 4.2 kW array generated 4,246 kWh of electricity despite June and November being

particularly cloudy months, producing a yearly electricity surplus of 591 kWh. The energy use breakdown of a ZESH remains essentially the same as that of a low energy solar house without the use of renewable energy generating systems. The only difference is that the generated electricity over the course of a year will equal to, or be greater than, the total electricity consumption and the amount of thermal energy generated by the solar thermal collectors will equal to, or be greater than, the amount of thermal energy consumed. The challenge is to reduce the energy consumption of the house substantially before implementing the renewable energy generating systems. For example, more energy efficient appliances, coupled with a ground source heat pump could be implemented in the Dumont house to help reduce the size and cost of the required PV system to reach the net-zero energy target.

With the expected advances in energy efficiency and renewable energy technologies, some Canadian and international groups would like all new homes constructed beyond 2030 to meet a net-zero energy standard (NZEHC, 2005). Achieving this goal would require a concerted effort from industry, government, and consumers. The government would need to instate new mandatory energy efficiency standards; in Canada, the logical first step would be to mandate that all new homes meet the R2000 standard. As seen in Figure 2.1, R2000 would only be a first step. Even the Advanced House standard, which aimed at half the energy consumption of R2000, still results in yearly energy consumption levels that are too high to feasibly achieve net-zero energy consumption through the use of renewable energy alone. Therefore, mandatory energy efficiency standards would need to be systematically improved such that energy consumption would be at a minimum by 2030.

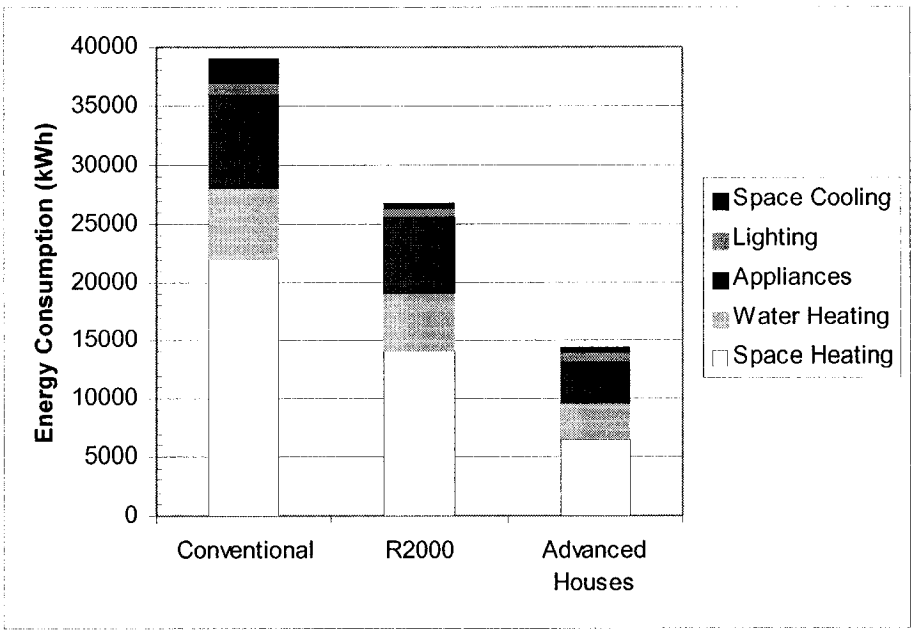

Figure 2.1: Typical total annual energy consumption (NRCan, 1993)

As mentioned in the introduction, the EQuilibrium demonstration program from CMHC will lead to 12 low and net-zero energy solar homes built across Canada in 2007 (CMHC, 2007). Examining the calculated energy breakdown of these houses can give us an idea of how much more energy reductions are needed beyond the levels shown in Figure 2.1 to achieve the net-zero energy target. The predicted annual consumption of the demonstration houses before counting PV generated electricity, but after including energy provided by solar thermal collectors, ranges from approximately 4,500 kWh to 7,500 kWh per year. The largest load comes from lighting and appliances and other plug loads, which ranges from assumed values of 2,734 kWh to 5,450 kWh per year. These consumption values are not modelled and are calculated based on assumptions of what future homeowners would have in terms of appliances and lights. In reality, these values would depend on the energy consuming behaviours of the future occupants. If the houses

come with energy efficient lighting with occupancy controls and the most energy efficient appliances, energy consumption will be reduced; however, secondary plug loads such as entertainment systems can result in a wide range of energy consumption levels. Since all of the teams are using some element of thermal energy for heating domestic hot water, this becomes the smallest load of the houses ranging from almost 0 kWh to 504 kWh per year. Almost none of the teams are installing formal cooling systems; although, some will have cooling from installed dual function heat pumps. All of the teams are using heat recovery ventilators (HRV) to supply fresh air to the space, with resulting ventilation and cooling loads ranging from 250 kWh to 1,700 kWh. Finally, given that the teams are using various configurations of solar energy and ground source heat pumps, the annual heating energy consumption is greatly reduced and ranges from 500 kWh to 2,000 kWh. From the predicted energy consumption results, we can see that stringent energy efficiency measures are implemented to reduce the annual consumption to less than half of the Advanced House standard of the early nineties, before adding PV to achieve the net-zero target.

The estimated energy consumption values for the EQuilibrium teams are based mainly on HOT2000 and RETScreen analyses. Some teams went further and utilized advanced tools such as TRNSYS and custom software developed for transient building simulation in Mathcad. Various teams are using solar thermal systems for both space heating and for domestic hot water heating (DHW), and two of the teams have BIPV/thermal systems where the heat generated from the PV panels is utilised for space and/or domestic hot water heating. Since HOT2000 does not have an option to include solar thermal for space heating, it is difficult to accurately calculate the fraction of space

heating that can be achieved with solar thermal systems using only these two programs. The hot water production calculated in RETScreen does not always match to when the space heating is needed. A couple of the teams calculated their space and domestic hot water consumption needs in HOT2000 without including solar thermal contributions. They then subtracted the predicted output of solar thermal collectors from RETScreen to the loads calculated in HOT2000. The problem this caused was that the combined space heating and DHW load calculated in HOT2000 was less than the estimated solar thermal energy production. In reality, the solar thermal collector would not be able to achieve 100% solar contribution for space heating and DHW and thus the amount of solar energy contribution was overestimated and the houses in question will likely not achieve the net-zero energy target with the specified system. Ideally, the teams would have used building energy simulation software that allow users to model all systems together, including the space heating and solar thermal at the same time.

No formal design guidance is available with HOT2000 or RETScreen that would help the EQuilibrium teams optimise their designs. Depending on the optimisation process that the teams followed, very different results were achieved; some teams claimed that ground source heat pumps could save them many thousands of dollars, whereas others found that they were too expensive. One of the teams detailed their design process in their project proposal and explained how the cost of various energy efficiency elements were compared to the cost of adding PV systems to generate an equivalent amount of savings. If it cost less to add more insulation compared to adding more PV, then more insulation was added. The issue with this methodology was that they considered many other energy efficiency measures before considering a ground source heat pump. The

cost effectiveness of adding more layers of insulation varies substantially depending on the heating system. With a ground source heat pump with a coefficient of performance (COP) of 3 or more, saving the last few watts of heating load with insulation will not be as cost effective as with other heating systems. Therefore, the cost effectiveness of energy efficiency measures should be compared not only with the cost of PV but also with the cost of various combinations of measures.

Finding the right mix of energy efficiency and renewable energy to achieve the net-zero energy target is not trivial since many factors are involved. Different standards may be required in different regions of the country depending on climatic conditions. The mix will change as new technologies emerge on the market. One of the most important aspects will be the cost differences between energy efficiency measures and renewable energy technologies. The cost of PV is expected to decline considerably before 2030 (Hoffmann, 2006). If PV and solar thermal technologies become less expensive than the cost of some energy efficiency measures, then the standards could change to reflect this by requiring less energy efficiency and more renewable energy technologies. Alternatively, performance standards that would simply regulate the net-energy use of houses would allow for more design flexibility as the technologies and economics change over time.

2.2 Research Needs and Motivation for Proposed Work

The design of ZESH involves the integration of various types of systems that can vary depending on the specific design objectives, the project location, the knowledge of the designers, and other factors, which leads to many different configurations of ZESH. This can be observed by examining the various zero and low energy building demonstration

projects from around the world (Charron, 2005). The projects generally depend on trial-and-error optimisation using dynamic energy simulation tools, coupled with the knowledge of the designers. Simulations are normally done on a scenario-by-scenario basis, with the designer generating one solution and subsequently using a computer program to evaluate it. This can be a slow and tedious process and typically only a few scenarios are evaluated from a large range of possible choices (Athienitis, 1989, Caldas and Norford, 2002).

Although a reduction in the energy use of residential buildings can be achieved by relatively simple individual measures, to achieve very high levels of energy savings on a cost effective basis requires the coherent application of several measures, which together optimise the performance of the complete building system. This multi-component optimisation problem can lead designers to feel ill-equipped to tackle such a task. The application of computerised optimisation techniques to the design of low and net-zero energy buildings would provide architects and engineers with a powerful design tool (Coley and Schukat, 2002). Another drawback of the traditional trial-and-error method is that since optimum designs are site specific, its functionality is limited by climate and other local factors. A design using an air-source heat pump might work well in Victoria, BC, but would most likely fail in the cold Edmonton, AB, climate. The use of optimisation coupled with building energy simulation is thus proposed to assist designers in finding optimal designs of ZESH.

2.2.1 Design Tool Programs

Over the years, there have been hundreds of different software tools developed to help evaluate energy efficiency, renewable energy, and sustainability in buildings. The

US DOE lists over 340 simulation tools in their tools directory (US DOE, 2007b). The majority of these tools offer a limited capability when it comes to optimising a given design. Tools such as DeST, DOE-2.1E, Energy Express, TRACE 700 and eQuest allow users to easily compare the energy consumption and costs of different design options; however, they rely on the user to develop the design alternatives, with the exception of eQuest which comes with an energy efficiency wizard that allows for the automatic implementation of common energy efficiency measures selected by the user from a list (Crawley, et al., 2005). Some tools such as HEED (UCLA, 2007), Energy10 (SBIC, 2007) and MIT Design Advisor (MIT, 2007), which were conceived specifically for early design stages, have relatively simple building models with user friendly interfaces, provide some assistance in finding more energy efficient buildings. Since these particular tools were developed in the US, the design options that are recommended may not all be suitable for colder Canadian climatic conditions and associated construction practices. In addition, their limitations in terms of the number of available HVAC and solar systems, limit their use as ZESH design assistance tools for Canada.

Based on the capabilities of existing tools, it was decided to link an optimisation program with a detailed energy simulation program that modelled both buildings and renewable energy technologies. TRNSYS, EnergyPlus, and ESP-r were selected as possible choices for the simulation software due to their capabilities in modelling different building envelope components, HVAC systems and solar technologies. Each of the three software packages has advantages and disadvantages. Table 2.4 provides a cursory comparison of the three software packages (Crawley, et al., 2005).

Table 2.4: Comparison of select features between ESP-r, EnergyPlus and TRNSYS from (Crawley, et al., 2005)

	Feature	TRNSYS	ESP-r	Energy +
Element heat conduction solution method	Admittance method	-	-	-
	Transfer function	X	-	X
	Finite difference	-	X	-
Thermal storage	Internal thermal mass	X	X	X
	Integral collector storage system	X	-	-
	Stratified thermal storage tank	X	-	X
	Rock bin thermal storage	X	X	-
	Stratified water heater tank	X	X	-
	Combi-tanks for space/water heating	X	-	-
Sky model	Isotropic	X	X	-
	Anisotropic	X	X	X
	User selected	X	X	-
Solar thermal collectors	Glazed flat plate	X	X	X
	Unglazed flat plate	X	X	-
	Evacuated tube	X	-	-
	Unglazed transpired	X	-	X
	High temp. concentrating collect.	X	-	-
Electricity generation	PV power	X	X	X
	Wind	X	X	-
Mechanical systems	Air-to-air packaged heat pump	X	X	X
	Water-to-air packaged heat pump	X	X	X
	Water-to-air heat pump	X	-	X
	Ground-source heat pump	X	X	X
	User configured solar systems	X	-	-
Consumption	Hot water consumption	X	X	X
	Complex energy tariffs	X	-	X
Daylighting	Illumination from windows/skylights	-	X	X
	Daylight shelves	-	X	X
	Radiosity analysis for interior light	-	X	X
	Shading device scheduling	X	-	X
	User specified shading control	X	X	X

ESP-r and TRNSYS were ranked in the top three tools to have undergone the most validation in the (Crawley, et al., 2005) report. Based on TRNSYS' modular structure, its validation history, available models, user interface, and the relatively straightforward manner in which it could be made to interact with an external optimisation program, it was selected as the simulation software for this research. However, the goal of this research is to establish the methodology of utilising optimisation software with building simulation programs; therefore it could be implemented using other software tools.

One of the solar design strategies that needs to be modelled in the design optimisation tool is the use of passive solar design. In passive solar design, additional thermal mass is included in the interior layer of the building. This allows solar gains that occur during sunny periods to be stored for release into the room at a later time when the sun is no longer shining. This helps regulate the room temperature, which improves thermal comfort, and can result in energy savings. Although the international scientific community has been involved in this field for more than 30 years, most of the available commercial software, produce some problems when utilised to simulate buildings with a lot of thermal mass (Beccali, et al., 2005a). Since TRNSYS uses the transfer function method (TFM) to calculate the heat transfer through walls, some inaccuracies are introduced when walls with high thermal mass are modelled.

One of the disadvantages of the TFM is its use of linearity assumptions, which cause some loss of information in the calculations. Previous studies have estimated that the linearity assumptions in the TFM, for most building materials and operation strategies, imply no significant difference between the results of this model and other numerical models (Beccali, et al., 2005a). On the other hand, this assumption can lead to errors

when used with non-linear control strategies that depend on heat storage in the building mass in order to make decisions. An example of a non-linear control strategy is the use of motorised shading control to regulate solar gains through windows. Other inaccuracies generated with the TFM are related to the truncation of the infinite coefficients that constitute the transfer functions (Beccali, et al., 2005b), and that most available commercial software for the non-steady-state thermal simulation do not assure the exact determination of the transfer function coefficients for building structures with significant thermal mass (Beccali, et al., 2005a). ESP-r utilises the finite difference method for calculating heat transfer through walls, which provides a more accurate simulation of the heat transfer; however, ESP-r is more limited in terms of modelling solar systems. In the future, either the TRNSYS building simulation model can be updated to better model high thermal mass buildings, or the simulation engine from the optimisation tool can be changed to a program that can produce better accuracy, while still offering flexibility in the simulation of a multitude of solar systems.

Another aspect to consider when developing a design tool is to get a good user base. When designing an advanced building, an integrated design process (IDP) should be followed where all the different design professionals work together from the start. Most of the current building energy simulation programs were developed by engineers and are used by engineers. It would be good to have a tool that is used by the whole design community, including both architects and engineers. For example, ECOTECT is a tool that was entirely designed by architects for architects. It provides users with a highly visual and interactive tool with a comprehensive 3D modeller and a range of analysis functions covering thermal, energy, lighting, shading, acoustics, resource use and cost

aspects (Crawley, et al., 2005). The tool also provides feedback to help users refine their designs in the conceptual design phase. Recent versions come with a comprehensive scripting engine that can facilitate the use of formal optimisation algorithms. One of the limitations of the tool is that it provides limited engineering analysis of HVAC and solar systems. It would be interesting if future development of this or other similar tools could incorporate the use of different engineering related systems combined with good visual representation demanded by architects so that the same design tools can be widely adopted by both architects and engineers.

2.2.2 NREL's BEopt Software

The US National Renewable Energy Laboratory (NREL) has developed BEopt that links an optimisation algorithm to building and solar simulation programs to help find cost effective ZESH designs (Christensen, et al., 2005). BEopt uses DOE-2 simulation program to calculate energy use functions related to the building and TRNSYS for solar domestic hot water and PV generation. For the optimisation, the tool uses a sequential search technique to automate the process of identifying optimal building designs along the path to ZESH (Christensen, et al., 2004). The sequential-search approach involves searching all categories (wall type, ceiling type, window glass type, HVAC type, etc.) for the most cost-effective combination at each sequential point along the path to net-zero energy (Anderson, et al, 2006). Based on the results, the most cost-effective combination is selected as an optimal point on the path and put into a new building description. The process is repeated based on this new configuration along the path to net-zero energy.

The BEopt optimisation is looking at the best ways to save energy. Once the cost of energy savings becomes greater than the cost of electricity generated with the PV system,

the building design is held constant, and the PV capacity is increased to reach the net-zero energy target. This concept can be seen in Figure 2.2, where after point 3, which represents approximately 50% energy savings, the cash flow line is linear until it reaches the net-zero target, point 4, since only PV is added which reduces the utility bills but adds costs to the mortgage. One interesting result that has been shown with BEopt is that significant energy savings can be achieved at a lower total monthly cost to the homeowner than a base-case house.

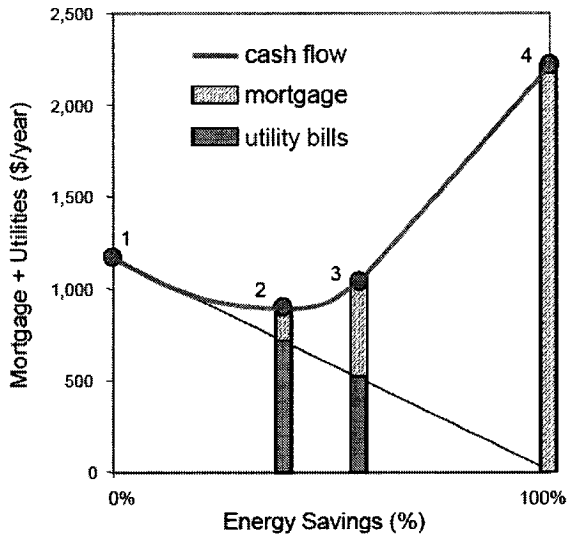

Figure 2.2: Conceptual plot of the path to net-zero energy (Christensen, et al., 2006)

One of the limitations of BEopt is that it separates the simulation of building components and solar energy technologies using both DOE2 and TRNSYS. The use of this technique makes it difficult to fully integrate the solar energy generation with the HVAC systems. However, a recent prototype version of BEopt was developed using only EnergyPlus as the simulation engine in order to test the feasibility of using a single simulation tool that would allow to extended the program's current capabilities (Anderson, et al, 2006).

The use of the sequential search technique offers advantages and disadvantages. The advantages include that it provides users with minimum-cost building designs at different target energy-savings levels; it uses discrete rather than continuous building options, which provides realistic construction options; and multiple near-optimal designs are identified at each particular energy-savings level which provides design alternatives (Christensen, et al., 2006). Unfortunately, it has one serious limitation; it depends on a sequential search that changes only one parameter at a time. For example, if the search starts by changing the heating system and finds that a ground-source heat pump is more cost-effective than an air-source heat pump, then the other parameters will be optimised assuming the use of a ground source-heat pump; however, there may be a case where the air-source heat pump gives more cost effective solution overall with a different combination of other energy efficiency options than any of the solutions that the ground-source heat pump could have provided.

This limitation is introduced since the interaction of various parameters is harder to consider using a sequential search technique. For example, if the user is interested in the interaction between south-facing glazing area and additional thermal mass, simply selecting available options within these two categories may not suffice (Christensen, et al., 2006). For the program to consider different combinations of mass and south-facing window area, either the thermal mass category or the glazing area category must first be independently cost-effective in order for the combination of additional thermal mass and glazing area to be evaluated. For experienced designers that would know to look for the interaction of these two options, an Include Combinations category, for example "Glass+Mass", was added that would force the search technique to search for

combinations of the selected combinations. This relies on the user to know beforehand those options that can interact positively. For less obvious combinations, or for interactions between 3 different options, say for example south-facing window area, thermal mass and heating system, the use of Include Combinations might not always work. Especially considering the complex interactions that are being considered between energy costs, upfront costs, financing costs, and maintenance costs, that make it difficult for a user to know how these factors interact, even for advanced users.

The limitation of the sequential search technique led to the evaluation of other optimisation algorithms. For the demonstration design tool developed in this thesis, GA was selected for the optimisation approach as detailed in Section 2.2.3. GA was selected in part since this methodology can accommodate for existing synergies between various design parameters. The results obtained with the GA program are evaluated in Section 6.7 to determine if the optimal configurations could have feasibly been obtained using a sequential search technique.

2.2.3 Genetic Algorithms

In recent years, GA have been used to optimise different building systems including optimising solar collector and storage tank size (Kalogirou, 2004); a low energy community hall including the shape of the perimeter, roof pitch, constructional details of the envelope, window types, locations and shading, and building orientation (Coley and Schukat, 2002); window size and orientation (Caldas and Norford, 2002); conceptual design of office buildings (Grierson and Khajehpour, 2002); HVAC sizing, control, and room thermal mass (Wright, et al., 2002) the design of an office building in Montreal considering an L-shape or a shape represented by a polygon with other parameters related

to structure, envelope configuration and window overhangs (Wang, et al., 2005, Wang, et al., 2006); and more. The use of GA in optimising buildings and other engineering problems is emerging since this global search technique is adequate for searching noisy solution spaces with many local and global minima. It has proved to have high efficacy in solving complex problems for which conventional hill-climbing derivative-based algorithms are likely to be trapped in local solutions (Caldas and Norford, 2002).

Another advantage of using GA is that it provides a population of optimal designs. Figure 2.3 shows the results of the use of GA in optimising the construction of a low energy community hall in the UK (Coley and Schukat, 2002). There are countless possible design solutions that would use less energy compared to the average energy intensity for similar buildings in the UK (137 kWh/m^2). Even more useful is that the optimum designs can vary, giving a number of choices to the designer and/or building owner. For example, two of the more optimal designs that evolved in this study had very similar energy use, but were very different. One used high levels of insulation with minimal window area to reduce losses, while the other focused on maximising passive solar utilisation by having more windows and thermal mass.

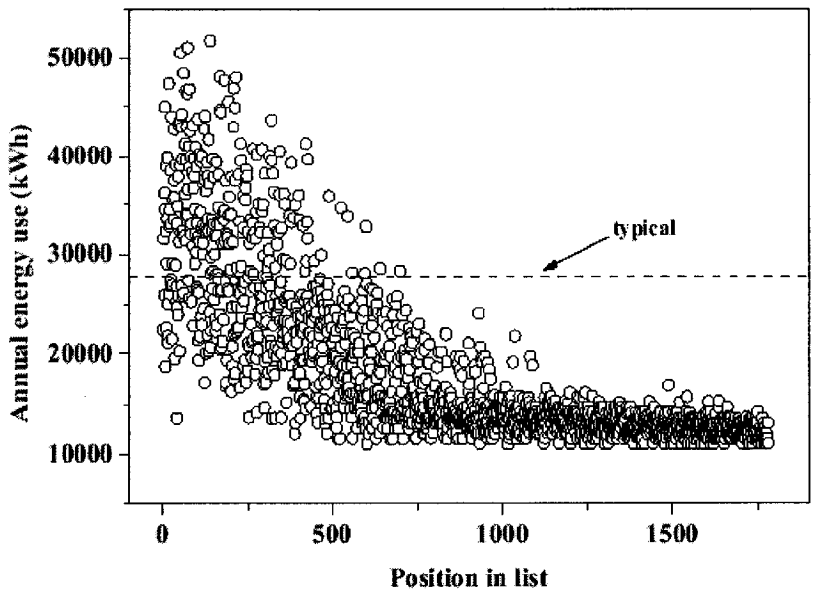

Figure 2.3: GA results for low-energy community hall design compared to typical UK energy use (137 kWh/m^2) for such a building (Coley and Schukat, 2002)

Wetter and Wright (2004) tested the performance of the following 7 optimisation algorithms by solving 6 optimisation problems in EnergyPlus (US DOE, 2007a):

1. Coordinate search method;
2. Hooke-Jeeves;
3. Two different versions of Nelder-Mead simplex algorithms;
4. Two different particle swarm optimisation (PSO) algorithms;
5. Simple GA;
6. Hybrid particle swarm Hooke-Jeeves algorithm; and
7. The discrete Armijo gradient algorithm.

They tested a simple optimisation problem with 4 independent variables that had small discontinuities, and a more detailed problem with 13 independent variables that had larger discontinuities in the range of 2% of their cost function. All the optimisation

methods, except for the GA, are available with the GenOpt optimisation software developed at the Lawrence Berkeley National Laboratory (Berkeley Laboratory, 2007).

Since EnergyPlus was used to evaluate the different design configurations, the optimisation was a computer intensive exercise. A 2.2 GHz processor took 2 minutes and 20 seconds for each simulation; a total of 500 simulations took 19 hours and 30 minutes to calculate. The long simulation time led the researchers to reduce the number of simulations for the PSO and GA to less than what is typically used for these types of algorithms. For the GA, a population size of 14, with a maximum number of 50 generations was used, for a maximum of 700 evaluated designs. The evaluation of only 700 design options represents only 3.8×10^{-13} percent of the possible designs in their solution space that had more than 1.8×10^{17} possible combinations. Table 2.5 lists the variables that were tested along with their initial value, lower and upper bound, step-size, and resulting total options.

The study evaluated the performance of the different algorithms by comparing the minimum cost function achieved by a given algorithm with the lowest value obtained out of all of the algorithms. The results showed that all non-hybrid PSO algorithms came close to the minimum using a low number of simulations, although the simple GA got consistently closer to the minimum with a comparable number of simulations. Both Nelder-Mead algorithms performed poorly. The Hooke-Jeeves and coordinate search methods worked well only in problems where there were small discontinuities in the optimisation function. The discrete Armijo gradient algorithm failed in all problems since it is sensitive to discontinuities, which are prevalent when using EnergyPlus or other similar software. The authors' conclusions were that the hybrid particle swarm

Hooke-Jeeves algorithm achieved the overall best performance. However, the limited number of tests done in their evaluation reduces the validity of this conclusion.

Table 2.5: Parameter variation in Wetter and Wright (2004) study

	Initial Value	Lower Limit	Upper Limit	Step-size	Total #
N window area	39.2%	13.6%	64.8%	2.6%	21
E window area	45.9%	20.4%	71.3%	2.6%	21
S window area	39.2%	13.6%	64.8%	2.6%	21
W window area	45.9%	20.4%	71.3%	2.6%	21
W window overhang	0.55 m	0.05 m	1.05 m	0.05 m	21
E window overhang	0.55 m	0.05 m	1.05 m	0.05 m	21
S window overhang	0.55 m	0.05 m	1.05 m	0.05 m	21
S shading setpoint	200 W/m^2	100 W/m^2	600 W/m^2	25 W/m^2	21
E shading setpoint	200 W/m^2	100 W/m^2	600 W/m^2	25 W/m^2	21
W shading setpoint	200 W/m^2	100 W/m^2	600 W/m^2	25 W/m^2	21
Night cooling setpoint (summer)	22°C	20°C	25°C	0.25°C	21
Night cooling setpoint (winter)	22°C	20°C	25°C	0.25°C	21
Cooling supply Temp.	15°C	12°C	18°C	0.25°C	25

The simple GA was tested with only one set of parameters including 1 elite point, a probability for recombination of 1 and a probability of mutation of 0.02. For the hybrid PSO Hooke-Jeeves, the algorithm was tested with two different sets of parameters. Table 2.6 gives the results of the evaluation of the detailed simulation model for the three cities tested. As seen, the hybrid PSO Hooke-Jeeves algorithm was not conclusively better than the GA algorithm. The authors' counted the two runs with the hybrid PSO Hooke-Jeeves as the same algorithm method. However, every time these types of optimisation algorithms are used, different results are obtained by simply changing the starting point of the algorithm, especially when considering the size of their solution

space. Therefore, if different parameters for the GA were tested, or if it was simply allowed more runs with different initial random populations, it may have come up with the optimal solution more often than the hybrid PSO Hooke-Jeeves as was the case for Chicago. In addition, the results were sufficiently close that the uncertainty in the problem related to using EnergyPlus makes them essentially equivalent. This is even more evident when looking at the average cost reductions predicted by the three methods. The simple GA's average cost reduction was between the two hybrid PSO Hooke-Jeeves algorithms.

Table 2.6: Results of detailed optimisation from Wetter and Wright (2004) study

	Houston, TX		Chicago, IL		Seattle, WA	
Optimisation Method	Cost Reduction	# of Simulations	Cost Reduction	# of Simulations	Cost Reduction	# of Simulations
PSO Hooke-Jeeves (1)	14.16%	653	10.94%	755	16.18%	843
PSO Hooke-Jeeves (2)	14.45%	740	10.96%	669	16.41%	889
Simple GA	14.06%	586	11.02%	592	16.35%	583

In the optimisation of a ZESH, there are typically more than 13 parameters that need to be optimised; however, the solution space needs to be kept to a reasonable size if meaningful conclusions are to be reached. Evaluating only 3.8×10^{-13} percent of the possible designs will generate doubt as to whether the actual optimum design was found. On the other hand, if the optimum designs that are found are generally better than could be achieved by simple trial-and-error methods, then it would still be a valuable design tool.

A large solution space can be acceptable for research applications; however, if this method were to be used in commercial applications, it would be best to use a smaller solution space, requiring less computation time, to find an optimal solution. One way to

reduce the solution space is to do a parametric analysis of the results. The first step would be to use a GA based optimisation with a large solution space to find optimum design solutions of ZESH in the various climatic regions in consideration. These optimal solutions could then be analysed on a parameter-by-parameter basis to determine if the optimal solutions are always in the same range. Say, for example, that in the initial algorithm the north-facing window area was allowed to vary from 5% to 50% of the façade area. If all of the optimum solutions were found to use 5%, then this parameter could be eliminated from the evaluation and simply be replaced by an input of the minimum allowable north-facing window area. This could also be used to reduce the range considered for a given parameter. Say the range considered for the east window area was the same as the north façade, and that the optimal solutions ranged from 5% to 25%. The range used in the optimisation of the east window area could be cut in half, which would in turn reduce the solution space by half. This method will be applied in this research in Section 5.2.

Another method that can be used to reduce the number of parameters included in the optimisation is to perform a sensitivity analysis on the parameters. If varying the value of a given parameter from its minimum value to its maximum value changes the results by less than a minimum value, say 1%, then it could be considered unimportant in the overall design and the parameter could be removed from the solution space. In addition, the results of a sensitivity analysis could be used to increase the step-size for some parameters. For example, if the difference between using a 0.50 m or 0.55 m overhang is negligible, but that the difference between using 0.10 m and 1.0 m is more substantial, then the step-size could be increased from 0.05 m to, say, 0.15 m while having a

negligible impact on the overall accuracy of the results. This method will be applied in this research in Section 5.2.

An alternative method to help reduce the size of the solution space is to do a simple model of the zone in the frequency domain, obtain the relevant transfer functions, and then perform a sensitivity analysis on the transfer functions to see how they are affected by fundamental design variables (Athienitis and Santamouris, 2002). With this method, one can see which variables will have the most effect on the results, which could be used to either eliminate some key variables from the optimisation, or to help determine what step-size increase between discrete options should be used. Although this method would be good to narrow down parameters in a temperature or energy related analysis, the methodology being developed for this thesis looks at the cost-effectiveness of various approaches, which would be hard to consider by simply looking at the transfer functions. For example, a small increase in the PV size will have a minor effect on net-energy consumption but will have a major effect on the overall cost of the design, due to the relatively high cost of PV. It would be interesting to include cost considerations in the type of sensitivity analysis carried out by (Athienitis and Santamouris, 2002); however that is beyond the scope of this thesis.

Even if the computing effort required in solving a problem remains significant (say greater than 24 hours), it may still have viable commercial applications. Computing times of this order should not be a problem for certain applications such as strategic policy and building code analysis, or for establishing a first design estimate in an energy efficient building project (Peippo, et al. 1999). It is questionable whether a building designer could come up with a complete set of optimal solutions, in the same amount of

time, using a combination of design tools, even if guided by professional experience. Design optimisation tools will prove even more powerful in the future, when the computational power of standard computers is increased. In fact, Christensen, et al., (2006) go as far as saying that with today's computers the bottleneck is no longer run times for individual simulations, but rather the time required to handle input and output data by the designer.

As mentioned, many optimisation methods, excluding GA, are available with the GenOpt optimisation software, which uses optimisation algorithms to minimise a cost function that is evaluated by an external simulation program, such as EnergyPlus or TRNSYS. With some knowledge of optimisation theory and basic skills in Java programming, a user can add different optimisation algorithms to the GenOpt library (Berkeley Laboratory, 2007). Initially, it was considered to implement a GA based optimisation algorithm within GenOpt, to encourage more uptake of the resulting research conducted for this thesis. However, in the course of gathering more information on how this could be implemented, it was discovered that the initial developer of GenOpt, Michael Wetter, was no longer at the Lawrence Berkeley National Laboratory, and that technical support for the tool was currently not available as a result[1]. Given that the estimated user population of GenOpt was only approximately 100 (US DOE, 2007b), and that there would be no technical support in implementing GA in GenOpt, this approach was not followed.

In their study, (Wang, et al., 2005) used multi-objective genetic algorithms to look at the optimisation of green building design. The multi-objective analysis used Pareto fronts to examine compromises between lifecycle cost performance and lifecycle

[1] Michael Wetter has since returned to Lawrence Berkeley National Laboratory.

environmental performance using exergy consumption. For the study, they developed a multi-objective GA based on a traditional approach (Dasgupta and McGregor, 1993) with modifications that allows the representation of the chromosome in a hierarchical genomic structure (Fonseca and Flemming, 1998). Given the extensive GA program that the researchers from the same research institution had developed for the optimisation of green building design, the researchers were approached to see if their GA program could be implemented for the GA Optimisation Tool being developed for this thesis. Unfortunately, the researcher in question felt that the program was not yet at a stage where it could be shared, since it required considerable cleaning up and the implementation of user instructions and comments within the code to make it easier to follow.

In an effort to develop something that would be easier to share with future researchers, and in an effort to save time, an existing GA program was sought out that could be applied for this research. Instead of opting for commercial software, it was decided to use algorithms developed by previous researchers that are available for free on the Internet to allow for the reproduction of the research being carried out in this thesis. Given that the researchers had previous experience in Fortran, a program written in this computer language was sought out. The search resulted in two viable alternatives of GA programs that have been used extensively in previous research applications (Carroll, 2005 and Coley, 2005). Either program could have worked; however the program by (Carroll, 2005) was selected since it was written for Fortran, whereas the (Coley, 2005) program was initially written in BASIC and converted to Fortran with a few alterations, making the coding not as ideal as it could be. The selected program also has more GA concepts

including creep mutations, uniform crossover, niching, elitism, and the ability to use a micro-GA as described in more detail in Section 3.3. The selected GA program has been used in hundreds of other research projects, including chemical engineering process development (Victorino, et al., 2007), an optimal variable air volume system controller (Jin, et al., 2005), a solar hot water system (Loomans and Visser, 2002), and in the development of a tool that estimates the lumped internal thermal parameters of a building thermal network model (Wang and Xu, 2006). With the energy simulation and optimisation programs selected, the next chapter details how the GA Optimisation Tool was developed.

3. OPTIMISATION TOOL DEVELOPMENT

3.1 Tool Overview

In Figure 3.1, a flow chart is presented that shows the basic principles in using a GA to optimise a ZESH. First, a random population of individual design configurations is generated. The GA program then calls an external energy simulation program to determine the energy use and thermal comfort of each individual in the population. Once all of the individuals in the population have been evaluated, the GA program calculates the fitness of each individual. If a set termination criterion is met, which was set based on evaluating a specified number of generations for this research, the program is stopped and the results are analysed. If the termination criterion is not met, then the GA program creates a new generation of designs by using selection, recombination, and mutation as detailed later in Section 3.3, and the program iterates until the termination criterion is met.

As shown in Figure 3.1, the GA program finds different configurations of ZESH to evaluate, and then calls TRNSYS to help determine their fitness. TRNSYS works with parameters that are set at constant values at the beginning of the simulation, and inputs that can vary throughout the simulation. The simplest way to update a large number of parameters at the beginning of a simulation is to use Type 70, which automatically updates parameters through an input file. Embedding this type within the TRNSYS model tells the simulator that parameters need to be updated in the listed units, and specifies the location of the file to read the new parameters. An alternative method would be to write a program that would update the whole deck file for each design

configuration. This method is much more difficult to implement as it requires an expert level of experience, and is more prone to implementation error. Type 70 was therefore selected in order to update the parameters. This decision meant that the more common and user-friendly Type 56 building model could not be used, as it currently does not interface with Type 70. In addition to Type 70 parameters, other values need to be updated at the beginning of the simulation that are used as inputs to components and to equations. Therefore, before the evaluation of an individual design, an input file and a parameter file are created in Fortran.

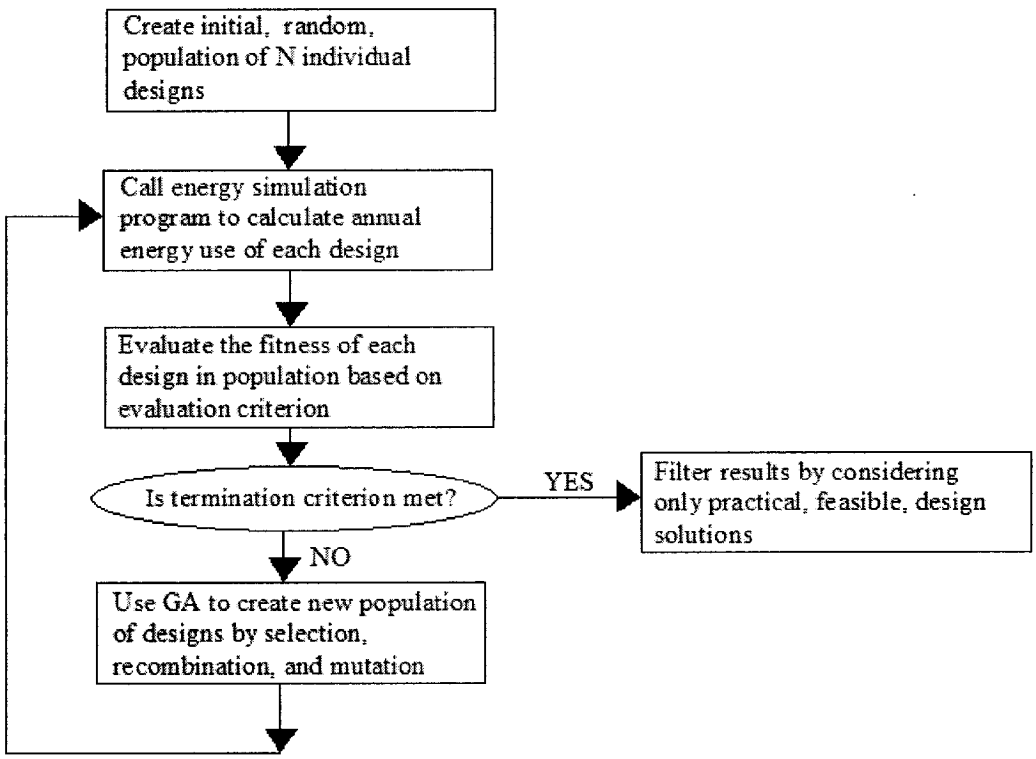

Figure 3.1: Flow chart outlining use of genetic algorithm

As the GA Optimisation Tool was setup, designs cannot be directly evaluated through TRNSYS. Instead, all the inputs and parameters need to be defined in the Fortran input file before the program calls TRNSYS. For this reason, two Fortran programs were

developed, one that is used for the main GA Optimisation Tool, and the other that is used to manually change parameters in order to run single TRNSYS evaluations. The manual program was required to test and validate the program. It is also useful for a user of the GA Optimisation Tool to test different design configurations around the optimal values obtained through the tool.

During the simulation, TRNSYS stores key values in two output files that are then evaluated by the Fortran program. The first file keeps track of the hourly electricity consumption and electricity costs calculated based on a time-of day schedule that allows for two price values depending on the hour of the day. This file also keeps track of the electricity generated by the PV and the revenue from selling 100% of the generated electricity based on the same time schedule used for the electricity costs. Revenues based on selling only excess electricity are not tracked, but they could be calculated in Fortran with the collected data. The second file keeps track of the hours in the year that the zone temperature is beyond $L95_h$, $L95_c$, $H95_h$, $H95_c$, MaxT_h, MaxT_c, MinT_h, and MinT_c as defined in Section 3.2.6. Based on this information, the Fortran program calculates the overall fitness of the individual design, which is then used to help generate the next generation of designs within the GA.

Initially, the idea was to develop one generic TRNSYS model that could represent all of the parameters to be optimised. However, adding multiple heating systems in a single model led to longer yearly simulation run-times that were not ideal for optimisation purposes. In the end, eight different TRNSYS files were needed, one for each heating system. This was not an ideal situation while developing the model, since when changes needed to be made on the base model, the changes needed to be made on all eight system

models. Evacuated tube and flat plate solar thermal collectors were specified in each model. The flow going through the collector is either turned on or off depending on which collector is chosen as depicted later in Figure 3.6. If a separate TRNSYS model was needed for each collector and each heating system, this would have led to 16 different TRNSYS files. One can see how this could easily become unmanageable if a number of different parameters would require their own TRNSYS model.

Currently the name of the weather file being used in TRNSYS needs to be updated manually. Therefore, before changing cities, each of the eight different TRNSYS files needs to be changed to specify the correct weather data. This is an acceptable situation for this initial tool, but would need to be changed such that the weather files could also be specified within Fortran.

3.2 TRNSYS Building Simulation Program

As mentioned in Section 2.2.1, TRNSYS uses the TFM to calculate the heat transfer through exterior zone surfaces, which introduces a certain level of error for building elements with more substantial thermal mass. The TFM is used for both the Type 56 multi-zone building model, and the Type 19 detailed single zone model that come with TRNSYS. The mathematical models used in the Type 56 and Type 19 building models are similar; however, they do have some differences. Type 56 has a more user-friendly interface and allows for more detailed modelling of the flow between zones. On the other hand, the Type 19 model allows for easier manipulation of individual parameters between simulations from an external program. As outlined in Section 3.1, the interface between the GA program and TRNSYS was done in part through the use of TRNSYS' Type 70 component, which allows the value of parameters to be updated at the beginning of a

simulation by reading an input file. This section provides an overview of the mathematical model used in Type 19 (Beckman, 2000), followed by a discussion on how separate elements were treated and modelled within TRNSYS.

As well as using the TFM, there are other approximations used in the TRNSYS Type 19 model that can reduce the overall accuracy of the calculations. An example is how the program deals with the long wave radiation exchange between surfaces. At the beginning of the simulation, the model calculates the view factors ($F_{i,j}$) between all the surfaces in a zone and the radiative heat transfer coefficient ($hr_{i,j}$) between each surface. The $hr_{i,j}$ is calculated once at the beginning of the simulation using the initial temperatures of the zone that are specified by the user and assumes that all surfaces are blackbodies:

$$hr_{i,j} = 4 \cdot \sigma \cdot F_{i,j} \cdot T^3. \qquad (3.1).$$

Using the initial zone temperature specified by the user to calculate Eqn. 3.1 introduces inaccuracy, since the T^3 represents the cube of the average temperature of the two surfaces. If the initial temperature is specified at 293K, and then increases to 298K, 303K, or even 308K, for surfaces with incident solar radiation, then the radiative heat transfer coefficient used in the model would be 5.2%, 10.6%, and 16.2% lower than if it were calculated with the actual temperature of the two surfaces for the particular time-step. However, if $hr_{i,j}$ was allowed to change at each time-step, then the **Z** matrix used to solve the zone model as described below, would become time dependent and would increase the computational power required to calculate the resulting temperatures at each time-step.

More uncertainty is introduced in calculating the radiation exchange between surfaces when the house model is simplified in fewer zones. For example, in the case where the

house is represented by a single zone, the model would calculate the radiation heat transfer between surfaces with higher incident solar radiation in the south part of the house, with surfaces with less incident solar radiation in the north part of the house. In reality, these surfaces, which may differ substantially in surface temperature, would not be in the same zone for surface-to-surface radiation heat transfer.

The Type 19 model uses a constant combined radiative and convective heat transfer coefficient for heat transfer calculation on the exterior surfaces. For this research, the default recommended value of 16.95 $W/m^2 \cdot K$ was used for all exterior surfaces. In reality, this coefficient varies depending on wind speed, outdoor and effective sky temperatures, and incident solar radiation. The model also uses a constant convective heat transfer coefficient for all of the interior surfaces. For this study, the default value of 2.66 $W/m^2 \cdot K$ was used for all surfaces. Again, these values would change based on temperatures, type and location of HVAC system, and other factors.

As for the model itself, the surface temperatures are calculated at each time-step using the following matrix multiplication:

$$T_s = Z^{-1} \cdot X, \tag{3.2}$$

where the matrix **Z**, which represents time-independent factors affecting surface and zone temperatures, is calculated and inverted once at the beginning of the simulation. The fact that **Z** is time-independent saves a lot of computational time, since it allows the inverse of the matrix to be calculated only once. The terms in **Z**, which are defined below in more detail, comprise the convective and radiative heat transfer coefficients of the surfaces and the transfer function (TF) relating the heat flux through the wall from the equivalent zone temperature. In reality, the convective and radiative heat transfer coefficients vary. In

addition, for the zone air nodes, since **Z** is time independent, two further simplifications are required. The first is that the zone temperature variations are considered to be linear over each simulation time-step, and secondly, the ventilation and infiltration energy gains are evaluated using the last estimate of the zone temperature. For typical interior surfaces, **Z** is defined as:

$$Z_{i,j} = \frac{h_{r,i,j}}{h_{c,i}} \cdot \left(\frac{c_{o,i}}{h_{c,i}} - 1 \right) \qquad i \neq j, \tag{3.3a}$$

$$Z_{i,i} = 1 - \frac{1}{h_{c,i}} \cdot \left(\frac{c_{o,i}}{h_{c,i}} - 1 \right) \cdot \sum_{j=1}^{N} h_{r,i,j}, \text{ and} \tag{3.3b}$$

$$Z_{i,N+1} = \frac{c_{o,i}}{h_{c,i}} - 1, \tag{3.3c}$$

where i=1 to N are interior surface nodes and N+1 is the room air node. The vector **X** in Eqn. 3.2 represents the time varying inputs affecting the surface and zone temperatures. For typical exterior envelope elements, it is calculated as:

$$X_i = \sum_{h=0} \frac{b_{h,i}}{h_{c,i}} \cdot T_{sa,i,h} - \sum_{h=1} \left(\frac{c_{h,i}}{h_{c,i}} - d_h \right) \cdot T_{eq,i,h} - \sum_{h=1} d_{h,i} \cdot T_{s,i,h} - \frac{s_i}{h_{c,i}} \cdot \left(\frac{c_{o,i}}{h_{c,i}} - 1 \right). \tag{3.4}$$

In cases where an exterior building envelope element cannot be represented by the TFM, such as the case for under-floor heating systems, Trombe walls, windows, etc., the heat flux from the surface is input into the zone model from another model, which changes the definition of **Z** and **X** to the following:

$$Z_{i,j} = \frac{-h_{r,i,j}}{h_{c,i}} \qquad i \neq j, \tag{3.5a}$$

$$Z_{i,i} = 1 + \frac{\sum h_{r,i,j}}{h_{c,i}}, \tag{3.5b}$$

$$Z_{i,N+1} = -1, \text{ and} \tag{3.5c}$$

$$X_i = \frac{\dot{Q}_i / A_i + s_i}{h_{c,i}}. \tag{3.5d}$$

Finally, the expressions for **Z** and **X** are the following for the zone air node:

$$Z_{N+1,j} = h_{c,j} \cdot A_j, \tag{3.6a}$$

$$Z_{N+1,N+1} = -\sum_{j=1}^{N} h_{c,j} \cdot A_j - \frac{2 \cdot Cap}{\Delta t}, \text{ and} \tag{3.6b}$$

$$X_{N+1} = -\dot{Q}_z - \dot{Q}_v - \dot{Q}_{infil} - \dot{Q}_{int} - 0.3 \cdot \dot{Q}_{s,people} - \frac{2 \cdot Cap}{\Delta t} \cdot T_{ZI}, \tag{3.6c}$$

where the heat transfer terms are from zone surfaces, ventilation, infiltration, internal gains other than from people or lights and sensible heat gain from occupants, respectively. Cap is the effective thermal capacitance of the zone air plus furnishings and any other thermal mass that is not considered in the zone surfaces, such as un-modelled interior partition walls. Cap was initially set at 12 times the capacitance of the zone air based on recommendations from the TRNSYS suppliers. However, the value used for this parameter is revisited in Section 5.1.5. The value of X_{N+1} is calculated based on the zone temperature of the previous time-step. Appendix A goes through a detailed example to demonstrate how Eqns. 3.3 to 3.6 relate to energy balance equations.

From Eqn. 3.4, we can see that the sol-air temperature and the equivalent zone temperatures are used in the model. The sol-air temperature is defined as the temperature of the outdoor air, which in the absence of all radiation exchanges gives the same heat transfer at the outside surface as actually occurs. There is an inconsistency in the

TRNSYS model in how T_{sa} is defined. It is calculated using an exterior surface convective heat transfer coefficient based on wind speed as follows:

$$T_{sa} = T_o + \frac{(\alpha I_T)}{h_{c,o}}, \tag{3.7}$$

where $h_{c,o}$ is calculated using the following equation:

$$h_{c,o} = 5.7 + 3.8 \cdot V_w. \tag{3.8}$$

Eqn. 3.8 is in W/m^2·K and the wind velocity is in m/s. The inconsistency in Eqn. 3.7 is that a variable convective heat transfer coefficient is used in its calculation, whereas a constant convective heat transfer coefficient is used in calculating the TF (16.95 W/m^2·K). In order to eliminate this discrepancy, a constant wind velocity of 2.96 m/s would need to be input in the model as opposed to using the wind velocity from the weather data; however, this would eliminate the effects of a varying wind velocity on the infiltration calculations. In order to not lose the effect of wind on infiltration, the weather data wind velocity was used in the model.

The use of constant exterior heat transfer coefficients and interior convective heat transfer coefficients are other factors affecting the accuracy of the results. As discussed, the TF coefficients were calculated using a constant exterior heat transfer coefficient of 16.95 W/m^2·K and an interior convective heat transfer coefficient of 2.66 W/m^2·K. In reality, both of these values vary significantly over the course of the year. For example, the use of a heater near a wall changes the convective heat transfer coefficient of that wall, as is the case with under-floor radiant heating. The TRNSYS Type 706 floor heating model does allow for a variable convective heat transfer coefficient as an input to the model, as it should, since the convection changes considerably depending on whether

the floor heating is on or off. However, Type 706 is linked with the conduction input wall, which has the convection heat transfer coefficient set as a constant. The use of a variable coefficient in Type 706 and a constant value in the zone floor model leads to inconsistencies. Therefore, the convection heat transfer coefficient for the floor model was assumed constant at a value of 2.66 $W/m^2 \cdot K$. The effect of using constant heat transfer coefficients was not analysed further since this is an issue directly related to the TRNSYS Type 19 model, and it is not the intention of this study to validate TRNSYS. It would be good to have a future study to quantify the effect of using constant convective heat transfer coefficients in the model. This would give TRNSYS users a better understanding of when it is not appropriate to use this particular model, which depends on using constant convective heat transfer coefficients to make **Z** time independent.

As mentioned in this section, the use of the TRNSYS Type 19 detailed single zone model brings a level of uncertainty in the calculation. This uncertainty arises since it uses the TFM, that is not as accurate for thermally massive walls, and that constant heat transfer coefficients are used. When doing the literature search for this work it was found that more research would be needed to clearly define the limitations of using the TFM for the modelling of thermal mass. It would be important to know how much mass these types of models can take while maintaining a good accuracy level. Quantifying the differences between using the TFM and finite difference methods for various levels of thermal mass would be a good starting point. In conjunction with this work, more accurate building models should be developed for use in these types of tools. However, any new models would need to be robust, and not be too computationally intensive since optimisation algorithms require many simulation runs as discussed earlier in this thesis.

Despite the limitations of the TFM, doing yearly simulation with real weather data and sub-hourly time-steps with TRNSYS should be more accurate than some methods based on monthly average weather data that are still in use today. In addition, the GA Optimisation Tool developed here is intended for use in the early design stages, which requires less accuracy than in the later stages of design. An in depth analysis of the uncertainty in the results due to using the selected building model is beyond the scope of this thesis. Only uncertainties introduced with the approximations made in developing the solar home model within TRNSYS are examined.

In terms of the zone definition, the height of the building was calculated assuming a typical floor height of 2.4 m (8 feet). If the user selects a two-storey house, then the height is double that of the default floor height. The east-west wall length of the zone is calculated as follows, where form is a parameter being optimised:

$$Len = \sqrt{\frac{Floor\_A}{\#\_Stories \cdot Form}}, \tag{3.9}$$

$$Form = \frac{Length}{Width}. \tag{3.10}$$

The width (south-north wall length) of the zone is equal to the floor area per story divided by the zone length.

Type 18, Pitched Roof and Attic model, is used to determine the heat loss through the ceiling. The model assumes that the ceiling is composed of 19 mm (¾") of plaster, followed by 0.051 m x 0.305 m (2" x 12") joists, followed by 19 mm (¾") of plywood, from the room to attic. In the 0.305 m (12") cavity formed by the joists, there is a choice of having 0.076 m, 0.152 m, 0.229 m or 0.305 m (3", 6", 9", or 12") of insulation. For this research, 0.305 m (12") of insulation was used in all cases. The model uses an

effective sol-air temperature calculated as a function of the various roof surfaces and the infiltration rate, which is used as a heat source (or sink) to drive the heat flux equation. One simple roof shape was considered for all designs as shown in Figure 3.2, with the slope of the roof being one of the parameters that was optimised.

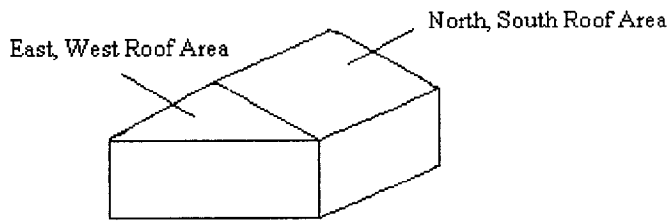

Figure 3.2: Diagram of roof shape considered in tool

3.2.1 Single Zone Approximation

One of the drawbacks of using genetic algorithms is the computational time it takes to run the optimisation. The level of detail used in the modelling, such as using one or more thermal zones, the interaction between the house and the ground, etc., and the simulation time-step used in modelling the house, play a large part in establishing the time it takes to run the GA Optimisation Tool. The number of thermal zones to be used for the tool needed to be decided in the early stages of the tool development. Should every room in the building be modelled as a separate zone, or should some or all rooms be grouped together to form larger aggregated thermal zones. Generally speaking, most solar homes would be expected to have a warmer south-facing zone and a colder north-facing zone. In two-storey homes, one may anticipate the use of a thermal zone for the basement, and both a south and north-facing zone for the first and second levels, for a total of up to five zones. When modelling multiple thermal zones, it is important to accurately model the

airflow between the different zones. However, few building energy simulation programs take into account the effect of airflow (Bastide, et al, 2006).

There are two methods of calculation: the microscopic method uses computational fluid dynamics (CFD) and the macroscopic method uses the simple multi-zonal (network) approach. Difficulties in using CFD are found in both defining the model, including the determination of boundary conditions (Bojic and Kostic, 2006), and the computational time required to run these models. The macroscopic method (multi-zonal model) uses a zonal approach and empirical knowledge to simulate the airflow inside the building and compute mass flows. It does not provide velocity and temperature distributions inside a room, which are often required for evaluating thermal comfort (Kuznik, et al, 2006). A third approach in evaluating airflow in zones is to couple energy simulation and CFD simulation in order to eliminate many assumptions that are used in the separate energy simulation and CFD computations and thus provide more accurate results (Farhanieh and Sattari, 2006). This hybrid method requires an iterative procedure in order to achieve the convergence and stability in the corresponding solution.

One popular multi-zonal airflow model, which can be coupled with TRNSYS, is COMIS (Feustel, 1999, Haas, et al., 2002). The use of COMIS within TRNSYS is done through the use of the multi-zonal building model Type 56, and not for the Type 19 zone that was used for this tool. To help define the pressure coefficients used in COMIS, it is recommended that the distribution of air pressure around the building be determined either by CFD or in a wind tunnel (Bojic and Kostic, 2006). Given the computational intensity of optimisation algorithms, it was not feasible to use CFD airflow modelling for this research. In addition, since the tool is intended for early design stages, the internal

layout of the house and the exact pressure coefficients required in the model are not known. The use of defined airflow modelling between possible zones was not considered for this tool since the level of detail required to accurately model airflow is not known at this stage of the design process.

Two simple models of a single-storey house using one and two zones were developed in order to determine how close their results were, and what difference there was in terms of simulation time. As mentioned, the interaction between the two Type 19 zones within TRNSYS is fairly limited. The wall separating the two zones was modelled as an internal partition, which is treated as an adiabatic wall with no heat transfer between the zones. Air transfer between the two zones was modelled using circulating fans that were turned on when either zone was 4°C hotter than the other zone, as recommended in (CMHC, 1998). In order to compare the approximate total calculation time of the optimisation tool, a total of 300 TRNSYS evaluations was assumed. GA have been shown to systematically find near optimum solutions of building optimisation problems that have large discrete search spaces (1.94×10^{22}), with as little as 300 evaluations of different building configurations (Wright and Alajmi, 2005). Table 3.1 shows the approximate time it took to go through a yearly simulation of the one and two-zone TRNSYS models using a simple electric auxiliary air heater using different time-steps, 200 m^2 floor area, Montreal weather data, and using a 3.2 GHz processor with 512 MB of RAM. The 2-zone results in the table are average results between having the south zone comprised of 25%, 50%, and 75% of the total floor area, with the north zone comprised of 75%, 50%, and 25%, respectively.

Table 3.1: Preliminary TRNSYS simulation results

Time-step (min)	1-Zone Run Time (sec)	1-Zone Heater (kWh)	2-Zone Run Time (sec)	2-Zone Heater (kWh)
60	15	15,680	268	17,313
30	28	14,685	407	16,568
20	38	14,680	483	16,393
10	72	14,615	619	16,446

It is apparent from Table 3.1 that there is a considerable difference in the time it takes for a yearly simulation of a one-zone model in comparison to a two-zone model. To run the simulation 300 times would take the one-zone model 1.25 to 6 hours depending on the time-step, and 22 to 51.6 hours for the two-zone model. If more than 300 runs are required for a given problem, or if multiple optimisation runs are needed, the time difference between using one and two zones can become even more significant especially as more modelling complexity is added. In terms of computational time, it was evident that it would be preferable to use a one-zone model with larger time-steps. However, it was imperative to further scrutinise the results in order to determine which model and time-step achieved the minimum level of accuracy required for this type of application. Since the fitness function of the GA is highly dependent on energy consumption and thermal comfort, the results were further analysed to compare the predicted zone temperatures and calculated yearly energy consumption between the one- and two-zone models.

Results in Table 3.1 show that the time-step used in the simulation plays an important role in determining the total time it takes to run the GA Optimisation Tool. Given that temperature level control is implemented, a 60 minute time-step is not recommended. This would imply having heating, cooling and ventilation equipment cycling at 60-minute

intervals, which is not a close approximation to what happens in reality. Determining how small a time-step can be taken needed to be done using a more final version of the model, one that had all of the different heating systems and other parameters implemented. An evaluation on the time-step used for the tool is presented in Section 5.1.5.

From Table 3.1 it can be seen that the two-zone model predicts an average heater consumption that is 11% higher than the one-zone model. One of the reasons for this is that the control strategy used in the two-zone model used the lowest temperature between the south and north zone to initiate the heating. Since it can be assumed that the one-zone model would gives more of an average temperature between the two-zones, it can be deduced that using a control strategy for the two-zone model based on the average temperature of the two thermal zones would result in closer calculated heating loads between the two models. Table 3.2 compares the results of the two-zone model and one-zone model assuming an even split between the south and north zone areas and a time-step of 20 minutes. Three control strategies were used: one identical to what was used for results in Table 3.1, one using the mixed zone temperatures, and one based on controlling the heater based on the highest zone temperature. Table 3.2 also provides the number of hours during the year that each zone was below 16°C and 18°C, and the number of hours that the zones were above 28°C and 33°C. The only cooling that was used consisted of using two stages of outdoor air at 3 air changes per hour (ach) and 6 ach when the outdoor temperature was lower than the zone temperatures, as discussed later in this chapter.

Table 3.2: TRNSYS control strategy results analysis

	1-Zone	T_{high} control	T_{mix} control	T_{low} control
Heater (kWh)	14,680	13,530	14,510	15,883
S_zone < 16°C	n/a	212	5	4
S_zone < 18°C	n/a	1,785	669	26
S_zone > 28°C	n/a	294	297	299
S_zone > 33°C	n/a	10	10	10
N_zone < 16°C	n/a	104	26	0
N_zone < 18°C	n/a	558	349	0
N_zone > 28°C	n/a	150	150	150
N_zone > 33°C	n/a	3	3	3
1-zone < 16°C	0	n/a	n/a	n/a
1-zone < 18°C	7	n/a	n/a	n/a
1-zone > 28°C	191	n/a	n/a	n/a
1-zone > 33°C	5	n/a	n/a	n/a

The results of Table 3.2 clearly show that using the mixed zone temperature for the two-zone heater control resulted in a much closer annual heating load to the one-zone model. In fact, the difference changed from the one-zone results being 11% lower than those of the two-zone, to being 1.2% higher. Provided that a mixed zone temperature is used for the heater control, the one-zone model should be adequate for calculating the annual heating load. These results indicate how important the control strategy is in building energy consumption. Since the one-zone model gives more of an average temperature between the zones, it averages out some of the peak temperatures and results in fewer hours in the year that the zone temperatures are outside the set thermal comfort range. To demonstrate the difference between the results, Figure 3.3 shows results for a one-day period that clearly demonstrates this tendency.

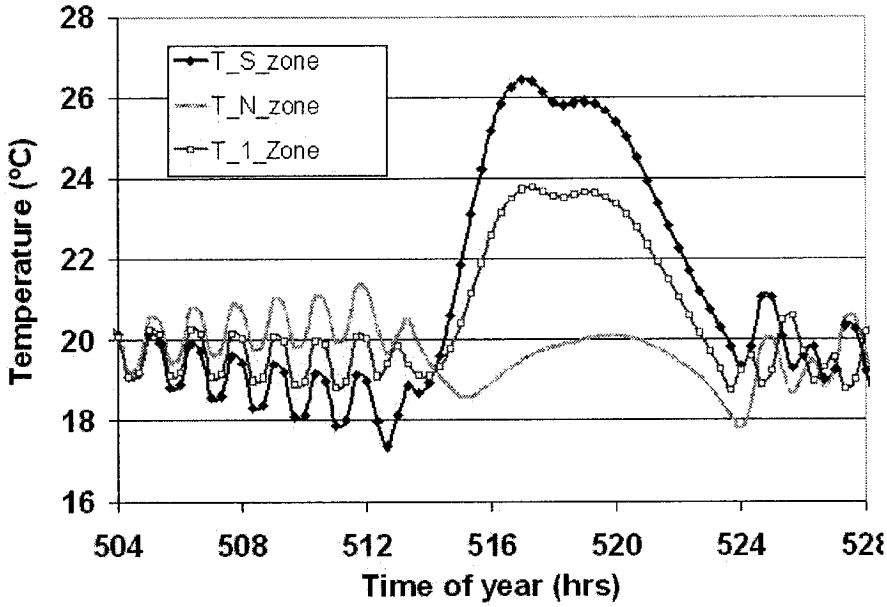

Figure 3.3: Comparison of predicted temperatures between one- and two-zone models

Based on the aforementioned results, it was decided that the additional information that could be gained by using the two-zone model did not justify the added complexity involved in developing the two-zone model, especially given the increased uncertainty in accurately representing the heat and air exchange between a multi-zone model and the order-of-magnitude increase in computational time. In the early stages of design, the HVAC control strategies between the north and south zones are usually not known; thus, the uncertainty arising in modelling the airflow between the different thermal zones introduces inaccuracies in the generic modelling approach implemented for modelling the house with two zones. Therefore, the house was modelled with a single thermal zone, even for the case of a two-storey house since the same issues arise in multiple stories as in modelling north-south interactions. A second tool, specific to the later stages of design when more critical information is known, could be developed that would have more

detailed modelling of the different thermal zones and help optimise control strategies. People using the tool need to keep in mind that the predicted zone temperature is an average temperature of the whole house and that the south zone would likely be hotter in the day and cooler at night than what is predicted. This difference would be less pronounced if a circulating fan was used to circulate air between the various zones in the house.

3.2.2 Radiant Floor System

The floor in the zone was modelled using TRNSYS Type 706 developed by (TESS, 2006), which represents a radiant slab with embedded pipes and ground storage effects. Unlike the other zone surfaces that rely on the TFM, this floor model relies on a three-dimensional finite difference method, which solves the resulting inter-dependent differential equations using an iterative approach. The floor model links with the zone model through the use of a conduction input wall. Type 706 calculates the rate of heat transfer from the floor surface and passes this information along to the Type 19 zone model. Note that Type 706 assumes that the heat transfer within the slab and the surrounding soil is conductive only and that moisture effects are negligible.

Type 706 was made for use with simplified building models that do not contain the concept of a boundary wall, where the surface temperature is calculated and transferred as an input to the zone model. Type 19 is somewhere between a more detailed zone model, and the simple zone model referred to in Type 706. In order to link Type 19 and Type 706 a few approximations needed to be made. Type 706 calls for three inputs from the zone: the incident solar radiation on the floor, the zone temperature, and the equivalent surrounding surface temperatures for long wave radiation exchange

calculations. For the research tool, the equivalent zone temperature from Type 19 for the floor surface was passed as the input zone temperature to Type 706, which took into account all three required inputs. The input incident solar radiation was set at 0 and the surrounding temperatures for long wave radiation calculations were set at the calculated floor temperature from the previous time-step, since these two parameters are included in the equivalent zone temperature.

A good way to verify if the two models are converging is to compare the output floor surface temperature of the zone model with the calculated floor surface temperature of the floor model. The floor temperatures were analysed using combinations of 20% or 80% south window coverage with either RSI 0 or RSI 6 insulation under the slab and with both an air based heating system and a radiant floor heating system. The case with 80% south window coverage with no under-floor insulation was also repeated with a slab thickness of 15 cm, as opposed to 7.5 cm. The amount of insulation under the slab had no effect on the performance of the models, nor did the slab thickness. The amount of south-facing windows did play a factor with the average difference between the models being 0.21°C at 20% coverage and 0.36°C at 80% coverage for the air based heating system 1. The difference between the models was slightly less using the radiant floor heating system with the differences being 0.20°C and 0.34°C, respectively. The floor model temperature was 0.03°C warmer with 20% coverage and 0.08°C warmer with 80% coverage with both heating systems. This temperature difference between the two models is well within acceptable limits. As discussed previously in this section, in order to match what was used in Type 19, a constant interior convective heat transfer

coefficient of 2.66 W/m^2K was assumed. In reality, this value would change over the course of the year, and would be larger with a floor heating system.

There were pipes embedded in the floor for all cases, even when no radiant heating was specified in order to keep the base TRNSYS model more consistent. When there was no radiant heating, the flow in the pipes was set equal to zero, which is essentially equivalent to a slab model. The pipes within the floor were spaced 20 cm apart based on the recommendation in (NRCan, 2002), which states that by placing the floor pipes 20 cm apart, rather than 30 cm apart, the water temperature required for heating can be reduced by 4°C to 5°C and the heating efficiency of the earth energy systems increases by about 10 percent. In reality this would depend on the thermal mass properties and thickness of the floor. For the finite difference calculations, the floor was divided in 4 sections along its length and 3 along its width. More division increases the accuracy, but increases the computational requirements of the model. The pipe was laid out as shown in Figure 3.4, with the same length of pipe given in each floor section. The pipe was assumed to have an inner diameter of 0.03 m and 0.033 m outer diameter. The total pipe length was calculated based on the following:

$$Pipe\_Len = \frac{(Width - 0.2) \cdot Length}{0.2}. \tag{3.11}$$

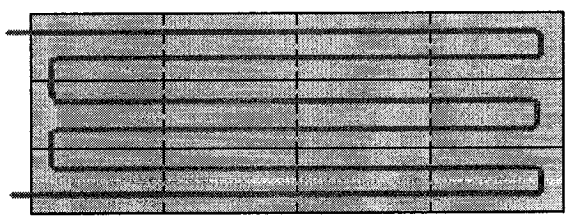

Figure 3.4: Representative pipe layout and floor division

There are various other parameters that need to be input into the floor model other than those required to specify the piping. Only one node depth below the floor and one node beyond the floor in the x- and y-axis were considered. Adding more nodes increases the accuracy, but also increases the computational requirements of the program. A horizontal and vertical far-field distance of 2 m was specified, which represent the distance away from the slab at which the soil is no longer influenced by the heat transfer from the slab into the soil. The ground thermo-physical properties surrounding the floor were initially set based on default values, which are 2.42 W/m·K for conductivity, 3,200 kg/m^3 for density, and 0.84 kJ/kg·K for specific heat. The soil surface temperature was calculated using the Kasuda correlation that is embedded in the Type 706 model using an assumed mean surface temperature of 10°C with an amplitude of 5°C and the minimum temperature occurring on the 36th day of the year.

The slab thickness of the base case that does not include additional thermal mass was initially assumed to be 0.10 m, and 0.20 m when added thermal mass was called for as discussed later. The thickness of 10 cm was selected based on recommendations found in (CMHC, 1998 and Chiras, 2002). Optimum thickness can vary based on specific design conditions, on the type of concrete that is used, and can be limited by the structural limitations of the house (Charron and Athienitis, 2006a). The slab properties were assumed to be 1.7 W/m·K for conductivity, 2,200 kg/m^3 for density, and 0.84 kJ/kg·K for specific heat (Athienitis, Santamouris, 2002). The perimeter insulation was assumed to go to one nodal depth, and was set to an RSI value of 4, the same as initially specified for the insulation under the slab. A hardwood floor was assumed to be installed on top of the slab with an emissivity of 0.9 and absorptance of 0.6, which also added RSI 0.12 above

the slab (McQuiston, et al., 2005). The sensitivity of the results based on these various parameters, including using different floor coverings, is investigated in Section 5.1.6.

3.2.3 Solar Thermal Collector Modelling

In TRNSYS, there are different models for both flat plate collectors and evacuated tube collectors. For the flat plate collectors, Type 1b was selected, which uses a quadratic efficiency equation of the form:

$$\eta = a0 - a1 \cdot \frac{T_{in} - T_o}{I_T} - a2 \cdot \left(\frac{T_{in} - T_o}{I_T} \right)^2, \tag{3.12}$$

and uses a 2nd order incidence angle modifier (IAM) to take into account effects on efficiency when the beam radiation is not normal to the collector as follows:

$$IAM = 1 - bo \cdot \left(\frac{1}{\cos \vartheta} - 1 \right) - b1 \cdot \left(\frac{1}{\cos \vartheta} - 1 \right)^2. \tag{3.13}$$

Model Type 538 was selected to model the evacuated tube collector. This model uses the same efficiency equation as written in Eqn. 3.12. For the IAM, Type 538 reads the modifiers from an input file for different transverse and longitudinal angles. Even though the cost data for the solar thermal collectors was obtained for generic panels as described in Section 3.5, real products were used for the performance data. For the flat plate collectors, the G Series glazed liquid flat plate solar collector from (Thermo-Dynamics, 2006) was selected. Specifications from the Mazdon Solar Collector from (ThermoMax, 2006) were selected for the evacuated tube collector. The performance specifications for both collectors can be found in Appendix B.

Various system configurations can be used with the solar thermal collectors and solar thermal storage tanks. Traditionally, the solar collectors heat a solar thermal storage tank

that feeds into a regular domestic hot water tank. This approach leads to the use of a large number of components, which can result in problems with the hydronic system and the controller, and the complex design can reduce efficiency. A new approach is emerging in Europe that uses a single stratified storage tank that serves as an energy manager (Weiss, 2003). Each energy source (solar and auxiliary) and different draws from the tank are connected to different heights to maintain the temperature layers in the tank, which avoids mixing and maintains stratification. These changes in approach approximately lower the required number of pipes from 17 to 8, reduce the space requirements from 4.8 m^2 to 2.2 m^2, and lower the system weight from 250 kg to 160 kg. One product that follows these innovations is the SolvisMax shown in Figure 3.5 (Solvis, 2005).

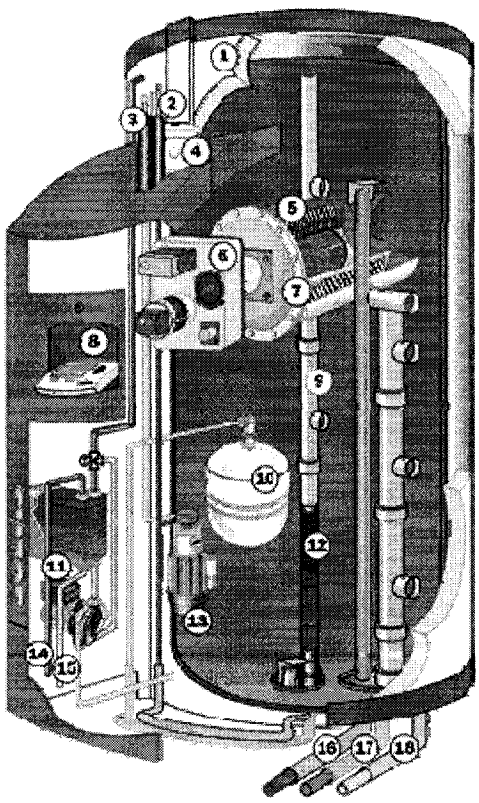

1. Insulation
2. Solar outlet
3. Solar return
4. Tail pipe connection
5. Combustion chamber
6. Oil burner
7. Waste gas heat exchanger
8. System automatic controller
9. Layer loader
10. Solar expansion tank
11. Warm water station
12. Solar heat exchanger
13. Solar pump
14. Warm water
15. Chilled water
16. Heater outlet
17. Heat return
18. Filling and emptying pipe

Figure 3.5: Diagram of SolvisMax solar combisystem energy manager (Solvis, 2005)

The solar thermal system in the GA Optimisation Tool follows a similar approach. The exception is that an external heat exchanger is used to transfer the heat from the solar collectors to the domestic hot water tank, and that an external water heater is used to boost the domestic hot water temperature going to the occupants. Figure 3.6 shows a diagram of the tank and collector arrangement as modelled in TRNSYS.

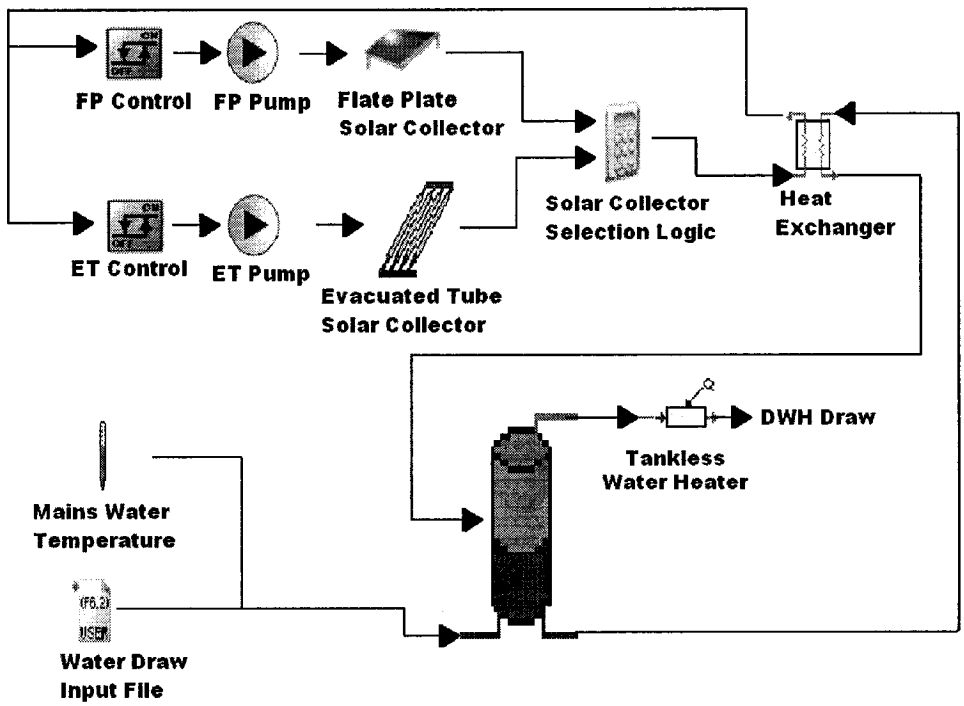

Figure 3.6: Solar thermal collector and storage configuration

The external heat exchanger used had an overall heat transfer coefficient (UA) of 300 W/K, as was used in (Ellehauge, 2002); however, this is a value that can have a significant impact on results and an actual value should be used if available. In the future, different heat exchangers could be modelled to make the UA a variable to be optimised. One study found that the value of the UA should vary depending on the size of the solar thermal collector in the range of 80 W/K per square metre of collector area in order to keep the collector inlet temperature as low as possible (Drück and Hahne, 1998).

The same study also found that the connections for the auxiliary and the space heating loop should be on the appropriate positions on the solar thermal storage tank. In the GA Optimisation Tool, the water heated from the solar thermal collectors is drawn from the bottom of the tank and returned to the middle of the tank. This configuration allows the top portion of the tank to be heated by an auxiliary heat source to a hotter temperature while maintaining thermal stratification in the tank (Ellehauge, 2002).

Various system configurations and control strategies can be employed for solar thermal systems. In depth studies could be carried out in order to optimise the performance of a given system based on the actual equipment that is selected. For the GA Optimisation Tool, a simple system with default parameters was assumed. In the future, more research could be devoted to the whole solar thermal system, depending on if it is used primarily for heating domestic hot water or if it is also used for space heating. For example, an area that could be improved would be the control strategy, with the implementation of P, PI, or PID control with a variable speed pump. In the model for this thesis, one constant pump speed was used with a simple on/off control with a given deadband. In the tool, the pump was turned on when the temperature leaving the solar collectors was 11°C higher than the temperature of the water coming from the bottom of the storage tank based on a recommendation given in (RS Means, 2005b), and it turned off when the difference went down to 2°C. The flow rate going through the solar collectors was set at 110 kg/hr based on simulation results of 1 to 4 solar collectors of 3 m^2 area, a 0.5 m^3 storage tank, a 30 minute time-step and default water temperature from the water main as outlined in Table 3.3. The default temperatures listed in Table 3.3 were used as default in the GA Optimisation Tool for all cases examined. In

reality, these temperatures vary depending on the location of the modelled house. Table 3.4 shows results of the DHW consumption for the different cases. The hot water consumption profile that was used is detailed later in Section 3.4.6. For the given conditions, if no solar thermal collectors were present and the hot water was simply heated with a 100% efficient tankless water heater right from the water main, the hot water consumption would be 4,236 kWh.

Table 3.3: Default water temperature coming from the utilities

Time (hr)	Temp. (°C)	Time (hr)	Temp. (°C)	Time (hr)	Temp. (°C)
0	9.4	3,624	10.5	7,296	9.7
744	9.6	4,344	10.7	8,016	9.6
1,416	9.7	5,688	10.6	8,760	9.4
2,160	9.9	5,832	10.4		
2,880	10.2	6,552	10.1		

Table 3.4: Domestic hot water consumption (kWh) with varying flow rate

Flow Rate (kg/hr)	Flat Plate Collector Area				Evacuated Tube Collector Area			
	3 m^2	6 m^2	9 m^2	12 m^2	3 m^2	6 m^2	9 m^2	12 m^2
100	2,498	1,836	1,493	1,299	2,354	1,373	904	664
110	2,498	1,830	1,485	1,288	2,362	1,373	903	662
150	2,501	1,820	1,467	1,264	2,378	1,381	905	661
200	2,519	1,828	1,466	1,256	2,406	1,405	916	665

The results of Table 3.4 show that the larger areas of solar collectors are more efficient with a higher flow rate. The value of 110 kg/hr produced near optimal performance in all cases, although this would depend on the actual thermal load and system configuration. The value of 110 kg/hr is within the range recommended for the selected flat plate collectors, which ranges from 48 L/hr to 150 L/hr. The same flow rate was assumed for the water flowing into the heat exchanger from the storage tank; a

variation in this velocity would affect the performance as in the above case. The working fluid in the solar collector loop was assumed to be a 40% mixture of propylene glycol and water in order to prevent freezing with a specific heat of 3.7 kJ/kg·K and a density of 1,030 kg/m^3 (M. Conde Engineering, 2005).

The solar thermal storage tank itself was modelled with a TRNSYS Type 4 tank with ten equal sized control volumes. The diameter of the tank was assumed to be constant for all cases at 0.80 m. As mentioned, the DHW was not heated to the desired setpoint in the tank itself, but instead was boosted to 60°C, when needed, by an external electric tankless heater, assuming 100% efficiency. This was done in order to allow the storage tank to be used as the heat source for a heat pump in a few of the heating systems considered. A heating element was set in the 9th node in the tank, controlled by a thermometer located in the 10th node, in order to prevent the tank from freezing for cases where a heat pump drew heat away from the tank at a rate that could not be replenished by the solar thermal collectors. The element was set to turn on when the tank reached 8°C using a deadband of 4°C. For other types of space heating systems, it would be possible to use the upper element to heat the water to 60°C, which would eliminate the need for the external tankless heater. This situation would use more electricity since the tank would be hotter, which would lower the amount of heat extracted from the solar thermal collectors and increase the heat loss through the tank walls. More care would be needed in the design in order to ensure good stratification in the tank. The way the system was modelled is equivalent to using a tankless water heater with an unheated solar thermal storage tank. Efficiencies for electric tankless heaters can range up to 99.5% (Builders Websource, 2006). The problem with tankless electric heaters is that they can substantially increase

peak loads, which is undesirable for utilities and for consumers with time-of-day billing rates. Gas tankless heaters, which have efficiencies in the low 80% range, would not generate these peaks in electricity consumption.

In order to verify the difference between the simulated DHW consumption using the tankless water heater and using the element at the top of the storage tank, a series of simulations were done to compare yearly consumption using the same basic assumptions that were used for those listed in Table 3.4. In cases without a solar thermal collector, the consumption more than doubled to 8,736 kWh, compared to the case where the tankless water heater heated the water directly from the water main. Figure 3.7 summarises the results using the default flow of 110 kg/hr. The solar thermal collectors reduced the DHW consumption substantially more in the configuration with the heater in the tank than with the tankless heater with the performance of larger evacuated tube collectors approaching that of flat plate collectors in the tankless heater configuration with the same collector area.

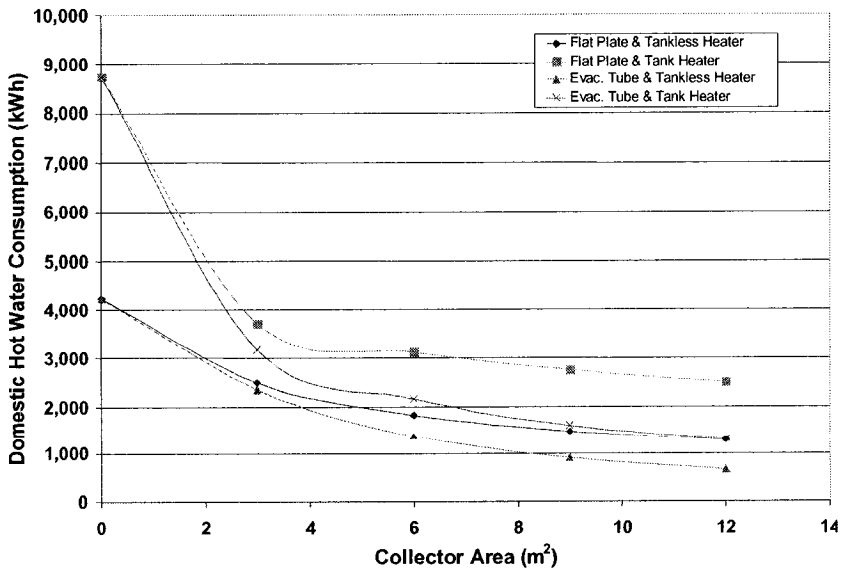

Figure 3.7: Comparison of DHW consumption using tankless and tank heaters

3.2.4 Infiltration and Fresh Air Ventilation

All houses, no matter how well constructed, have air that infiltrates into the building through cracks and other unintentional openings, and through the normal use of exterior windows and doors. Typical infiltration values can vary significantly from one house to the next, varying by a factor of about ten in North America. For tightly constructed houses, the seasonal average air exchange rates are in the range of about 0.2 ach, whereas loosely constructed houses can have air exchange rates as high as 2.0 ach (ASHRAE, 2001). Various studies have evaluated the air exchange rates of different houses. One such study looked at two groups of houses: the first comprising of 292 energy efficient houses that were built incorporating measures to reduce air infiltration, and the second comprised of 331 control houses. Tests showed that the first group of houses had average air exchange rates of about 0.25 ach, whereas the second group had average rates of about 0.49 ach (range: 0.05 to 1.63 ach) (ASHRAE, 2001). ASHRAE Fundamentals 2001 lists various studies done to test the accuracy of the models used to predict air exchange rates due to infiltration; it found that the models exhibited average errors on the order of 40% for many measurements on groups of houses and were off by as much as 100% in certain individual cases. Therefore, regardless of the model used, the predicted values of air exchange rates due to infiltration introduce some inaccuracies to the overall building model.

The TRNSYS Type 19 zone model utilises the following equation to calculate the ventilation flow rate from infiltration based on a model given in the 1981 book of ASHRAE Fundamentals:

$$\dot{m}_{infil} = \rho_{OA} \cdot V_{zone} \cdot (K_1 + K_2 \cdot (T_{OA} - T_Z) + K_3 \cdot V_w), \quad (3.14)$$

where K_1, K_2, and K_3 are empirical constants. For this design tool, values for the constants were initially taken based on new building construction, where special precautions are taken to prevent infiltration (K_1=0.10, K_2,= 0.011, and K_3=0.034) (Klein, et al., 2000). The predicted infiltration rates for various building configurations and locations were examined to determine if they were within the range of values expected for airtight construction as detailed in Section 5.1.3.

The infiltration experienced by a house varies depending on the type of fresh air ventilation system that is in place in the house. One recent study found that for exhaust-only ventilation, the stack effect was too small compared to the indoor under-pressure induced by the extract fan to produce an increase in the ventilation rate, and that infiltration was mainly related to wind speed (Mattsson, 2006). The same study found that for an exhaust-supply HRV type system, the stack effect was sufficient to influence ventilation rates, and that it was the wind speed that had less of an effect. The overall air change rate between the two systems was more or less the same. These results show that for exhaust-only systems, the value K_2 should be negligible and a larger K_3 value should be present, and the opposite is true for HRV type systems.

Conventional homes do not necessarily need to introduce fresh outdoor air into the space to maintain indoor air quality since they may have a sufficient amount of fresh air entering the space through infiltration; however, for airtight buildings, this may not be the case. ASHRAE *Standard 62* specifies that the minimum outside air ventilation per person for any type of space is 8 L/s (ASHRAE, 2001). This minimum rate ensures that maximum CO_2 concentrations are 0.07% of the outdoor concentration, and it satisfies the

odour perceptions of 80% or more of people. On top of the 8 L/s, 0.1 L/s of outdoor air needs to be introduced per square meter of floor space.

In the design tool model, additional outdoor air was introduced into the space to satisfy ASHRAE *Standard 62*. The flow rate was calculated at each time-step based on the following expression:

$$\dot{m}_{OA} = \text{Max}\,(0, \dot{m}_{AS\_62} - \dot{m}_{infil} - \dot{m}_{NV}). \qquad (3.15)$$

The third term in Eqn. 3.15 represents the fresh air introduced into the zone for free cooling purposes as detailed later in this chapter. Note that in reality, the infiltration rates are not known and thus, the amount of fresh air introduced to the space is not based on the actual infiltration rate. In order to precondition the outdoor air entering the building, the air exhausted from the zone to satisfy the fresh air requirements is passed through a HRV with a fixed effectiveness of 60%.

3.2.5 Windows, Overhangs, and Blinds

The building model includes windows, blinds, and overhangs. Overhangs are included in all orientations but the north, as the north orientation rarely has a problem with beam radiation (in the Northern hemisphere). Even if the lot orientation is not set at due south, other studies looking at the optimisation of overhangs have found that there is minimal need for overhangs on east and west orientations (Wang, et al, 2005). The benefits of using east and west overhangs is scrutinised later in Section 5.2. The TRNSYS Type 34 Overhang Model calculates the amount of beam and diffuse solar radiation that is incident upon the window, while taking into consideration the overhang. For the design tool, it was assumed that the overhangs were all located 0.25 m above the windows, and that they extended beyond both sides of the window by 0.1 m.

Two window models were needed to take the windows into account. The first window model provides inputs to the second window model, which is included in the Type 19 zone component models. The first window model was TRNSYS Type 35 Window with Variable Insolation using mode 2, which considers beam and diffuse radiation separately. Type 35 calculates the following parameters:

$$\dot{Q}_s = A \cdot \tau_b \cdot I_{bT} + \textit{diffuse and ground reflected}, \tag{3.16a}$$

$$\dot{Q}_t = U \cdot A \cdot (T_o - T_Z), \text{ and} \tag{3.16b}$$

$$\dot{Q}_n = \dot{Q}_s + \dot{Q}_t. \tag{3.16c}$$

Eqn. 3.16a calculates the rate of solar energy gain through the window. The effect of diffuse and ground reflected radiation is computed internally as the transmittance of beam radiation at an angle of 60°. Eqn. 3.16b calculates the rate of thermal energy transfer through the window, and Eqn. 3.16c calculates the net rate of energy transfer through the window.

The window transmittance in Type 35 is calculated internally based on the number of window panes, the extinction coefficient multiplied by the window pane thickness (*kL*), and the refractive index of each pane. For this model, it was assumed that the *kL* coefficient was constant at 0.02088 and that the refractive index was constant at 1.52 (Athienitis and Santamouris, 2002). The type of window used was then included as a parameter to be optimised in the GA Optimisation Tool. In all, four windows were initially considered as detailed in Table 3.5 (ASHRAE, 2001). All windows were assumed to be operable with wood or vinyl frames. Different low-e coatings and different frames would produce different U-values. Note that the low-e coatings would also reduce the window transmissivity but this factor is not considered in Type 35. A

wider selection of windows could be included in future versions of this tool to better consider the effects of the different window parameters.

Table 3.5: Four different windows to be considered in optimisation (ASHRAE, 2001)

Description	Number	U-Value (W/m^2K)
2-pane, 12.7 mm air cavity	1	2.87
2-pane, 12.7 mm argon cavity, 1 low-e coating of 0.1	2	2.10
3-pane, 12.7 mm argon cavities, 2 low-e coatings of 0.1	3	1.56
4-pane, 12.7 mm argon cavities, 2 low-e coatings of 0.1	4	1.48

The Type 35 window model calculates, and then sends the calculated values of total solar radiation, thermal energy, and beam solar radiation to the room to the Type 19 window model. These inputs are then used directly in the zone energy balance calculations. In the Type 19 window model, the beam radiation is treated in a rudimentary manner. The user must input how many surfaces the beam radiation is incident upon and the fraction of beam radiation that each of these surfaces receives. In the design tool, it was assumed that the incident beam radiation was incident on only two surfaces, the floor and the wall on the opposite side of the room (i.e. the north wall for the south window, etc.). The floor was given 90% of the beam radiation and the opposite wall 10%. The effect of this assumption is verified in Section 5.1.4.

In the design tool, the window areas for each wall are set through the optimisation. The areas are calculated such that the windows occupy a certain percentage of their respective wall. Only one window is placed on each wall. The window is centred, and is assumed to have the same form as the wall it occupies. The vertical positioning of the window is calculated as follows:

$$Wdw\_vertical = \frac{2}{3} \cdot (Wall\_Height - Wdw\_Height). \quad (3.17)$$

In passive solar buildings, roller blinds and Venetian blinds can play an important part in controlling the amount of solar radiation entering a window in order to help prevent overheating. In the design tool, roller blinds that allow some diffuse solar radiation penetration were considered. Venetian blinds introduce more complexity since they can allow a portion of the beam radiation to be transmitted and redirected based on the angle of the blind position. Adding Venetian blinds to the design tool could be done in the future, but is beyond the scope of the present work. The outputs of the Type 35 window model are modified as follows before they are passed on as inputs to the Type 19 window model to take into consideration the effects of the blind, when the blind is in use:

$$\dot{Q}_{s,blind} = \tau_{blind} \cdot \dot{Q}_s, \quad (3.18a)$$

$$\dot{Q}_{b,blind} = 0, \text{ and} \quad (3.18b)$$

$$\dot{Q}_{t,blind} = \dot{Q}_t + \alpha_{blind} \cdot \dot{Q}_s. \quad (3.18c)$$

Eqn. 3.18a calculates a new value of the solar radiation through the window by multiplying the total solar radiation through the window by the transmittance of the blind. Eqn. 3.18b ensures that all of the solar radiation calculated in Eqn. 3.18a is diffuse radiation. Finally, Eqn. 3.18c adds the amount of solar energy that is absorbed by the blind to the heat transfer to the room. Note that this approach does not consider the effects of the radiation inter-reflected between the blind and the window. In addition, the effective U-value of the window changes if the blind is down; however, this effect was not considered in this thesis. Eqns. 3.18a-c are only applicable to roller blinds installed on the inside of the zone. If they were attached outside the zone, then it is the inputs to

the Type 35 window model that would need to be modified. Attaching the blinds outside would reduce the heat load to the zone from the windows. Since the most common approach is to install the blinds inside the room, this was the only method considered. Future upgrades to the tool could add the choice of placing the blinds inside or outside the zone. It was assumed that the blind used had a transmittance of 20% and an absorptance of 30%. The effect of this assumption is verified in Section 5.3.4.

There are several ways that the roller blinds can be controlled. In office settings, blinds are often used to reduce glare. In the design tool, glare considerations were not taken into account. The blinds' primary purpose was to limit over-heating. It was assumed that the blinds were motorized and controlled based on zone temperature setpoints. In the heating season, the blinds were utilised when:

$$T_Z \geq H95h - \Delta 2_h, \tag{3.19a}$$

whereas in the cooling season, the blinds were utilised when:

$$T_Z \geq H95c - \Delta 2_c \tag{3.19b}$$

where the terms $H95_h$, $H95_c$, $\Delta 2_h$, and $\Delta 2_c$ are described later in the next sub-section.

3.2.6 Heating and Cooling Control Strategy

There are countless HVAC control strategies that can be used to try to maintain the thermal comfort of a space given specified user inputs. In fact, a whole research project could be devoted to the optimisation of control strategies for a specific house and system. The objective of this research was not to implement optimisation of the control strategy. Instead one control strategy was implemented for all eight systems that would allow for adjustable setpoints based on comfort requirements, and would allow for the temperature in the room to fluctuate in order to maximise passive solar heating. Two different control

periods were considered, one for the heating season, from October 15th to April 15th, and the other for the cooling season, from April 16th to October 14th. In reality, the length of the heating season depends on the house design and local weather. A change to the set heating season could be part of optimising the control strategy in later stages of design.

Different setpoints were used based on a high and low 95% limit specified for the heating and cooling season. In the heating season, the heating system turns on ($T_{H,on}$) when the zone indoor air temperature reaches the low 95% limit plus a predetermined $\Delta 1_h$ temperature difference. The heating then turns off ($T_{H,off}$) once the temperature increases by the heating deadband (db_h) temperature difference. In passive solar design, there is a chance of overheating even in the winter, due to excessive solar radiation entering through large south-facing windows. In order to limit the chances of overheating, outdoor air (OA) is introduced into the zone once the indoor air temperature reaches the high 95% ($H95_h$) limit minus a predetermined $\Delta 2_h$ temperature difference through an on/off control. Figure 3.8 shows a fictitious temperature plot following the described heating control strategy. As shown, the temperature drops until it reaches $T_{H,on}$ and overshoots a little, hence the use of $\Delta 1_h$ to limit the temperature from reaching the low 95% ($L95_h$) limit too often. The temperature oscillates once around the deadband and then increases once the sun starts to shine until the OA ventilation is turned on. The effect of using different values of $\Delta 1_h$, $\Delta 2_h$ and db_h is examined in Section 6.6.

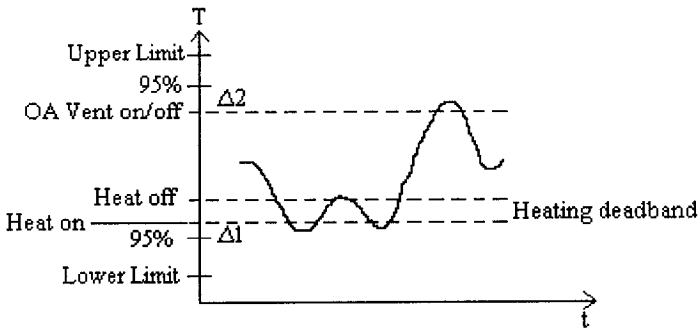

Figure 3.8: Diagram of heating control strategy

In the cooling season, if a cooling system was included in the design, it turns on ($T_{C,on}$) when the indoor air temperature reaches the high 95% ($H95_c$) limit minus a specified $\Delta 1_c$ temperature difference. Two rates of OA ventilation were considered. If no cooling system is included, the upper OA ventilation rate turns on instead of a cooling system. The cooling, or upper OA ventilation rate, turns off once the temperature decreases by the cooling deadband (db_c) temperature difference. Note that in all cases, OA ventilation only occurs provided that

$$(T_Z - T_{OA}) \geq 1^\circ C . \qquad (3.20)$$

The lower OA ventilation rate turns on when the zone's indoor air temperature reaches the $H95_c$ limit minus a predetermined $\Delta 2_c$ temperature difference. The lower OA ventilation turns off when $T_{C,on}$ is reached.

The lower OA ventilation rate was set at 3 ach, and the upper OA ventilation rate, used when there is no cooling system, was set at 6 ach. These values are less than the 10 ach recommended in (CMHC, 1998) since it was assumed that super-insulated houses would require less cooling. Further study would be required to optimise the natural ventilation strategies, which could change the set flow rates or call for a variable speed

fan that would allow for the volume to vary based on the cooling potential of the outdoor air compared to the cooling requirements of the house. It was assumed that the 3 ach could be achieved through passive measures, and would therefore not result in any electricity consumption for a fan. The use of a fan was modelled to supply the upper ventilation rate. It was assumed that the GA Optimisation Tool would be used for houses between 100 m^2 and 300 m^2 in floor area; at 6 ach this translates to airflow rates between approximately 0.33 m^3/s and 1 m^3/s (700 cfm and 2,100 cfm). Given the wide range in possible airflows, different fan sizes would most likely be used depending on the size of the house. For the model, the power consumption was calculated assuming a forward-curved blade fan with a 23 cm (9 in) wheel diameter and a 660 cm^2 (0.71 ft^2) outlet with static pressure of ¾ in wg (McQuiston, et al, 2005). At 0.6 m^3/s, the fan turns at 1100 rpm, and consumes 254 W. Fan laws were applied to calculate the power consumption of the fan at the various flow rates as follows:

$$\dot{W} = 254 \cdot \left(\frac{Flow}{0.6\, m^3/s} \right)^3 \cdot watt\,. \tag{3.21}$$

In the case of unseasonably cold temperatures and low available solar radiation, heating is available in the cooling season and turns on ($T_{H,on/off}$) when the zone's indoor air temperature reaches the low 95% ($L95_c$) limit plus a predetermined $\Delta 3_c$ temperature difference. The heating in the cooling season is controlled through on/off control.

Figure 3.9 shows a fictitious temperature plot following the described cooling control strategy. As can be seen, the temperature drops until it reaches $T_{H,on/off}$ and oscillates once until it starts to increase. Once the temperature reaches the low ventilation rate it stabilises until it starts to increase again, at which point cooling (or high OA ventilation

rate) is turned on to lower the temperature. The effect of using different values of $\Delta 1_c$, $\Delta 2_c$, $\Delta 3_c$ and db_c is examined in Section 6.6. Since the control strategies for the radiant heating and cooling are based on zone air temperatures alone, this may cause overheating of the floor in the winter and condensation in the summer. The analysis will verify how these heating and cooling control strategies compare between air-based and radiant-based heating systems.

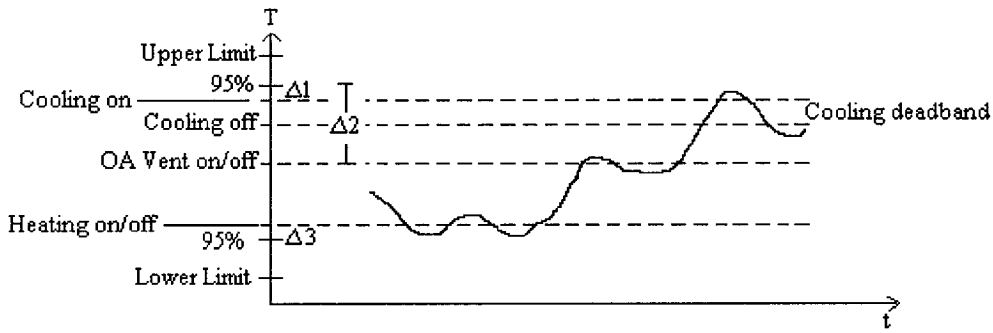

Figure 3.9: Diagram of cooling control strategy

3.2.7 Heating and Cooling System Selection

It may not always make economic sense to install a ground source heat pump when other energy efficiency and passive solar measures can lower the annual heating load substantially. The GA Optimisation Tool considers eight different heating systems in its optimisation process. The system types vary between air-based systems and radiant floor heating systems, and range from simple electric heaters, to ground source heat pumps. In order to limit the number of systems in consideration, only one capacity of each system type was considered and the same control strategy was used for each system. In future versions of the tool, various sizes of the same system could be considered or possibly the same system could be varied using different control strategies. As detailed further in this section, the performance data needed in TRNSYS to run the simulation was selected from

existing high efficiency products. The products were selected from an Internet search identifying products that had the required data for modelling purposes in their technical specifications. The selection of a given product is not to be considered as an endorsement of the product. It was assumed that the selected product was representative of the performance of a given system type across various high efficiency products. In the future, different products of the same system type using actual cost data could be considered. The eight different heating systems under consideration are as follows:

1. Air system with electric heater,
2. Hydronic system with solar thermal and electric heater,
3. Air-to-air heat pump system,
4. Ground source heat pump using an air system,
5. Ground source heat pump using a hydronic floor heating system,
6. Water-to-air heat pump using solar thermal heat source and a desuperheater,
7. Water-to-water heat pump using solar thermal heat source, and
8. Water-to-air heat pump using solar thermal heat source.

For cooling, the optimisation only considered whether there was a cooling system in place or not. It may be possible to maintain comfort conditions without a cooling system if good passive solar design approaches and natural ventilation measures are included. Different cooling system types were implemented depending on the given heating system. It would not make sense to install a separate cooling system when a ground source heat pump or air source heat pump was specified for heating. Therefore, if a heat pump was present for heating and could be utilised for cooling, then when cooling was selected the heat pump functioned for both heating and cooling. If there were no heat

pumps present, then an efficient central air conditioner was used as detailed later in this section. A cooling system was included in all eight TRNSYS models; however, when no cooling system was called for, the control setpoint was set to zero.

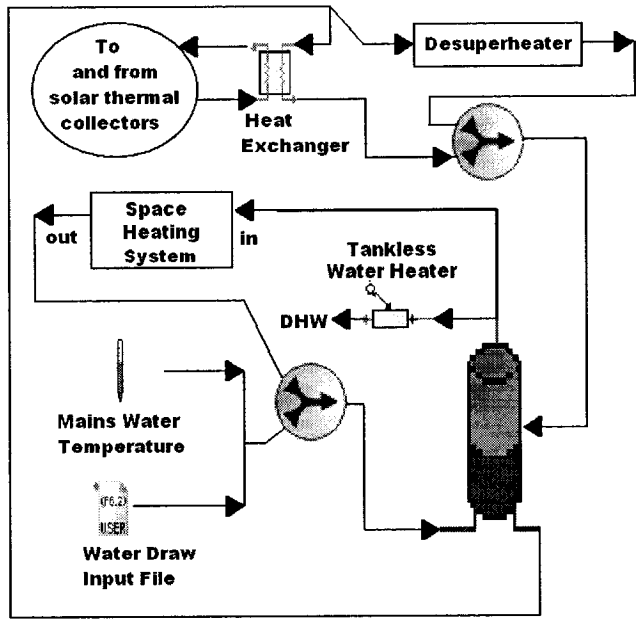

Figure 3.10: Revised Figure 3.6 to account for space heating and desuperheaters

For the systems that either take heat from the solar thermal storage tank or supply heat to it as in the case of the heat pump desuperheaters, the configuration of the solar thermal tank was slightly changed as depicted in Figure 3.10. The water to the desuperheater comes from the same tank outlet as the water going to the solar thermal heat exchanger and the heated water returns to the same inlet as the water exiting the solar thermal heat exchanger. As for space heating, the water comes from the same outlet as that going to the DHW tankless heater and after the heat is extracted for space heating purposes, it returns to the tank at the same inlet as the water coming from the water mains. The modelled system uses the same source of water for both the floor heating and for domestic hot water. With this type of configuration, special care must be taken not to

use stagnant water for the floor heating system as a source for the DHW tank. This can be accomplished by plumbing the system such that any fresh water needs to run through the floor system (Radiant Floor Company, 2007). In the future, an optimisation analysis could be done to determine the most appropriate place to have each of the inlets and outlets to ensure good tank stratification, maximising the solar fraction.

System 1: Air based system with electric heater and central AC

Heating for system 1 was based on a simple electric air heater modelled with the TRNSYS auxiliary heater Type 6. A total capacity of 10 kW with an efficiency of 99% was assumed. The airflow rate was set at 1,428 kg/hr (~700 cfm) with a setpoint of 60°C. Cooling was provided by the 2 Ton York Affinity R-410A Split System Air Conditioner rated at seasonal energy efficiency ratio (SEER) of 15. The input files used for this unit are shown in Appendix B (York, 2006). The air conditioner was modelled using TRNSYS Type 756 developed by (TESS, 2006). The flow rate through the evaporator was set at 1,428 kg/hr (~700 cfm), which corresponds to the unit's second stage of operation. The performance data from the unit was provided for only one indoor dry bulb temperature (26.7°C) but with a number of airflow rates, outdoor dry bulb temperatures and indoor wet bulb temperatures. Type 756 then extrapolates to obtain the performance at other conditions. Data was provided at indoor temperature of 23.89°C, but at only one dry bulb temperature, which was not enough to be included in the input performance data. Note that the air for both the heating and cooling system was set at 100% return air from the zone since the fresh air was delivered directly to the room, as in the other systems.

System 2: Under-floor radiant heating system with electric heater and central AC

System 2 draws water from the solar thermal storage tank and uses an electric tankless heater to boost the temperature to a setpoint of 45°C before it is circulated in the under-floor heating system. Model 240 water heater from (e-tankless, 2006) was chosen which has a total capacity of 24 kW and operates at an efficiency of 98.5% with specifications for this unit shown in Appendix B. Note that the hydronic system was sized at a larger capacity than the air-based system in order to be able to meet the temperature setpoints for a variety of different conditions. The flow rate going through the heater was set at 0.19 L/s (3 gpm). The same air conditioning unit used in system 1 was used for cooling in system 2.

System 3: Air-to-air heat pump

The performance data for the air-source heat pump was taken from a York 2 Ton Affinity R410-A Split-System Heat pump with a SEER rating of 15 (York, 2006). The heating and cooling input files for this unit can be found in Appendix B. The heat pump was modelled using TRNSYS Type 665 model developed by (TESS, 2006). This model uses a constant airflow rate across the indoor coil. For the simulation, the flow rate was set at 330 L/s (700 cfm), which represents the lower operating range of stage 2 of the selected heat pump. The air supplied to the room was 100% return air from the zone since the fresh air was delivered directly to the room without passing through the heat pump, as with the other systems. The cooling data required in TRNSYS includes the performance of the system at a minimum of two indoor dry bulb temperatures, each with performance data at various wet bulb temperatures. The performance at 26.7°C was given for 4 different wet bulb temperatures; however, the performance at 23.9°C was only

given at 1 wet bulb temperature. In order to satisfy the data requirements, the performance at 23.9°C was extrapolated from the one data point provided such that its performance curve matched the performance curve for 26.7°C but offset by the same amount as for the one data point provided.

Air-source heat pumps work well at moderate temperatures. At very cold temperatures, the COP approaches unity and back-up electric heaters are needed to help maintain the setpoint. For the given unit running at 330 L/s (700 cfm) with an outdoor air temperature of −12.2°C and an indoor temperature of 21.1°C, the COP is rated at 1.9. Assuming that at colder temperatures, the unit would drop to a COP of 1, then the heating output would be in the range of 2 kW. This would typically not be enough to meet the heating needs. Type 665 allows for two stages of auxiliary heating. In order to match the total capacity set for the heater in system 1 (10 kW), two 4 kW auxiliary heaters were implemented. The control strategy was modified slightly in order to implement the auxiliary heaters. The heat pump heating starts when the zone indoor air temperature reaches the low 95% limit plus ($\Delta 1_h$ + 1°C) temperature difference, auxiliary 1 at plus $\Delta 1_h$ and auxiliary 2 at plus ($\Delta 1_h$ −1°C). Each heating component turns off once the zone temperature increases by db_h.

System 4: Ground source heat pump using an air system

The performance data for the ground-source heat pump was taken from a Next Energy 2 Ton Tranquility 27 TT series (NextEnergy, 2006). The heating and cooling input files for this unit can be found in Appendix B. The heat pump was modelled using TRNSYS Type 505 developed by (TESS, 2006). The given model uses a constant air flow rate across the indoor coil. For the simulation, a flow rate of 378 L/s (800 cfm) was

set, which represents the lower operating range of stage 2 of the selected heat pump. The performance data for the selected unit was given at both part load and full load operation. In the Type 505 model, either full load or part load data can be entered. Since the unit was already selected with a low capacity, the full load data was used. The flow rate through the ground heat exchanger was set at 1,400 kg/hr which is the middle value given in its performance data. The performance data uses cooling correction factors to account for different entering air wet bulb and dry bulb temperatures. A correction factor of 1.7 was used for situations when the cooling output was 100% sensible, as this boosts the sensible fraction to over 100% for all conditions, which TRNSYS corrects by setting the sensible fraction at 100%.

Type 505 also works with the option of using an auxiliary heater. For system 4, one 5 kW auxiliary heater was implemented to help maintain the desired setpoint. The control strategy was modified slightly in order to implement the auxiliary heaters. The heat pump heating starts when the zone indoor air temperature reaches the low 95% limit plus ($\Delta 1_h$ + 1°C) temperature difference and the auxiliary heating starts at plus ($\Delta 1_h$ – 1°C). Each heating component is turned off once the zone temperature increases by db_h.

System 5: Ground source heat pump, under-floor radiant heating system

The performance data for the water-to-water heat pump was based on the Trane 2 Ton water-to-water heat pump, model number WSHP-PRC009-EN (Trane, 2006). The heating and cooling input files for this unit can be found in Appendix B. The heat pump was modelled using the TRNSYS Type 668 model developed by (TESS, 2006). The heating and cooling data was entered based on a load flow rate of 0.24 L/s (3.8 gpm), and a source flow rate of 0.44 L/s (7 gpm). Type 668 allows the variation of the load and

source flow rates; however, there can only be one flow rate in the performance data that is entered in the model. Therefore, in order to match the performance data, the load and source flow rates were kept constant. The Type 668 heat pump model does not have any auxiliary heating capacity like the other heat pump models. In order to match the capacity of the systems, a 5 kW auxiliary heater was added using the same control strategy as for system 4.

The ground-source heat pump can be used for cooling purposes. However, in order to take advantage of the ground heat sink, 0.24 L/s (3.8 gpm) was set to circulate through the under-floor radiant system directly from the borehole, bypassing the heat pump. In this arrangement, the only cooling energy that is consumed is from the circulating pump.

System 6: Water-to-air heat pump using solar thermal and a desuperheater

The same heat pump used in system 4 was used in system 6, with the exception of adding a desuperheater for the heat pump. The desuperheater was set to run at a flow rate of 400 kg/hr. The major difference between system 4 and system 6 is that the system was connected to the solar thermal storage tank, as opposed to a ground heat exchanger. Since there was already a solar thermal system in place, it could make economic sense to use the heat from this system as opposed to having to drill boreholes. In order to ensure that the storage tank did not freeze, its electric heating element, situated in the 9^{th} node, was set to maintain a minimum temperature of 8°C with a 4°C deadband. The heat output of this element was added to the calculated total zone heating energy. The water from the solar thermal storage tank was also used for cooling. It is not ideal to use hot water for a heat pump for cooling; however, this is what was implemented. The efficiency of a heat pump drops with increasing input temperature, but it was decided that it would not make

economic sense to include a separate cooling system when a heat pump was already in place. The performance data from the heat pump was given up to entering liquid temperature of 48.8°C. For higher temperatures, the heat pump model extrapolated the performance data. Note that even though the cooling performance dropped at higher temperatures, the use of the tank for cooling helps increase the tank temperature, which reduces the DHW load. However, there may be cases when the temperatures become too elevated, which may require a heat dump.

System 7: Water-to-water heat pump using solar thermal

The same heat pump used in system 5 was used in system 7. As was done in system 6, the solar thermal storage tank was used as opposed to the ground heat exchanger for both heating and cooling.

System 8: Water-to-air heat pump using solar thermal

System 8 is identical to system 6 with the exception that the desuperheater option was not used.

Systems 1 through 8 represent 8 discrete heating systems. In theory, there could be various different configurations of the same system implemented. For example, the use of different heating and cooling capacities will produce different results both in terms of performance and costs. The capacity of the system was taken based on what a typical low energy house would require. In the later design stages, it would be important to revisit the exact capacity and control strategy. The required heating capacity would be different in Victoria than in Iqaluit even though the same systems were used for this tool. Another factor that will need to be addressed in the later design stages relates to staged

capacity. A single stage 2-ton system will not perform the same as a 2 or 3 stage system of the same total capacity. Eight discrete heating systems were used in an effort to give the user a good indication of what system would be the most cost-effective for a given situation. The results should offer valuable guidance in the final product selection.

3.2.8 Ground Heat Exchanger

Systems 4 and 5 used a vertical loop ground heat exchanger, modelled using the TRNSYS Type 557 model developed by (TESS, 2006). Sizing a borehole is highly dependent on soil type, which varies significantly from one region to the next. The RETScreen ground source heat pump model version 3.0 (RETScreen International, 2007) was used to verify the effect of soil type on recommended borehole length for a closed-loop system. The program was used assuming a 5 kW peak heating load, a standard ground heat exchanger layout, a high efficiency heat pump system, and a mean earth temperature of 9°C with a yearly amplitude of 14°C. Table 3.6 shows possible variations in borehole length depending on soil type.

Table 3.6: Variation in RETScreen-calculated borehole length by soil type

Soil Type	Conductivity (W/m·°C)	Density (kg/m^3)	Heat Capacity (kJ/kg·°C)	Borehole length (m)
Light soil - damp	0.9	1,600	1.05	196
Light soil - dry	0.3	1,400	0.84	428
Heavy soil - damp	1.3	2,100	0.96	141
Heavy soil - dry	0.9	2,000	0.84	196
Light rock	2.4	2,800	0.84	90
Heavy rock	3.5	3,200	0.84	70
Permafrost light	1.4	1,580	0.76	137
Permafrost dense	2.0	2,070	0.69	99

For the design tool, soil conditions for the damp heavy soil were used, which resulted in the use of two 70 m deep boreholes in series. The default parameters of Type 557 are based on heavy soil conditions. Except for the borehole reference flow rate which was set based on the selected heat pumps, and the fluid specific heat and density which were set to the values for glycol, all other parameters are set to Type 557 default values.

3.2.9 Inputs, Constants, and Optimised Variables

When setting up the model, a distinction needed to be made between which parameters would be allowed to be varied by the user as inputs, which values would be fixed, and which variables would be optimised.

Inputs: The objective of developing this optimisation tool was to provide assistance in the early design stages when little is known about the design. The following would be the only inputs a user would need to run the program:

- Area: The desired area of the residence.
- Number of Stories: The option between a one and two storey home.
- Orientation: The default orientation was set as south-facing; however, the orientation was set as an input for cases where a user would already have a specific property in mind that has restrictions with regards to orientation. In the future, orientation could be added as a variable to optimise since the introduction of time of day pricing could change the optimal orientation (Rowlands, 2005).
- Minimum Energy Target: The goal of this research was to develop the concept of a tool that could lead designers to achieve the net-zero energy consumption target; however, to make the tool more generic, the total yearly net-energy consumption of the building was set as an input in the program.

- Control Temperature Setpoints: Since optimal designs would vary based on how large of a temperature swing the future occupants are willing to tolerate, the user was given the ability to vary the control temperature setpoints.
- Electricity costs: Since the optimisation tool aims to reduce costs, it was required to allow for the input of both the cost of electricity and the rate at which electricity will be sold back to the grid. The flexibility to input two different rates based on the time of day was provided. In addition, an electricity cost escalator was included in order to better compare the average cost of purchased and generated electricity.
- Mortgage Details: The added cost of utilising more efficient technologies, solar thermal and PV was amortised over the life of the mortgage. Therefore, there is a monthly cost associated with these measures. The inclusion of a mortgage cost allows for a better comparison between the costs of reducing energy requirements through energy efficiency and renewable energy measures and the cost of purchasing more energy.
- Location: The desired location of the project is required in order to utilise the correct weather data.

Constants: There are certain parameters that were kept constant within this research project in order to reduce the scope of the problem. In the future, once the benefits of the GA Optimisation Tool have been demonstrated, some of the constants could be either moved to inputs, or added to the optimisation variables.

- House Type: The house model was limited to a single zone. In order to facilitate the modelling, if the house is a two-storey house, the two floors were combined to maintain a total of one zone.
- Rectangular Shape: As a general rule, a rectangular floor plan works best for passive solar design (Chiras, 2002). There has been some work done on the optimisation of shape using GAs (Coley and Schukat, 2002, Marks, 1997, Caldas, 2001, Wang, et al., 2006). Only a rectangular zone shape was considered in this analysis. One study that considered an 'L' shape in the optimisation had results that converged to a rectangular shape; this is because a rectangular shape has a more compact floor plan with less area for external walls, which reduces the initial construction cost, the environmental impacts due to material production and construction, and the operating energy consumption (Wang, et al., 2005). An L-shape could be optimal if floor layout patterns and minimum room sizes based on architectural and functional considerations were included. Other possible shapes can be considered in future versions of this tool, since the same authors demonstrated that different polygon shaped zones could offer some advantages (Wang, et al., 2006). The length to width ratio of the house was one of the parameters optimised.
- HRV: A 60% efficient heat recovery ventilator was included in all cases.
- Floor Height: A standard floor height of 2.44 m (8 feet) was used. This parameter can easily be added as an input to the program, if users desire.
- Control Strategies: The same control strategy was used in all cases. The results from the use of the same control strategy for both air-based and radiant-based

heating systems are analysed in Section 5.1.6. Various control strategies could have been considered for the optimisation; however, this would have significantly increased the solution space. This tool would be used in the preliminary design stages in order to help in the design of the building itself and in the selection of the equipment. Once the design and equipment are selected, then a second optimisation tool could be used to optimise the operation of the equipment by varying control strategies and variables.

- Airtightness: Airtightness in the house was initially set at levels found for airtight construction.
- Photovoltaic Panels: No parameters of the PV panels were directly optimised. The type and size of the required PV panels were calculated based on the results of the generation of a 1 kWp array. The PV panels were modelled using the TRNSYS Type 94a. The total PV system size (kWp) was calculated in order to reach the energy use target specified by the user. In the case of ZESH, the size of the panels was calculated as follows:

$$\text{kWp required} = \frac{\text{Total consumed electricity}}{\text{Total electricity generated per kW}} \cdot \text{kWp}. \qquad (3.22)$$

The modelling inputs used for the PV panels were based on the Shell Module SQ160-PC as shown in Appendix B (JATS Alternative Power Company, 2005). A total of six 160 W modules were used in parallel in the model. All PV panels were assumed mounted on the south-facing roof. In reality, the PV panels could be mounted in locations other than a south-facing roof, such as the façade or as overhangs. In addition, the implementation of heat recovery from the PV panels to form a PV/Thermal (PV/T) product could also bring some advantages.

Unfortunately, the GA Optimisation Tool developed was based on existing building integrated PV technologies. PV/T technologies are in their infancy, and it would be difficult to include them as an option without knowing their true cost and performance. In an attempt to reduce the number of optimisation parameters, façade integration was not included. This assumption was based on the fact that this approach is seldom used. PV overhangs were not included, as overhangs would generally not provide adequate area to generate enough electricity to achieve the net-zero energy target. Therefore, overhangs would have to be added in conjunction with roof integrated PV in a future version.

Optimised Design Variables: Houses can be constructed with various configurations, with different technologies, and with a wide range of costs, which made it difficult to narrow the scope of variables that were optimised. Table 3.7 provides a summary of the variables optimised in this research. Note that the values in Table 3.7 were the values used at the initial stages of the research. Some parameters were removed and the allowable range and step-size modified in Section 5.2 based on the results of a sensitivity analysis. The number of parameters, their range, and their step-size were limited in order to try to minimise the size of the solution space; the solution space was still quite large at over 137 billion possible solutions, but was over 1.3 million times smaller than the one used in (Wetter and Wright, 2004). The shear size of the solution space introduces doubt as to whether the most optimum solution is reached; however, this doubt is even more pronounced with the use of traditional trial and error approach to the optimisation.

Table 3.7: Summary of optimised variables

	Type of Parameter	Parameter	Minimum Value	Maximum Value	Total #
1	Building Form	Length/width	1	2	8
2	Building Envelope	Window type	1	4	4
3		N window area	5%	20%	4
4		E window area	5%	20%	4
5		S window area	10%	80%	8
6		W window area	5%	20%	4
7		E overhang	0 m	1.26 m	4
8		S overhang	0 m	1.26 m	4
9		W overhang	0 m	1.26 m	4
10		Wall construction			8
11		Thermal mass			4
12		Roof slope	Flat	21 in 12	8
13	HVAC System	Heating system			8
14		Cooling system			2
15	Solar Systems	Thermal collector type	Flat plate	Evac. tube	2
16		Thermal collector area	3 m^2	12 m^2	4
17		Storage tank size	250 L	681 L	4

The description of the parameters considered and their allowable ranges is described below:

Form (Length/Width): According to Chiras (2002), the ideal length to width ratio for passive solar design is 1.3 to 1.5. In the initial stages of the design tool, a range from 1.0 to 2.0 was used. In reality, this parameter would be limited to the lot size and shape, and would also be influenced by other factors such as daylight penetration into the space and in the desired interior room layout.

Window Type: There are various window types (double-, triple-, quadruple-glazed) that can be used, varying in costs, U-value, and solar heat gain coefficient (SHGC). The four window types listed in Table 3.5 were used.

Window Area: The optimum window area varies depending on orientation, total thermal mass in the building, window shading, etc. Large windows can lose a lot of heat in the winter and allow too much heat gain in the summer.

Window Overhang: In general, the use of overhangs is an inexpensive way to reduce cooling loads in the summer, without losing too much heat gain in the winter. Overhangs were considered in all but north-facing windows.

Wall Construction: In the early nineties, typical exterior wall construction on the east and west coast of Canada comprised of standard 51 mm x 102 mm (2" x 4") construction with RSI 2.11 (R12) insulation, whereas in Manitoba, Saskatchewan, Alberta and the north 51 mm x 152 mm (2" x 6") construction with RSI 3.52 (R20) insulation was more common (Prowskiw, 1992). Replacing the exterior fiberboard sheathing with an exterior insulating sheathing is a good way to increase the thermal efficiency of these standard walls, which are still very common today. In addition, new wall types have emerged that can be used as an alternative to the standard stick frame construction. For this study, eight different wall configurations were implemented with varying insulation using the standard 51 mm x 152 mm (2" x 6") stick frame, insulated concrete forms (ICF), and structural insulated panels (SIP). The desired walls were not included in the ASHRAE wall types provided in TRNSYS; therefore, the transfer functions for each wall were calculated using the PREP program that comes with TRNSYS. Each wall was composed

of siding, an air gap, the part of the wall as described below, followed by an interior layer of gypsum board:

Wall 1: Standard 51 mm x 152 mm (2" x 6") construction with fiberboard exterior sheathing- RSI 3.96 (R22.5),

Wall 2: Standard 51 mm x 152 mm (2" x 6") construction with 5 mm (2") of insulating exterior sheathing - RSI 5.20 (R29.5),

Wall 3: ICF wall with 64 mm (2.5") EPS on both sides and 15 mm (6") concrete core - RSI 4.91 (R27.9),

Wall 4: ICF wall with 100 mm (4") EPS on both sides and 15 mm (6") concrete core - RSI 6.83 (R38.8),

Wall 5: ICF wall with 100 mm (4") EPS on both sides and 20 mm (8") concrete core - RSI 7.13 (R40.5),

Wall 6: SIP wall with 89 mm (3.5") EPS - RSI 3.18 (R18.1),

Wall 7: SIP wall with 190 mm (7.5") EPS - RSI 5.87 (R33.3), and

Wall 8: SIP wall with 292 mm (11.5) EPS - RSI 8.59 (R48.8).

Thermal Mass: A major issue in passive solar design is the inclusion of the right amount of thermal mass. Four different levels of thermal mass were considered as part of the optimisation parameters, which include:

Mass 1: No additional thermal mass.

Mass 2: Increasing the floor thickness from 10 cm to 20 cm.

Mass 3: An additional brick layer added on the inside of the exterior wall before the gypsum board layer. Material C4 in Table 4.8.3.5 of the TRNSYS manual was chosen (Klein, et al., 2000), which represents 100 mm of common brick.

Mass 4: A combination of mass options 2 and 3.

Heating System: Eight different heating systems were considered initially:

System 1: Air system with electric heater,

System 2: Hydronic system with solar thermal and electric heater,

System 3: Air-to-air system,

System 4: Ground source heat pump, air system,

System 5: Ground source heat pump, hydronic system,

System 6: Water-to-air heat pump using solar thermal and desuperheater,

System 7: Water-to-water heat pump using solar thermal, and

System 8: Water-to-air heat pump using solar thermal.

Cooling System: Two options were made available for cooling:

Option 1: No mechanical cooling provided.

Option 2: Mechanical cooling that utilised the heating system's heat pump, if it existed, or a regularly sized efficient air conditioning system.

Thermal Collector Type: Both flat plate and evacuated tube solar thermal collectors were included.

Thermal Collector Area: Four sizes of solar thermal collectors were considered with the assumption that 1 to 4 panels would be used with a standard size of 3 m^2 (4' x 8'). In general, the expected range of collector area is 4 m^2 to 8 m^2 for DHW systems and 10 m^2 to 30 m^2 for combisystems (Weiss et al. 2003). The range covered in the optimisation (3-12 m^2) represented the range of expected sizes for DHW systems, and only touched

the lower end of the range for combisystems. The allowable solar collector area and thermal storage volume is revisited in the results analysis of Section 5.2.

Thermal Storage Volume: Four sizes of solar thermal storage tanks were included: 250 L, 303 L, 454 L, and 681 L (66 gal, 80 gal, 120 gal, and 180 gal). The tanks were assumed to have a diameter of 0.7 m, which was chosen to limit the height of the tank to under 2 m when the 681 L tank was used. With the exception of the 681 L tank, the tank sizes are standard water tank sizes as listed in (RS Means, 2005a). The 681 L tank was selected in order to have a larger tank available for situations where more thermal storage may be called for. The range used for the solar collector area and thermal storage volume is revisited in the results analysis of Section 5.2.

3.3 Genetic Algorithm Program

There is an abundance of literature on various optimisation concepts using GAs (Beasley, et al., 1993, Mitchell, 1998). The basic idea is that anlgorithm mimics Darwinian theory of survival of the fittest. By mimicking this process, GAs are able to evolve solutions to real world problems. The basic process starts with the random generation of a population of individuals, each representing a possible solution to the problem. Each individual is then assessed and assigned a particular fitness score with higher scores representing better designs. These individuals are then given a chance to reproduce by crossbreeding with fitter individuals who have a higher probability of mating. There are some key mechanisms that are included within the process such as random mutations, different processes to select which individuals should mate, and different ways of recombining individuals that that can change the characteristics of a

given GA program. Generally, each parameter that is optimised is assigned a binary number and each binary number is put together to form one long binary string, or chromosome. The GA program being used for this tool (Carroll, 2005) uses the mechanisms listed below.

Tournament Selection: There are various ways to select which parents will mate to form the next generation; in (Carroll, 2005) tournament selection is used. In tournament selection, two individuals are randomly chosen from the population and the fittest individual of the two is selected to mate with the fittest individual from a second randomly chosen pair.

Crossover: One of the main distinguishing features of a GA is the use of crossover (Mitchell, 1998). The program allows for the choice between single-point or uniform crossover. Single-point crossover is the simplest form, where a single crossover position is chosen at random and the parts of the two parents after the crossover position are exchanged to form two offspring as depicted in Figure 3.11. In uniform crossover, each pair of bits is swapped with a given probability. A 50% probability of bit crossover gives the greatest mixing of genetic information between paired individuals.

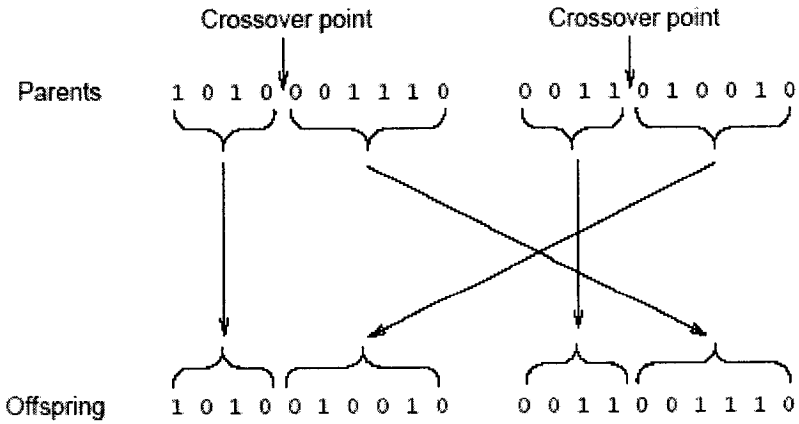

Figure 3.11 Single point cross-over (Beasley, et al., 1993)

Number of Children per Parent: The program gives the choice of either forming one or two children per set of parents.

Elitism: When elitism is used, the fittest individual from a generation is passed on to the next generation intact, preserving its genetic makeup.

Niching: Niching techniques have been developed to maintain population diversity by allowing the GA to investigate multiple peaks in parallel to prevent the GA from being trapped in local optima. The sharing method is the niching technique implemented in this GA. The basic idea is that the GA perception of the fitness function is changed in such a way that when individuals tend to concentrate around a high peak, the fitness around this point is reduced by a factor proportional to the number of individuals in the region (Imrani, et al., 1999).

Jump Mutations: Jump mutation is a traditional mutation approach in GA programs, which is applied to each child individually after crossover. Each gene has a random chance of being flipped from 0 to 1, or vice-versa, based on a small probability that the user assigns. This mutation provides a small amount of random search, and helps to ensure that no point in the search space has a zero probability of being examined.

Creep Mutations: In creep mutation, a randomly chosen parameter from the binary string is randomly increased or decreased by one step with the specific parameter being decoded, adjusted, and encoded into the string again (Loomans and Visser, 2002).

Micro-GA: A micro-GA starts with a small population (5-15) of individuals and quickly makes it converge to a solution. Convergence is measured by comparing the chromosomes of the individual solutions. If they differ by less than 5% (arbitrarily set by the program writer), it is considered that the population has converged and a new random

population is generated carrying over the individual with the best fitness from the previous generation. An advantage of using the micro-GA procedure is that the algorithm tends to perform a local search around the best solutions during the generations prior to convergence. This local search is important in finding local minima around good solutions, and is usually hard to implement in conventional GA (Caldas and Norford, 2002).

The program developer recommends using a micro-GA with a population size of five since he has had success with this setting for various problems (Carroll, 2005). One should note that when the micro-GA option is selected, the program automatically resets the jump and creep mutation probability to zero, turns on elitism, turns off niching, and only one child is generated per set of parents. Unless otherwise stated, the GA Optimisation Tool will use the recommended settings that came with the program, namely a micro-GA with a population of five and uniform crossover.

Some optimisation algorithms rely on the use of continuous variables, whereas others use discrete variables. For the GA program, discrete values are used. The lower and upper limits for a given parameter are inputs, along with the number of discrete values to use within the specified range. For many parameters, the use of discrete rather than continuous building options reflects realistic construction practices (Christensen, et al., 2005); however, there can be a combination of both. For example, there are a discrete number of window types available, whereas the overall window area is a continuous variable. The fact that only discrete values are considered is not considered a limitation since the GA Optimisation Tool looks for a range of optimal designs. If results indicate that a 30% window area is optimal, instead of 20% or 40%, the user should interpret this

as the optimal window coverage being in the range of 25% to 35%. Further refinements around specific values can be made in later stages of design. With all the limitations in accuracy that go with an early stage design tool, it would not be realistic to accurately determine the optimal window size with a single discrete value.

The GA program developed by (Carroll, 2005) did not verify whether a particular configuration had been evaluated, instead every individual in the population is evaluated at every generation. This is not a problem if the function evaluation is not computationally intensive; however, in this case, every individual that was evaluated by TRNSYS took on the order of a minute to compute. Since elitism was used, which means that the fittest individual in a generation was passed on to the next generation without change, this could have led to many unnecessary TRNSYS evaluations. To avoid these unnecessary evaluations, a new checking subroutine was implemented in order to ensure that no individual was evaluated more than once. Each design configuration was composed of 17 different parameters, each having a range of possible values. Given the large number of possible combinations, it is unlikely that the sum of the parameter values would have been repeated between different design configurations. Therefore, the sum of the parameter values of an individual up for evaluation was first taken and compared with the sums of individuals that had already been evaluated; if the sum was unique, TRNSYS was called. If the sum matched a sum that was already stored, then the parameters of the individuals with the matching sums were compared to see if the individual was in fact a repetition. If the parameters all matched, then the stored results of the matching individual were assigned to the new individual. The sums of the parameters were compared in order to save time compared to verifying each individual

parameter. One possible way to speed up the tool for a commercial release would be to store all the computed configurations in an online database that could be accessed by users such that they would not have to redo a simulation that had already been done. Unfortunately, this would only save time in situations where all the same inputs would be used.

3.3.1 Evaluating the Fitness of Design Configurations

Optimisation problems can be formulated with either a single objective function or a multi-objective function having two or more objective functions. Single objective optimisation aims at finding one global optimum solution, while multi-objective optimisation aims at finding compromises between different design objectives, such as maximising thermal comfort while minimising energy consumption in a building. Since building design involves the consideration of many different aspects including aesthetics, thermal comfort, code compliance, energy efficiency, etc., various studies have relied on multi-objective optimisation. With multi-objective optimisation, a set of global Pareto optimal solutions are found, with each Pareto optimal solution not dominated by any other solutions in the decision variable space (Wang, et al., 2005). A Pareto optimal solution has at least one objective function that is higher than the same objective function compared to other individuals in the solution space. For example, the GA Optimisation Tool could have used both the objective to minimise the annual electricity consumption and to minimise the upgrade costs in a multi-objective function. Let us compare four fictitious solutions to this problem: solution A has an annual consumption of 4,300 kWh at a cost of $60,000, solution B has a consumption of 6,700 kWh at a cost of $30,000, solution C has a consumption of 4,800 kWh at a cost of $65,000, and solution D has a

consumption of 5,500 kWh at a cost of $53,000. Of the four solutions, 3 are Pareto optimal, A, B and D, whereas C is dominated by A. This example is represented in graphical form in Figure 3.12. When analysing the results, all the points in the objective function space corresponding to Pareto optimal solutions form a Pareto front, which is useful to understand the trade-off relationship between the performance criteria as depicted in Figure 3.12.

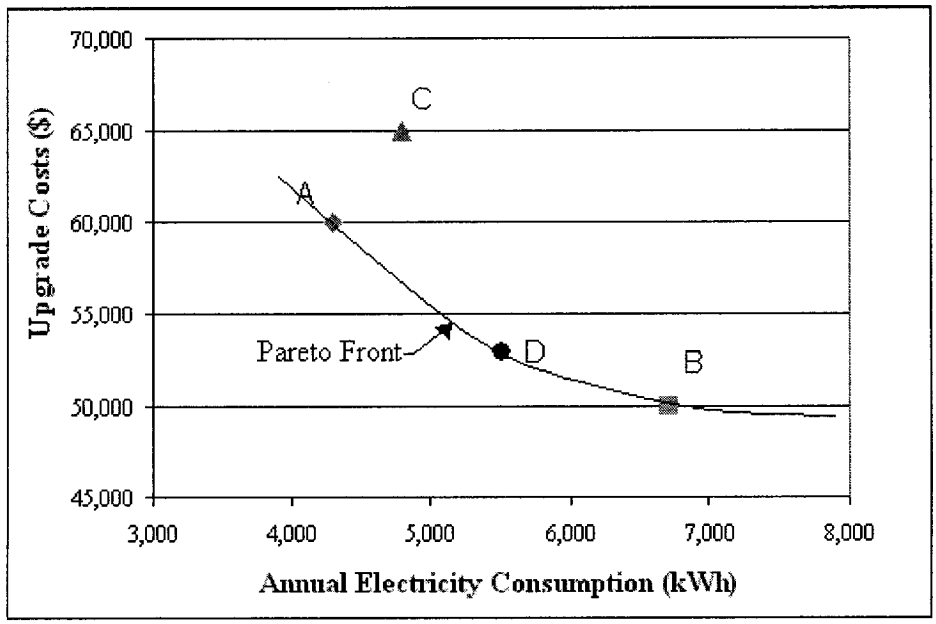

Figure 3.12: Example representation of a Pareto optimal solution and a Pareto front

There are numerous studies that have used either single or multi-objective functions for the optimisation of certain building design elements. For single criterion optimisation, end-use operating energy consumption is used in many studies, as well as life-cycle costs (Wang, et al., 2005). There is a lot of potential to use costs as an optimisation criterion. Caldas (2001) used this concept in her doctoral thesis by evaluating energy efficiency using different wall construction materials. For a building in Phoenix, the energy level reduction was 6% on average, compared to the initial

random population; however, cost reductions were in the order of 41%. In Chicago, where building envelope design is more important in terms of energy efficiency, average energy consumption levels decreased by 33% in relation to the initial random population, while costs were reduced by 68%. In order to save money, lower performing and lower costing insulation materials were used in the south wall, but the north wall remained highly insulated. Results showed that for the same energy consumption, a wide range of costs could be obtained.

In the case where the house not only consumes energy, but also generates energy, it becomes difficult to use energy consumption as an optimisation criterion. One would have to ensure that the trivial solutions of adding large solar thermal collectors and PV panels to meet the loads of an inefficient house would not be considered to have high fitness. One would have to separate the energy generation from the energy needs of the house. It would be difficult to differentiate between these factors when the solar thermal energy is used by the heating systems.

The costs of materials and equipment play an important part in determining a cost effective ZESH. For example, say that in 30 years, advances in PV make it so that their costs are reduced substantially; it may not make sense to spend a lot of money on energy efficiency if electricity could be generated at a low cost. Even at current cost levels, when the marginal costs and benefits of an investment in increased equipment efficiencies have to compete with the additional simultaneous alternative investments, maximum equipment efficiency is not always the optimal solution when looking at cost effectiveness (Carroll, 1991). Therefore, using life-cycle costs is important in

determining optimal ZESH configurations, and mechanisms to keep the costs up-to-date within the program are essential.

Under the limiting assumptions that externalities are accounted for and appropriate pricing of energy and material resources is possible, then the life-cycle cost of a building is the preferred objective function to minimise in order to achieve maximum economic efficiency. The use of incremental initial costs and incremental energy (or utility costs) savings, relative to a reference configuration offers practical advantages during computation, and intuitive advantages during interpretation of the optimisation results (Carroll, 1991). With more criteria considered in the optimisation objective function, pay-off characteristics become increasingly difficult to interpret (Wright, el al., 2002). For instance, the Pareto front goes from a line to a surface when the number of criteria is increased from two to three.

As an alternative to multiple criteria in the objective function through Pareto ranking, one can use a single objective function that lumps together multiple criteria. For instance, a cost value can be given to thermal comfort through a weighting function that tries to give good relative costs to different criteria. The usefulness of this objective weighting technique depends on the appropriate selection of weighting functions. One cannot easily assign a monetary value to interior thermal comfort, indoor air quality, and other qualitative design aspects. However, when trustworthy weights are available its use is highly recommended, since this approach reduces the size of the search space and provides adequate direction into the solution space (Alcalá et al., 2005). For an example of its application, one can look at the study done by (Alcalá et al., 2005) that optimised the fuzzy control of an HVAC system using a single objective function with vector

weights that considered the following five criteria: upper thermal comfort limit, lower thermal comfort limit, indoor air quality requirements, energy consumption, and system stability.

One of the difficulties in the use of weighting functions is that they should be user specific. For example, one building owner might be concerned with energy consumption, whereas another might place occupant comfort at a higher priority level. The advantage of the Pareto optimisation is that the user can decide which non-dominated solution to choose; however, this can only work when the user is knowledgeable on how to read and evaluate Pareto curves. For the tool developed in this research, it was decided to use a single optimisation criterion based on life-cycle costs. Due to the limited data and uncertainty related to maintenance costs, only initial costs and operating costs were considered. As described in the next section, cost penalties were used to consider thermal comfort, and to ensure that the designs had sufficient roof area to install the required PV systems and solar thermal collectors.

For the GA Optimisation Tool, the objective function represents an equivalent monthly cost based on the sum of the amortised initial incremental cost, the net energy costs, and the monthly cost penalties. In general, this value should be compared to the typical household monthly energy costs. As shown in Table 2.1, the average Canadian residence consumes 33,963 kWh of energy. If one assumes that all the energy needs are met with electricity at a rate of $0.10/kWh, this translates to a monthly cost of $283. Note that the monthly costs would vary across the different jurisdictions as the utility rates vary across the country depending on the utility. If the energy cost reductions could

equal the monthly-amortised upgrade costs, the resulting monthly cost of a ZESH would be equivalent to the monthly energy costs of a typical Canadian residence.

The objective function considers the time value of money where the user inputs the mortgage details, the incremental energy costs, and the yearly inflation rate. The advantage of a mortgage is that the money that the homeowner pays stays constant over the life of the mortgage, if interest rates are assumed constant. For example, assuming incremental costs of $500/month with a 2% annual inflation rate, in the last year of a 25-year mortgage, this would be equivalent to $308/month in the first year's dollar value. The monthly mortgage cost is calculated as follows (Kurtz, 1995):

$$Mortgage = Incremental\_Cost * \frac{\left[(1+i)^{1/12} - 1\right]}{1 - \left[(1+i)^{1/12}\right]^{-n \cdot 12}}, \tag{3.23}$$

where i is the annual interest rate and n is the mortgage period in years. The following pseudo-code loop is then used to calculate the objective function (Kurtz, 1995):

$sum1 = Cost(1); sum2 = PV(1); sum3 = Mtge(1)$ *initial year values*

Do $kk = 2, n$

$$Cost(kk) = Cost(1) \cdot \left[1 + \frac{util\_inc - \text{inflat}}{100}\right]^{kk-1}$$

$$PV(kk) = PV(1) \cdot \left[1 + \frac{sell\_inc - \text{inflat}}{100}\right]^{kk-1} \tag{3.24}$$

$$Mtge(kk) = Mtge(1) \cdot \left[1 - \frac{\text{inflat}}{100}\right]^{kk-1}$$

$sum1 = sum1 + Cost(kk); sum2 = sum2 + PV(kk); sum3 = sum3 + mtge(kk)$

End do

$$Objective\ Cost\ Function = -\frac{sum1 + sum3 - sum2}{n \cdot 12} - Monthly\ Penalties$$

Note that the negative term in the objective cost function definition was added since the GA program is trying to maximise the cost function.

3.3.2 Cost Penalties

Maintaining thermal comfort in a house is essential. The designs found with the GA Optimisation Tool could both overheat and underheat the zone over parts of the year. Overheating can often occur in buildings when solar gains are maximised and losses simultaneously minimised (Coley and Schukat, 2002). This is especially a concern in the GA Optimisation Tool for the optimal designs that do not include a mechanical cooling system. In terms of under-heating, the heating systems are modelled at a relatively low capacity that may not be sufficient to meet the heating loads of some house designs in colder climates, which would lead to uncomfortable periods.

There are various ways to evaluate thermal comfort such as the predicted mean vote (PMV) index, predicted percent dissatisfied (PPD), PMV-PPD model, adaptive models, and more (ASHRAE Fundamentals, 2001). Since different individuals experience thermal comfort at different temperature ranges, it may be beneficial to offer the GA Optimisation Tool user, a choice in setting thermal comfort requirements. Thermal comfort conditions are evaluated to ensure that the majority of occupants are comfortable. This is a good strategy to use in office buildings that have a wide range of occupants. For a house, one is not generally concerned that a wide percentage of the population is comfortable; instead the focus is on ensuring that the actual house occupants are comfortable. Women and older people tend to prefer warmer environments, since women often wear lighter clothing and older people are generally more sedentary compared to younger people (ASHRAE, 2001). In addition, different homeowners may tolerate cooler or hotter temperatures in order to achieve greater energy savings. For example, the author of this thesis maintains winter setpoints in the bedroom

at around 15°C, in the living space between 17-20°C, and in the office at 15-18°C through the use of individually controlled electric baseboard heaters. Additional layers of clothing and blankets help maintain thermal comfort at lower temperatures.

Thermal comfort can either be included as part of the fitness evaluation, or be included as a penalty. Since this study utilised a single objective function, weighting functions were needed to include thermal comfort in the fitness evaluation. The basic idea in determining a weighting function is to find a financial equivalent to thermal comfort. Such equivalences are difficult to define and there is a lack of confident data on this topic (Alcalá et al., 2005). However, Alcalá et al. (2005) did find that some weights were emerging when used for commercial buildings as recent studies showed a direct correlation between improvements in office workers' thermal comfort and indoor air quality, and productivity improvement for these workers. Based on typical salaries and a quantification of this improved productivity, such equivalences could be defined.

In residential applications, one cannot directly assign a monetary value to thermal comfort by examining improvements in productivity, unless of course there is a home-based business in the residence. Given the fact that the user was given the choice of allowable temperature ranges for design, it made it even more difficult to justify a specific monetary value for thermal comfort. This does not mean that thermal comfort should not be included in the evaluation of specific design configurations. Thermal comfort was included as a constraint to ensure a minimum level of thermal comfort set by the user of the tool.

In order for the user to be able to set the thermal comfort constraint, eight different inputs are required from the user, four for the heating and four for the cooling season. The four inputs required for both the heating and cooling seasons are:

1. Upper limit: temperature that should never be exceeded,
2. Lower limit: minimum temperature maintained at all times,
3. High 95% limit (H95): temperature should be below this setpoint a minimum of 95% of the time, and
4. Low 95 limit (L95): temperature should be above this setpoint a minimum of 95% of the time.

The high and low 95% limits were based on the CMHC (1998) recommendation that the temperature in the heating season should only go above 25°C for 4% of the heating season. Instead of setting a predetermined temperature limit, the user is given the choice as to what the temperature should not go above for more than 5% of the time, and what it should not go below for more than 5% of the time. The upper and lower limits are included to ensure that temperature extremes are avoided. If the temperature only goes above 25°C for 5% of the time, but reaches as high as 35°C during that 5% of the time, the occupant may not be satisfied. These H95 and L95 limits are the same values that were used for the heating and cooling control strategies. Therefore, if a user can tolerate a wider range of allowable temperatures, the control setpoints reflect this.

Even if the control strategies implemented should maintain temperatures within these bounds, it may happen that the heating and cooling capacities are not sufficient to maintain the specified temperature setpoints. If this occurs, the thermal comfort constraint is not met for the specific design configuration. In order to ensure that these

designs were not considered as fit in the optimisation, a high cost was given to the objective function. In summary, for every hour that the temperature exceeds the upper limit, goes lower than the lower limit, is higher than the upper 95% limit for more than 5% of the heating/cooling season, or is lower than the lower 95% limit for more than 5% of the heating/cooling seasons, a cost penalty of $5/month per uncomfortable hour over the entire year is added to the objective function. This equates to being paid $60 per year to endure every uncomfortable hour. A maximum penalty of $500/month was implemented. One must keep in mind that even though the cost value associated with uncomfortable conditions may be high, since we are using a single zone model, actual temperatures in some of the zones will be higher or lower than calculated, which would worsen the uncomfortable conditions.

In addition to the cost penalty given for uncomfortable conditions, a penalty was given to designs that do not have sufficient roof area to hold the calculated PV area plus the solar thermal collector area. A cost penalty of $10/month per square metre of missing roof area was added over the entire year to the objective function. This equates to being paid $120 per year per square metre. In practice, either specifying more efficient PV or solar thermal panels that generate more energy per square metre, or by placing the solar technologies on other support structures other than the roof of the house could deal with a situation where the roof area does not fit. Note that the size of the PV system is calculated based on the panel specifications, which are 1.32 m^2 per 160 W panel. A maximum penalty of $500/month was implemented for the roof size. The effect of removing the cost penalty for insufficient roof sizes is verified in Section 5.3.3.

3.4 Consumption Patterns

3.4.1 Behavioural Effects on Overall Consumption

One thing that needs to be considered when designing a ZESH is the effect of behaviour on overall consumption. A given ZESH might be able to reach the zero energy target for a family of four that is aware of their energy consumption, whereas it may be short by as much as 50% for a family of four that pays no attention to the amount of energy that they consume. In fact, "occupant effects" can result in an annual energy use ranging from 70-140% of the average use in commercial and residential buildings (Chiras, 2002). Studies in the US, the Neatherlands, and the UK estimate that 26-36% of in-home energy use is due to resident behaviour (Wood and Newborough, 2003). Factors that influence consumption include the number of occupants, the average time spent at home by the occupants, the age of the occupants, and the feedback given to the occupants on their energy consumption. One study found that the number of occupants was more important than the average time stayed at home (Lucas, et al., 2001). They also found that occupants aged between 6 years old and 42 years old in Argentina showed the highest consumption.

A study performed to determine the variation of energy used in cooking found a 50% variation in electricity consumption between six chefs cooking the same meal with the same equipment (Wood and Newborough, 2003). All of these results show that there is promising potential in energy conservation that could theoretically be achieved by changing behaviour. For the GA Optimisation Tool, a set consumption pattern was assumed in all cases. Section 5.3.2 examines the impact that changing the consumption pattern has on the optimal configurations.

3.4.2 Electricity Consumption from Lighting

The electricity consumption due to lighting varies based on a number of factors. The type of lighting used plays a large role in determining consumption. For example, conventional incandescent light bulbs consume a lot more electricity than compact fluorescents light bulbs (CFL); a 13 W CFL has the same light output as a 60 W incandescent. Another advantage that CFL have over incandescent bulbs is that they have a longer life, in the range of 6,000 hours to 10,000 hours, compared to around 1,000 hours for an incandescent bulb (Energy Star, 2005). New light bulbs made with light emitting diodes (LED) are starting to emerge on the market that have even larger electricity savings and longer life spans. Current LED light bulbs on the market have lower overall lumen output than either CFLs or incandescent lighting; however, they could be used in some applications where lower light output is acceptable, such as hallways, porches, accent lighting, etc.

Other factors affecting the overall consumption are the number of occupants in the house, proper use of daylighting to eliminate the need for some electric lighting, the controls used to turn lights on and off, and the behaviour of the occupants, just to name a few. No two houses will have the same electricity consumption for lighting, especially as houses transition from incandescent to CFL to LED lighting. In the optimisation tool, only one consumption level and pattern was used for lighting irrespective of the inputs. Another strategy would be to use a wattage per square metre of house; however, if one assumes that the same family occupies a 100 m^2 house, or a 250 m^2 house, the overall consumption should not change drastically provided that controls are used. In larger houses, more instances would be found of unoccupied, unlit, rooms.

In order to establish the overall expected electricity consumption due to lighting, certain assumptions were made. First, it was assumed that 13 W CFL were used throughout the house. A number of lights were distributed to the various rooms of a house (3 in the kitchen, 2 in the dining room, 2 in bedroom 1, 2 in bedroom 2, 3 in bedroom 3, 2 in washroom 1, 1 in washroom 2, 2 in the living room, 2 in the den/office, and 2 outside) for a total of 213 W. After the lights were distributed, a schedule was made up that tried to take into account the expected daylighting contribution and occupancy. Appendix C shows the details of how the lights were distributed and the assumed usage frequency. The resulting lighting consumption was 400 kWh per year. One daily profile was used for all 365 days of the year. If more details were known about the occupants and their behaviours, it would be better to have different daily profiles based on different day types such as weekdays, weekends, vacations, and holidays.

Internal loads in TRNSYS can be either input as radiative gains or other internal gains. The gains associated with the lights were assumed to be 67% radiative and 33% convective based on recommendations made in (McQuiston, et al., 2005), for suspended, unvented fluorescent lights.

3.4.3 Loads from House Occupants

When the energy consumption of a building is modelled, it is important to consider the energy released into the room from the occupants. This is especially important in low energy buildings where the overall space conditioning loads are much smaller and that the heat gains from occupants contribute a higher percentage of the load. As with the other occupancy and consumption profiles developed for the GA Optimisation Tool, only one set of occupancy patterns and degree of activity was used. This could be changed to

an input with different schedules in future releases of the software. As it stands, the occupancy schedule was developed based on a family of four (two parents with two children). Different activity levels can be associated with the occupants that would vary the total heat released by an individual as well as the split between sensible and latent heat. Two different activity levels were considered in the schedule: activity level 1, where the occupants are seated at rest with a total heat load of 100 W (60 W sensible), and activity level 4, where the occupants are seated doing light work for a total head load of 150 W (75 W sensible) (Klein, et al., 2000). Appendix D shows the details of the occupancy schedule. One daily profile was used for all 365 days of the year. If more details were known about the occupants and their behaviours, it would be better to have different daily profiles based on different day types such as weekdays, weekends, vacations, and holidays.

3.4.4 Loads from Major Appliances

Every household has a number of major appliances that not only consume electricity, but that also release heat into the space. Table 3.8 outlines the average number of appliances that were used in each Canadian residence in 1990 and 2003 (NRCan, 2005b). The data presented in the table is for all types of residences, from detached homes to apartments. One would expect that the number of detached homes that have a clothes washer and dryer would be higher than for apartments. In 2003, approximately 54% of households had a dishwasher, a more than 30% increase from 1990. Freezers were found in approximately 56% of residences. Again, one would assume that the number would be higher in detached houses than in apartment dwellings. In order to represent what was found in the majority of Canadian detached houses, one of each of the following major

appliances was considered: refrigerator, freezer, dishwasher, clothes washer, clothes dryer, and range.

Table 3.8: Number of major appliances in Canadian households (NRCan, 2005b)

Appliance	Average number of appliances in 1990	Average number of appliances in 2003	Percent increase from 1990 to 2003
Refrigerator	1.18	1.24	5.2%
Freezer	0.57	0.57	-1.0%
Dishwasher	0.42	0.54	31.2%
Clothes washer	0.75	0.81	8.9%
Clothes dryer	0.73	0.81	11.9%
Range	0.98	0.99	1.1%

With the number and type of major appliances selected, the unit energy consumption (UEC) of each appliance was needed. Each appliance type had a wide range of available models, each with a different UEC. In future versions of this tool, the user could be given the choice of the type and number of appliances to include, along with a selection of different available models. In this case, the exact models of the appliances were not known; however, it is a reasonable assumption to make that someone choosing to purchase a low or net zero energy solar home would opt for more energy efficient appliances. The load associated to each appliance was selected based on the average energy consumption of the top 10 appliances in each category from the EnerGuide database (NRCan, 2005d).

The energy consumption rating for clothes washers and dishwashers includes the electricity consumption from the actual machine and the energy consumption to heat the hot water that is consumed. The hot water consumption was already included in the domestic hot water profiles used for this tool, as defined further in this section. To separate the hot water energy consumption from the appliance electricity consumption is

not straightforward since each given model is different. The EnergyStar (2005) website has a calculator that allows the user to test the impact of different parameters for both dishwashers and clothes washers. In the calculator, assumptions are made relating to the split between the energy used for hot water and for the appliance. These same assumptions were used in this tool to calculate the split in energy consumption of these appliances. The portion of rated energy used to run the actual appliance was assumed to be 44% for dishwashers and 10% for clothes washers.

Standard size, front-loading, Energy Star qualified clothes washers were selected for this study. There were a total of 122 models from 25 different brands in this category ranging from 48 L to 94 L in size and from 125 kWh to 341 kWh in yearly energy consumption. The energy consumption was based on 392 cycles per year (NRCan, 2006). The top 10 models came from 5 different brands and varied in size from 49 L to 75 L and the energy consumption varied from 125 kWh to 192 kWh with an average value of 137 kWh. Given that only 10% of the rated energy consumption was assumed for running the actual appliance, and that the hot water was included elsewhere, the electricity consumption from clothes washers was assumed to be only 13.7 kWh.

There were 214 different models of clothes dryers from 30 different brands ranging in size from 125 L to 212 L. The EnerGuide energy rating for dryers was calculated based on 416 cycles per year to dry clothes with predetermined water content (NRCan, 2006). If one uses the fast spin cycle on a front-loading clothes washer, the clothes get drier than with conventional clothes washers and therefore consume less energy to dry. Also, the rating assumed that the clothes were never hung to dry. It even assumed that the dryer went through 24 more cycles per year than the clothes washer. Of the top 10 dryers, the

top 2 had a consumption of 785 kWh; however, their size was only 125 L, the smallest possible size before being considered compact. There were 19 models tied for second place in terms of energy consumption, all having a capacity of 198 L and an annual consumption rated of 898 kWh. The energy consumption of the top dryers was taken as 898 kWh. This particular researcher and his wife do not use a dryer, even with a young child using cloth diapers, opting instead for indoor drying racks and an outdoor clothesline. It was assumed that the use of the dryer could be cut by a minimum of 30% through the use of hang-drying and using the fast spin cycle of the clothes washer. Therefore, the overall electricity consumption for the clothes dryer was assumed to be 629 kWh per year.

For freezers, there were again a wide range of types and sizes available. EnergyStar qualified chest freezers in the size category of 382 L to 436 L (13.5 ft^3 to 15.4 ft^3) were selected. The EnerGuide had a total of only seven freezers from four different manufacturers. Each had the same average annual electricity consumption of 354 kWh per year, which was used as the electricity consumption for the house freezer.

For refrigerators, there were again a wide range of types and sizes available. EnergyStar qualified fridges with auto-defrost, freezer-on-top, and sizes between 524 L (18.5 ft^3) and 578 L (20.4 ft^3) were selected. A total of 50 fridge models were available from 6 different brands. Of the top 10 fridges, 9 were 532 L (18.8 ft^3) from Kenmore, and 1 was 535 L (18.9 ft^3) from Gladiator. The energy consumption for the top 10 fridges ranged from 387 kWh to 393 kWh, with an average consumption of 391 kWh.

Standard size, built-in, Energy Star qualified dishwashers were selected for this study. There were a total of 628 models from 44 different brands in this category having yearly

energy consumption ranging from 125 kWh to 341 kWh, and using between 12.6 L to 29.9 L of hot water per cycle. The energy consumption was calculated assuming 215 cycles per year (NRCan, 2006). Four different dishwashers tied for tenth place with an energy consumption of 247 kWh; therefore, the top 10 category had 11 different models, 9 of which were from Asko and 2 from Ultraline. The average hot water consumption per cycle for the top 11 dishwashers ranged from 12.6 L to 15.5 L and the average energy consumption was 233 kWh. Given that only 44% of the rated energy consumption was assumed for running the actual appliance, and that the hot water was included elsewhere, the electricity consumption from the dishwasher was assumed to be 103 kWh.

Freestanding, normal width ranges with a single, non-self cleaning oven, and a conventional top were selected for this study. A total of 127 models from 17 different brands were in this category having an annual energy consumption ranging from 416 kWh to 579 kWh. The top 10 models included 7 brands and had yearly electricity consumption ranging from 416 to 459 kWh, with an average consumption of 449 kWh.

Table 3.9 summarises the electricity consumption of each appliance that was used in this study. The table also includes the average electricity consumption of new appliances from 1990 and 2003 (NRCan, 2005b) to compare with the selected values for this study. The consumption of the refrigerator and freezer used in this tool are reasonably close to the average consumption of a new appliance from 2003. The consumption of the dishwasher is almost twice as high, which likely indicates that a different split was used between the appliance and hot water energy consumption. This may also be the case for the energy used for the clothes washer, or it may be that the NRCan data includes both

front and top loading washers, whereas the present study only considers front-loading washers, which consume less energy. The energy used for the dryer is less in this study since it was assumed that energy efficiency practices would be followed in order to reduce the electricity consumption of the dryer. The range in the current study consumes only 62.5% of what a new 2003 range consumed. The total electricity consumption for the appliances used in this study was 1,940 kWh.

In general, the electricity consumed by appliances is released as heat into the house. It was assumed that 70% of this heat would be released through radiation and 30% through convection (McQuiston, et al, 2005). The exception was the clothes dryer, which loses a significant part of its heat through the exhaust. It was assumed that 85% of the heat energy was lost through the exhaust. Further analysis would be needed to confirm this assumption, but was not done for this study. Therefore, over the course of the year, 1,405 kWh was released into the room as heat, 984 kWh through radiation, and 421 kWh through convection.

Table 3.9: Average electricity consumption of household appliances (NRCan, 2005b)

Appliance	Avg. 1990 UEC (kWh)	Avg. 2003 UEC (kWh)	% Decrease 1990 to 2003	Current Study (kWh)
Refrigerator	956	487	49.1	391
Freezer	714	369	49.3	354
Dishwasher*	101	52	48.9	103
Clothes washer*	97	57	41.8	13.7
Clothes dryer	1,103	914	17.1	629**
Range	772	718	7.0	449

* Values do not include energy used for hot water consumption.
** Value assumes reduced use of dryer and use of more efficient clothes washer.

Finally, the times that the appliances were used needed to be assumed in order to distribute the loads in the building simulation program. The schedule for which

appliances are used varies from household to household. The energy use of the refrigerator and freezer was assumed to be spread out evenly over 24 hours. For the clothes washer and dryer, the energy use was spread out such that 25% of the consumption occurred between 07:00 and 09:00 and that the remaining 75% occurred between 17:00 and 20:00. For the dishwasher and range, the energy use was spread out such that 25% occured between 07:00 and 09:00, 25% between 11:00 and 13:00, and the remaining 50% between 16:00 and 19:00. An overview of the energy used by the appliances over a 24-hour period is given in Appendix E.

3.4.5 Minor Appliances and Other Loads

Minor appliances do not consume a significant amount of electricity on their own; however, when all of the consumption from the various appliances is added up, it can represent a significant amount. One study found that electricity use for minor appliances in the US and the UK was growing rapidly, and was responsible for an ever-increasing proportion of total household electricity use (Herring, 1995). The author reported that this area of appliance energy use was only beginning to be studied, in part due to the lack of consensus of what the definition of a minor appliance should be.

In the UK, the proliferation of minor appliances masks the real trend in electricity use for some end uses, such as cooking. If one only looks at the energy consumption for major appliances, it appears that electricity use for cooking is in decline. The cooking habits of people are changing with the use of minor cooking appliances, such as microwaves, toasters, coffee makers, and deep fat fryers steadily increasing; their energy use quadrupled in the decade preceding the study, which resulted in an actual increase in the electricity used for cooking of 5% (Herring, 1995). A similar trend was found for

entertainment and communication appliances. Even though the total energy consumption of televisions declined due to increases in efficiency, energy consumption in this category increased due to the increasing popularity of new entertainment and communication appliances including computers, compact discs, faxes, cordless telephones, and more.

The actual energy consumption of minor appliances in a typical household depends on a number of factors: the type and number of minor appliances used, the energy efficiency of individual appliances, the amount of time each appliance is used, and user behaviours. These variations, along with a limited amount of published data in this field, introduce some uncertainty in the data used in the tool. Table 3.10 lists what minor appliances were considered in this research, along with their estimated energy consumption, and the source that the consumption came from. The data coming from (Herring, 1995) was based on estimates from the US from 1988.

A miscellaneous load of 351 kWh/year was added for any loads that may have been missed. For example, the only appliance that was assumed to be duplicated was the clock; however, a house may have two TVs, stereos, DVD players, etc. In addition, some houses may have minor appliances that were not included in the list, such as slow cookers or electric grills. Herring (1995) reported that 4% of US households had block heaters for their cars, which consumed on average 250 kWh/year, which would likely be higher in colder climates. There may be some items listed that could be more efficient than what is listed since the data is dated.

Table 3.10: Assumed electricity consumption for minor appliances

Appliance	Electricity Consumption (kWh/year)	Source
Iron	50.0	(Herring, 1995)
Microwave	120.0	(Herring, 1995)
Vacuum	30.0	(Herring, 1995)
Clocks	25.0 x 2	(Herring, 1995)
VCR	25.6	(Energy Star, 2005)
Radio	27.0	(Guler, et al., 1999)
Hair dryers	40.0	(Herring, 1995)
Coffee maker	50.0	(Herring, 1995)
Toasters	50.0	(Herring, 1995)
Stereo	53.6	(Guler, et al., 1999)
Colour TV	147.5	(Energy Star, 2005)
CD player	94.0	(Guler, et al., 1999)
Cordless phone	9.1	(Energy Star, 2005)
DVD Player	22.5	(Energy Star, 2005)
Computer	169.8	(Guler, et al., 1999)
Printer	41.0*	(Energy Star, 2005)
Modem	12.0	(Guler, et al., 1999)
Miscellaneous other	351	Present assumption
Stand-by power	106.8	Present assumption
TOTAL	1,450	

*Assumed an Energy Star qualified inkjet printer

The other item that was added, stand-by power requirements, accounted for electricity used by major and minor appliances when they are not in use that had not already been included in the yearly consumption total. Standby power accounts for a 20 W to 60 W continuous load per home in developed countries and represents about 2% of the total electricity consumption in OECD countries (Fung, et al., 2003). Fung, et al. (2003) completed a study on the standby power requirements in Canada. They measured the standby power requirements for 268 new appliances in 4 large electronics stores as

well as 1,393 appliances in 75 households. More than half of the new stock appliances had a higher mean standby power requirement than the existing stock appliances. Two likely reasons for this increase were attributed to the increased features in newer appliances, and insufficient attention given towards energy efficiency in product design.

Standby power requirements varied significantly from one product to the next. For example, it was observed that all televisions from one manufacturer had a 0 W standby power requirement, while televisions from another manufacturer had 20 W or more. Another example was that the standby power requirements of computers varied by a factor of 15.6. There are currently no standards regulating standby power requirements. However, studies have reviewed the power consumption levels of the major components of household appliances responsible for standby functions, and found that nearly all standby functions could be performed with a total appliance standby power consumption of 1 W or less, with little or no extra cost to the manufacturers (Meier, et al., 1998). Several countries including the US and Canada, are considering a 1-W standard for standby electricity use for household appliances (Fung, et al., 2003).

The Canadian study on standby power requirements found that the mean household standby power requirement was 49 W, and the average annual household standby electrical energy consumption was approximately 427 kWh. This estimate was likely lower than the actual consumption since major hard-wired and white appliances were not included in the study (Fung, et al., 2003). If the standby power requirements of all appliances were reduced to 1 W, the annual standby electrical energy consumption in Canada per home could be reduced by over 59% to below 177 kWh. A lot of the minor appliances included in Table 3.10 already included the standby power requirements in

their total consumption. In addition, with the assumption that more energy efficient major and minor appliances would be selected, they should, in general, have lower standby power requirements, since this is one of the items regulated by the Energy Star program. Therefore, it was assumed that the standby power requirements not yet considered in the analysis accounted for one quarter of the average standby power requirements, or 106.8 kWh.

For the GA Optimisation Tool, it was assumed that 75% of the total load for minor appliances came from general equipment that are not internally cooled with fans, which have 70% radiative and 30% convective loads, and that the other 25% came from computers and electronics that are cooled by fans, which have 20% radiative and 80% convective loads (McQuiston, et al., 2005). This resulted in 833.8 kWh of radiative loads and 616.2 kWh of convective loads. It was assumed that the load was distributed evenly over a 24-hour period. In summary, the total electricity consumption for major and minor appliances and standby power requirements used in this study was 3,389.7 kWh. Table 2.1 showed that the average Canadian dwelling consumed 4,490 kWh of electricity for major and other appliances (NRCan, 2005b). This represents a less than 25% decrease in energy consumption, which is a reasonable expectation for the reduction that can be achieved through energy efficiency. This reduced consumption value is within what was approximated for the 12 EQuilibrium homes being built across Canada, which ranged from an estimated value of between 2,734 kWh/yr and 5,450 kWh/yr. The effect that the total assumed electricity consumption for major and minor appliances has on the optimal design configuration is verified in the analysis in Section 5.3.2.

3.4.6 Domestic Hot Water Profiles

A set of realistic domestic hot water profiles in different time scales was developed within the scope of the Solar Heating and Cooling Program of the International Energy Agency (IEA SHC), Task 26: Solar Combisystems (Ulrike and Klaus, 2001). Sets of load profiles for the domestic hot water demand for a period of one year with time scales of 1 min, 6 min, and 1 hour were developed. Each profile consists of a value of the DHW flow rate for every time-step of the year.

For the IEA-Task 26 simulation studies, a mean load volume of 200 L/day was chosen for a single-family house. The load profiles were developed with a series of assumptions on the type of water draws that a typical family would make. The draws were separated into four categories: category A was for short loads, such as washing hands; category B was for medium loads, such as for a dishwasher; category C was for baths; and category D was for showers. For each of these loads, assumptions were made related to flow rates, duration, number of incidences per day, and the statistical distribution of the loads. Table 3.11 shows the assumptions that were made in order to reach a mean load of 200 L/day. The basic load in each set of DHW profiles is then reduced to 100 L/day and the profiles are generated for higher demands by superposition to get load profiles for any number of occupants or multi-family dwellings (100 L, 200 L, 400 L, 800 L, etc.).

For the 6-minute profiles, only draws with duration of 6 minutes or more are taken into account. This means that only one category of loads is defined for the 6 minute profiles, representing all 4 water draw categories. Taking hourly mean values of the 6-minute profiles produces the DHW load profiles for the 1 hour time scale. Due to the

fact that the flow rates become very small when calculating mean values, they may not be regarded as realistic flow rates. However, the effect of averaging out the DHW draws becomes smaller for an increasing total load (Ulrike and Klaus, 2001). For the ZESH being modelled by the GA Optimisation Tool, the simulation time-scale was limited to one hour. The same mean load volume of 200 litres per day was used for all cases as was used for the single-family house in the IEA-Task 26 simulation studies. As with other consumption patterns, the DHW load could be varied based on the size of family expected to occupy the dwelling. Table 3.12 represents the assumed temperature of the water coming into the storage tank from the water main depending on the time of year.

Table 3.11: Assumptions used for daily DHW draws (Ulrike and Klaus, 2001)

	Category A Short Loads	Category B Medium Loads	Category C Baths	Category D Showers
Flow (liters/min)	1	6	14	8
Duration (min)	1	1	10	5
Incidences/day	28	12	0.143	2
Volume/load (liters)	1	6	140	40
Volume/day (liters)	28	72	20	80
Portion of total load	0.14	0.36	0.1	0.4

Table 3.12: Assumed water mains temperature for varying time of year

Hour Range	Temperature	Hour Range	Temperature	Hour Range	Temperature
0 – 744	9.4°C	2880 – 3624	10.2°C	5833 – 6552	10.4°C
744 – 1416	9.6°C	3624 – 4344	10.5°C	6552 – 7296	10.1°C
1416 – 2160	9.7°C	4344 – 5088	10.7°C	7296 – 8016	9.7°C
2160 – 2880	9.9°C	5088 – 5833	10.6°C	8016 – 8760	9.6°C

3.5 Calculating Costs

As mentioned, initial costs and operating costs were considered in the objective function. In terms of operating costs, only costs associated with the purchase and sale of electricity were considered. A cost structure that allowed for two different prices over the course of a 24-hour period was used. The user is asked at what hour the price would initially change and at what rate the electricity would be purchased and sold at that time. A second time is then entered when the price changes to a second set of prices for the purchase and sale of electricity. The operating costs were calculated based on the sale and purchase of electricity separately (i.e. the revenue from the sale of electricity assumed that all the generated electricity was sold, as opposed to only the surplus generation.) The user also inputs the rate at which the sale and purchase price would escalate every year.

The major cost in the objective function was associated with the initial costs. In this analysis, one is concerned with the incremental costs of the implementation of various levels of energy efficiency and renewable energy options. For the parameters that were assumed as part of standard construction practices, no associated costs were included. On the other hand, if the optimal configuration called for 5 cm more insulation than what is typical, then the costs were calculated based on adding 5 cm, as opposed to the cost of the whole wall. The additional costs associated with each parameter were then lumped together and assumed fully financed in a mortgage. The user inputs the number of years that the mortgage would be amortized and the interest that would be paid.

In order to maintain the accuracy of the optimisation tool over the long term, it is important to have the capability to periodically update the costs. In addition, it would be

important to be able to account for the different costs associated with different regions. Finding and updating location specific costs for the construction of a ZESH is not a simple task, and it would be unreasonable to expect this to be done for one research tool. Instead, the tool must rely on specific sources of information that publish the required costs on a periodic basis. One often used source is the RS Means cost data that provides cost information on building construction costs, building assemblies, mechanical equipment, and on electrical equipment on a yearly basis (RS Means, 2005a,b,c,d). It also provides cost factors to relate the costs given in its manuals to specific cities in North America that include currency conversions, as shown in Table 3.13. Based on the availability of the data, and the fact that it is updated annually and is location specific, the RS Means cost data was used where possible. For parameters that are not included in RS Means, other sources were utilised as specified.

Table 3.13: RS Means location cost factors (RS Means, 2005a)

City	Material cost factor	Installation cost factor	City	Material cost factor	Installation cost factor
Kamloops	117.8	84.3	Thunder Bay	114.8	85.4
Vancouver	125.6	88.2	Montreal	118.8	81.4
Victoria	119.1	84.8	Québec	119.6	81.8
Calgary	124.6	82.0	Sherbrooke	115.8	81.1
Edmonton	126.2	82.0	Dartmouth	117.7	69.2
Medicine Hat	117.0	81.0	Halifax	119.3	70.3
Regina	116.0	64.9	Charlottetown	117.8	58.7
Saskatoon	114.7	64.7	Fredericton	117.1	66.9
Brandon	117.1	70.7	Moncton	115.5	62.8
Winnipeg	124.3	71.0	St. John's	120.0	62.8
Ottawa	120.7	88.1	Yellowknife	114.3	79.8
Toronto	124.4	95.0	Whitehorse	114.0	63.8

Note that a similar approach of finding costs was used for BEopt, which used construction costs based on user specified or national average cost data from sources such as RS Means (Christensen, et al., 2006). For window and HVAC costs, they used quotes from manufacturers' distributors and appliance costs were based on manufacturers' suggested retail prices. In the future, the developers of BEopt wish to incorporate a database of different costs from different sources and allow the user to select from a among several different cost assumptions for each option (Christensen, et al., 2006).

Table 3.14: Roof cost at different pitches (RS Means, 2005b)

Roof Slope	Approximate Angle	Pitch Cost Factor	Roof Cost ($/m^2 floor area)	Incremental Cost ($/m^2 floor area)
Flat	0°	1.000	54.36	-6.46
3 in 12	14.0°	1.031	56.08	-4.74
6 in 12	26.6°	1.118	60.81	0.00
9 in 12	36.9°	1.250	67.92	7.10
12 in 12	45.0°	1.414	76.86	16.04
15 in 12	51.3°	1.601	87.08	26.26
18 in 12	56.3°	1.803	98.06	37.24
21 in 12	60.3°	2.015	109.58	48.76

For the exterior walls, the base case wall was taken as Wall 1 from the wall selection. The cost per square foot of the base case wall is itemised in Table 3.15. Wall 1 was given a cost of $0, and for the other walls, their incremental costs were calculated as any costs over $64.48/m^2 ($5.99/ft^2). For wall 2, the difference in cost was associated with changing the plywood sheathing to 51 mm (2") of rigid insulation and reducing the stud spacing to 406 mm (16") in order to provide more structural stability. The replacement of the plywood sheathing with expanded polystyrene (EPS) and the reduction of the stud

spacing to 406 mm (16") resulted in incremental costs of $-0.75/m^2 ($-0.07/ft^2) for materials and $2.48/m^2 ($0.23/ft^2) for labour, for a total of $1.73/m^2 ($0.16/ft^2) (RS Means, 2005a).

Table 3.15: Cost of base case exterior wall (RS Means, 2005a)

Layer	Layer description	Material ($/m^2)	Labour ($/m^2)	Total ($/m^2)
1	Painted aluminium siding	9.26	14.85	24.11
2	Asphalt felt building paper (15 lb)	0.43	1.29	1.72
3	16 mm pneumatic nailed plywood sheathing	6.67	3.44	10.11
4	8' pneumatic nailed 2" x 6" studs with 24" O.C.	5.06	5.38	10.44
5	6" thick, 23" wide, fibreglass batt insulation	4.95	2.15	7.10
6	16 mm level 5 finish fire resistant gypsum	3.34	7.64	10.98
-	TOTAL	29.71	34.77	64.48

The cost of insulated concrete form (ICF) walls was not found in the RS Means data. The costs used for this study were estimated based on the cost of reinforced concrete ready mix with EPS on both sides, which replaced layers 3 to 5 of the base case wall. Two layers of 64 mm (2.5") EPS cost $10.12/m^2 ($0.94/ft^2) for material and $8.18/m^2 ($0.76/ft^2) for labour, for a total cost of $18.30/m^2 ($1.70/ft^2), and 2 layers of 102 mm (4") thick EPS costs $14.85/m^2 ($1.38/ft^2) for material and $8.18/m^2 ($0.76/ft^2) for labour, for a total cost of $23.04/m^2 ($2.14/ft^2), (RS Means, 2005a). The reinforced ready mix concrete cost $20.99/m^2 ($1.95/ft^2) for material and $9.69/m^2 ($0.90/ft^2) for labour, for a total cost of $30.68/m^2 ($2.85/ft^2), for a thickness of 150 mm and $26.70/m^2 ($2.48/ft^2) for material and $9.69/m^2 ($0.90/ft^2) for labour, for a total cost of $36.38/m^2 ($3.38/ft^2) for 200 mm (RS Means, 2005b). The incremental costs for layers 3 to 5 for wall 3 were $14.42/m^2 ($1.34/ft^2) for material and $1.61/m^2 ($0.15/ft^2) for labour, for a

total incremental cost of $16.04/m^2 ($1.49/ft^2). For wall 4, incremental costs were $18.08/m^2 ($1.68/ft^2) for material and $1.61/m^2 ($0.15/ft^2) for labour, for a total incremental cost of $19.70/m^2 ($1.83/ft^2). For wall 5, incremental costs were $24.87/m^2 ($2.31/ft^2) for material and $1.61/m^2 ($0.15/ft^2) for labour, for a total incremental cost of $26.48/m^2 ($2.46/ft^2).

For walls 6 to 8, made of structural insulating panels (SIP), layers 3 to 5 of the base case wall were replaced by SIP with 11 mm of oriented strand board (OSB) on one face and varying levels of EPS insulation. For wall 6, the costs of layers 3 to 5 were replaced with $20.13/m^2 ($1.87/ft^2) for material and $6.89/m^2 ($0.64/ft^2) for labour, for a total cost of $27.02/m^2 ($2.51/ft^2); for wall 7 it was $25.30/m^2 ($2.35/ft^2) for material and $9.80/m^2 ($0.91/ft^2) for labour, for a total cost of $35.09/m^2 ($3.26/ft^2); and for wall 8 it was $29.60/m^2 ($2.75/ft^2) for material and $16.15/m^2 ($1.50/ft^2) for labour, for a total cost of $45.75/m^2 ($4.25/ft^2) (RS Means, 2005a). Therefore, incremental costs for wall 6 were $3.44/m^2 ($0.32/ft^2) for material and $-4.09/m^2 ($-0.38/ft^2) for labour, for a total incremental cost of $-0.65/m^2 ($-0.06/ft^2); wall 7 it was $8.61/m^2 ($0.80/ft^2) for material and $-1.18/m^2 ($-0.11/ft^2) for labour, for a total incremental cost of $7.43/m^2 ($0.69/ft^2); and for wall 8 it was $12.92/m^2 ($1.20/ft^2) for material and $5.17/m^2 ($0.48/ft^2) for labour, for a total incremental cost of $18.08/m^2 ($1.68/ft^2). Table 3.16 summarises the costs of the eight different walls.

For the thermal mass optimisation parameter, there were three costs that needed to be obtained. The option of no additional thermal mass had no costs associated with it. For the exterior walls, the addition of a brick layer with an interior veneer finish costs $31.00/m^2 ($2.88/ft^2) for material and $68.68/m^2 ($6.38/ft^2) for labour, for a total cost of

$99.68/m^2 ($9.26/ft^2) (RS Means, 2005a). The interior veneer finish was selected, adding 15% in labour costs, since it is likely that the interior gypsum board would either not be installed or be removed at a later date for some of the walls. The cost difference between a 10 cm thick concrete floor and a 20 cm thick concrete floor was $11.84/m^2 ($1.10/ft^2) for material and $1.61/m^2 ($0.15/ft^2) for labour (RS Means 2005a). The costs for any additional support structure that would be required to add an interior brick layer or for doubling the concrete thickness were not considered.

Table 3.16: Summary of costs for exterior walls

Wall	Total Material ($/m^2)	Total Labour ($/m^2)	Total Wall ($/m^2)	Incremental Material ($/m^2)	Incremental Labour ($/m^2)	Total Incremental ($/m^2)
1	29.71	34.77	64.48	0	0	0
2	28.96	37.24	66.20	-0.76	2.48	1.72
3	44.14	36.38	80.52	14.43	1.61	16.04
4	48.87	36.38	85.25	19.17	1.61	20.78
5	54.58	36.38	90.96	24.87	1.61	26.48
6	33.15	30.68	63.83	3.44	-4.09	-0.65
7	38.32	33.58	71.90	8.61	-1.18	7.43
8	42.63	39.94	82.56	12.92	5.17	18.08

One parameter for which it was more difficult to associate a cost was the building form since there is no conventional form for houses. The rectangular shape presents some cost savings for the building envelope compared to an L-shaped house or an H-shaped house. Since incremental costs were used in the optimisation and that some of the exterior wall types had a negative incremental cost, then one could imagine that the algorithm would try to maximise the building envelope area in order to capitalise on the this negative cost value. In order to counter this problem, and to introduce incentive to

reduce building envelope costs, a cost factor was associated with different building forms. The base case was set as a square house since this is the form that has the lowest exterior envelope area per interior space. Therefore, to calculate the incremental cost of the building form, the exterior wall costs were calculated with wall type 1 and then the exterior wall costs for a square building with wall type 1 are subtracted. Note that wall type 1 is used in the calculation as the cost difference associated with using different wall types is already considered in the calculation of the incremental costs in the wall type selection.

Window costs are very difficult to specify since they vary based on window size, number of windows, quality, among other factors. For this tool, average cost values between wood framed, double glazed, sliding windows were used (RS Means, 2006a). The costs were given for double glazed windows. However, RS Means recommends adding $\$25.83/m^2$ ($\$2.40/ft^2$) to upgrade from a double glazed to a triple glazed window, which is the value that was used to determine the cost of triple glazed windows, and an additional $\$25.83/m^2$ ($\$2.40/ft^2$) was assumed for quadruple glazed windows. In addition, the cost for the low-emissivity (low-e) coating was assumed to be 50% more for the triple and quadruple glazed windows since they have two coatings instead of one. The cost for the argon fill was not included in RS Means for these windows; however, window manufacturers tend to add argon at little or no extra cost. For this model, an additional material cost of 4% was assumed for the argon fill. The costs for the four different window types are summarised in Table 3.17.

Table 3.17: Assumed window costs

Description	Material ($/m^2)	Labour ($/m^2)	Total ($/m^2)	Relative ($/m^2)
2-pane, 12.7 mm air cavity	147.69	23.68	171.37	0.00
2-pane, 12.7 mm argon cavity, low-e	190.31	23.68	213.99	42.62
3-pane, 12.7 mm argon cavities, low-e	235.52	23.68	259.20	87.83
4-pane, 12.7 mm argon cavities, low-e	263.51	23.68	287.19	115.82

The Type 34 window overhang model in TRNSYS assumes that the overhang projects perpendicular to the wall. The perpendicular projection can be placed on the top edge of the window or a specified distance on top of the window. In reality, a lot of window overhangs are angled downwards as seen in Figure 3.13, and shade a larger portion of the window. For this tool, it was assumed that the overhang was installed horizontally 0.25 m above the window, and that it extended 0.10 m on both sides of the window. The price and length of the overhangs were taken from the Series 3100 window awning kits from (Patio Concepts, 2006), as summarised in Table 3.18, with the assumption that they were installed horizontally as opposed to at an angle.

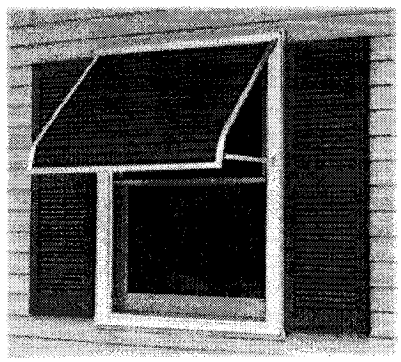

Figure 3.13: Window awning (Patio Concepts, 2006)

The cost of PV panels is not yet included in the RS Means cost data. Every year, the IEA PVPS releases reports on the price of the installation of PV systems in different countries (IEA PVPS, 2005). In 2004, the cost to install grid-connected PV systems of

less than 10 kW in Canada ranged from $13.52 and $14.56 per Watt, and for systems over 10 kW the cost was $8.97 per Watt. The costs for Canada were quite a bit higher than those of most other countries. For example, in Japan the cost of systems under 10 kW was reported as $8.06/W. For the initial version of the tool, PV system costs of $13.52 per Watt were assumed. The effect that using different PV costs has on the determination of the optimal design is examined in Section 6.4.

Table 3.18: Window overhang costs (Patio Concepts, 2006)

Protrusion Length	Cost for first 0.61 m ($)	Cost per additional 0.30 m ($)
0	$0	$0
0.65 m	$120.00	$40.20
0.94 m	$199.00	$40.40
1.26 m	$279.00	$40.60

The cost of solar thermal collectors is relatively small compared to the overall system costs, with more than 50% of the costs associated with labour costs (RS Means, 2005b). There are various different types of system configurations that can be used. In order to determine the cost of the solar thermal system, the system cost given in (RS Means, 2005b) for a closed loop, add-on hot water system with external heat exchanger was selected, since it was the closest to the system being modelled. Costs are given for a flat plate solar collector. It was assumed that the collector cost would be the only difference when using evacuated tubes for the system. In addition, a cost for evacuated tube collectors was only given for a 1.22 m x 1.83 m (4' x 6') collector, which is 1.4 times smaller than the system that was modelled. It was assumed that the material costs would be 1.4 times higher, and that the installation costs would match the installation costs of a flat plate solar collector of the same size, which was the case for the 1.22 m x 1.83 m (4' x 6') collectors. The balance of system costs that were assumed to be the same regardless

of the size and type of collector are listed in Table 3.19. Table 3.20 gives costs of components that were varied depending on the number and type of collectors.

Table 3.19: Solar thermal balance of system constant costs (RS Means, 2005b)

Component	Quantity	Material Cost ($)	Installation Cost ($)
Heat exchanger fluid-fluid package including 2 circulators, expansion tank, check valve, relief valve, controller, hi temperature cutoff and 2 sensors	1	765.00	355.00
Thermometer 51 mm (2") dial	3	66.00	91.50
Fill and drain valve, brass, 19 mm (¾") connection	1	5.20	20.50
Air vent, manual, 3 mm (1/8") fitting	2	4.92	30.70
Air purger	1	47.50	41.00
Strainer, Y type, bronze body, 19 mm (¾") IPS	1	19.15	26.00
Valve, gate, bronze, NRS, soldered 19 mm (¾") diam	6	165.00	147.00
Neoprene vent flashing	2	19.60	49.00
Relief valve temp & press, 150 psi, 98.9°C self closing	1	10.00	16.35
Pipe covering, urethane, ultraviolet cover	20'	38.20	91.80
Pipe covering, fibreglass, all service jacket	50'	45.50	183.50
Valve, swing check, bronze, regrinding disc	2	77.00	49.00
Pressure gauge, 60 psi, 51 mm (2") dial	1	24.50	15.35
Valve, water tempering, bronze, sweat connections	1	70.50	24.50
Copper tubing, type L	6.1 m	48.40	129.00
Copper tubing, type M	21.3 m	133.00	441.00
Sensor wire	0.15 m	5.68	24.25
Wrought copper fittings and solder	76	88.92	1,976
Propylene glycol antifreeze*	7.6 L	19.40	35.10
TOTAL	N/A	1,653.47	3,746.55

*Assume 7.6 L (2 gal) in system, and 7.6 L (2 gal) per solar collector

Table 3.20: Size and collector type dependant costs (RS Means, 2005b)

Component	Quantity	Material Cost ($)	Installation Cost ($)
Collector panels, liquid with copper absorber plate with flat black aluminium frame 1.2 m x 2.6 m	1	490.00	107.00
Liquid vacuum tube solar collectors 1.2 m x 1.8 m	1.4	1,232	107.00
Roof clamps for solar thermal panels	1	1.77	12.65
Propylene glycol antifreeze*	7.6 L	19.40	35.10
TOTAL PER FLAT PLATE	N/A	511.17	154.75
TOTAL PER EVACUATED TUBE	N/A	1,253.17	154.75

* Assume 7.6 L (2 gal) in system, and 7.6 L (2 gal) per solar collector

The costs of three different tank sizes, 250L, 303 L, and 454 L (66 gal, 80 gal and 120 gal), were obtained from (RS Means, 2005a). The material costs for the 250L, 303 L, and 454 L tanks were $730, $835, and $940, respectively, and labour costs were $204, $204, and $233. There were no 681 L (180 gal) tanks listed in (RS Means, 2005a). Instead, an approximate cost was obtained through the addition of the same price differential that exists between the 250 L and 454 L tanks to the 454 L and 681 L tanks. Therefore, the resulting assumed cost for the 681 L tank was $1,150 for materials and $262 for labour. The base case cost of a house includes a DHW storage tank. Depending on the system, the solar thermal storage tank can be the same tank as the DHW tank. In the design tool, only one tank was modelled with an additional tankless heater. However, two tanks are often used with solar thermal systems. To be conservative, the cost of the whole storage tank was included in the upgrade costs. Note that the cost of the tankless DHW heater was not included.

The cost of heating system 1 was set to zero to reflect the reference cost for a heating system. The reference costs were based on that of an electric hot air furnace with blowers and standard controls taken from (RS Means 2005c) for a 10 kW system, which

was listed at $405 for materials and $169 for labour. No tankless water heaters were found in RS Means for heating system 2. The cost for the selected product was used instead, which came to $949 (e-tankless, 2006). An additional cost of $120 for materials and $37 for labour was added for a circulating pump (RS Means, 2005c). A 2 Ton air-to-air heat pump with supplementary heating was listed at $1,425 for materials and $490 for labour (RS Means, 2005c). A 2 Ton water-to-air heat pump was listed as $1,238 for materials and $345 for labour (RS Means, 2005c) including auxiliary heating. It was assumed that the water-to-water heat pump was set to the same cost as the water-to-air heat pump since it was not listed in RS Means. Note that heating systems 4 and 5 used a borehole for a ground source heat exchanger. The cost of the system would be highly dependent on soil type. When published in 2002, The Buyer's Guide to Ground Source Heat Pumps (NRCan, 2002) listed the average costs for a vertical ground loop in clay for a 8.8 kW (2.5 ton) system to be between $1,400 and $1,800, and in rock to be between $2,400 and $3,200. The cost of a vertical loop for a ground source heat pump was not available in RS Means; therefore, a cost of $2,200, between the clay and rock soil, inflated at 3% per year until 2005 was used, which came to $2,404. No additional costs, other than for the heat pump, were given to systems 6 to 8 in order to connect them to the solar thermal storage tank. The cost of the desuperheater for system 6 was assumed to be $400. For systems 1 and 2, an additional cost of $975 for materials and $445 for labour was assumed when cooling was called for. Table 3.21 summarises the costs of the heating and cooling systems.

Table 3.21: Summary of costs for heating and cooling systems

System Type	Material Costs ($)	Labour Costs ($)	Total Costs ($)
Electric furnace - no cooling	0	0	0
Electric furnace - cooling	975	445	1,420
Hydronic – solar thermal + electric – no cooling	664	0	664
Hydronic – solar thermal + electric – cooling	1,639	445	2,084
Air-to-air heat pump	1,020	321	1,341
GSHP- air	833 + hole	176 + hole	3,413
GSHP - hydronic	833 + hole	176 + hole	3,413
Water-to-air HP using solar thermal + desuperheater	1233	176	1,409
Water-to-water HP using solar thermal	833	176	1,009
Water-to-air HP using solar thermal	833	176	1,009

4. MODEL VERIFICATION

4.1 TRNSYS Model Verification

One of the reasons for selecting TRNSYS as the energy simulation tool was that there has been a considerable amount of work done to validate its different components and systems (Crawley, et al., 2005). The objective of this section is not to validate TRNSYS itself, but to verify whether the component models were correctly implemented, such that the results obtained were comparable to what happens in reality. Due to the large number of heating and cooling systems and other parameters with varying setpoints, it is impossible to validate the entire model including all the possible parameter combinations. Instead, the analysis focuses on the results obtained for one specific situation.

In order to verify that the model is sufficiently accurate at predicting the energy consumption and zone temperatures of a house, a highly efficient house built according to the Advanced House standard (NRCan, 1993) in Saskatoon in 1992, was monitored for a one-year period in order to compare actual zone temperatures and energy consumption with results obtained from the TRNSYS zone model. The test house monitoring started March 6, 2005, and results from a full year of monitoring are presented in Table 4.1. The house (Figures 4.1a,b) features very high levels of insulation, passive solar heating, an active solar thermal system, energy efficient lighting (mostly compact fluorescent lamps), and relatively efficient appliances (vintage 1992). The house, which features double-thick 51 mm x 102 mm (2" x 4") constructed walls with blown-in cellulose insulation in a 406 mm (16") cavity, was reported to be the best-insulated house on earth in Home Energy magazine (Dumont, 2000). Whether this claim is true or not, the house is super-insulated with a ceiling R-value of R-80, walls (including basement) at R-60,

windows at R-5, and the basement floor at R-35. The house is also very airtight with blower door tests showing only 0.47 ach at 50 Pa.

Figure 4.1a: North façade of the house in winter

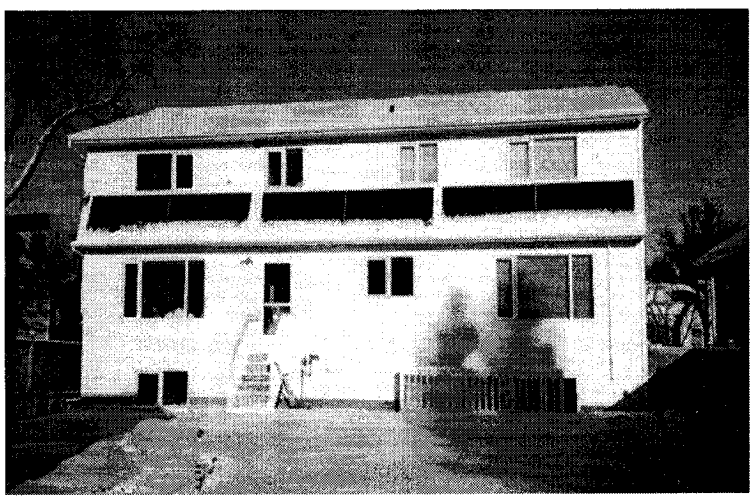

Figure 4.1b: South façade of the house in winter

Table 4.1: One-year electricity consumption breakdown of test house from March 6, 2005

Load	1 year consumption from March 6th, 2005 (kWh)
Electric heaters	8,349
Dryer	1,340
Electric water heater	1,114
*Monitoring equipment	1,086
Oven + range top	851
Freezer	499
*HRV	482
Refrigerator	323
*Computer + DSL modem	301
* 2 televisions	170
Microwave	112
Dishwasher	91
*Solar pump	85
Clothes washer	79
*Humidifier	44
*Toaster	31
*CD player	10
Misc. (lighting, outdoor use, garage, car block heaters, small plug-in appliances, doorbell, 6 smoke detectors, garage door openers, etc)	1,360
TOTAL	**16,327**

* Estimated consumption based on spot monitoring of consumption and extrapolating over a year

For the duration of the monitoring period, the house was heated primarily with 3 electric baseboard heaters including: a 1,000 W natural convection baseboard heater located in the hallway of the second floor, a 1,500 W fan forced convection heater located in the dining room, and a 1,500 W natural convection baseboard heater located in the family room. The total electricity consumption monitored for the baseboard heaters

for a one-year period starting March 6, 2005 was 8,349 kWh. This consumption was higher than expected by the house owner based on previous monitoring experiences.

The heating load was higher than expected due to two reasons. The first reason was that one of the windows in the basement was improperly closed for the majority of the monitoring period. In August of 2005, a monitoring wire was passed through the window, and the window did not close properly afterwards. An infrared thermogram of the leaky basement window is shown in Figure 4.2. The second reason that the heating load was higher than normal was due to the fact that the bird screen on the intake duct for the HRV was found blocked by debris in the spring of 2006, when the monitoring was completed. It was assumed that it was blocked for most if not all of the monitoring period. Although air filters were cleaned regularly, the homeowner neglected the bird screens. Flow measurements at the exhaust of the HRV indicated a flow of about 40 L/s throughout the monitoring period. Essentially the ventilation system was likely acting as an exhaust only system with very little heat recovery.

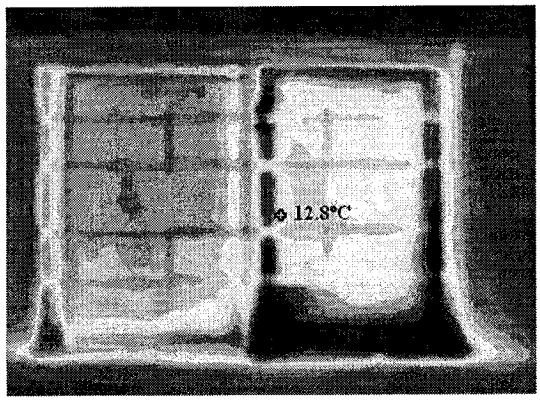

Figure 4.2: Infrared thermogram of leaky basement window

In order to use the data from the advanced house in Saskatoon to compare with results obtained with the low energy solar home model, the portion of the loads attributed to the basement needed to be evaluated. The house was modelled using HOT2000 version 9.31.

The effects of the leaky window were not considered, but the HRV was modelled simply as an exhaust fan operating continuously at 40 L/s. The HOT2000 report is presented in Appendix F. It was assumed that the main floors were heated to 20°C and the basement to 15°C based on the monitored data. The total consumption for heating was calculated with HOT2000 at 9,552 kWh. This is 14.4% higher than the monitored value. Three factors likely led to this higher predicted heating load: the HRV duct may have been only partially blocked, which would have allowed for some heat recovery; some of the unoccupied rooms in the house were left unheated by closing the room doors; and finally, HOT2000 used default weather data, which would differ from what actually occurred during the monitored year. Nonetheless, the data from HOT2000 was useful to determine what portion of the monitored heating load was attributed to the basement, which was not included in the low energy solar home model.

The heat losses for the house were divided at 41.9% for the upper floor's envelope, 14.8% for the basement envelope, and 43.2% due to infiltration and ventilation. It was assumed that only 15% of the ventilation load was due to the basement since the basement was unheated for the great majority of the year, it has smaller windows, and is partially underground restricting infiltration. The energy lost through the floor in the low energy solar home model, should be close to the heat lost in the basement floor modelled in HOT2000. Given that the floor represents 63% of the below grade foundation area, which itself represents 65.6% of the basement heat losses, the heat lost through the foundation floor should represent approximately 41.3% of the basement load, which represents 6.1% of the total heat lost. Therefore, a house without a basement would have a heating consumption of approximately 84.7% (41.9% + 36.7% + 6.1%) of the heating

energy consumption of a house with a basement. Therefore, for the house in question, the monitored consumption would drop to 0.847 x 8,349 kWh, or 7,072 kWh, without a basement.

In order to compare results with the test house to the results obtained with the low energy solar home model, the following modifications were made to the model to represent the actual house:

- the weather data file was changed to what actually occurred during the monitored time period with weather data obtained for the Saskatchewan Research Council;
- the house was modelled with a floor area of 243.9 m^2 on two floors;
- the hot water consumption pattern was changed to the measured data;
- the major and minor appliances and lighting consumption was changed to the measured data;
- the form was changed to 1.4725;
- the window type was set at window number 3 described previously;
- a new type of exterior wall was added to match what is in the test house;
- the percent glazing on the walls: 17.2% on the south wall, 11.5% on the north wall, and 1.5% on the east and west walls;
- overhang 2 was used on the south windows, and none on the east and west façade;
- a flat plate solar thermal collector with 6 m^2;
- a roof with a slope of 18.4°;
- thermal mass option 1; and,
- H95, L95, MinT, and MaxT were not changed; however, the value of db_h was increased from 2.0 to 2.7 and Δ1h increased from 0.5 to 0.9.

The loads used in the GA Optimisation Tool were modified to reflect the monitored data of the test house. For the major appliances, the split between radiative and convective loads was assumed to be the same as that used for the tool. The lighting load was assumed to be the same as that for the tool, with a total of electricity consumption of 400 kWh per year. The consumption for the desktop, toaster, televisions, and CD player was evenly distributed from 8am to 8pm. The remaining loads were distributed evenly over a 24 hour period. Forty percent of the miscellaneous loads were assumed to take place outside the residence, releasing no heat inside the house. The split between convective and radiative loads was consistent with the approach used in the development of the TRNSYS model.

The heating system also needed to be modified, as none of the heating systems considered for the GA Optimisation Tool were electric baseboard heaters. Since there were multiple heaters in operation in the house, these would work similarly to a multi-stage heating system. In order to represent the heating system, a heater of 2 kW was connected to the heating control. The heat released from the heater was input directly into the zone's input radiative and convective gains with an assumed split of 20% radiative and 80% convective. A second stage 2 kW heater was added that turned on when the zone temperature dropped below 19°C with a deadband of 1°C. .

A final modification was done to the specified infiltration in the TRNSYS program before the simulation was run. In the current model, infiltration was calculated based on Eqn. 3.14. The test house in question has a very tight envelope. Given that the HRV was acting similar to a constant exhaust of 40 L/s, there would not be much more air infiltrated above the amount needed to replace the exhausted air. Based on measured

infiltration properties and exhaust fan, HOT2000 calculated the total ventilation and infiltration at 0.192 ach. This infiltration rate at an assumed constant air density of 1.21 kg/m^3 translates to a continuous introduction of outdoor air into the space of 138.1 kg/hr. Therefore, the infiltration constants were all set to 0, and a fan was added to introduce 138.1 kg/hr of outdoor air into the zone all year round.

A one-year simulation starting March 6th, 2005, was done based on the above modifications to the low energy home model. The heating consumption was calculated at 6,619 kWh, or 6.8% less than monitored heating adjusted to remove the basement loads. The calculated and measured temperatures seemed to be different; the calculated temperature fluctuated more than the measured temperatures. The temperature difference between the measured and calculated was more pronounced in the shoulder season when there was little heating and no natural ventilation for cooling, as seen in Figure 4.3. One of the reasons for the differences between the measured and calculated data might have to do with how the blinds were modelled. As mentioned earlier in Section 3.2.5, the blinds were only assumed to be down in the model when the room temperature was too hot based on a temperature setpoint. In reality, people close blinds due to glare, privacy, or other reasons and may not actively use them to help with heating or cooling. Figures 4.1a and b, show the case of a cold winter day where half of the blinds in the house are down, which reduces the impact of solar gains. The blinds are also a mix of Venetian blinds and Silhouette^{TM} type blinds that have different properties than the blinds used in the model. In order to verify the impacts of the blinds, the control strategy was modified such that blinds were controlled with the same temperature conditions as before, but also lowered when solar radiation incident on a given window (by orientation) was higher than

150 W/m^2. For this new blind control strategy, the yearly heating energy was increased to 8,917 kWh, and the temperature profile for May is shown in Figure 4.4. The calculated temperature profile was now closer to what was measured, but the heating energy was 26% higher than expected. As seen from the pictures of the house, not all of the blinds are down, which would affect the results. The current modelled blind properties have the transmissivity set at 10% and the absorptance at 30%. If one assumes that only half the blinds are down at any given time, this would increase the effective transmissivity to 55% and decrease the absorptance to 15%. At these conditions, the calculated heating load was 7,695 kWh, which was closer to the monitored value, but the temperature profiles were again closer to those seen in Figure 4.3. These results seem to indicate that the blind properties and control strategy used in the modelling can have a significant impact to the calculated heating load and temperature profiles.

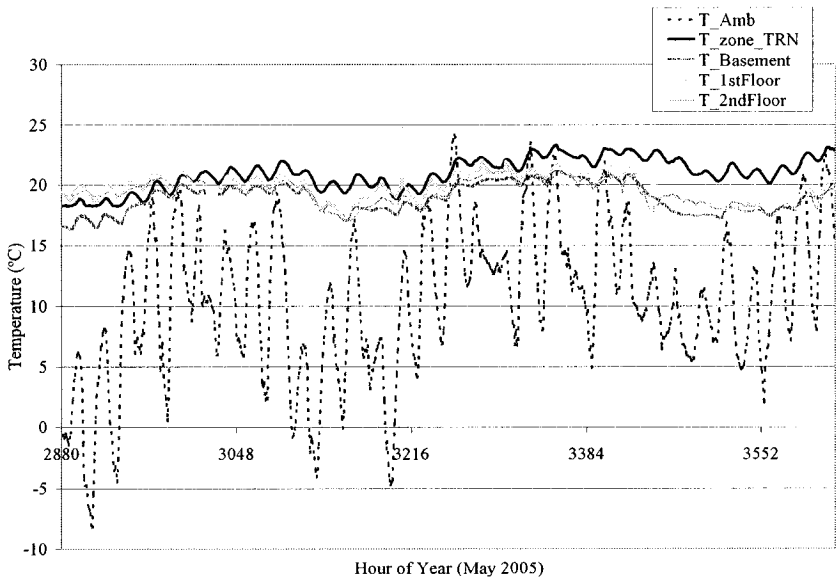

Figure 4.3: Comparison of simulated temperature versus monitored for May 2005

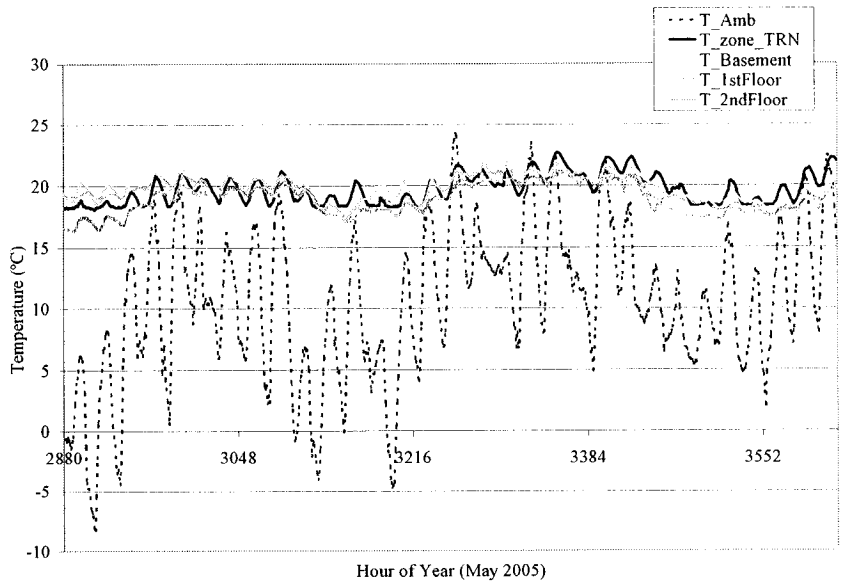

Figure 4.4: Temperature comparison for May 2005 with new blind control strategy

Figure 4.5 shows the calculated and measured temperatures from November 1, 2005 to February 28, 2006 with the new blind control strategy in place with blind properties of 10% transmittance and 30% absorptance. As can be seen from the figure, the zone temperature calculated with the low energy home model is in between the temperatures measured on the first and second floors, which is expected using a one zone model. In fact, over the course of the year, the calculated zone temperature is on average 0.5°C cooler than the main floor, 0.2°C hotter than the 2nd floor zone, and 0.1°C cooler than the average of the two zones together. If the average of the absolute temperature difference is taken, the difference is greater. On average, the calculated zone temperature is 4.4% different than the average measured temperature.

The effect of changing the split between radiation and convection for the baseboard heaters was verified and it had little effect on the overall results. When the split was 10% radiative the heating was 8,838 kWh, at 20% it was 8,917 kWh, and at 30% it was

8990 kWh. Therefore, tripling the radiative fraction increased the heating consumption by only 1.7%. The current model assumed that all of the ventilation going into the house came directly from outside due to an exhaust fan. If instead we assume that all of the ventilation would go through a HRV at 75% efficiency, with no infiltration, then the heating for the year would go down to 5,664 kWh from 8,917 kWh. Even if the HRV was working, there would have still been some air infiltration into the house. It is quite possible that the HRV duct was not blocked during the whole monitoring period, or that a fraction of the air did manage to go through the HRV intake, which resulted in a consumption that was between the two calculated values. The results indicate that the TRNSYS model is able to reproduce the monitored results within acceptable limits. The calculated zone temperature was on average only 0.1°C cooler than the measured average temperature of the first and second floor, and the heating electricity consumption was within the right range of the revised monitored electricity consumption that was attributed to the heating load without considering the basement. One cannot achieve a more accurate result without the precise blind properties and their opening and closing schedule, a more precise assessment of how much energy was lost through the basement, and more details on how the HRV was affected by its blocked inlet duct. Section 5.1 looks at the impacts of other critical assumptions used in the low energy house model.

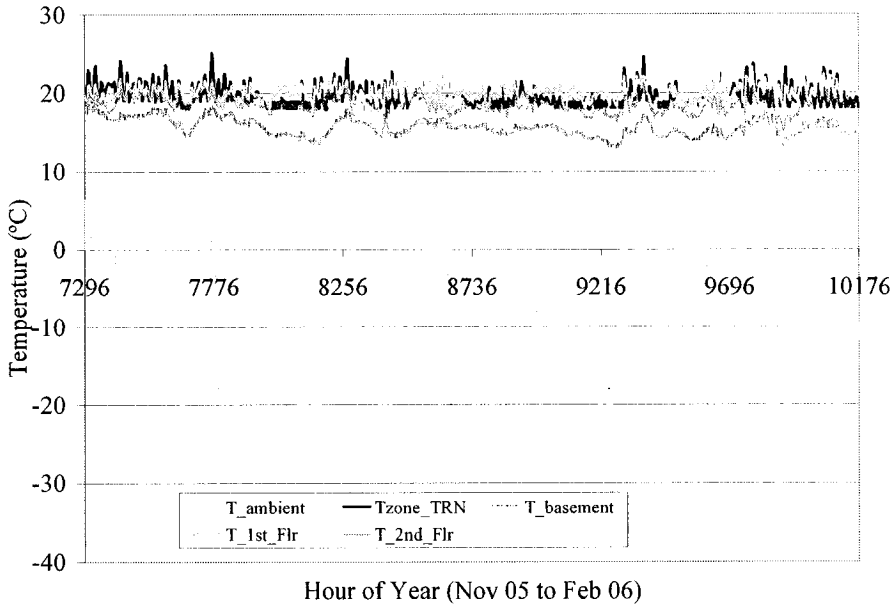

Figure 4.5: Measured and calculated temperatures for winter 2005-06

4.2 GA Program Verification

In order to test whether the GA program was implemented correctly based on the files provided by (Carroll, 2005), the code came with a test function subroutine. The GA program was run with this subroutine and achieved the expected results finding the optimal function value of 1.0000 at generation 187 with the specified inputs. The problem is an N-dimensional version of a multimodal function with decreasing peaks presented in (Goldberg and Richardson, 1987). In N dimensions, the function has $(\text{nvalley-1})^{\text{nparam}}$ peaks, but only one global maximum. This is a reasonably challenging problem for a GA, especially for higher dimensions and larger values of nvalley. The fact that the expected results were obtained confirms that the initial installation of the code was done correctly.

In order to verify that the GA program was able to find optimal solutions for the problem investigated in this study, the results were analysed by performing a manual optimisation around the optimal results obtained, in order to test if better solutions could be found. Based on the limited number of evaluations performed by the GA program, better solutions were bound to be found; however, the GA program would be considered to be running correctly if it could consistently find solutions that were close to the best solution found manually. The results of this analysis are found in Section 6.7. This approach was used since no analytical solution exists for realistic building optimisation problems and the extent to which the solutions are optimal can only be confirmed by inspection of the solutions (Wright, el al., 2002). In the manual optimisation, the parameters were varied one at a time and were updated to the fitter values of parameters. This approach is similar to the sequential search technique that is used in the BEopt tool (Anderson, et al., 2006).

5. TOOL ANALYSIS AND REFINEMENT

5.1 Impact of Critical Assumptions on Zone Modelling

As highlighted throughout this thesis, various assumptions need to be made in the development of a generic house model. Some assumptions can have a significant impact on the overall results obtained, whereas others have a minimal impact. The purpose of this section is to examine some of the key assumptions that were made in the development of the model to test the impact that they have and to make appropriate changes in order to improve the accuracy of the model.

5.1.1 Weather Data

One approximation that is bound to have some effect on the overall results of the model is the use of weather from a database. The estimated performance of a house based on archived weather data, compared to what actually happens, will always be different than the monitored performance. With our climate changing due to global warming, the use of weather from old databases may tend to overestimate heating energy consumption and underestimate cooling energy. Christenson, et al. (2006) looked at the climate trends in Switzerland to see how heating degree-days (HDD) and cooling degree-days (CDD) have changed. Their results indicated that from 1901 to 2003, the HDD decreased by 11–18%, depending on the threshold temperature (8°C, 10°C or 12°C) and location. The scenario calculations projected a further decrease of between 13% and 87% by 2085. For CDD, a significant increase in cooling potential was found to have occurred between 1901 and 2003 (between 50% and 170% based on CDD with a threshold of 18.3°C). The CDD were projected to increase by up to 2,100% by 2085!

The results of the study indicate that weather data used in energy simulation programs should be updated regularly. It would be interesting to examine the impacts of the results of the optimisation with projected weather data for different climate change scenarios, to see if climate change will affect the best approach to design a ZESH. Unfortunately, this type of analysis is beyond the scope of this thesis.

One can look at the impact that the use of actual weather data versus the standard weather data that comes in the TRNSYS weather database would have on the overall results of the test house case. The Saskatoon weather data from TRNSYS is from 1995. In order to compare for the same year period from March 6th, the TRNSYS data from January 1st to March 5th, 1995, was copied to the weather data following December 31st. The case of the test house with the modified blind control strategy was used with the added case that the blinds were used when the incident solar radiation went above 150 W/m^2. Recall that the total heating electricity calculated for that year was 8,917 kWh. With the database weather data, the heating electricity increased by 17.6% to 10,358 kWh. Figure 5.1 shows the temperature profile calculated with TRNSYS compared to the monitored values. Given that the heating setpoint was the same, the temperatures are not very different. The only exceptions were two very cold spells, where temperatures were below -30°C for over 24 hours; the calculated zone temperature dropped to a low of 13.8°C due to an insufficient heating capacity. Over the year, the average calculated zone temperature was the same as the average measured temperature of the test house; however, the average difference between the TRNSYS temperature and the measured temperature at each time-step was 6.5%. The fact the average temperatures over the year were the same indicates that the temperature was overestimated as much as

it was underestimated. With double the heating capacity, the heating electricity in the base case went up to 9,433 kWh, and for the TRNSYS weather data, it went up to 10,984 kWh. With the increased capacity, the temperature only fell to a low of 18.0°C.

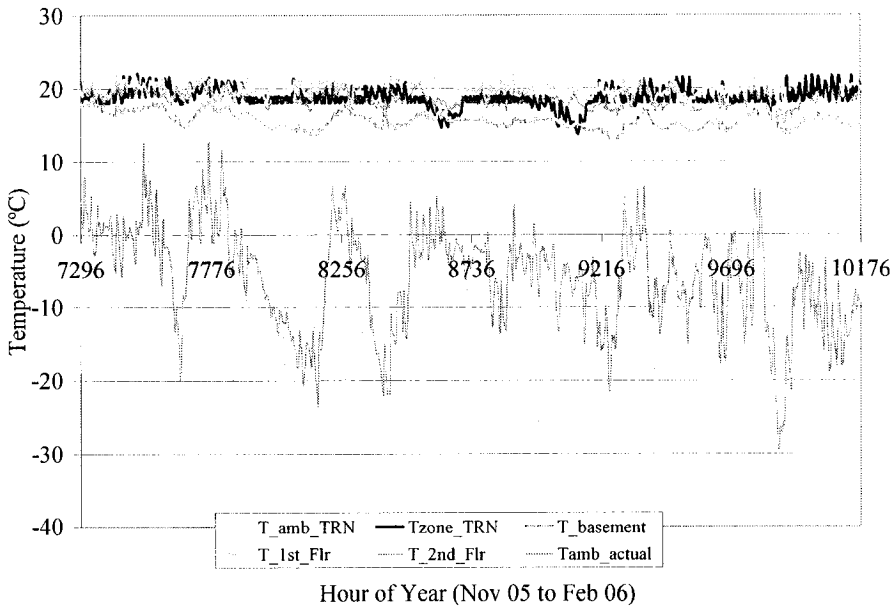

Figure 5.1: Measured and calculated temperature with TRNSYS weather data

With double the heating capacity, with a 4 kW primary heater and a 4 kW second stage heater, the heating consumption increased from 8,917 kWh to 9,433 kWh, a 5.8% increase. A big difference was also noticed in the zone temperature in the winter. With the increased heating capacity, the zone temperature mainly fluctuated between the heating setpoints at a high frequency. In reality, the temperature in the test house did not have that profile. The temperature profile obtained with the lower heating capacity was much closer to what actually happened. Therefore, it seems that it is important to have the heating capacity as close to what will be installed in order to predict the heating consumption and to obtain more realistic temperature profiles.

5.1.2 Program Robustness

Since the GA optimisation tool performs simulation runs with various different parameters in different combinations, the program needs to be robust such that it can compute an answer regardless of which parameters are selected. For example, while performing preliminary optimisation runs with the tool, it was found that TRNSYS would freeze during simulations on occasion. The only way to continue with the simulation when the program freezes is to stop TRNSYS from the computer's task manager. When it takes over 24 hours to complete an optimisation run, it is inconvenient to have to continually ensure that TRNSYS is still running. The difficulty in trying to debug the program when it freezes is that when TRNSYS freezes while it is in a simulation, it does not provide any indication as to what could have caused the problem. Without feedback it is quite difficult to determine what caused an error. This is unlike when an error is detected by the program during a calculation; in that case, TRNSYS simply stops the simulation and provides feedback as to what could have caused the error. In the case mentioned above, it was found that the majority of the instances that caused TRNSYS to freeze was when too few coefficients were used to define the B, C, and D transfer functions for certain walls. It was found that with 8 B coefficients, 10 C coefficients, and 8 D coefficients the problems were eliminated. The number of coefficients needed is dependent on the amount of thermal mass in the wall. If different walls are modelled that have more thermal mass and insulation, more coefficients may be required.

The task to eliminate all cases where TRNSYS freezes is an ongoing one. For example, when the analysis of the effects of the use of real versus archived weather data was done, TRNSYS inexplicably froze after completing 80% of the yearly simulation

with the new Saskatoon weather data. This freezing episode coincided with a period in the weather data that was exceptionally cold at the end of December when the outdoor temperatures went as low as -34.5°C and stayed below –30°C for over 30 hours. The calculated zone temperature dropped to 13.1°C before the program froze. In an effort to test whether this low zone temperature caused the program to crash, the heating capacity was doubled; the temperature dropped to 18.1°C before the program froze again after calculating 19 more hours than the previous case. Changing the heating system to heating system 1 with an 8 kW capacity, the temperature never dropped below 19°C, but the program still crashed after computing one additional hour. The outdoor temperature for all of December 25th up to noon on December 26th was increased by 2°C, which allowed the program to not freeze at that time. However, 1995 was a particularly cool year, with a second cold spell in early January with temperatures on January 12th and 13th reaching below -36°C, which again caused the program to freeze.

After a lengthy debugging procedure, it was found that it was the HRV Type 667 that was causing the problem. It was causing the problem whether or not its output air temperature and flow rate were connected to the zone. For some reason, when the outdoor temperature was connected to the fresh air input temperature and it dropped to below –33°C, it would cause TRNSYS to get stuck in its calculations and thus freeze the program[2]. The flow rates in the HRV were changed to 0, which eliminated the errors. Not only that, but the program ran 2.8 times faster when the HRV was not in operation. This example highlights the difficulty to eliminate all of the bugs in the program, as it

[2] Since doing the analysis the problem has been identified and eliminated. The Type 667 model calls the steam subroutine to get the enthalpy of the water vapour in the air and at low temperatures the steam subroutine gets into some sort of infinite loop. The problem was fixed by setting the enthalpy of the vapour at a constant value below –34°C.

may work well with one set of parameters and weather data, but changing one element can cause any one of the components implemented in the model to malfunction. In the final version of the tool, the only known instance where TRNSYS still gets stuck is when the heating and cooling setpoints are changed to allow very little temperature fluctuation. Since a limited number of test cases were tried, there may be other combinations of inputs that result in a program malfunction.

5.1.3 Fresh Air Ventilation and Infiltration

In order to test the effect of infiltration and fresh air ventilation, an example house was developed. Table 5.1 gives a summary of the parameters that were used for the example house. The house was 150 m^2 and 1 storey high. Table 5.2 shows the results from the change of various parameters related to infiltration and the envelope itself. Three sets of values for K1, K2 and K3 were used; the two highest are based on the TRNSYS guidelines for tight construction (0.10, 0.011, 0.034) and regular construction (0.10, 0.017, 0.049). The last values were based on a linear extrapolation from the two previous values in order to represent the more airtight envelopes that have emerged, which use more recent construction practices. The resulting infiltration rates with the use of the new coefficients were closer to results from a study mentioned earlier in the thesis that looked at 292 energy efficient houses that had average air infiltration rates of 0.25 ach (ASHRAE, 2001). More research would be needed to accurately define new coefficients that would be applicable to new construction practices.

Table 5.1: Summary of variables in example house

Parameter	Type of Parameter	Parameter	Value
1	Building Form	Length/width	1.5
2	Building Envelope	Window type	2
3		N window area	5%
4		E window area	5%
5		S window area	50%
6		W window area	5%
7		E overhang	0 m
8		S overhang	0 m
9		W overhang	0 m
10		Wall construction	Varying
11		Thermal mass	Varying
12		Roof Slope	# 4
13	HVAC System	Heating system	Varying
14		Cooling system	None

As mentioned earlier in the thesis, infiltration models are not the most accurate with average errors ranging at 40%, going up to 100% for individual houses. From the results in Table 5.2, we can see that differences in infiltration of 40-100% can make a big difference in heating energy consumption. A change in the constants from those for tight construction to regular construction increased infiltration by 37%, which resulted in an increase in the heating electricity by 28.4%. The derived infiltration constants resulted in significantly lower heating energy compared to the constants suggested in TRNSYS for tight construction practices. The most significant reduction in heating electricity occurred when wall 8 was used. This is not surprising as when the heat loss through the envelope is reduced with more insulated walls, the heating demand due to ventilation becomes more important.

Table 5.2: Heating load results summary varying infiltration coefficients

K1	K2	K3	Wall #	Therm Mass #	Heating System	City	Avg. ach	Avg. HRV (kg/hr)	Heating Electricity (kWh)
0.10	0.005	0.019	1	1	1	Montreal	0.255	43.9	5,503
0.10	0.011	0.034	1	1	1	Montreal	0.408	15.2	7,243
0.10	0.017	0.049	1	1	1	Montreal	0.559	5.6	9,298
0.10	0.005	0.019	8	1	1	Montreal	0.256	43.3	4,287
0.10	0.011	0.034	8	1	1	Montreal	0.409	14.6	5,967
0.10	0.005	0.019	1	4	1	Montreal	0.255	44.0	5,085
0.10	0.011	0.034	1	4	1	Montreal	0.407	15.0	6,795
0.10	0.005	0.019	1	1	4	Montreal	0.258	43.1	1,613
0.10	0.011	0.034	1	1	4	Montreal	0.413	14.7	2,145
0.10	0.005	0.019	1	1	1	Nanaimo	0.208	62.6	2,820
0.10	0.011	0.034	1	1	1	Nanaimo	0.317	31.0	3,438
0.10	0.005	0.019	1	1	1	Iqaluit	0.331	0*	17,198
0.10	0.011	0.034	1	1	1	Iqaluit	0.572	0*	23,472

* Temperatures in Iqaluit were too low for the HRV model, which made the program freeze

The effect that weather has on infiltration rates was also analysed by testing three cities: Montreal, which has a yearly average temperature of 6.1°C, a high monthly average of 20.9°C, and a low monthly average of –10.4°C; Nanaimo, which has a yearly average temperature of 9.8°C, a high monthly average of 17.9°C, and a low monthly average of 2.7°C; and Iqaluit which has a yearly average temperature of –9.8°C, a high monthly average of 7.7°C, and a low monthly average of –28.0°C (Environment Canada, 2007). As expected, the effects of infiltration for the heating demand were more significant in areas with colder weather. A change in the infiltration constants from the derived low values to those for tight construction increased the heating energy by 21.9% in Nanaimo, 31.6% in Montreal, and 36.4% in Iqaluit. Note that the HRV model was not working for the Iqaluit test case since the outdoor temperature drops below -33°C on a

regular basis, which caused a bug in the HRV model as described in Section 5.1.2. Therefore, in order to get results, the HRV was removed from that case, which had some impact on the results. Given the importance of airtightness regardless of the parameters, it was assumed that people building low and net-zero energy solar homes would implement an airtight envelope. Therefore, the new infiltration constants were implemented in the model (K1=0.1, K2=0.005, K3=0.019) as opposed to the tight construction values suggested in TRNSYS.

The HRV model Type 667 was selected since it takes into account both latent and sensible heat recovery; the effectiveness of the HRV was set at 60% for sensible heat recovery and 30% for latent heat recovery. The analysis brought out two issues related to the use of Type 667. The first was that it is not dependable for cold climates due to an internal coding problem. The second was that using Type 667 in the model significantly increased the calculation time for the simulation. A simpler heat exchanger model Type 91 was implemented in the model to see if it would solve the above problems and it did. The model no longer had difficulty with very cold temperatures, and Type 91 did not noticeably affect the run-time of the model. With Type 667, the run-time for a one year simulation was 360 seconds, whereas with Type 91 it was only 171 seconds. The downside with the simplified model is that it does not consider both latent and sensible heat recovery. It also does not calculate the changes in relative humidity of the air as it flows through the heat exchanger. Therefore, as a simplification, it was assumed that the relative humidity of the fresh air did not change as it flowed through the heat exchanger. To compare the results, the heat exchanger was tested using a 60% efficiency. The heating energy calculated changed from 5,503 kWh with the Type 667 HRV to

5,505 kWh, an insignificant difference. Given the negligible impact on the heating energy calculation, the significant time difference in the computational time, and the need to have a robust model for the optimisation, Type 667 was replaced in the model with Type 91 using a constant heat exchanger effectiveness of 60%. The fact that the model does not consider latent heat recovery has more of an impact in the cooling load calculation; however, the cooling load is generally small in Canada in comparison to the entire house loads, and the possible increases in accuracy are outweighed by the limitations of Type 667.

The amount of air flowing through the HRV was calculated to maintain 8 L/s per occupant in the house plus 0.1 L/s per square metre. This amount was calculated at every time-step based on the occupancy, the amount of air infiltrated, and the amount of outdoor air brought in through natural ventilation. This would be very difficult to implement in a real situation; however, it was done this way to bring flexibility to the controls, such that the fresh air introduced into the zone depended on the size of the house and on the projected number of occupants. A control strategy that would be more likely to be implemented would have a constant flow of outdoor air through the HRV. To see the impact of the use of a constant flow rate as opposed to a varying flow rate, the flow rate through the HRV was set to the average yearly flow rate that was calculated with the variable flow rate approach. This changed the calculated heating consumption from 5,503 kWh to 5,517 kWh, or a negligible 0.2% difference. Therefore, provided that the same average flow rate goes through the HRV, it does not seem make a noticeable difference in the heating energy consumption, whether the flow rate varies throughout the day or stays constant.

5.1.4 Window Properties and Modelling

Four different types of windows were included in the optimisation parameters. The window U-values were taken from the 2001 ASHRAE Fundamentals assuming the use of wood or vinyl frames. The values would be different if aluminium frames with thermal breaks were chosen, or if insulated vinyl or fibreglass frames were used. Table 5.3 shows the calculated heating electricity for the same example house that was used in the infiltration discussion using heating system 1, thermal mass 1, and wall 1. The results indicate that if aluminium frames with thermal breaks are used instead of wood or vinyl, that the electricity consumption for heating increases by an average 2.9%. If insulated vinyl or fibreglass frames are used instead, the consumption decreases by an average of 9.2%. Note that the relative difference depends on the surface area of the windows that are implemented. Differences between 2.9% and 9.2% are noticeable. In future versions of the model, it would be good to include different framing options within the window parameters. This would provide more feedback to the user as to whether it makes economic sense to spend money on more expensive window frames or on other energy efficiency measures.

Table 5.3: Effects of window framing type on annual heating load

Window	Aluminium w/ thermal breaks (U: W/m^2K)	Annual heating (kWh)	Wood/Vinyl (U: W/m^2K)	Annual heating (kWh)	Insulated Fibreglass/Vinyl (U: W/m^2K)	Annual heating (kWh)
1	3.00	7,180	2.87	6,932	2.53	6,305
2	2.22	5,730	2.10	5,505	1.79	4,962
3	1.61	5,043	1.56	4,957	1.30	4,498
4	1.54	5,267	1.48	5,155	1.23	4,705

One result that may be a surprise in Table 5.3 is that the performance of the triple glazed windows is better than that of the quadruple glazed windows. The reason for this is that the window model calculates the effects of each glazing within the window. As it is implemented, the relatively small improvement in U-value is not enough to compensate for the reduction in transmitted solar radiation due to the fourth glazing. The difference almost vanishes if the percentage window area between the south and north facades is switched, so that the north has 50% windows and the south has only 5%. Window type 3 is still the better performing window at 7,918 kWh, but window 4 is only slightly higher at 7,948 kWh. It is possible that the interior glazing properties for triple and quadruple glazed windows to be different than for the exterior glazings. However, the TRNSYS Type 35 window model does not allow varying glazing properties within the same window. Given that window type 4 is more expensive than window type 3, yet has a poorer performance, it does not make sense to include it in the optimisation since it will never give more optimal results than window type 3. In order to keep four window options, window type 4 was replaced by the same type of window as window 3, but with an insulated fibreglass frame. For simplicity and due to lack of data, it was assumed that this new window type 4 would have the same cost as the previous window type 4. The fibreglass frame with three glazings has a better U-value (1.30 W/m^2K) than the quadruple glazed window with a vinyl or wood frame (1.48 W/m^2K).

Another assumption that needed to be made with the window modelling was to set where the beam radiation would be incident. As implemented in the model, 90% of the beam radiation through windows was assumed to be incident on the floor, and the other 10% was assumed to be incident on the wall opposite the window. Table 5.4 shows the

effects of the use of different splits between the floor and back wall for beam radiation. The results show the effects for an air based heating system (System 1) and a hydronic based heating system (System 2). A window centred on a wall in a large room has most of its incident beam radiation incident on the floor; however, a corner window in a smaller room has more of its incident radiation on the walls and not only on the back wall. When large overhangs are included, a lot of the beam radiation comes through the window at a lower angle, which results in a higher percentage that strikes the back wall as opposed to the floor. Despite the variability in the fraction of incident radiation on the floor and the other wall, Table 5.4 shows that this input does not significantly affect the results. If the fraction of incident radiation on the floor is lowered from 99.5% to 50%, the heating load of system 1 increases by only 1.3% and by 3.0% for system 2. Based on these results, it was decided to keep the assumed default values of 90% of the beam radiation through windows to be incident on the floor, and the other 10% to be incident on the wall opposite the window.

Table 5.4: Effects of location of incident beam radiation

% Floor	% Back wall	System 1 heating (kWh)	System 2 heating (kWh)
99.5	0.5	5,492	7,801
95	5	5,505	7,867
90	10	5,505	7,870
75	25	5,532	7,911
50	50	5,565	8,032

5.1.5 Determining Time-Step and Zone Air Heat Capacitance

The results presented up to this point in this section were obtained with a time-step of 10 minutes. As was shown in Section 3.2.1, the time-step affects both the calculated

heating and cooling energy use and the calculated zone temperatures. Table 5.5 presents the results of the heating energy calculation for both an air-based (system 1) and a radiant based (system 2) heating system.

Table 5.5: Heating energy calculated using different time-steps

Time-step (minutes)	Sys 1 heat (kWh)	Sys 1 cool (kWh)	Sys 2 heat (kWh)	Sys 2 cool (kWh)	Sys 2 heat Tank 38 (kWh)	Sys 2 cool Tank 38 (kWh)
60	6,860	33.2	4,898	49.6	9,416	51.2
30	5,925	33.8	6,215	37.6	9,234	36.8
20	5,663	27.8	7,016	37.3	9,241	37.3
15	5,530	26.3	7,460	32.7	9,277	32.7
10	5,507	24.5	7,874	30.2	9,249	29.4

As can be seen from the results, the heating energy calculation varied more significantly with heating system 2. After scrutinising the results, it was found that it was the TRNSYS Type 4 stratified fluid storage tank model that was varying significantly with the time-step. The reason that the results were affected with system 2 is that it uses the water from the tank to pre-heat the water for the under-floor radiant heating system, whereas system 1 does not use the heat from the solar thermal storage tank. Type 4 tank was chosen after a more detailed tank model was tried, Type 60, which slowed down the program and was less robust. The user manual does not recommend a specific time-step to use with Type 4. However, the description for the Type 38 algebraic tank (Klein et al., 2000), which models the behaviour of a temperature stratified tank with variable size segments of fluid, states that:

> "*A time-step of 1 hour in the Type 38 tank model is sufficient for many stratified tank systems, whereas simulation time-steps of a few minutes are necessary in a Type 4 model with a large number of fixed nodes.*"

The 10 nodes used to model the tank required small time-steps to obtain more accurate results. Based on these findings, the heating load for system 2 was recalculated with tank Type 38 and the results are shown in Table 5.5.

The results from Table 5.5 show very little variation in the heating energy calculation with system 2 and Type 38. The energy calculated was higher than with Type 4; however, the energy use calculated with tank Type 4 was increasing with smaller time-steps, which reduced the gap between the two models. A change in the tank models will affect the DHW energy consumption calculations. Table 5.6 shows the calculated energy consumption to heat the DHW with system 1 and 2 with the evacuated tube (ET) and the flat plate (FP) solar collectors. As expected, the calculated DHW electricity consumption stays fairly constant with Tank 38, and not with Tank 4. Given the need for a smaller computational time with the implementation of optimisation, Tank 4 was replaced with Tank 38 in the tool. The auxiliary heater was located at 0.85 the tank height, the control thermometer at 0.95, and the collector return at 0.5 the tank height. The tank height was calculated based on the specified storage diameter (default 0.7 m). The location of the auxiliary heater, the thermometer, the inlets and outlets, and other tank parameters affect the tank's performance. Different overall designs would result in different optimal tank configurations. A search for these optimal configurations is left for later stages in the design process, when more information is known about the overall system.

Based on the results from Table 5.5, three time-steps were chosen for further analysis: 30, 20 and 10 minutes. These time-steps were tried with the other heating systems not considered to date, systems 3 to 8, and the results for the heating energy calculated are

found in Table 5.7. The same example house was used with the evacuated tube collector and no cooling. The effect of changing the time-steps on the DHW consumption would be similar to the results presented in Table 5.6 using Tank 38, regardless of the heating system. The average absolute difference between the heating calculated with time-steps of 10 minutes and 20 minutes was 0.6%, and from 10 minutes and 30 minutes was 2.3%; the longer time-steps generally had a higher calculated heating energy consumption.

Table 5.6: Yearly DHW electricity consumption (kWh) using Type 4 and 38 tanks

Time-step (min)	Heating System 1		Heating System 2			
	Tank 4 ET	Tank 38 ET	Tank 4 ET	Tank 4 FP	Tank 38 ET	Tank 38 FP
60	1,006	1,412	1,174	1,756	1,606	1,904
30	1,198	1,417	1,414	1,946	1,617	1,899
20	1,311	1,413	1,547	2,043	1,599	1,890
15	1,386	1,412	1,630	2,108	1,599	1,893
10	1,474	1,409	1,718	2,173	1,598	1,885

Table 5.7: Heating energy calculated for all heating systems varying time-steps

Time-step (min)	Sys 1 (kWh)	Sys 2 (kWh)	Sys 3 (kWh)	Sys 4 (kWh)	Sys 5 (kWh)	Sys 6 (kWh)	Sys 7 (kWh)	Sys 8 (kWh)
30	5,925	9,234	3,927	1,655	1,805	2,583	8,416	6,358
20	5,663	9,241	3,913	1,612	1,791	2,552	8,122	6,340
10	5,507	9,249	3,902	1,613	1,769	2,539	8,105	6,343

In order to determine which time-steps would be more appropriate, the zone and solar thermal storage tank temperatures were compared for heating systems 1 and 2 with varying time-steps. Figures 5.2a and b show the zone temperatures and 5.3a and b the tank temperatures for January 11th and 12th for systems 1 and 2 respectively, which correspond to one of the two coldest days of the year. As expected, with the new tank model, the tank temperatures are very similar between the different time-steps. With

heating system 2, the zone temperature is fairly consistent with the different time-steps. For system 1, the 30 minute time-step predicts slightly higher temperatures; the 10 and 20 minute time-steps fluctuate within the same range of upper and lower temperatures; the 10 minute time-step fluctuates at a higher frequency, as expected.

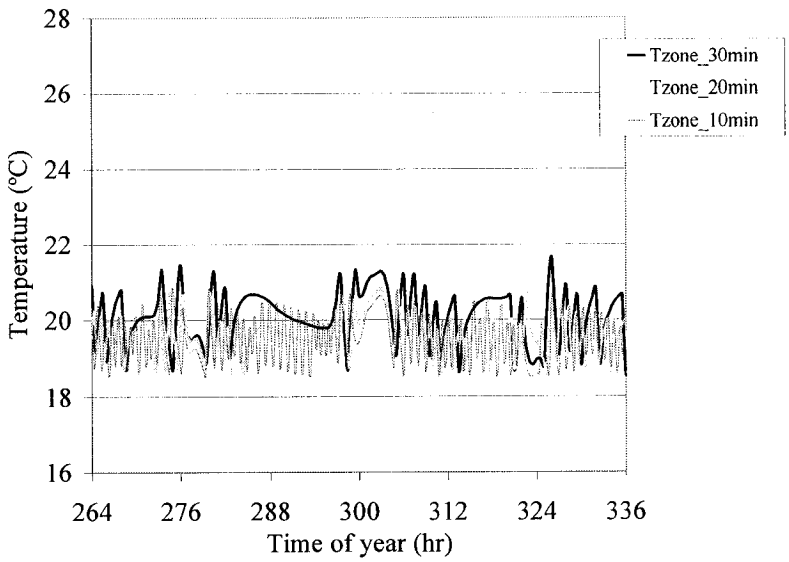

Figure 5.2a: Zone air temperature using system 1 with different time-steps

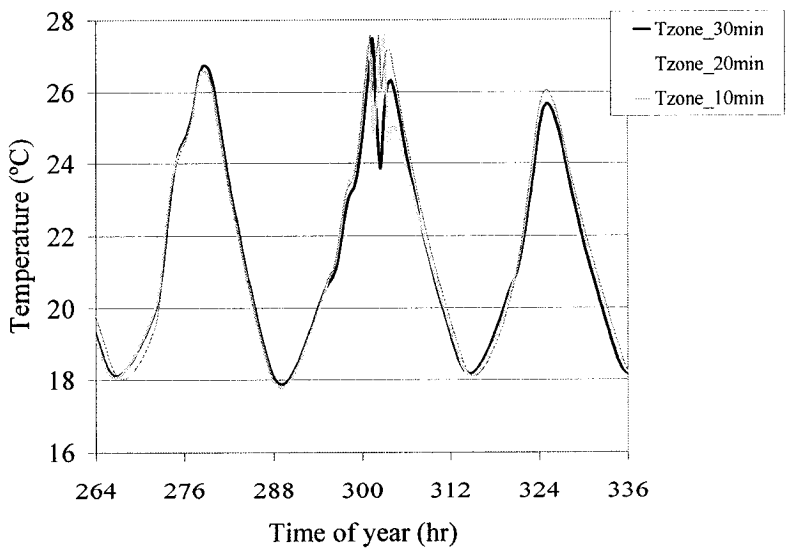

Figure 5.2b: Zone air temperature using system 2 with different time-steps

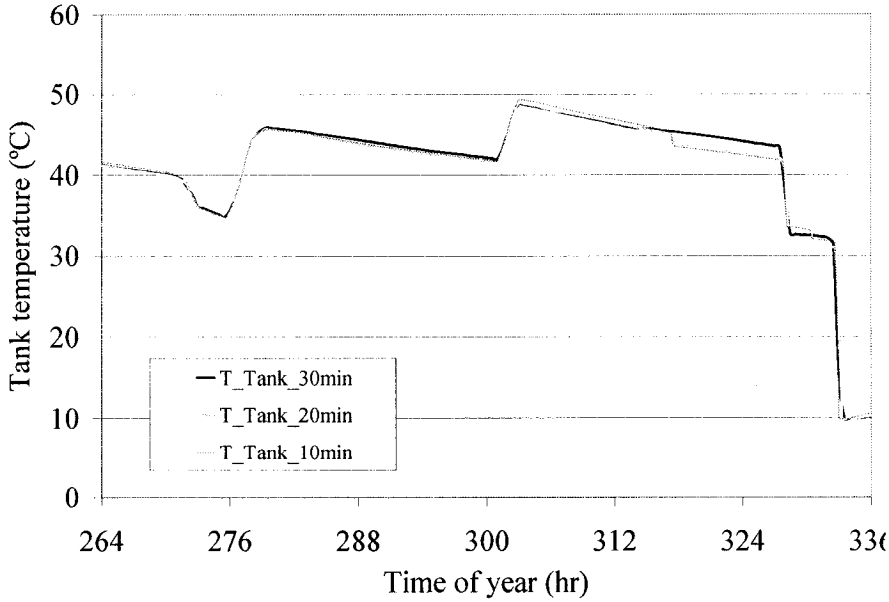

Figure 5.3a: Tank temperature using system 1 with different time-steps

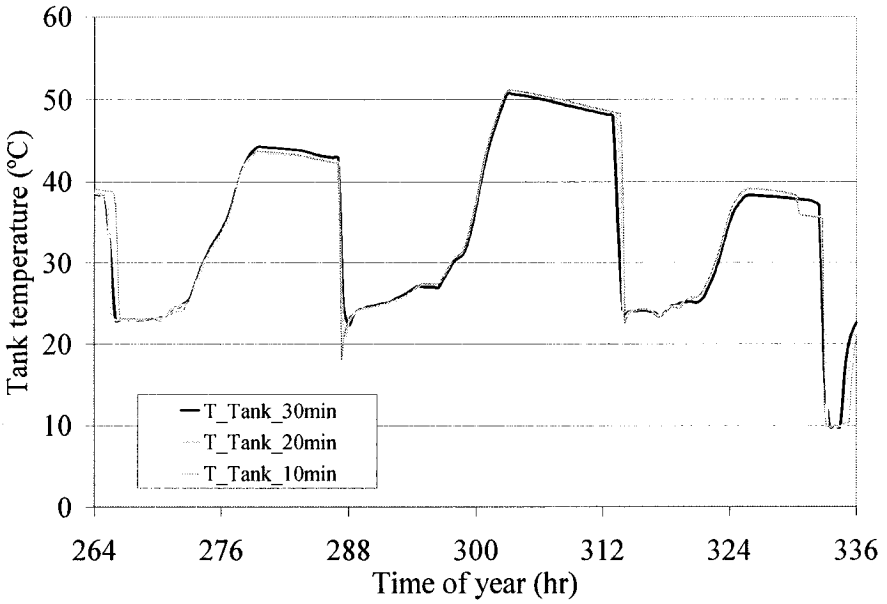

Figure 5.3b: Tank temperature using system 2 with different time-steps

The Type 19 zone model uses an effective thermal capacitance of the room air and furnishings plus any mass not considered in the building envelope as discussed in Section 3.2. The value of this effective capacitance can have a significant effect on the

calculated temperature, but tends to have smaller impact on the calculated heating load. At the start of this study, the TRNSYS software providers recommended to use a capacitance value equal to 12 times the room air capacitance. However, Jeff Thorton, the president of Thermal Energy System Specialists (TESS), answered the following questions related to the thermal capacitance on the TRNSYS user group on March 4th, 2006:

Q: Is there any basic criteria for selecting capacitance?

A: It depends entirely on the type of zone that you are modelling. For residential and commercial zones I usually multiply the volume by 10 to 50 times the default value (1.2 x Zone Volume) to account for non-wall capacitance.

Q: Will it make major changes in inside temperature or heat transfer calculation?

A: Heat transfer calculation - no. Inside temperature - yes. The higher the capacitance the slower the building will respond to changes. Try different values until the building behaves like you think it should to a step-change in temperature.

Therefore the effective zone air capacitance that was used up to this point, with the inclusion of the model verification, was on the low end of the values used by TRNSYS experts despite the fact that it was the recommended value. Figures 5.4a and b are analogous to Figures 5.2a and b but they use an air capacitance of 50 times the zone air capacitance instead of 12. The heating electricity consumption for system 1 went down to 5,245 kWh, 5270 kWh, and 5,275 kWh for the 30 minute, 20 minute, and 10 minute time-steps, respectively. For system 2, the heating energy also went down to 7,966 kWh, 7,991 kWh, and 8,058 kWh for the 30 minute, 20 minute, and 10 minute time-steps, respectively. The capacitance does seem to have an effect on the calculated heating

electricity consumption; the heating load dropped by approximately 13% for system 2 with the longer time-steps. The figures show that the zone air temperature does not change as much between the different time-steps when the higher room air capacitance was used. In system 1, the frequency of zone temperature oscillation was decreased and the trend in temperatures between the different time-steps was closer. In system 2, the zone temperature oscillates between 18°C and 24°C instead of 18°C and 26°C. Another attribute of the higher effective capacitance is that calculation time decreased by approximately 30% with the higher capacitance. The calculation run-time savings were due to the fact that the program required less iteration for each time-step in order for the solution to converge; this was because there was less fluctuation in the zone air temperature from one time-step to the next. The next challenge was to determine which capacitance value gave the most accurate results.

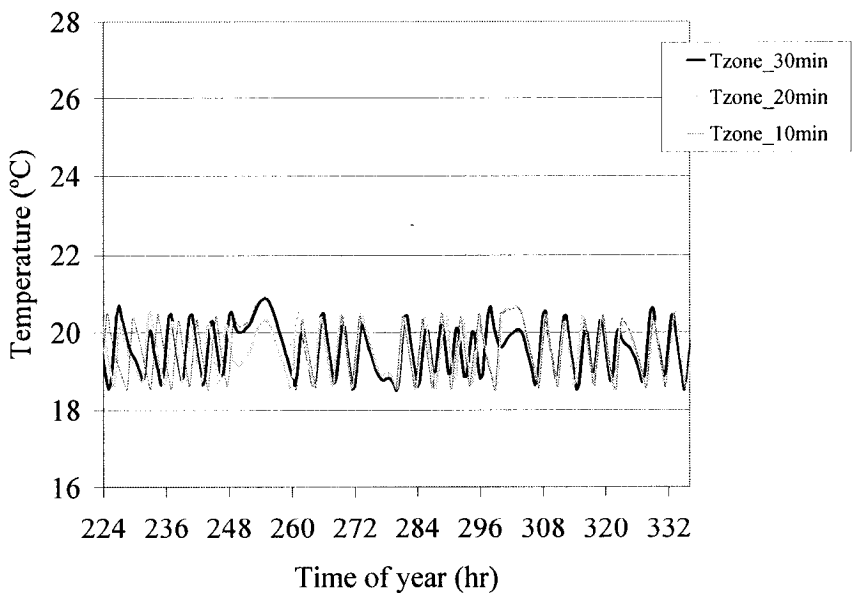

Figure 5.4a: Repeat of Figure 5.2a with new effective air capacitance

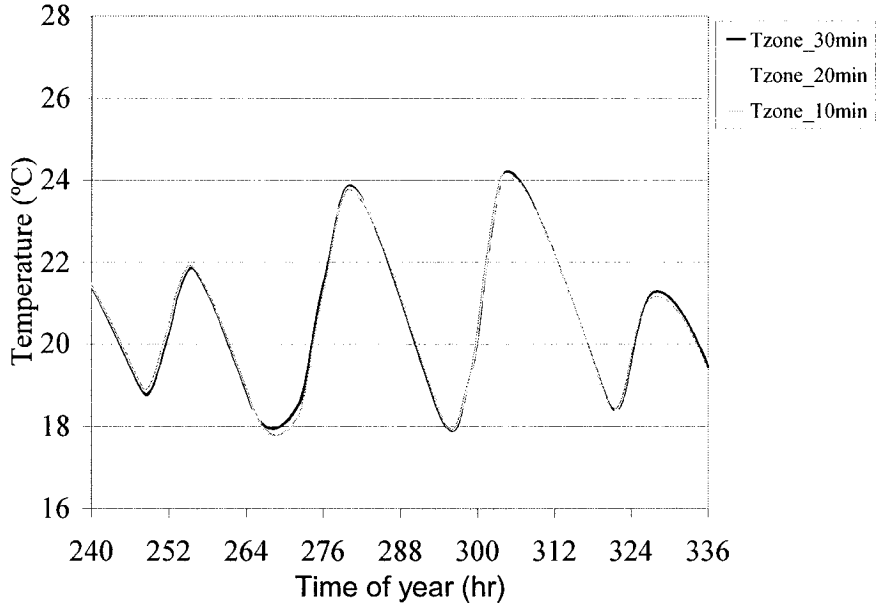

Figure 5.4b: Repeat of Figure 5.2b with new effective air capacitance

In order to determine which capacitance value to use, the results from the test-house were re-visited. In the zone model verification, it was assumed that the main difference in zone temperature calculation was due to a difference between the modelled blind control and the actual blind control strategy. Although this did explain part of the variation, there were still some differences with regards to the amplitude of the temperature oscillations that were larger in the calculated values than the measured values. It is likely that the differences between the calculated and measured temperatures were mainly due to a combination of the blind control and the zone air capacitance values that were used. In the tool verification analysis, the blind control strategy that used revised effective blind properties to represent the situation where not all of the windows are covered with blinds led to more realistic results. Several air capacitance values were modelled with this blind control strategy in order to get a closer correlation in the zone air temperature between the measured and calculated values. The value that seemed to offer

the best results over the whole year had the capacitance multiplied by 40. The calculated heating electricity consumption was 7,534 kWh, which is 6.5% higher than the modified measured results but it is still within the range of uncertainty associated with the assumptions used to account of the basement. Therefore, the effective air capacitance in the model was changed to:

$$Cap = 40 \cdot Zone\ Volume \cdot 1.006 \frac{KJ}{m^3}. \qquad (5.1)$$

The analysis on the effects of this effective capacitance has shown that the value that is used has an effect on the air temperature profile, the calculated heating and cooling loads, and the program computational time. Values in the recommended range of 10 to 50 times the zone air capacitance result in a range of possible different solutions. The suggested strategy to experiment with different values until the building behaves as expected to a step-change in temperature is far from ideal. One of the reasons that people use modelling is to try to determine how a building will behave. The capacitance value will change on a case-by-case basis and will depend on the amount of capacitance in the furniture and interior wall layers that is not included in the modelling. This value should be re-visited and refined in later stages of design. In addition, it would be good to have a future research project that would develop a more defined method to determine an appropriate value to use.

With the new solar thermal storage tank and a higher effective air capacitance value, the difference in results between the different time-steps is small. However, this might not always be the case when different combinations of parameters, different weather data, different consumption profiles, etc., are used. Given that this thesis is in pursuit of a methodology to develop a robust tool that works well for all different parameter

combinations and climatic conditions, balanced with shorter computational time, a time-step of 20 minutes was implemented in the GA Optimisation Tool. Although a time-step of 30 minutes would probably have resulted in acceptable results for an early-stage design tool, the shorter time-step was used in order to have a higher level of certainty in the results.

5.1.6 Heating System Configuration and Control

In Figures 5.2a and b we can see that the resulting zone temperature is quite different for each heating system used. This is despite the fact that the same control strategy was used in both cases. For heating system 1, the temperature fluctuates between approximately 18.5°C and 20.5°C. This corresponds well with the control strategy that is set to turn on the heat at 0.5°C above the L95 temperature, currently set at 18°C with a deadband of 2°C. The actual zone temperature would depend on the setpoints selected by the occupants. The temperatures for L95 and H95, which determine the heating and cooling control setpoints, will be input by the program user. Some users like to have a warm house, or a house with a fairly constant temperature throughout the year, whereas other users might endure more fluctuations in temperatures based on season in order to consume less energy. With the default settings and the new time-step and effective zone air capacitance, the heating load was 5,577 kWh and cooling was 5.3 kWh. A change in the heating setpoint to have the temperature remain between 20°C and 22°C increased the heating electricity consumption to 6,563 kWh; between 22°C and 24°C the heating load increased to 8,107 kWh; and between 24°C and 26°C the heating climbed to 10,013 kWh. Similarly, a decrease in H95 to 26°C from 28°C increased the cooling load to 63.1 kWh. These few cases show that the HVAC control strategy and setpoints used in the

modelling should be as close as possible to what the future house occupants will use. Section 6.6 examines if the selection of different setpoints leads to different optimal designs.

One of the advantages of an under-floor hydronic radiant heating system, such as in systems 2 and 5, is that it results in a higher mean radiant temperature (MRT), at the same zone air temperature, than an air-based system. This allows for a higher level of comfort to be achieved at the same temperature, or the same level of comfort to be achieved at a lower zone temperature. However, from Figure 5.2b, it is shown that the zone temperature for system 2, with the present control strategy, is higher than for system 1. For the month of January, the average zone temperature for system 1 is 19.8°C, and for system 2 it is 21.5°C. This difference in temperature is one of the reasons that system 1 consumes less heating energy then system 2. Another problem with the current control strategy is that it does not limit the floor temperature. If one again looks at January, the floor temperature often exceeds 30°C and has a peak of 33.8°C with system 2. ASHRAE Fundamentals 2001 recommends that the floor temperatures not exceed 27°C to 29°C in order to maintain comfort. There are two reasons why the zone temperature was higher with the hydronic heating. The first reason is that the floor has a high thermal capacitance, and when the room air temperature reaches the setpoint, there is still a lot of stored heat in the floor that increases the zone temperature beyond the setpoint. The second reason is that the current time lag of the system results in the heating generally being turned on in the early morning right before the sun comes out. The heating system tends to turns off right before the sun starts to shine on the floor, which then further increases the floor temperature, which boosts the zone temperature

higher. For example, system 1, which does not have active under-floor heating, has a maximum floor temperature in January of 26.8°C. If the floor almost reaches its maximum allowable range passively, one can see how it overheats with system 2, when the floor can be as hot as 29°C before the sun even starts to shine on it. Note that this would be even worse with south-facing windows larger than 50% and/or more insulation in the exterior walls. For example, with system 1, wall 8, 80% south-facing window coverage, and option 4 for the thermal mass, the heating load drops to 4,420 kWh, and the average zone temperature in January increases to 20.4°C with a maximum floor temperature of 31.9°C.

Due to the maximum floor temperature requirements, ASHRAE Fundamentals 2001 recommends against thermostatic controls based on air temperature to control the zone temperature in cases where the slab is the primary heating system. Instead, the heating system should be wired in series with a slab-sensing thermostat. Their recommended control strategy sets the slab temperature setpoint based on the outdoor temperature; at -19°C, the slab temperature would be set at 29°C, and for every 5°C increase in outdoor temperature, the slab temperature should be decreased by 1°C. This control strategy with recommended setpoints was implemented with system 2 and produced poor results. The heating went from 8,678 kWh to 13,087 kWh, the average zone temperature in January increased from 21.5°C to 24.6°C, and the maximum floor temperature increased from 33.8°C to 34.2°C. The reason for this decrease in performance is that the recommended setpoints are based on a typical house. With a highly insulated and airtight envelope, less heat input is required to maintain the setpoint at colder outdoor temperatures.

With the ASHRAE control strategy, the under-floor heating system is controlled based on the outdoor temperature, and it is not directly regulated with the zone temperature setpoints. This did not fit with the proposed user input zone temperature allowances, therefore, a modification was implemented that followed the same ASHRAE control setpoints, with the added stipulation that the under-floor heating system would only be turned on if heating was called for based on the previous control strategy using zone-air temperature. Hence, when heating is called for with the original control strategy, the floor is heated to a set-temperature related to the outdoor temperature. This was tried with the default setpoint, which had the $L95_h$ at 18°C. Different floor setpoints were tried to see the effects on zone and floor temperatures. It was found that using a floor temperature of 23°C at -19°C or colder, and a linear decrease in the floor temperature setpoint to 18°C when the outdoor temperature increases to 21°C produced the best results; this led to an annual heat consumption of 7,236 kWh, an average zone temperature in January of 20.6°C, and a maximum floor temperature of 29.1°C. However, as noted before, the optimal floor setpoints would vary based on the envelope configuration, and the desired zone temperature setpoints. The development of such a sophisticated control strategy for hydronic heating systems with varying floor setpoints based on each unique configuration and desired zone temperature setpoint is beyond the scope of this research. The determination of an optimal control strategy based on a specific design could be part of a later stage optimisation tool that refines the design and systems selected in the early design stages.

In the results analysis, it was observed that the zone temperature control with the hydronic heating system was better in the beginning of the cooling season, when heating

was occasionally needed. There seemed to be fewer fluctuations and better control. In the cooling season, the heating was set to turn on when the zone temperature was $\Delta 3c$ (0.3°C) above $L95_c$ (18°C) with zero dead-band. This control strategy was implemented for the whole year with system 2 to test its performance. This test case resulted in a yearly heating consumption of 7,340 kWh, with an average zone temperature in January of 20.0°C, and a maximum floor temperature of 30.3°C. This approach limits the floor temperature to the temperature required to maintain the minimum zone temperature at the desired zone setpoint. The floor temperature was above 29°C for 10.3 hours in January and above 30°C for 1.7 hours. A more detailed control strategy developed with the specific design configurations in the later design stages could better control the maximum floor temperature. Figure 5.5 shows the January zone temperature for system 2 with this new control strategy, and for system 1 with the existing control strategy.

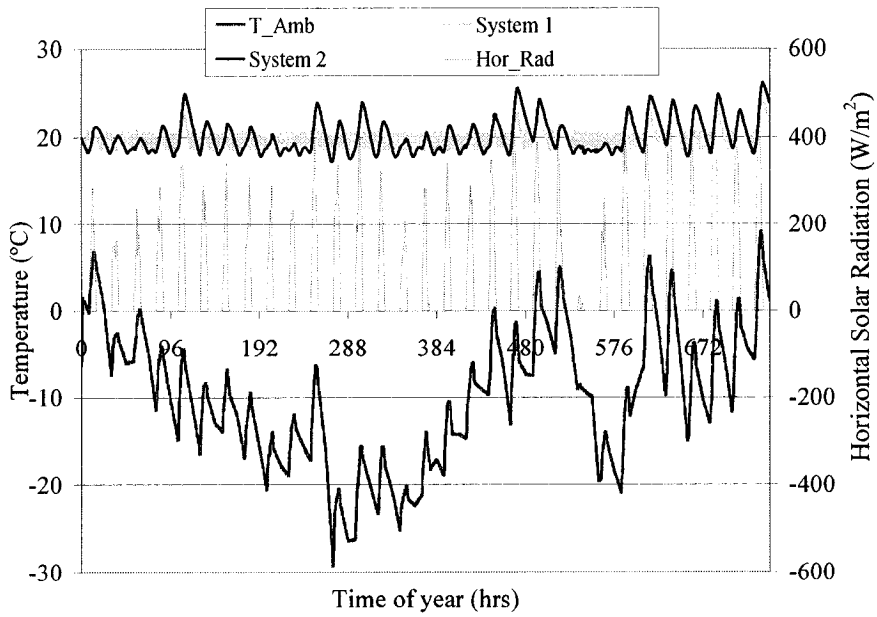

Figure 5.5: January temperatures for system 2 with new control strategy and system 1

As can be seen from Figure 5.5, the two heating systems stay reasonably well within the same bounds. System 2 has temperatures that oscillate on a frequency of 1-day whereas system 1 oscillates at a higher frequency. Near the end of the month, when the outdoor temperatures are warmer and the solar radiation is high, the predicted zone temperatures from the two systems converge, as expected, since this represents a situation with more passive heating. With lower outdoor temperatures and solar radiation as seen just after hour 500, system 2 maintains a lower temperature than system 1, which is acceptable as radiant based systems offer a more comfortable environment at lower temperatures. Finally, the peak zone temperatures from both systems occur at the same time, when the solar radiation peaks; the peaks are more pronounced with system 2, due to the higher initial floor temperature before the sun starts to heat up the floor, which then heats up the zone. As this new control strategy provided zone temperatures for radiant based systems that were closer to what is experienced with air-based systems, and allowed for the zone-temperature setpoints to be varied by the program user, it was implemented in all radiant based systems. Therefore, the under-floor heating systems (2, 5, and 7) have the same control strategy all year round, which corresponds to the initial heating control strategy applied in the cooling season, and the air-based systems have the same control strategy as initially specified.

It should be noted that the temperature fluctuation of the zone and floor, as well as the system performance, is dependent on the properties of the flooring material that is used above the radiant slab. In the simulation, 19 mm thick hardwood floor with an equivalent RSI value of 0.120 was assumed. If carpet is used instead, the RSI value increases to 0.366, and with tiles it decreases to 0.0088 (McQuiston, et al. 2005). When more

insulation is placed between the slab and the zone, it reduces the heat transfer from the slab to the zone, and it reduces the amount of solar radiation that can be stored in the slab. With more insulation, the solar radiation is released more quickly into room, which leads to higher peak temperatures. Table 5.8 shows the heating energy used for systems 1 and 2 along with the average temperature and peak floor temperature in January for the three different flooring options. The results show a large difference in maximum floor temperature for both heating systems. As expected, the difference in heating and mean zone temperature is more pronounced for the under-floor heating system. The use of carpet instead of tile increases the heating consumption by over 30%. Given that the difference is so pronounced, the model was changed to include a flooring option as an input, with hardwood flooring as default. No difference in cost was assumed between the different flooring options as this decision is based more on owner preference than costs. The inclusions of a flooring choice as an input in the program will allow owners to see how their floor type selection will affect the house's energy efficiency and comfort.

Table 5.8: Differences in results using different flooring options

	System 1			System 2		
	Heat (kWh)	Mean Zone Temp Jan.	Max Floor Temp. Jan.	Heat (kWh)	Mean Zone Temp Jan.	Max Floor Temp. Jan.
Carpet	5,303	19.19	28.86	8,605	20.56	33.51
Hardwood	5,143	19.03	26.02	7,340	20.00	30.30
Tile	5,067	18.87	23.06	6,517	19.32	25.66

Since the flooring RSI-value had a significant impact on the results, the other inputs to the flooring model were modified to see which inputs had the largest impact on energy consumption. Note that the number of nodes used in the model, the pipe length and configuration, and the floor temperature model were not examined as part of this

analysis. Default soil properties were used in the TRNSYS model; the thermal conductivity was 2.42 W/m·K, the density was 3,200 kg/m^3, and the specific heat was 0.88 kJ/kg·K. The properties for the specific heat and density seemed to be higher than what a typical soil would have; for sand the specific heat is generally 0.83-1.67 kJ/kg·K and the density is approximately 1300 kg/m^3, and for clay the specific heat should be 1.17-2.25 kJ/kg·K and 1,200-1,400 kg/m^{3}for density, respectively, (Abu-Hamdeh, 2003); the thermal conductivity for silt loam should be 0.2-1.4 W/m·K, for clay 0.1-1.5 W/m·K, and for sand 0.2-2.5 W/m·K (Usowicza, et al., 2006). A change in the soil properties did have an effect on the overall results; therefore, the default soil conditions in the model were changed to 1.0 W/m·K for thermal conductivity, 1,300 kg/m^3 for density, and 1.3 kJ/kg·K for specific heat in order to be more representative of a typical soil. These changes decreased the heating consumption of system 1 by 3.7% and of system 2 by 5.2%; the average zone temperature and peak floor temperature changed by less than 0.1°C for both systems.

Two other parameters had a noticeable impact on the simulation results: the mean ground temperature, and the under-floor insulation R-value. A mean ground temperature of 10.0°C had been implemented. A decrease to 5°C increased the heating consumption by 8.6% for system 1 and 7.7% for system 2. Given that this parameter varies with the local climate, the mean ground temperature, the ground temperature amplitude, and the day with the coldest ground temperature were added as inputs, with default values of 10°C, 10°C, and day 28, respectively. As for the under-floor insulation, the value that was initially used was RSI 4 (R-23). An increase in the insulation to RSI 5.3 (R-30), decreased the heating consumption by 2.7% for system 1 and 4.7% for system 2, whereas

a decrease to RSI 2 (R-11.5), increased the heating by 9.5% and 13.2%, respectively. Given the relative impact that the under-floor insulation had on the overall results, this parameter was added to the list of parameters to be optimised. The RSI values used for the optimisation were 0, 2, 4, and 6 (R-0, R-11.5, R-22.7 and R-34.1). The cost of the different options was approximated with a multiple of RSI 2 EPS, which are 3" thick, have a material cost of $\$5.60/m^2$ ($0.52/ft^2$), and labour costs of $\$4.09/m^2$ ($\$0.38/ft^2$) (RS Means, 2005a).

Most of the analysis thus far has been comparing systems 1 and 2, as this served as a good comparison between radiant and air based heating. Table 5.7 shows results from all systems, some of which have heating consumption values that call for further scrutiny. For example, the only difference between systems 6 and 8 is the fact that system 6 uses a desuperheater, yet the consumption varied significantly. Given that a few parameters had changed in the model since the analysis began, the two systems were re-evaluated. System 6 had a heating consumption of 2,180 kWh, and a DHW energy consumption of 1,179 kWh, and system 8 was 5,670 kWh for heating and 2,524 kWh for DHW. Typical desuperheaters work with geothermal heat pumps. In this case, there is a feedback loop, since the heat pump draws its heat from the top of solar thermal storage tank, and the desuperheater then heats up the bottom of that same tank. The main reason for the large difference in heating consumption is that the tank temperature for system 8 often drops below the setpoint temperature of 8°C. This drop in temperature causes the auxiliary heater to turn on, which is less efficient than a heat pump. In fact, if the auxiliary heater component is removed, the heating energy for system 8 drops to 1,499 kWh. In a typical situation, using a GSHP and a desuperheater in the heating season, the reduction in DHW

consumption is gained at the expense of the space heating capacity (Lee and Jones, 1997). However, this only implies that the heat pump has to operate for a longer period of time to meet the space heating requirements, but the hot water produced is still obtained with a relatively high coefficient of performance (COP) (Biaou and Bernier, 2005). Biaou and Bernier (2005) found that the DHW consumption dropped by 1,710 kWh (37.1%) with a desuperheater, and the heating energy increased by only 490 kWh (11.6%) for a total decrease in energy of 13.8%. In this case, there was a substantial drop in both DHW and heating.

Since system 6 is a novel configuration, it is difficult to determine what an appropriate performance would be. In addition, the product specifications for the heat pump state that a desuperheater can be added as an option, but they do not give any performance specifications for that option. To model the desuperheater, the six following parameters were used as inputs in Type 505:

1. Inlet DHW Temperature: Temperature from the storage tank
2. Inlet DHW Flow: Default value of 400 kg/hr used.
3. Refrigerant Temperature, Cooling: Default value of 60°C used.
4. Refrigerant Temperature, Heating: Default value of 55°C used.
5. Desuperheater UA, Cooling: Default value of 1,500 kJ/hr·K used.
6. Desuperheater UA, Heating: Default value of 1,500 kJ/hr·K used.

A variation in the parameters around the TRNSYS default values changed the results slightly, but not enough to account for the overall difference between systems 6 and 8. A variation in the refrigerant temperature had the most noticeable influence. To determine if the performance of system 6 was reasonable, its performance was compared with that

of system 4, which uses the same heat pump but with geothermal energy as the heat source. For system 4, the heating was 1,380 kWh, and the DHW was 1,896 kWh. System 4 had a combined heating and DHW load that was 83 kWh (2.5%) lower than system 6. If system 4 is used with the desuperheater with the same settings, the heating increases to 1,743 kWh (26.3%) and the DHW decreases to 756 kWh (60%), for a total 777 kWh (23.7%) reduction. This increase in performance is much better than what was achieved in (Biaou and Bernier, 2005); however, this does not mean it is not accurate as a lot of other parameters are different between the two studies. To err on the side of caution, the refrigerant temperature was reduced by 15°C. For system 4, this resulted in a heating load of 1,590 kWh (15.2%) and a DHW energy consumption of 1240 kWh (34.6%). This led to an overall decrease in energy consumption of 446 kWh (13.6%) with the desuperheater, which closely matches what was achieved in the previous study. For system 6, the heating energy decreased to 2,067 kWh and DHW energy consumption increased to 1,688 kWh.

Note that the above results were obtained with a 6 m^2 flat plate collector. If a 12 m^2 evacuated tube (ET) collector is used instead, the performance of system 8 improves to 1,470 kWh for heating and 1,771 kWh for DHW, which is slightly better than system 4 with a 6 m^2 flat plate collector. System 6, with a 12 m^2 ET solar thermal collector still performs better with 1,981 kWh for heating and 1,065 kWh for DHW. However, the difference in energy consumption between the two systems is smaller at only 195 kWh, which may make it more cost effective to use system 8 over system 6 for larger solar thermal collector.

From Table 5.7 we also see a large difference in heating consumption between systems 5 and 7. This is again a result of the tank temperature in system 7 that goes below the setpoint temperature of 8°C. With a 6 m^2 flat plate collector, the heating consumption of system 5 is 1,327 kWh and 1,890 kWh for the DHW consumption, and for system 7 it is 6,479 kWh for heating and 2,684 kWh for DHW. If we remove the auxiliary heater component of system 7, the heating energy is only 1,655 kWh. One item that was noticed in the results was that the auxiliary heater in the tank did not have a sufficient capacity to maintain the tank temperature above freezing. When the heat pump draws heat away from the tank, the temperature in the tank drops below –20°C, which is unrealistic. A re-examination of the results for system 8 found that the temperature in the tank dropped to –0.2°C. An increase in the tank auxiliary heater capacity from 4.5 kW to 10 kW improved the results; the tank temperature did not drop below 4°C for either case. This change in auxiliary heater capacity increased the heating energy consumption in system 7 to 7,847 kWh and to 5,752 kWh for system 8, and decreased the DHW consumption to 2,349 kWh for system 7 and 2,490 kWh for system 8. The DHW energy consumption dropped because it only considers the tankless heater component; the auxiliary heat is considered part of the heating load. The default auxiliary heater capacity was increased to 10 kW for all of the heating systems.

A look at more results with the 12 m^2 evacuated tube collector instead of the 6 m^2 flat plate collector shows the heating consumption of system 5 unchanged at 1,327 kWh and the DHW energy consumption drops to 878 kWh; for system 7 energy consumption for heating drops to 7,424 kWh and for DHW to 1,530 kWh. There is a slight improvement in the heating consumption and a more considerable drop in the DHW consumption with

the larger solar thermal collectors for system 7. However, the improvement was not as significant as it was for system 8 for the same change in solar collector area. This is due to the fact that system 8 cycles on and off over a 24 hour period, which permits it to take advantage of the solar energy. System 7 however, generally turns on for longer periods of time and generally at night when there is no solar radiation; therefore it can take advantage of some stored solar energy in the tank, but soon depletes it and requires the auxiliary heater. The system was using tank 1, the smallest option, and if the tank size is increased it should improve the performance. With tank 4, the energy consumption drops to 6,731 kWh for heating, increases to 1,781 kWh for DHW. For these same conditions, system 2 has an energy consumption of 6,072 kWh for heating and 1,154 kWh for DHW.

Given that system 7 performs worse than the base radiant system 2 and costs more money, it does not make sense to keep it as a heating system option, since it will never be more cost effective. In order to keep eight heating systems, it was decided to replace system 7 with a different option. One option was to use a variation of system 2 with a heat pump water heater (HPWH) to heat the water. This type of heat pump system extracts heat from the zone air to heat the hot water. However, instead of this option, it was decided to use the geothermal system 4 with a desuperheater, since it can offer good energy savings. The HPWH option would be more appropriate in hotter climates as the heat extracted from the air acts as an air conditioning unit, which provides cooling for the house.

5.2 Optimisation Parameter Refinement

In this section, the impacts that different inputs and assumptions have on the performance of the GA Optimisation Tool and on the optimal configurations are tested.

The analysis done in this section will help determine whether some parameters should be eliminated from the optimisation, or their ranges changed, as well as determine the effects that certain assumptions and inputs have on the overall results. Unless otherwise stated, the following default inputs will be used in the tool:

- A 150 m^2, two-storey house in Montreal, with southern orientation and hardwood flooring;
- A target energy consumption of 0 kWh per year;
- A constant rate for electricity purchase and sale at $0.10/kWh, escalating at 2% per year;
- A 25 year mortgage at a 5% interest rate;
- Inflation of 2% per year;
- The default thermal comfort and control parameters listed previously; and
- As recommended by the GA program developer, a uniform crossover with a cross-over probability of 50% with the micro-GA (Carroll, 2005).

A total of 40 different cases, as listed below, were run through the GA Optimisation Tool in order to both test the performance of the tool and to analyse how variations of the inputs alter the optimal design, with the results summarised in Appendix G:

- Case 1: Default values, 5 individuals per generation, 160 generations;
- Case 2: PV cost of $7000/kW, 10 individuals per generation, 80 generations;
- Case 3: Lot orientation 45 deg SW, 5 individuals per generation, 250 generations;
- Case 4: Iqaluit weather data, Montreal costs;
- Case 5: Nanaimo weather data, Montreal costs;
- Case 6: Sacramento weather data, Montreal costs;

- Case 7: Montreal weather, 1 story house, Sacramento latitude;
- Case 8: House at 300 m^2;
- Case 9: One storey house, Montreal latitude;
- Case 10: Target consumption of 2,000 kWh per year;
- Case 11: Target consumption of 4,000 kWh per year;
- Case 12: Target consumption of 6,000 kWh per year;
- Case 13: Target consumption of 8,000 kWh per year;
- Case 14: Target consumption of 10,000 kWh per year;
- Case 15: Target consumption of 15,000 kWh per year;
- Case 16: New parameter ranges, default values;
- Case 17: Lot orientation 45 deg SW;
- Case 18: Lot orientation 45 deg SE;
- Case 19: Montreal weather, high-cost city (Toronto);
- Case 20: Montreal weather, low-cost city (Charlottetown);
- Case 21: Variation 1 in heating system costs (see Table 5.10);
- Case 22: Variation 1 in heating system costs, Nanaimo weather (latitude);
- Case 23: Variation 1 in heating system costs, target 8,000 kWh per year;
- Case 24: Time of day rates 1, $0.15/kWh days, $0.03/kWh nights, 2% inflation;
- Case 25: Time of day rates 2, $0.30/kWh days, $0.03/kWh nights, 2% inflation;
- Case 26: Time of day rates 3, $0.45/kWh days, $0.03/kWh nights, 2% inflation;
- Case 27: PV buy-back at $0.25/kWh (no inflation of sale price);
- Case 28: PV buy-back at $0.50/kWh (no inflation on sale price);
- Case 29: PV buy-back at $0.75/kWh (no inflation on sale price);

- Case 30: Financing options as used in BEopt (30 years, 7% interest, 3% inflation);
- Case 31: Objective function + [0.0915*electricity consumption];
- Case 32: Controls: L95 20°C, H95 26°C, Min: 18°C, Max 29°C;
- Case 33: Carpet as floor finish;
- Case 34: PV cost of $11,250/kW;
- Case 35: Change base loads to 75% of default values;
- Case 36: Change base loads to 150 % of default values;
- Case 37: Remove roof and comfort penalties;
- Case 38: Remove blinds;
- Case 39: Change blind control so that blinds are on when incident solar radiation is greater than 200 W/m^2; and
- Case 40: Change fitness function so that it optimises to minimise energy.

The first case uses 5 individuals per generation with a total of 160 generations, the second case uses 10 individuals per generation with a total of 80 generations, and third uses 5 individuals per generation with a total of 250 generations. As mentioned earlier, the GA samples only a minute fraction of the total possible design configurations. In order to determine how well a GA algorithm performs, one should repeat the optimisation more than once with different initial populations to test for repeatability. Without a repetition of the run with different initial populations, it is impossible to determine whether the results were obtained by chance through a good initial population or if they can be achieved regardless of the initial population. The GA program itself works with an embedded random number generator. To change the numbers that are generated, and hence the initial population, the seed value to the random number generator is changed.

Case 1 and 2 were repeated five times, and the remaining cases were repeated three times as in (Wang, et al., 2005). The average cost function of the fittest individuals for case 1 was 1.9% above the fittest value found with the manual sequential search around the fittest individuals. For case 2, the average fittest individual was 5.3% above the fittest manual individual, and for case 3 it was 0.2% above the fittest individual. Based on these preliminary results, the remaining 37 cases used 5 individuals with 250 generations. Although 5 individuals over 250 generations leads to 1,250 individuals, approximately 900 unique configurations were tested per run, for a total of around 18 hours of computation. So, for three runs, each case resulted in approximately 2,700 TRNSYS evaluations, which took approximately 54 hours to compute.

After the first 15 cases were finished, a preliminary analysis was done to determine if certain parameters could be changed. The performance of the GA program for cases 1 through 15 is summarised in Appendix G; the results indicate that in general, the GA program finds close to optimal solutions for a range of different inputs. Provided that the best manual solution was indeed the fittest possible solution, all of the best GA solutions were from 0.07% to 9.1% above the fittest value. Case 2, which used 10 individuals instead of 5 in each generation, performed the worst, although fewer unique configurations were evaluated than in subsequent cases. The best performance was achieved with case 3, which was on average only 0.2% away from the fittest value. Looking at the repeatability in the performance of cases 3 to 15 with the same GA parameters, one can see that the performance of individual runs with those GA parameters ranged from 0% to 5.8% above the fittest possible value. The best performing

individual with the GA were within 1% of the optimal value 61.5% of the time and found the optimal solution 5.1% of runs.

With the parameters set as they were for cases 1 through 15, there are a total of 549,755,813,888 different possible design configurations. Given that fewer than 1,000 different design configurations are evaluated per run, it is unlikely that the fittest individual will be found. In many cases, the fittest design solution only had 1 or 2 parameters that were different than the fittest design found manually. In this section, a parameter-by-parameter examination is done to see if refinements can be made to improve the tool either through the expansion or reduction of the range of parameters considered.

Form: This parameter was set at a range between 1.0 and 2.0 divided into 8 equidistant discrete values. In general, form was often one of the parameters that was off from the most optimal value due to its relative low cost value from one discrete value to the next. For example, a change in the form from 1.00 to 1.14 led to differences in the cost function of between $0.05 and $1.10, depending on the case in question. Of the 15 cases studied, the form of the fittest value ranged from 1.00 to 1.29. Given the relatively low cost of varying form, higher form values may be preferable due to increased daylight penetration and other architectural considerations including interior layout and aesthetics. It is possible that with a non-south-facing lot, that an optimal form of less than 1.00 could be optimal, which was not considered up to now. Given the results obtained, the range of form was reduced from 0.8 to 1.4 with increments of 0.2 between each value. A reduction in the possible values from 8 to 4, and an increase in the difference between the values should improve the performance of the tool when it finds the most optimal form

for the given optimisation cost function. The user should be aware that if a form of 1.2 is found to be optimal, then values plus or minus 0.1 around the optimal value are within the optimal range.

Heating System: With the current setup, 14 of the test cases had system 7 as the optimal system, with the exception of case 6, which had system 1. However, given that there can a big difference in the system prices, compared to what was used in the study, and that the system price can play an important role to find the most cost effective system, the different heating systems were not changed at this point. Instead, different price scenarios were evaluated to see how they affect the overall results.

Cooling: The optimal configurations varied between having active cooling on or off, therefore no changes were made to this parameter.

Window Type: Optimal window types varied between options 1, 2, and 4, therefore, no changes were made to this parameter.

South Window Area: Optimal window area varied from 20% to 80% wall coverage. In most cases, a change in the window coverage of 10% changed the optimal cost function by less that $1. The range of south window area was reduced from 20% to 80% with a step-size of 20%. As with form, the user must be aware that the optimal value obtained is a range of plus or minus 10% of the value obtained. An optimal range gives more flexibility to the designer with minimal repercussions in terms of cost effectiveness.

East and West Window Areas: The minimum allowable window area (5% wall coverage) was found to be the most optimal value, with the exception of the cases where the house orientation was not south-facing. In case 3, when the lot faced 45° SW, the optimal east window area was at its maximum allowable value of 20%. In fact, the best performance

was obtained at an area of 25%. In order to keep the functionality to find optimal window sizes at non-south-facing orientations, the range of window areas was increased to between 5% and 35%, with 10% increments.

North Window Area: For all cases studied, the north window area was optimal at its smallest allowable value of 5% wall coverage. This parameter was changed from a parameter that is being optimised, to a user input; the user will input the minimum allowable north window area. For the remainder of the cases studied in this thesis, a value of 5% is used.

Overhangs: In all cases, the most optimal design was found with no overhangs. Given the position of the sun, typically south overhangs are more efficient than other orientations. Note that another study that evaluated optimal building design in Montreal with a GA resulted in convergence of window sizes to their lower bounds for the north, east, and west facades and varying results for the south façade, and no overhangs on the north, east, and west facades, and minimal overhangs on the south (Wang, et al, 2005). One of the reasons that overhangs were found to be non cost-effective for the cases evaluated in this study is that the house was modelled as one zone, which reduced the simulated peak zone temperatures. As is shown in Figure 3.3, the one zone simplification reduces the modelled peak temperatures. If two zones are used, overhangs may work well to reduce the peak temperatures in the south zone. In the current model, overhangs for the east and west windows were removed, and in the south orientation, only having no overhang or a 1 m overhang was considered. The user will be informed of the limitations of this model, and will be encouraged to evaluate the potential benefits of the use of overhangs with a more detailed model in the later stages of design.

Collector Type: Both collector types were found to be optimal depending on the case and therefore both are kept.

Collector Area and Tank Size: Collector areas that ranged from 3-12 m^2 were found to be optimal. In more than half of the cases, a collector area of 12 m^2 was found to be the most optimal. It is possible that a larger collector area would be more optimal. In Europe, systems vary in size such that the solar contribution of the heating systems ranges from 10% to 100% (Weiss et al., 2003). In the Netherlands, small systems which comprise of 4-6 m^2 of collector and a 0.3 m^3 (79.3 gal) storage tank are typical, whereas in Switzerland, Austria, and Sweden, larger systems with 15-30 m^2 of collector area and 1-3 m^3 of thermal storage are typical. Therefore, the collector area range was expanded to 3-24 m^2 with a 3 m^2 step-size. In order to accommodate the larger allowable collector area, the tank size was also expanded by adding 4 more increments of 0.227 m^3 (60 gal) above the largest tank. The tank sizes range from 0.250 m^3 to 1.590 m^3 (66-420 gal). Costs for these additional collectors and tanks sizes are assumed to increase linearly with the costs that were already used.

Roof Slope: Optimal roof slopes varied from 1 to 8 and this parameter was left as is.

Wall Number: The most efficient wall varied between walls 2, 7, and 8. ICFs were not found to be cost effective at this time. However, if the costs between the different walls were to change, it is likely that the most cost effective wall would also change. The wall selection is not changed.

Thermal Mass: The addition of thermal mass was not found to be cost effective. This can be due in part to the fact that only one zone was modelled which reduces the amplitude of the temperature variation. As well, the addition of a brick layer on the inside of each wall

can be expensive. Depending on the floor layout, which is not known in the early stages of design, a brick layer can be added to one select wall that would have the most benefit. In addition, the base case has 10 cm of concrete, which is already a significant amount of mass. The thermal mass parameter options were changed such that the use of an internal brick wall was no longer an option, and the slab thickness was set to vary between 7.5 cm and 15 cm, instead of 10 cm and 20 cm. In later stages of design, the addition of more thermal mass in the form of an interior brick wall can be considered.

Slab Insulation: In most cases, no insulation under the slab was found to be most cost effective. However, with the colder Iqaluit weather, a slab insulation of RSI 4 was found optimal. Given that the floor concrete thickness was decreased, the slab insulation parameter was kept as is. For cases where under-floor heating is used, it is likely that some level of insulation under the slab would be optimal.

With the above changes to the parameters and their allowable ranges, the solution space was reduced to 2,147,483,648 possible designs, which represents only 0.4% of the initial solution space. For the first 15 cases with the original parameters, the GA Optimisation Tool found an optimal design that had a monthly cost function that was on average 1.13% above the optimal value. With the new set of parameters and reduced solution space, the average performance actually deteriorated with the average performance being 2.65% above the fittest configuration. However, the new set of parameters found the fittest individual 16.0% of the time, whereas with the old set it was only 4.5% of runs. This translates to the new set of parameters finding the fittest individual in 48.0% of cases tested compared to 14.3% of cases with the old parameters. The reason the average performance of the tool deteriorated with the new set of

parameters was because the range of collector area and tank size was doubled. The optimisation program had difficulty finding the optimal combination of collector area, tank size, and roof slope, and the combination of these parameters had a larger effect on the overall cost function than some of the other parameters that were considered in the first set of parameters. Therefore, with the smaller solution space, the program was more capable of finding the fittest individual, yet when it did not, the optimal cost function that was found was generally slightly greater than the fittest value in comparison to cases which used the first set of parameters.

5.3 Effects of Modelling Assumptions on Optimisation

5.3.1 Effects of Assumed Costs

In this subsection, the assumed cost of the energy efficiency upgrades and renewable energy technologies are examined to determine if this parameter has a large impact on the determination of the optimal configuration. As a reference, the costs associated with the base case house in Montreal (Case 16), are shown in Table 5.9. The PV accounts for 73.9% of the costs, and the combined active solar costs represents 86.5% of the upgrades, without including the cost of the bigger storage tank. Recall that the costs associated with a very airtight envelope and more energy efficient appliances are not considered in the analysis.

Table 5.9: Breakdown of the cost of the upgrades in the base case

Upgrade Item	Associated Costs		
	Base case ($) [% of total]	Updated heating system costs ($) [% of total]	PV system cost of 7 $/W ($) [% of total]
Heating system	$2,804 (3.1%)	$15,000 (14.5%)	$2,804 (4.9%)
Exterior walls	$2,335 (2.6%)	$2,335 (2.2%)	$134 (0.2%)
Window type	$3,081 (3.4%)	$3,081 (3.0%)	$2,800 (4.9%)
Roof slope	$2,391 (2.6%)	$2,391 (2.3%)	$2,391 (4.2%)
Solar collector	$11,473 (12.7%)	$11,473 (11.1%)	$9,858 (17.2%)
Thermal storage	$1,579 (1.7%)	$1,579 (1.5%)	$1,306 (2.3%)
PV system	$66,842 (73.9%)	$67,898 (65.4%)	$37,981 (66.3%)
TOTAL COSTS	**$90,506**	**$103,757**	**$57,292**
Monthly mortgage	$523.25	$599.86	$331.23
NPV monthly mortgage	$414.97	$479.72	$262.69

As mentioned, one of the benefits with RS Means to obtain cost data is that it provides a table of material and labour cost multipliers that account for differences between cities. In order to determine if the use of different prices based on these multipliers made a difference, two runs were done with different city cost multipliers; everything else was kept constant, including climate. Recall that in the program, the cost multipliers affect the cost of each parameter, except the PV and overhang. The cost multipliers for Toronto are 124.4 for material, and 95.0 for labour; in Charlottetown they are 117.8 for material and 58.7 for labour; and in Montreal they are 118.8 for material and 81.4 for labour. For the given problem, the most cost effective solution remained the same with all three cost multipliers. The only change was in the total costs of the upgrades ($88,900, $90,506, $92,123) and the resulting optimisation cost function ($407.12, $414.98, $422.34) for Charlottetown, Montreal, and Toronto costs, respectively. The GA program found similar solutions for these three cases, yet it used

different paths to get there. In this case, the relative cost difference with the different cost multipliers was not enough to change the cost effective design. For different initial conditions, such as a different house size or energy target, or larger regional differences in prices, the effect of regional cost differences could change the optimal design. However, the differences in regional costs will likely be less substantial than differences attributed to regional solar and climatic differences.

One of the disadvantages with RS Means is that there is generally only one cost given per item, with no differentiation between high quality energy efficient products and lower efficiency products, which makes the costs less accurate. In general, the costs given by RS Means seem lower than what one would expect. The author replaced all the windows in his four-plex in 2006 with energy efficient low-emissivity coated argon filled windows, and can attest that he paid quite a bit more than the value calculated with the RS means costs. Without significant costing experience, one can also neglect to consider balance of system costs. For example, a quadruple pane window might require more framing around the window, which increases the installed costs beyond simply the additional costs of the window system.

RS Means also seems to underestimate the true costs for heating systems. The Ph.D. thesis supervisor for this thesis, Dr. A.K. Athienitis, recently constructed a low energy solar home as his personal residence (Athienitis, 2007). Dr. Athienitis found that a 2-ton one-stage air source heat pump with ducting and an HRV cost between $15,000 and $17,000, whereas the price went up to $23,000 for a high-quality 2-stage system. To upgrade to a geothermal air based heat pump, the price increased by approximately $4,000, which included a 122 m (400 ft) deep vertical borehole. To change the heat

pump to a water-to-water geothermal heat pump added an additional $2,000. Note that all of these are the installed costs that include ducting, HRV, circulation pumps, etc, which would be more than the prices used from RS Means in which we focused primarily on the heating system costs and not the whole balance of system costs. An optimisation run was done with new costs outlined in Table 5.10. To consider the base case cost for system 1, an assumed cost of $12,000 was used that would include all ducting and the HRV. In addition, the cost of the desuperheater was increased to $1,000 as indicated by (Earth Energy Society, 2007). It was also assumed that the use of the solar thermal tank instead of the geothermal borehole as the heat source would cost $1,000 in labour and accessories. As system 2 generally consumes more energy than the other systems, the price for this system was assumed to be half the cost of system 1, in order to see if a substantial price reduction would make the system more cost effective.

Table 5.10: Modified heat system costs

System Number	New Costs ($)	Original Costs ($)
1 – Simple electric furnace	$0	$0
2 – Under-floor heating solar + electric backup	$(6,000)	$664
3 – Efficient air-source heat pump	$11,000	$1,341
4 – Ground source heat pump, air heating	$15,000	$3,413
5 – Ground source heat pump, hydronic heating	$17,000	$3,413
6 – Water-to-air heat pump, solar sourced, desuperheater	$13,000	$1,009
7 – System 4 with desuperheater	$16,000	$3,813
8 – System 6 without desuperheater	$12,000	$1,009

These revised costs seem to be closer to costs provided by various sales representatives, when the author visited the National Home Show in Montreal in March 2007. Various vendors were approached and asked what it would cost to install a 2 ton

heat pump in the author's residence. For a complete system, the geothermal system costs in the range of $20,000 to $25,000. This cost includes the costs for ducting and a HRV ($10,000 to $15,000), the cost to drill the borehole ($6,000 to $7,000) and the cost of the heat pump itself ($5,000 to $6,000). The cost of an efficient air source heat pump was approximately the same cost as a geothermal heat pump minus the cost for the borehole. One manufacturer who sold ENERGY STAR windows was asked about the price differential between different window types. A double-glazed window with a low emissivity coating and an argon fill was said to be approximately 8% more expensive than a typical double glazed window. To change to a triple glazed window with low emissivity coatings and argon fill was said to increase the price by approximately an additional 20%. Based on the costs from RS Means that were used for this study, the costs for the low emissivity coating and argon fill were estimated at an additional 24.8% for the double glazed windows and the upgrade to a triple glazed window was assumed to cost an additional 21.1%, or 51.3% more than a standard double glazed window. One vendor from an insulated concrete form manufacturer was asked about the cost premium for their product compared to standard construction and it was said to cost approximately 3-4% more. The cost difference used in the tool between walls 2 and 3, which have comparable R-values, put the ICF at 21.3% more expensive. This large discrepancy might explain why walls 3 to 5 were never found to be cost effective. Only the effect of the heating system prices is considered in the analysis. It is evident that a commercial release of this type of tool that uses product costs should involve various manufacturers of the different products in order to identify more accurate costs.

A significant increase in costs for the heating system resulted in very little change to the most cost-effective solution. The only difference from the default case is that the most optimal system is now heating system 4. The increase in the cost of the desuperheater from $400 to $1000 made it more cost effective to increase the overall PV capacity rather than to use the desuperheater. The annual electricity consumption increased from 5,034 kWh to 5,113 kWh. The overall costs of the upgrades increased from $90,506 to $103,757, which resulted in an increase in the optimisation cost function from $414.98 to $479.72. As can be seen in Table 5.9, with the new heating costs, the PV accounts for 65.4% of the costs, and the combined active solar costs represent 76.5% of the upgrades, without including the cost of the bigger storage tank. In order to test if these new heating system costs might play out differently for different scenarios the optimisation was repeated with these costs for two other scenarios: one with Nanaimo weather and a target annual net-energy consumption of 0 kWh, and one with Montreal weather with a target consumption of 8,000 kWh.

In the case with the Montreal weather data and a target consumption of 8,000 kWh, the resulting optimal configuration is completely different with the new heating system costs. Instead of having heating system 7 as optimal, the optimal design uses heating system 1, namely the electric furnace. With the ground source heat pump there was less need to minimise the energy consumption with the other parameters, so one saw a minimisation of costs with the minimum window sizes of the basic double glazed window, minimum collector area with the smallest tank, flat roof, and wall 2. Now with heating system 1, the window went from the least efficient to the most efficient, the south window coverage went from 20% to 60%, the collector area from 3 m^2 to 9 m^2, the tank

from 250 L to 303 L, the roof from flat to a 14° slope and the wall from wall 2 to wall 8. The new optimal configuration with the higher heating system costs has a monthly cost function of $126.69 compared with $103.12 with the old costs. However, if we were to use the same configuration as the old optimal, with the new costs, this would result in a monthly cost function of $165.58.

The use of the new heating system costs with the Nanaimo weather data also led to different optimal configurations. In fact, two optimal configurations emerged, one with heating system 7 and the other with system 1. There was not much difference in the new optimal configuration with system 7 compared to the optimal configuration obtained with the previous heating system costs. Given the new window step-size of 20%, the optimal window size dropped to 20% from 30%, and the wall changed from wall 2 to wall 8. On the other hand, there are many differences when looking at the optimal configuration with heating system 1. The optimal window coverage is 40% instead of 30%. The collector went from a 12 m^2 evacuated tube collector to an 18 m^2 flat plate collector. The change in collector resulted in the optimal tank size to increase from 681 L to 908 L, and the roof slope changed from 45° to 56.3° in order to accommodate the larger areas so to avoid roof size penalties. The optimal with heating system 1 also called for RSI 2 insulation under the slab. The monthly electricity consumption for the optimal configuration of system 1 is 5,583 kWh compared to 4,932 kWh with system 7. The monthly cost function for the optimal configurations with the new heating system costs was $468.56 for heating system 7 and $465.81 with heating system 1 up from $400.07 for the optimal configuration with the old heating system costs. These results show that the program can find two very different optimal configurations of almost identical monthly costs. The differences are

also not very intuitive, which would make it difficult to arrive at both optimal designs with only manual iteration. The sequential search technique used in BEopt (Anderson, et al., 2006) would also fail to find two different design configurations of a net-zero house since it would not optimise all the parameters for two different heating systems.

Another area where differences in assumed costs might play a large difference is in the prices assumed for the installed PV. The price of an installed PV system can vary significantly from one country to the next, and even within a given country. The installed costs of a grid connected PV system under 10 kW in size in 2004 was between 10.40-11.20 $/W in Canada, 7.00-10.00 $/W in the US, 4.90-14.80 $/W in France and was reported as 6.20 $/W in Japan and 6.50 $/W in Germany, all in US denomination (IEA PVPS, 2005). Based on these numbers, a cost of 13.52 $/W (CDN) was used in the GA Optimisation Tool. If prices were to drop to say 7 $/W, which would be comparable to the price indicated for other countries, this could significantly affect the optimal design. For the default case, a change in the installed PV cost to 7 $/W increased the optimal form from 1.00 to 1.14, decreased the south window area from 60% to 50% wall coverage, reduced the collector area from 12 m^2 to 9 m^2, reduced the tank size from 681 L to 454 L, and found that wall 2 was more cost effective than wall 8. The resulting optimal design had an electricity consumption of 5,374 kWh and upgrade costs of $56,260 for an optimal cost function of $258.00. As expected, these new PV costs resulted in a significant improvement in the cost effectiveness of ZESH. If one used the optimal design found with the higher PV costs with the new PV costs, it would result in an upgrade cost of $57,515 and an optimisation cost function of $263.71. Note that the assumed cost of 13,52 $/W was based on data from 2004. The 2005 data shows a cost

between 10,04 $/W and 12,46 $/W for an average of 11,25 $/W (IEA PVPS, 2006). Therefore, the reported installed price of a PV system dropped by 16.8% in a single year. As can be seen in Table 5.9, with a PV system cost of 7 $/W the PV now accounts for 66.3% of the costs, and the combined active solar costs represents 83.5%, only down by 3% from to the base case.

The effect of the assumed costs of renewable energy and energy efficiency measures does play a role in the design process. The author had the privilege to look at the internal design submissions for the EQuilibrium competition, and the submissions were a good demonstration of this. Many, if not all of the teams, used some element of cost optimisation in their design charrettes. They would compare the cost of an energy efficiency upgrade with the cost to use PV to generate the equivalent amount of electricity. The assumed costs of the PV and other energy efficiency measures had an effect on the amount of insulation used, the selected heating system type, and on the type and size of the active solar technologies. Given that in the near future, many low and net-zero energy homes will be designed using an integrated design process, it would be of great value for design teams to have up-to-date costs of various design alternatives. Designers could then use these costs in combination with their own internal costs to more accurately determine a cost-effective combination of energy efficiency with active and passive solar technologies.

5.3.2 Effects of Using Different Base Loads

As discussed earlier, the behaviour of the individuals who live in the house has an impact on the overall energy consumption. In Section 6.6, the effect of changing the thermostat control setpoints will be discussed. Depending on what appliances are used,

and how they are used, the major and minor appliance electricity consumption can vary. In order to test what impact this had on the resulting optimal configuration, the optimisation was run with 75% and 125% of the base loads, which includes lighting and the major and minor appliances. Note that the loads were simply multiplied by a factor of 0.75 or 1.25 to change the total electricity.

There were very few changes in the optimal design when the base load was changed. The main difference was that the roof slope increased from 36.9° to 45.5° to 51.3° as the base load increased, in order to accommodate larger PV panels. The only other difference occurred with the 125% base load design, which had RSI 2 under the slab in the optimal configuration. The reason for this was that there was a monthly roof penalty of $7.72 without insulation, which dropped to $2.75 when it was added. The addition of a further RSI 2 dropped the penalty to $1.03, which was not enough to compensate for the cost of the added insulation. Without the penalty, the case without the insulation has a lower monthly cost function.

Although there were few changes in the optimal configuration, Table 5.11 shows that there were some significant differences in terms of costs. The assumption of a base load that consumes 25% less electricity, changed the roof slope and reduced the required PV size by 800 W, which translated to an initial cost savings of $12,888, and a 14.2% reduction in the monthly cost function. Whereas increasing the consumption by 25% increased the up-front costs by $15,254 and the cost function by 17.5%.

Table 5.11: Optimisation results changing base electric load

% Base load	Electricity Generated & Consumed (kWh/yr)	PV Size (kW)	Roof Penalty ($/mth)	Efficiency Upgrade Costs ($)	Monthly Cost Function ($)
75%	4,189	4.1	0	77,618	355.88
100%	5,034	4.9	0	90,506	414.98
125%	5,863	5.8	2.75	105,759	487.66

5.3.3 Effects of Assumed Penalties

The optimisation was repeated with the comfort and roof size penalties removed in order to see if a different optimal design would emerge. The comfort penalties had no effect on the resulting optimal configuration. The removal of the roof penalties did result in a few slight changes, namely the optimal roof slope went down to 36.9° from 45° and the optimal tank size decreased from 681 L to 454 L. Note that the available roof area is highly correlated with the roof slope. At 0°, the available area is only 37.5 m^2 and at the maximum roof slope of 60.3° it is 75.7 m^2. In this particular situation, the available roof area at 36.9° is 6.1 m^2 less than at 45°. The roof penalty of the new optimal design would have been $61.56, representing 6.16 m^2 of inadequate roof area. The annual electrical consumption of the new optimal design actually increased by 63 kWh; however, the cost function without the penalty was $409.59/mth instead of $414.93/mth. This difference came from the savings of the reduction of the roof slope and the use of a smaller storage tank, which resulted in savings of $1,175 in upfront costs. Other cases, such as when hotter or colder climates or stricter heating and cooling control setpoints are used, would likely have resulted in different optimal configurations, with the comfort penalty removed. However, the effects of this were not tested in this study due to the time

constraints imposed by the computational time required to evaluate each hypothetical case. A more elaborate study, which is beyond the scope of this thesis, should be done to find the exact value of the cost penalties to use, through a variation of the penalties on multiple design cases that are constrained by comfort and roof size.

5.3.4 Effects of Blind Modelling Approach

The use of blinds is often not considered when modelling the energy consumption of a house. When blinds are included, different modelling and control approximations are assumed. Two cases were run through the optimisation program to see what effects the blinds had on the optimal configuration. The first case considered a removal of the blinds completely to verify if a different optimal solution would have been reached if blinds had not been included in the modelling. The second case used the same temperature control strategy, with the added assumption that the blinds would be lowered when the incident solar radiation on a window exceeded 200 W/m^2 to represent a case where someone systematically lowers the blinds to avoid glare. These two cases were selected to see how the different extremes of blind use played into the optimal design configuration.

Both cases resulted in some changes to the optimal configuration. Without the blinds, the cooling load increased, which increased the size of the required PV panel, which added more restrictions on the roof size. Without considering the penalties, the optimal configuration was that of the base case with an increase in the annual electricity consumption of 135.3 kWh. However, the optimal design did have \$8.53/mth in roof penalties and \$500/mth in comfort penalties. The zone temperature exceeded Tmax_c for 2.7 hours and $H95_c$ for 103.3 hours. To eliminate the comfort penalties, the new optimal design has only 40% south window coverage and the form changes to 1.2. The form and

window coverage are interrelated; for a form of 1.2, the window area is slightly larger than at a form of 1.0 and still avoids comfort penalties. An increase in the form to 1.4 produces better results in terms of energy without the incurred comfort penalties by reducing the yearly electricity by 15.8 kWh, which was not enough to compensate for the increased cost of the envelope, although the difference was negligible at $0.11/mth. To compensate for the roof penalties, the collector area decreases to 9 m^2, which reduces the optimal storage tank size to 454 L. Compared to the base case, the new optimal consumes 7.6% more electricity at 5,415 kWh, but the cost function is only 2.8% higher at $426.62/mth. It is interesting to note that although the addition of RSI 2 of insulation under the slab reduces the annual electricity consumption by 80 kWh, it results in $11.33/mth of comfort penalties, since the added insulation keeps the solar gains in the house in the summer.

For the case with the blinds down when the incident solar radiation increases beyond 200 W/m^2, the solar gains from the windows are reduced. Therefore, the optimal south window coverage becomes the lowest allowable at 20% since it becomes a source of heat loss as opposed to a heat gain. An interesting result is that the optimal heating system becomes system 5, the ground source heat pump with radiant heating. The reason that the radiant heating system might be underperforming with more solar radiation is based on the simple control strategy that is in place. There are interesting dynamics that are occurring when radiant heating systems are coupled with passive solar heating with solar radiation incident on the same floor. To take advantage of these dynamics and maximize energy savings, more advanced control algorithms need to be used (Athienitis and Chen, 2000). Therefore, with more sophisticated control strategies, it is possible that system 5

would be more efficient even with higher solar gains. The lower amount of solar radiation going through the windows increased the annual energy consumption, which increased the roof slope to 51.3° to avoid roof penalties. With the larger roof area, the optimal collector area increased to 15 m^2 with the optimal storage tank volume unchanged at 681 L. One last difference with the optimal configuration compared to the base case is the use of RSI 2 insulation under the slab. Compared to the base case, the new optimal consumes 5.7% more electricity at 5,319 kWh, and the cost function is 9.5% higher at $454.51/mth.

These results show the importance to properly model the blinds and their control. As most houses use some type of window coverings, it is important to include their effects in the modelling. However, often times the coverings are typically used for aesthetics and/or privacy concerns, the control of which changes depending on the occupants; this makes it difficult to properly model the controls in the simulation. The use of motorised blinds with automated controls might change that. However, although the use of these types of technologies is emerging in commercial buildings, it might take a while longer before they become commonplace in houses. Alternatively, a manual blind control could be assumed that would optimise energy efficiency and minimise occupant interaction. Homeowners could then be given a lesson on how best to operate the window coverings in order to improve the performance of their house.

5.3.5 Effect of the Objective Function

Up to this point, the objective function used in the optimisation has been the net-present value of the monthly costs associated with the utilities and the financing costs of the energy efficiency and renewable energy upgrades. The use of this objective

function should lead to a family of very nearly optimal designs. The objective function was changed such that the GA would try to minimise the annual electricity consumption, without the inclusions of penalties for comfort and insufficient roof size. Some interesting design features emerged with electricity as the objective function. As one might expect, the solar thermal collector area was maximised at 24 m^2. The roof slope did not optimise at 36.9°, which would lead to maximum PV production, but it reached is maximum value of 60.3°. At a higher slope, the production of solar hot water reaches a more stable production throughout the year. The reduction in peak hot water generation in the summer was offset by higher production in the winter. With such a large collector area, there could still be problems with overheating in the summer due to the larger slope. The optimal solar thermal storage tank size was 908 L.

With such a large solar thermal collector area, the domestic hot water consumption was reduced to less than 200 kWh per year, which made the use of the desuperheater less efficient than the use of the ground source heat pump without the desuperheater. Therefore, the most optimal design used heating system 4. Other features were as expected: the maximum under-floor insulation (RSI 6), the thicker slab, minimal east and west-facing windows, and maximum south-facing windows. However, 80% window coverage on the south-facing façade led to overheating in the summer. The penalty for insufficient cooling was $426.33/month with the given value of $5.00/mth for every uncomfortable hour. The zone temperature exceeded 33°C for 5 hours, and was above 28°C in the cooling season for 80.3 hours beyond the allowable 5% of the cooling season. A reduction in the window coverage from 80% to 60% eliminated the comfort penalties and increased the electricity consumption by only 0.7% (31.4 kWh).

Table 5.12 compares the results of the initial objective function with the yearly electricity consumption as the cost function. The use of electricity as the cost function translates to a 9.9% decrease in annual electricity consumption, but results in a 16.5% increase in the monthly costs, with the comfort penalties excluded. As the objective of different homeowners may vary, there could be some benefit to the use of multi-objective function, with monthly costs and yearly electricity generation. This would lead to tradeoffs between the minimisation of the costs and the annual electricity consumption. As an alternative, a single objective function could be used with appropriate weights. For example, if equal emphasis is placed on yearly electricity consumption as to the monthly costs, the annual electricity consumption can be multiplied by 9.15% such that the lowest weighted electricity consumption equals the lowest cost function. The optimisation was repeated with this new weighted objective function. The resulting optimal configuration had few differences compared to the base case. The optimal collector area increased from 12 m^2 to 18 m^2, the tank size from 681 L to 908 L. To accommodate the larger collector area without incurring a roof penalty, the roof slope increased from 45° to 51.3°. Finally, the optimal had RSI 2 of insulation under the slab. With this hybrid objective function, the electricity generation decreased by 5.2% and the monthly costs increased by 4.5% compared to the initial objective function. Whereas the annual electricity consumption is 4.5% higher and the monthly costs 10.0% lower with the weighted objective function compared to using annual electricity consumption as the objective function.

Table 5.12: Comparison of results with yearly electricity as objective function

Case	Electricity (kWh/year)	PV Size (kW)	Upgrade Cost ($)	Cost Function ($/mth)	Cost Function Without Penalty
Base case	5,034	4.94	90,506	414.98	414.98
Minimum electricity – no penalties	4,534	4.70	105,484	909.98	483.65
Minimum electricity	4,565	4.73	105,102	481.90	481.90
New weighted objective function	4,771	4.76	94,539	433.47	433.47

Note that the weighting would change depending on the modelled scenario since the balance between energy consumption and costs varies. With the single objective function, the user could run the optimisation once to minimise costs, once to minimise yearly electricity consumption, then with the results of the first two runs, find the appropriate weights to use for a weighted objective function. More research to compare the use of a single objective function, a weighted objective function, or a multi-objective function with Pareto analysis is needed to determine the most appropriate approach. The potential user community would have to be polled to determine its needs. Ideally, a commercial tool would allow the user to choose between different approaches in order to define the objective function.

6. RESULTS ANALYSIS

6.1 Effects of Climate on Optimal Configuration

One of the advantages of a GA Optimisation Tool is that it can find the optimal configuration for a variety of different climates. Given that Canada is quite a large country and has various different climate zones, it is not always apparent what design strategies should be followed when one zone is compared to the next. In order to see the impacts of climate on the optimal design configuration, the optimisation was run with climate data from one of Canada's coldest cities, Iqaluit, one of its milder cities, Nanaimo, and from a hotter US city, Sacramento. Table 6.1 presents the average HDD, CDD, and daily solar radiation for these cities (RReDC, 2007, NRCan, 2007a, Environment Canada, 2007, California Climate Data Archive, 2007). The results for the optimal design configurations are summarised in Table 6.2.

Table 6.1: Average HDD, CDD and solar radiation for varying cities

City	HDD base of 18°C	CDD base of 18°C	Mean Daily Solar Radiation South-Latitude Tilt (kWh/m^2)
Iqaluit, NU	10,117	0	3.9
Montreal, QC	4,891	158	4.3
Nanaimo, BC	3,056	77	3.6
Sacramento, CA	2,691	1185	5.5

The difference in optimal design between Montreal and Nanaimo varied only by the south window coverage and the exterior wall type. Nanaimo required less insulation in the exterior walls and called for fewer south-facing windows. It is interesting to note that despite their very different climates, the overall yearly electricity consumption of Nanaimo and Montreal varied by only 12 kWh per year. As expected, the most costly

design was for Iqaluit, which had an annual electricity consumption that was 55.3% more than in Montreal. This was not a surprise since it has 106.8% more heating degree-days. Even with a roof slope of 60.3°, the roof area is still 3.2 m^2 too small to accommodate the required PV and solar thermal collectors. Note that the addition of RSI 2 more insulation under the slab or the increase in the slab thickness could reduce the heating consumption and thus the PV size; however, these measures were not as cost effective as the imposed PV roof penalty. The heat pump cooling or the natural ventilation resulted in the same cost function in Iqaluit as there was no cooling load, and the heat pump cooling was assumed to cost nothing. The optimal design for Sacramento had a monthly cost function that was 30.8% lower than in Montreal, despite an annual electricity consumption that was only 7.3% lower. The cost effectiveness of building net-zero energy homes in Sacramento is better due to cost savings in other parameters and in the higher PV generation per installed kW. These results start to explain why more net-zero energy homes have appeared in California than in Canada, especially if the higher electricity costs and increased government support for solar technologies are factored in.

Table 6.2: Resulting optimal configurations with cities of varying climates

Parameter	Montreal, QC	Iqaluit, NU	Nanaimo, BC	Sacramento, CA
Form	1.0	1.1429	1.0	1.1429
Heating System	7	7	7	1
Cooling	0	0 or 1	0	0
Window Type	4	4	4	4
S_Wdw	60%	50%	30%	20%
E_Wdw	5%	5%	5%	5%
W_Wdw	5%	5%	5%	5%
S_Overhang	none	none	none	none
Collector Type	evacuated	evacuated	evacuated	flat plate
Collector Area	12 m^2	9 m^2	12 m^2	12 m^2
Tank Size	681 L	454 L	681 L	454 L
Roof Slope	45°	60.3°	45°	26.6°
Wall Number	8	8	2	8
Thermal Mass	1	1	1	1
Slab Insulation	0	RSI 4	0	0
Electricity	4,924 kWh/yr	7,649 kWh/yr	4,936 kWh/yr	4,563 kWh/yr
PV Size	4.8 kW	8.5 kW	5.0 kW	3.6 kW
Roof Penalty	0	$32.22/mth	0	0
Cost Function	$408.27/mth	$692.27/mth	$400.07/mth	$282.40/mth

6.2 Effects of Building and Lot Characteristics on Optimal Configuration

One of the areas where this type of design optimisation tool can have the most impact is for design cases that are not ideal. For example, say that there is a tall building that blocks 25%, 50%, 75% or 100% of the direct sun from the south orientation on a given lot, what would be the best approach to take in order to achieve a low or net-zero energy building? There are typically no rules of thumb that can be followed for these non-ideal situations. This type of tool would also be beneficial in retrofit applications where there would be more limitations imposed on the problem that would make the optimal

configuration less obvious. Future versions of this tool could be developed that apply directly to the case of renovations. This would require a slightly different setup for the program, with different input and optimisation variables and costs.

One typical restriction that occurs with new construction is a building lot that does not face south. The optimisation tool was used to compare the base case that faced south in Montreal, versus a lot that faced 45°SW and one that faced 45°SE. Overall window areas, solar thermal collector area, and roof pitch were the only parameters that varied from one situation to the other, with the differences summarised in Table 6.3. As expected, the south-facing orientation reached the most favourable results. The only difference between the optimal configuration for the south and the 45°SE orientation was the roof slope. For the 45°SW orientation, the optimal window area became smaller on the south façade and larger on the east façade. The overall electricity consumption is not very different between the cases at an increase of only 4.9% and 6.8% for the SE and SW orientations, respectively. Higher costs are attributed to the need for more PV panels, and for the larger roof slope. An increase in the slope from 45.0° to 56.3° is estimated to cost $3,161, and results in a less than optimal PV performance.

Table 6.3: Variation in optimal results with different lot orientations

Case	S_wdw (% wall)	E_wdw (% wall)	W_Wdw (% wall)	Collector Area	Roof Slope	Electricity (kWh)	PV (kWp)	Cost Function
South	60%	5%	5%	12 m^2	45.0°	5,034	4.9	$414.98
45°SW	20%	35%	5%	16 m^2	56.3°	5,378	6.2	$515.77
45°SE	60%	5%	5%	12 m^2	51.3°	5,282	5.4	$450.39

After a scan of the results, one might conclude that higher slopes are needed to generate more electricity for off-south orientations. However, the effect of the roof penalty must be kept in mind, which adds $10/mth for every square metre of missing roof

area required to accommodate the PV and solar thermal collectors; this is due to the fact that higher sloped roofs have a larger overall area, which can accommodate more solar panels. Table 6.4 shows the results of the simulations for varying roof slopes around the optimal configuration, without the inclusion of the cost penalty for the roof area. In this case, the optimal slope for the south and south-east orientations is actually 36.9°, and it is actually the lowest for the south-west orientation at 26.6°. What these results show is that for this case, reducing consumption further, through either the addition of more thermal mass in the floor or through the addition of insulation under the floor, is not as effective as an increase in the roof slope to accommodate the larger solar panels.

Table 6.4: Effect of roof penalty on optimal results with varying lot orientations

	South Orientation			45°SW Orientation			45°SE Orientation		
Slope	kWh/kW of PV	Penalty $/mth	Cost Function w/out penalty	kWh/kW of PV	Penalty $/mth	Cost Function w/out penalty	kWh/kW of PV	Penalty $/mth	Cost Function w/out penalty
14.0°	959.6	$198.32	$443.55	910.1	$273.90	$483.22	946.2	$223.71	$462.63
26.6°	1010.4	$124.49	$416.04	926.6	$219.01	**$470.04**	988.3	$153.65	$437.95
36.9°	1024.5	$60.63	**$410.14**	920.4	$166.78	$472.88	999.1	$92.00	**$433.71**
45.0°	1018.2	$0.00	$414.98	903.0	$112.10	$484.03	992.3	$30.44	$439.70
51.3°	1002.4	$0.00	$425.32	882.0	$53.33	$499.03	977.8	$0.00	$450.39
56.3°	-	-	-	860.9	$0.00	$515.77	-	-	-

If the goal was not to achieve net-zero annual consumption, but to instead reach a configuration that has the roof fully covered, different optimal roof slopes would have been found. In addition, instead of the decision to opt for a larger roof area, one might consider more efficient solar panels that would produce as much electricity with a smaller roof area. In future versions of the tool, different PV technologies could be included as an optimisation parameter to vary efficiencies and costs. Alternatively, different roof configurations could be used that would allow PV panels to be installed in more than one

orientation, or PV panels could be installed on overhangs or on the vertical south-facing façade. It is clear that when the effects of different orientations, roof slopes and areas, PV technologies with varying efficiencies, and different possible roof shapes are considered that multiple solutions are possible. This type of tool could give designers some answers to help solve this problem.

Another area where one might expect to have differences in the optimal configuration is if the house would be built on one storey instead of two. With the mobility challenges that face the aging baby boomers, it is expected that more of them will chose to live in single storey homes, in an effort to avoid the daily use of stairs (Turner, 2002). The base case house was run through the optimisation with the assumption that it was built as a single storey house. Quite a few of the optimal parameters changed with this new scenario. Given that the south wall would be relatively smaller, the south window percent coverage increased from 60% to 80%. In addition, the form of the building increased from 1.0 to 1.3 to give the south wall more area. The roof area became larger, which allowed the roof slope to decrease from 45° to 36.9° without an incurred penalty. With this new roof slope, the optimal storage tank size dropped from 681 L to 454 L. Given that more of the exposed exterior envelope was in the floor and ceiling, the optimal now called for 0.05 m (2 in) of EPS under the basement, and the exterior wall went from the SIPS wall of RSI-8.59, to the 0.05 m x 0.15 m (2"x6") wall of RSI-5.20. All of these changes made it such that even though the single storey house consumed 5.1% more electricity, the monthly cost function only increased by 2.1% or $8.63/mth.

Unlike the change from 2 stories to 1, the change in the overall floor area from 150 m^2 to 300 m^2 did not change the optimal configuration significantly. The south

window percent coverage increased from 60% to 80%, the optimal roof slope decreased from 45.0° to 26.6°, which dropped the optimal storage tank size from 681 L to 454 L. It was also now more cost effective to cool the house with the heat pump, as opposed to the free cooling strategy. The increase in the area resulted in an increase in the annual electricity consumption of 15.7% and in the monthly cost function of 13.0% or $53.26. Note that the same loads were assumed for both houses. One could expect that a larger house would consume more energy for lighting and minor appliances, which would change the results.

As was discussed previously, the floor finish can have an impact on the heating load of the building. In order to test if the floor finish would have an impact on the overall optimal configuration, the GA Optimisation Tool was run with carpet as the floor finish instead of hardwood flooring; carpet has an RSI-value that is three times that of hardwood. The resulting optimal configuration did not change. Given that the optimal configuration used a highly efficient ground source heat pump air heating system, the effect of the carpeting was minimal. The annual electricity consumption increased by 0.5% (22.8 kWh/yr) and the monthly cost function increased by 0.3% ($1.39/mth). If the optimal heating system had used radiant heating, then the effects would have been more pronounced and would likely have led to changes in optimal configuration depending on the floor finish.

6.3 Impacts of Varying Utility Rates and Financing Costs

A variation in the rate structure at which electricity is both bought and sold can have a significant impact on the economic benefits of solar technologies. This section examines how a change in the rate structure can impact the optimal design configuration. First,

time of day pricing is examined where the utility charges more for electricity during the day and offers a reduced rate at night. The rate the utilities buy back the electricity also varies, which has been shown to help encourage the use of PV and allow for some loads to be shifted at night. In fact, one can reach a point where a house achieves net-zero utility costs before the actual net-zero energy target is reached. This is the case in Japan where some electric utilities buy and sell electricity at 26 yen/kWh (~$0.24/kWh CDN) from 7:00 to 23:00, and at 6 yen/kWh (~$0.06/kWh CDN) at night (Charron, 2005). The scheme works well for both the PV owner and the utility companies as the peak production of solar electricity generally occurs at around the time when the utility companies face peak electricity demand.

In order to test the effects of time-of-day pricing on the generated optimal configuration of the base case, three separate sets of prices were used: electricity was sold at $0.03/kWh from 22:00 to 7:00, and was sold and purchased at $0.15/kWh, $0.30/kWh, and $0.45/kWh. In each case, both prices were assumed to escalate at the same rate as the assumed inflation rate of 2%. The results showed no variation in the optimal design to the base case that used a rate of $0.10/kWh day and night for both sale and purchase of electricity. The only thing that changed in the results was the amount paid for electricity, the revenue from the PV and the overall optimisation cost function, as summarised in Table 6.5.

It is likely that the designs did not change because the consumption patterns were assumed to stay constant; however, in Japan, people try to do more of the household chores that require electricity such as vacuuming, dishwashing, laundry, etc, during off-peak rates. Another reason is that the control strategy was not varied from one case to the

next, whereas people could try to pre-heat their house or hot water tanks at night. In fact, a whole PhD thesis could be carried out to study different load management strategies that would shift loads from day to the night. Even if the overall energy consumption were to increase, if the peak utility loads could be reduced, the overall environmental benefits could be greater as dirtier electricity generation is often used to meet peak demands. With a daytime rate of $0.45/kWh, the monthly cost function dropped by 12.1%, the electricity consumption costs increased by 228%, and the PV revenue increased by 348%. One can see how this rate structure would encourage people to conserve more electricity during the day in order to maximise the benefits of the rate differential between day and night.

Table 6.5: Results of using different time of day rates

Rate (night, daytime, $/kWh)	Electricity Generated & Consumed	Electricity Costs ($/year)	PV Revenue ($/year)	Efficiency Upgrade Costs ($)	Monthly Cost Function
0.10 – 0.10	5,034 kWh	$503	$503	$90,506	$414.98
0.03 – 0.15	5,034 kWh	$579	$752	$90,506	$400.60
0.03 – 0.30	5,034 kWh	$1,114	$1,503	$90,506	$382.63
0.03 – 0.45	5,034 kWh	$1,650	$2,253	$90,506	$364.66

Another mechanism that has been used to promote PV technologies is to offer homeowners a guaranteed premium rate on the solar electricity that they generate, also called feed-in-tariffs. These are quite common in the European Union (EU); 11 of the 15 member countries have programs that offer a range of rates from $0.023/kWh to $1.091/kWh (Rowlands, 2005). This type of mechanism could go a long way to help grow the Canadian solar industry at a relatively low cost (Rowlands, 2005). This is likely one of the reasons that Ontario announced in 2006 that it would offer a feed-in-tariff of

$0.42/kWh for electricity generated with PV (OPA, 2007). In order to test the possible impacts of different feed-in-tariffs to the optimal design of a ZESH, three rates were tested: $0.25/kWh, $0.50/kWh, and $0.75/kWh. Note that these rates were constant, whereas the price to purchase electricity was the same as the base case at $0.10/kWh escalating at 2% per year.

Unlike the time-of-day rates, the use of feed-in-tariffs did result in some changes to the optimal configuration. For all three of the feed-in-tariffs, the size of the solar thermal tank decreased from 681 L to 454 L, which was the only change for the $0.25/kWh rate. For the $0.50/kWh rate, the solar collector area decreased from 12 m^2 to 9 m^2. For the case of the $0.75/kWh rate, the south-facing window wall coverage decreased from 60% to 40%, the solar thermal collector area decreased to 6 m^2, and cooling was now more optimal from the heat pump than with the passive ventilation fan. The results of the yearly electricity consumption and economic factors are summarised in Table 6.6. As can be expected, the optimal electricity consumption increases since it becomes more cost-effective to purchase more PV than to purchase some of the energy efficiency options. For example, for the case of the optimal design with the $0.75/kWh rate, the cost of the energy efficiency upgrades not including the cost of PV dropped by $4,324 (total $19,340) compared to the base case, whereas the PV cost increased by $9,229 for a total cost of $76,071 at the assumed PV cost of $13,52/W. At a monthly cost function of $201.25, this is comparable to the utility costs of a typical home without the ZESH upgrades.

Now that it has been shown that the utility rates can change the optimal configuration, it would be interesting to see if the assumed financing costs also have an effect. Results

of the use of BEopt presented by NREL often show that equivalent monthly costs can be obtained with energy efficiency measures that reduce the energy consumption by 40-50% (Anderson, et al., 2006). With their simulation they assume a 30-year mortgage at a 7% interest rate with a 3% general inflation rate. The other cost data is also different; their PV system used an installed cost of 7.50 $/W, with the inclusion of the present value of future operation and maintenance (O&M) costs. In order to see how the financing costs affected the optimal configuration, the base case assumption of a 25-year mortgage at 5% interest and 2% inflation, was changed to the BEopt numbers, including a 3% utility cost escalation. Note that the PV system cost was kept at 13,52 $/W. The resulting optimal configuration remained the same as the base case. However, with the more favourable financing rates, the monthly cost function decreased by 5.5% to $392.09/mth.

Table 6.6: Results of using different PV feed-in-tariffs

Utility Rates (buy, sell, $/kWh)	Electricity Generated & Consumed (kWh/yr)	Electricity Costs ($/yr)	PV Revenue ($/yr)	Efficiency Upgrade Costs ($)	Cost Function ($/mth)
0.10 – 0.10	5,034	$503	$503	$90,506	$414.98
0.10 – 0.25	5,057	$506	$1,264	$90,547	$373.75
0.10 – 0.50	5,238	$524	$2,619	$91,330	$289.32
0.10 – 0.75	5,729	$573	$4,297	$95,411	$201.25

6.4 Impacts of Declining Costs of Solar Energy

All of the results, unless otherwise stated, used an assumed cost of 13,52 $/W for the PV system, which was based on data from 2004. If the cost data from 2005 had been used, which had an average cost of 11,25 $/W (IEA PVPS, 2006), the optimal configuration might have been impacted for some of the tested scenarios. However, this

was not the case for the base case that had the same resulting optimal configuration, the only difference was that the monthly cost function decreased by 12.4% to $363.52/mth. One can see that the monthly costs is highly correlated with the PV cost as a 16.8% drop in PV cost resulted in 12.4% savings in monthly costs for the same optimal design configuration.

The reported installed price of a PV system dropped by 16.8% in a single year from 2004 to 2005. At this rate of decline, the price would drop to 7 $/W between 2007 and 2008. At this cost, the optimal configuration and cost function would change. The optimal collector area drops from 12 m^2 to 9 m^2, the tank volume from 681 L to 454 L and the wall changes from wall 8 to wall 2. These changes increased electricity consumption by 9.1%, which increased the required PV capacity from 4.8 kW to 5.3 kW, and resulted in a decrease in the monthly cost function of almost 37% to $258. These results show that as the price of PV systems decrease that the economic viability to achieve the net-zero energy target is improved, and they show the importance of keeping costs up-to-date in order to find the optimal configuration.

6.5 Impact of Varying Target Energy Consumption

The net-zero energy target is arbitrary. Some building owners might be content with an annual consumption of 2,000 kWh, or more, which would still be considerably lower than the consumption of the average Canadian residence. The optimisation was run with an increasing energy target, from net-zero energy to 15,000 kWh per year. The optimal design converged to a specific design at target levels of 8,000 kWh and above. As mentioned before, when the effects of the assumed heating system costs were analysed, the converged optimal design was less concerned to minimise energy consumption than

to minimise costs. Other than the ground source heat pump with desuperheater and the exterior wall, which have less energy efficient options, the other parameters all converged to the least costly value. This indicates that the energy savings achieved by these two parameters resulted in greater cost savings due to a reduction in electricity consumption than their monthly financing costs. Note that this was not the case when the higher heating system costs were used. For this case, heating system 1 became more optimal, and the other parameters changed in order to reduce the heating consumption. An increase in the energy target would likely result in varying designs but it would eventually converge to a design that would be different than if the ground source heat pump were used, since its higher COP reduces the impact of the increased heating load through less costly design alternatives. Table 6.7 summarises the optimal design configurations that emerged with the various targets for yearly energy consumption.

Table 6.7: Optimal design progression with increasing energy target

Parameter	Target – kWh per year					
	0	2,000	4,000	6,000	8,000	8,000 New costs
Form	1.0	1.0	1.0	1.0	1.0	1.0
Heating System	7	7	7	7	7	1
Cooling	0	1	0	1	0	0
Wdw #	4	4	4	2	1	4
S_Wdw	60%	60%	70%	40%	20%	60%
E_Wdw	5%	5%	5%	5%	5%	5%
W_Wdw	5%	5%	5%	5%	5%	5%
S_Overhang	0	0	0	0	0	0
Collector Type	Evacuated	Evacuated	Evacuated	Evacuated	Flat	Flat
Collector Area	12 m^2	12 m^2	12 m^2	9 m^2	3 m^2	9 m^2
Tank Size	681 L	681 L	454 L	303 L	250 L	303 L
Roof Slope	45°	36.9°	36.9°	14°	0°	14°
Wall Number	8	8	7	7	2	8
Thermal Mass	1	1	1	1	1	1
Slab Insulation	0	0	0	0	0	0
Electricity	4,924 kWh/yr	4,996 kWh/yr	5,080 kWh/yr	5,964 kWh/yr	7,556 kWh/yr	8,001 kWh/yr
PV Size	4.8 kW	2.9 kW	1.0 kW	0	0	0
Cost Function	$408/mth	$300/mth	$196/mth	$119/mth	$103/mth	$127/mth

6.6 Impact of Changing Heating and Cooling Control Setpoints

With the control strategy that has been used throughout this thesis, the zone temperature was allowed to fluctuate between 18°C and 28°C without penalty, and could drop to 16°C for 5% of the year and go up to 33°C for 5% of the year without penalty. Some occupants might not tolerate such a wide range of temperatures, especially with the limitations of the one-zone modelling that under-predict maximum and minimum temperatures. In order to see the effects of a change in the control setpoints, the optimisation was run with $L95_h$ and $L95_c$ at 20°C, $H95_c$ and $H95_h$ at 26°C, MinT_c and MinT_h at 18°C, and MaxT_c and MaxT_h at 29°C.

The new control strategy resulted in three changes to the optimal configuration. The optimal window size for the south window was decreased from 60% to 40%, to reduce the cooling load, cooling from the heat pump was used as opposed to the natural ventilation, and finally, the optimal roof slope increased from 45° to 51.3° to accommodate the larger required PV array. Natural ventilation resulted in $55 of monthly penalties related to comfort. The annual electricity consumption increased by 10.6% to 5,565 kWh, the required PV size increased by 12.3% to 5.6 kW, and the monthly cost function increased by 9.8% to $455.90.

6.7 Performance of GA Optimisation

The objective of this thesis was not to prove that a GA was the best optimisation algorithm to use. It was selected as it has been shown to be effective to find optimal solutions for building design problems with a limited number of evaluations. Even within the GA, there are different approaches and parameters that could be changed that would affect its performance. In this section, a review is done to show how well the GA program was able to find the optimal configuration. Only cases 16 through 40 are considered in order to eliminate differences that could have occurred with the two different sets of parameters to be optimised. As mentioned previously, the fittest value found by the GA Optimisation Tool was on average 2.65% above the fittest value. On a case-by-case basis, i.e. combining the performance of the three runs per case, the GA Optimisation Tool found the fittest value 48% of cases, an optimal value less than 0.5% higher than the fittest for 80% of cases, and an optimal value less than 1% above the fittest for 84% of cases. In only 2 cases (8% of cases) the optimal value was more than 3% above of the fittest individual.

Three different initial populations were tested (i.e. three different seeds were given to the random number generator). The first random population was on average 2.06% above the fittest value, the second 2.37% above the fittest value, and the third 3.64% above the fittest value. A deeper analysis reveals that the second population performed better, the fittest individual was found 28% of cases, compared to 8% for the first random population, and 12% for the third. The reason that the average performance for the first random population was better is due to one case in the second population that was 29.8% above the fittest value. If the worst performing run for each initial population is ignored, the first random population becomes on average 1.85% above the fittest value, the second 1.23% above the fittest value, and the third 2.50% above the fittest value. These results indicate that the composition of the random population in the first generation has an effect on the performance of the GA Optimisation Tool. However, the better performance is not directly correlated to the average cost function of the first generation. The average cost function of the first generation for the first population was $1305.82/mth, for the second population $1123.04/mth, and for the last $1060.29/mth. If only the fittest run per case is considered, the GA Optimisation Tool was on average only 0.49% above the fittest value. This highlights the importance of doing multiple runs per case, as this performance is more than twice as good as what was achieved with the best performing initial population.

It is likely that there would be a different set of GA parameters that would have performed better. It is possible that a regular GA with different mutation and crossover rates or a micro-GA with a different population size and number of generations would have found the fittest individual more often, or would have been on average closer to the

fittest individual with fewer computations. It is also possible that different GA parameters or even optimisation algorithms would work differently for different test cases; this makes it difficult to identify the best strategy. Mitchell (1998) reported that since GA parameters interact with one another nonlinearly that they could not be optimised one at a time, which makes it difficult to identify the most performing combination of parameters. In addition, it was noted that it was unlikely that any general principles about parameter settings could be formulated a priori, in view of the variety of problem types, encodings, and performance criteria that are possible in different applications. Even within an individual case, it is believed that optimal population size, crossover rate, and mutation rates likely change over the course of a single run. One proposed approach is to have the parameter values adapt in real time to the ongoing search. An in depth analysis to help find the most performing GA parameters or the implementation of an optimisation algorithm to vary the GA parameters within the simulation is beyond the scope of this study. If an analysis was done to optimise the performance of the GA, it would be of value to compare the performance with other optimisation algorithms.

One must keep in mind that in the analysis, the fittest values were found manually with a sequential search technique with parameters optimised one at a time around the fittest individual found with the GA program. However, over the course of the analysis for this thesis it was found that it is sometimes difficult to find the fittest value in this fashion as many of the parameters are inter-related. A good example of this is when the building form and south window coverage are optimised. In case 28, the fittest individual found with the GA program had a form of 1.2 and south window coverage of 40%. With

a form of 1.2, the optimal south window coverage is 40%. Therefore, since parameters are changed only one at time, this combination is always fittest. However, if the form is changed to 1.0 and the south window coverage to 60% at the same time, then a better solution is found. The difference in monthly cost function between a form of 1.2 with a south window coverage of 40%, compared to a form of 1.0 with a coverage of 60%, is very small at only 0.01%, but it highlights how sometimes analysing parameters one at a time can fail. Only after the completion of the analysis for a great majority of the cases did this correlation between form and south window coverage emerge. The results of the manual optimisation from previous cases were reviewed, and in two other cases it was found that there existed a fitter individual than what was found in the initial manual optimisation, due to the combination of form and window coverage.

Another example of a design that would be difficult to optimise manually occurred when the annual electricity consumption was used as the objective function. The case with 24 m^2 of solar thermal collector area resulted in an optimal configuration, where the desuperheater on the ground source heat pump was no longer optimal. However, the optimal south window coverage was found to be dependent on whether the desuperheater was used or not. Without the desuperheater, the optimal window coverage was 80%, but resulted in 85.3 hours of overheating. A 60% window coverage eliminated the comfort penalties, but increased the yearly consumption by 31 kWh. With the desuperheater, 60% coverage resulted in a consumption that was 2 kWh less than with 80% coverage, with neither coverage resulting in overheating. Therefore, if the south window coverage parameter was optimised first in the sequential technique and the system with the

desuperheater was default, then the optimal that would have been found would have had 60% window coverage, instead of the more efficient 80%.

Another parameter that may lead to problems with the use of a linear sequential search is the roof slope. In most cases, the optimal roof slope was found to be 45.0°; however, a slope of 36.9° would have been more cost effective without the consideration of the cost penalties for insufficient roof sizes. In some of the cases, it was found that a reduction in the roof slope, in conjunction with the addition of insulation under the slab resulted in a more optimal configuration, whereas either reducing the slope or adding insulation independently would not have resulted in a better solution. Finally, if one looks at case 22, which had two designs with very similar cost functions but with very different design configurations as discussed in Section 5.3.1, one sees that only one of these designs could have emerged with a sequential search technique, depending on which heating system the sequential search technique started with. This phenomenon was noticed when the winning submissions for the EQuilibrium competition were reviewed. Various teams followed a cost optimisation approach, where they would compare the cost of an energy efficiency measure with the cost of the generation of an equivalent amount of energy with a PV system. It appears that the different optimal designs were reached depending on if teams started their analysis with a geothermal heat pump or with a standard gas or electric furnace. The use of a heat pump that has a COP of 3 or 4 reduces the cost effectiveness to use other energy efficiency measures to reduce heating energy consumption. Generally, the teams that had a geothermal heat pump called for less insulation. Ideally teams should have started with a heating system and

then optimised the house based on that heating system; the analysis should have then been repeated for the other heating systems that were considered.

7. CONTRIBUTIONS AND FUTURE WORK

7.1 Contributions

This thesis examines the process used to develop a GA based design optimisation tool for low and net-zero energy solar homes. The use of formal optimisation tools for building design is not commonly used in practice. However, if such tools could be commercialised, they could be used for various applications with a partial list of applications put forward in (Carroll, 1991):

- Provide information for the development of energy standards and mechanisms for the evaluation of the impact of their implementation;
- Provide a quantitative mechanism for the evaluation of economic inefficiency that result from non-optimal current design practices;
- Provide ways of rationally building flexibility into building energy standards. The use of the tool for this type of activity was demonstrated in this thesis by examining different design configurations that emerge with different yearly net-energy targets. This would be helpful to provide different design options for performance based energy standards;
- Identify new design and/or construction techniques and related new products, which are not currently available that need to be developed or marketed in order to build optimally designed buildings;
- Provide quantitative mechanisms to determine what types and corresponding levels of incentives are justified to encourage new building designs and new product development. The use of the tool for this type of activity was

demonstrated in this thesis by examining different utility rate structures that could be put in place to encourage the use of PV;

- Identify optimal configurations for the design community, and thus, ways to design buildings that meet or exceed the energy budget requirements of standards. The use of the tool for this type of activity was demonstrated in this thesis by examining how optimal configurations change with various different input conditions;
- Provide information to designers in regards to the best way of optimally allocate costs to the various design features in order to achieve prescribed performance levels; and,
- Provide design trade-off mechanisms that maintain optimality. The use of the tool introduced in this thesis is based on being able to find the most cost-effective trade-offs between energy efficiency and renewable energy generation.

In fact, the type of tool developed in the thesis could be used to support any of the activities highlighted by (Carroll, 1991). The use of these types of tools has started to emerge in real applications. The results generated with BEopt provided a starting point to determine the most cost-effective approaches to achieve the near-term and long-term performance targets for the DOE Building America Program with targets that will be updated over time based on analysis with BEopt (Anderson, et al., 2006). Despite this recent application of a design optimisation tool for low energy buildings, research still needs to be carried out before their use becomes mainstream. The research conducted as part of this thesis starts to address some of these research needs with the following main contributions:

1. First use of genetic algorithms to find optimal configurations of net-zero energy solar homes. Genetic algorithms are an improvement over sequential search techniques because they take into account interactions between different parameters in the optimisation process;
2. Clearly demonstrated the extent to which local climate, economic factors, and specific design constraints can have a major impact on the optimal design configuration, which limits the usefulness of generic design guidelines;
    - A specific look at the impact of heating system and PV costs shows the importance of finding appropriate costs, while at the same time it highlights the difficulties to find accurate costs as these vary with product, location, and change over time.
3. Examination of the effects of certain modelling assumptions on the accuracy of the program to help designers focus their attention on the parameters that are more important.
    - Highlighted limitations of the use of a single zone in terms of comfort predictions. Other programs for the design of energy efficient houses like Energy 10 (choice of 1 or 2 zones) (SBIC, 2007) or HEED (UCLA, 2007) use the single zone approximation.
    - The analysis showed that blinds can have a significant effect on the optimal configuration that is reached, which demonstrates the need to include blinds in building energy simulation programs.
4. Novel use of whole building design optimisation with TRNSYS as the design tool. TRNSYS comes with the capability to do parametric analysis and to

connect with GenOpt to use formal optimisation algorithms; however, this new approach allows for more flexibility.

7.2 Future Work

Despite the research contributions of this thesis, many areas need further investigation. This section summarises some of the research needs identified within the thesis.

7.2.1 Modelling

The choice of TRNSYS as the simulation engine brought advantages and disadvantages. As various simulation tools progress, they can be considered for the simulation engine if they bring advantages in terms of modelling speed and capabilities. Compromises need to be made between available technologies to model within the program, simulation run-times, model accuracy, etc. For example, either TRNSYS can improve its accuracy in modelling high mass buildings, or different software such as ESP-r could be implemented in its place. In order to increase the user base of a future tool, the GA optimisation can be added as a feature to current programs that are already widely adopted by industry. For example, a GA Optimisation wizard could be added in a future release of HOT3000 (NRCan, 2007b) that would allow a user to optimise parameters in a given design. This would be advantageous in Canada if HOT3000 becomes the tool that builders and architects are required to use to show compliance with national EnerGuide or R2000 programs, which currently use HOT2000 (NRCan, 2007b). The methodology could easily be adapted in other software that are used to support various international low and net-zero energy building initiatives.

If TRNSYS is to remain the simulation engine, there are various aspects of the modelling that could be improved. Either a different method to interact with TRNSYS from the GA program or to update the software to permit parameter updates for the Type 56 building type, could allow for an easier implementation of a multi-zone building. The current Type 19 zone model relies on constant convective heat transfer coefficients on its surfaces. The effect of this approximation would need to be quantified to have a better understanding of the accuracy of the program. A better methodology would be required to determine the effective room air capacitance, since it has an effect on both the accuracy of the program and the run-time.

The capability of modelling a multi-zone building in the early design stages could introduce some benefits. Currently, the use of a single zone model reduces the accuracy of the thermal comfort estimations. The actual internal layout of the zones could be one of the parameters optimised. Alternatively, two optimisation tools could be developed: one that uses a single zone for the early design stages, and a second tool that is used in the later design stages to help refine the design. The second stage tool could help determine the best internal layout of the space, and it could help choose between different control strategies and other parameters that are selected in later design stages. Either approach requires further work to determine how to implement a multi-zone building within a GA program, this includes the determination of the number of zones to be used, the airflow between zones, the zone layout, etc. The current tool is also limited to a rectangular zone. However, other possible shapes could be considered in future versions of the tool, as another recent study has demonstrated that different polygon shaped zones could offer some advantages (Wang, et al., 2006). The introduction of multi-zone

modelling with different shapes other than rectangular, would introduce a new set of modelling challenges.

Other modelling issues could also be examined to help improve the accuracy of the simulation. The fraction of the dryer load that is lost to the outside could be examined. The use of a better model for the blinds, or simply the use of different types of blinds such as Venetian blinds could affect the results. Currently only one set of occupant loads was included in the program. It would be good to have varying occupant loads depending on the planned occupancy that would allow for varying the total consumption and schedules. This could either be a choice from a list or a user input.

7.2.2 Parameters

In the analysis of the tool, the number and range of parameters that were optimised was revised. It could be even further revised since the overhang was never optimal even with the Sacramento climate, and the additional thermal mass and some of the heating systems were also never found to be optimal. Note that these parameters might become more important with the use of a multi-zone building model for the overhang, or if a different simulation engine was used that was more accurate in modelling thermal mass effects. Other parameters could be added to the tool for the analysis as identified in the thesis. Also, there could be a list of parameters that could be chosen by the user at the beginning of the simulation instead of evaluating every available parameter. For example, the east and west window coverage are always minimised unless the lot orientation is off-south and other items such as the use of radiant floor heating or a ground source heat pump might be mandated by a given client.

The following is a list of parameters that were identified in the thesis as possible choices to be included in future versions of the tool:

- Different solar thermal heat exchangers with the overall heat transfer coefficient made as an optimised variable;
- Different PV technologies could be included as an optimisation parameter with varying efficiencies and costs. Alternatively, different roof configurations could be used that would allow PV panels to be installed in more than one orientation, or PV panels could be installed on overhangs or on the vertical south-facing façade. It is clear that when the effects of different orientations, roof slopes and areas, PV technologies with varying efficiencies, and different possible roof shapes are considered, that multiple solutions are possible. The inclusions of these options would give the designer some answers to help solve this problem. Another alternative would be to have the solar thermal collectors mounted on the building façade and the PV on the roof. This configuration would allow room for more PV and solar thermal collectors. Another advantage of placing the solar thermal collectors on the façade is that a more constant energy production is generated in this configuration with more energy available in the winter months than with inclined installations;
- Allow for the choice of different blinds such as Venetian blinds or the choice of interior or exterior mounted blinds.
- Different products of the same system type with varying performance and cost (i.e. ground source heat pump, solar thermal collector, etc.); and,
- Different framing options within the window parameters.

7.2.3 Reduction in Optimisation Run-Times

One of the limitations of the GA Optimisation Tool is that it can take days to find the optimal configuration. Various approaches could be implemented in order to reduce the overall simulation time. It is possible that using other optimisation algorithms or with the use of different GA parameters could lead to the need for fewer evaluations of different design configurations to find the optimal. Another possible approach to speed up the tool for a commercial release would be to store all of the computed configurations in an online database that could be accessed by users such that they would not have to redo a simulation that was already done. However, this method would be limited to cases where the exact same simulation is repeated, which would be unlikely. Alternatively, the initial population of designs used in the optimisation could be stacked with highly performing individuals for similar design cases found in the online database.

Another approach to speed up the process would be to focus on the energy simulation tool. A more simplified tool or other simplifications could be made to speed up the simulation. The challenge would be to speed up the simulation time without significantly affecting the program accuracy. The level of accuracy would depend on whether the tool is simply used for early design stages, or if it would be used at all stages of design. A methodology could be developed to find the optimal design configuration based on a peak winter and summer design day. However, it would be difficult to predict the yearly performance of low or net-zero energy solar homes based solely on a design day methodology. Instead, perhaps the energy simulation tool could evaluate only one or two weeks out of every month or every second or third day, and it could use an analytical approach to find the yearly consumption based on this reduced simulation period. The

challenge would be to find a method that would be accurate to estimate the full year load for varying climates and different design configurations.

7.2.4 Controls

This thesis barely touches on the subject of optimal control strategies. It showed that the use of different heating and cooling setpoints, or different blind control strategies led to differences in the final results. As mentioned, a whole research project could be devoted to optimisation of control strategies for a given house and system design. Different optimal control strategies would result depending on the desired goal, whether it be to minimise energy consumption, or to shift loads from day to night to lower peak energy demands with the implementation of different load management strategies. In order to develop a detailed control strategy, it would be good to know the room layouts and ventilation requirements, which are more defined in the later stages of the design. This would be another situation that would benefit from a second phase optimisation tool that would help refine the design and systems selected in the early design stages. For example, an area that could be improved would be the control strategy implemented for the solar thermal collector and storage, which could vary between P, PI, or PID control with a variable speed pump. The heating and cooling setpoints could be varied depending on the time of year or predictive control could be implemented with weather forecasting. Different sizes or makes of heating and cooling systems could be considered or possibly the same system could be varied through the use of different control strategies. Although the inclusion of the control strategies in a second stage optimisation tool would be helpful, more work is needed to fine tune the control strategies used in the

early stage design tool, to ensure that the controls are the most representative of what would actually happen; this would result in better modelling accuracy.

Another control aspect that would require more analysis relates to natural ventilation. The two levels of outdoor air of 3 ach and 6 ach would need to be verified, this would include whether 3 ach could be achieved through passive means alone, as was assumed in this study. Further study would refine the natural ventilation airflow rates and control strategy. The resulting analysis may change the set flow rates or call for a variable speed fan that would allow for the volume of outdoor air to vary based on the cooling potential of the outdoor air compared to the cooling requirements of the house.

7.2.5 Further Study

There are various other aspects that concern the development and use of formal optimisation techniques in the design of low and net-zero solar energy homes that would be of interest to pursue further research. A more elaborate study should be done to refine the value of the cost penalties to use to account for comfort, roof size, and possibly other important design elements or constraints. More research that compares the use of a single objective function, a weighted objective function, or a multi-objective function with Pareto analysis would be helpful to identify which approach is most appropriate for different end-uses of the tool. The end make-up of the tool should depend on the project end-users of the optimisation tool. Policymakers may require different features than design professionals. The design community may wish to use the tool for both renovations and new construction. This may result in one tool that has various features for different user groups or in different versions of the tool adapted to specific user communities.

The use of a GA Optimisation Tool can be useful to a wide variety of users. A study that looks at the impacts of projected weather, based on climate change models, could help policymakers not only understand the effects of climate change, but be ready to offer optimal design guidelines to meet the changing needs of the building industry. Another use of the tool would be to identify which subsidy improves the cost effectiveness to build and own low and net-zero energy solar homes in the most efficient manner. This could be a combination of time-of-day day rates, feed-in tariffs, preferential financing options, and subsidies for the purchase of renewable energy or energy efficiency upgrades.

8. CONCLUSIONS

The growing concern in regards to global warming, the continual development of energy-efficient appliances and HVAC systems, the expected drop in PV and solar thermal collector prices, and other driving factors should lead to the eventual emergence of solar homes that either consume zero net energy or generate a surplus of energy. Advances in computing power and costs have helped facilitate the task to design net zero and low-energy solar homes. They have helped improve the accuracy and capabilities of building energy performance simulation tools and can soon help in the emergence of a different type of tool altogether, the building optimisation tool. In order to help accelerate the uptake of low and net-zero energy solar homes, new design tools, such as the GA Optimisation Tool presented in this thesis, need to emerge that help designers and policymakers determine the most cost-effective mix of technologies that needs to be utilised in order to achieve their various possible design objectives.

Different tools can be developed that are geared towards different stages of the design process, with the present tool for the early design stages. The limited amount of data available to accurately model the building is a key issue that arises when models are run in the early design stages. The verification of the low energy solar home model developed for this thesis focused on the comparison of the modelled results with monitored data. For the GA Optimisation Tool, no existing house will be available to help set the inputs and parameters, which will present more unknowns with the introduction of more uncertainty as more assumptions will need to be made. For example, the analysis on the effects of the effective capacitance showed that the value that was used had an effect on the air temperature profile, the calculated heating and

cooling load, and the program computational time. Values in the recommended range of 10-50 times the zone air capacitance, result in a range of possible different solutions. Another area that can affect the accuracy of a simulation model occurs in the modelling of infiltration. In super-insulated houses, infiltration can account for a larger percentage of the overall heating load. However, without a measured infiltration value, it is difficult to know how much infiltration to expect since typical infiltration values can vary significantly from one house to the next. In the verification analysis, real weather data was used; however, when the tool is used to make predictions about future consumption, one does not have that luxury. With our climate changing due to global warming, the use of weather from old databases may tend to overestimate heating energy consumption and underestimate cooling energy. Another area that becomes more critical in modelling low energy solar houses relates to the occupant loads, which are dependent on occupant behaviour; whether a house actually achieves a specified energy consumption target will depend on the energy consumption of the eventual house occupants. However, when used with the GA Optimisation Tool, designs are compared on a relative basis, which reduces the impact of most of these modelling inaccuracies in order to help find an optimal design configuration.

From the contributions and future work in Section 7, one can see that a lot more future work was identified than current contributions. This is typical of any new research area, where the more that is learned reveals the extent of what still needs to be learned. Ideally more answers would have been provided in this thesis; however, the nature of the problem makes it time-consuming to delve deep into any particular area in order to help answer specific questions such as the best GA parameters to use in the analysis. The

objective of this thesis was to look at the broader picture and to develop a methodology to apply a GA optimisation approach to the design of low and net-zero energy homes to highlight its advantages and the work that remains to be done.

The research did show that genetic algorithms were capable to find near optimal solutions with three runs per case and approximately 2,700 TRNSYS evaluations, which represented 0.00012% of the solution space of 2,147,483,698 for the reduced set of optimised parameters. On average, the GA found a solution that was within 0.5% of the optimal, which represents a difference of approximately $2.00/mth. Such a small difference would not have a noticeable effect on the cost effectiveness of building a net-zero energy solar home.

Early in the thesis, it was shown that the average Canadian home consumes 33,963 kWh of energy per year, which translates to a cost of $283/mth, under the assumption that it is all electric at $0.10/kWh. This is almost identical to the monthly cost value found for building a net-zero energy house in Sacramento, CA. Even in Canada, equivalent monthly costs can be achieved with a significant reduction in energy consumption; the analysis showed that a monthly cost value of $300 can be achieved with a net-energy consumption of only 2,000 kWh per year. The best mechanisms shown to improve the cost-effectiveness to achieve the net-zero energy target are to offer favourable utility rates for PV energy such as feed-in-tariffs, or to reduce the cost of PV systems. At a PV system cost of 7.00 $/W, which is expected within a few years, the monthly cost value to achieve the net-zero energy target for the Montreal test case reduced to $258. Alternatively, with a feed-in-tariff of $0.50/kWh the monthly cost value was $289, and reduced to $201 at a tariff of $0.75/kWh. Therefore, current energy

consumption levels can be reduced significantly, down to net-zero energy consumption in the near future, while current cost levels are maintained. When this becomes known by consumers, this could lead to a relatively quick change in the building industry in an effort to build highly performing solar houses. With a quick transition, tools like this GA Optimisation Tool will be helpful to assist less knowledgeable developers in the design process as they gain experience in designing more energy efficient houses with integrated solar technologies.

9. REFERENCES

Abu-Hamdeh, N, 2003. Thermal Properties of Soils as Affected by Density and Water Content. *Biosystems Engineering* **86** (1), 97–102.

Alcalá, R., et al., 2005. A genetic rule weighting and selection process for fuzzy control of heating, ventilating and air conditioning systems. *Engineering Applications of Artificial Intelligence* **18,** 279-296.

Anderson, R., C. Christensen, S. Horowitz, 2006. Program Design Analysis using BEopt Building Energy Optimisation Software: Defining a Technology Pathway Leading to New Homes with Zero Peak Cooling Demand, *ACEEE 2006 Summer Study Pacific Grove*, California, NREL/CP-550-39827.

ASHRAE, 2001. *ASHRAE Fundamentals 2001,* SI Edition, ASHRAE. Atlanta, GA

Ayoub J., et al., 2001. Photovoltaic for Buildings: Opportunities for Canada, Natural Resources Canada, CANMET Energy Technology Centre, Varennes.

Athienitis, A.K., 1989. A Computer Method for Systematic Sensitivity Analysis of Building Thermal Networks. *Building and Environment* **24**, 163-168.

Athienitis, A.K., 2007. Design of a Solar Home with BIPV-Thermal System and Ground Source Heat pump, Joint SESCI 32nd & SBRN 2nd Annual Conferences, Calgary, AB.

Athienitis A.K., E. Akhniotis, 1993. Methodology for computer-aided design and analysis of passive solar buildings. *Computer Aided Design* **25,** 203-214.

Athienitis, A.K., M. Santamouris, 2002. *Thermal Analysis and Design of Passive Solar Buildings*, James and James, London, UK.

Athienitis A.K., Y. Chen, 2000. The effect of solar radiation on dynamic thermal performance of floor heating systems. *Solar Energy* **69** (3), 229-237.

Bastide, A., P. Lauret, F. Garde, H. Boyer, 2006. Building energy efficiency and thermal comfort in tropical climates Presentation of a numerical approach for predicting the percentage of well-ventilated living spaces in buildings using natural ventilation. *Energy and Buildings* **38,** 1093–1103.

Beasley, B., D. Bully, R. Martinz, 1993. An Overview of Genetic Algorithms: Part 1, Fundamentals, *University Computing*, **15**(2) 58-69.

Beccali, G., M. Cellura, V. Lo Brano, A. Orioli, 2005a. Is the transfer function method reliable in a European building context? A theoretical analysis and a case study in the south of Italy, *Applied Thermal Engineering* **25,** 341–357.

Beccali, G., M. Cellura, V. Lo Brano, A. Orioli, 2005b. Single thermal zone balance solved by Transfer Function Method, *Energy and Buildings* **37**, 1268–1277.

Beckman, W.A., 2000. TRNSYS A transient system simulation program, TRNSYS Manual, Version 5, Solar Energy Laboratory, University of Wisconsin, Madison USA.

Berkeley Laboratory, 2007. http://gundog.lbl.gov/GO/

Biaou, A.-L., M. Bernier, 2005. Domestic Hot Water Heating in Net-Zero Energy Homes. *Ninth International IBPSA Conference,* Montreal, Canada, 63-70.

Bojic, M., S. Kostic, 2006. Application of COMIS software for ventilation study in a typical building in Serbia, *Building and Environment* **41,** 12–20.

Brogren M., B. Karlsson, 2002. Low-Concentrating Water-Cooled PV-Thermal Hybrid Systems for High Latitudes", *Photovoltaic Specialists Conference. Conference Record of the Twenty-Ninth IEEE*, May 19-24, 1733-1736.

Builers Websource, 2006. *Tankless Water Heaters: Consideration and Comparisons,* www.builderswebsource.com/techbriefs/tankless.htm.

Caldas L., 2001. *An evaluation-based generative design system: using adaptation to shape architectural form*, MIT Press, Ph.D. Thesis, 299 pp.

Caldas L., Norford L., 2002. A design optimisation tool based on a genetic algorithm. *Automation in Construction* **11,** 173-184.

California Climate Data Archive, 2007. www.calclim.dri.edu.

Carroll D., 2005. http://cuaerospace.com/carroll/ga.html.

Carroll W., 1991. Life Cycle Cost Optimisation of Residential Building Designs. *Proceedings of Building Simulation '91,*638-644.

CEPHEUS, 2005. www.cepheus.de/eng/index.html.

Charron, R., 2004. *One- and two-dimensional modelling of ventilated facades with integrated photovoltaics*, M.A.Sc Thesis, Concordia University, Montreal, Canada.

Charron, R., 2005. *A Review of Low and Net-Zero Energy Home Initiatives.* NRCan/CETC report, http://cetc-varennes.nrcan.gc.ca/en/er_re/pvb/p_p.html?2005-133.

Charron R., A. Athienitis, 2005. An international review of low and zero energy home initiatives, *ISES Solar World Congress 2005,* Orlando, FLA.

Charron R., A.K. Athienitis A.K., 2006a. Design and Optimisation of Net-Zero Energy Solar Homes, *ASHRAE Transactions*, Vol. 112, Pt. 2.

Charron, R., A.K. Athienitis, 2006b. The Use of Genetic Algorithms for a net-Zero Energy Solar Home GA Optimisation Tool. *23rd International Conference on Passive Low Energy Architecture*, Geneva, Switzerland.

Charron R., A.K. Athienitis, I. Beausoleil-Morisson, 2005. Tools for the Design of Zero Energy Solar Homes, *SESCI 30th Annual Conference*, August 2005, Burnaby, BC.

Chiras D., 2002. *The Solar House: Passive Heating and Cooling*. Chelsea Green Publishing.Vermont, 274 pp.

CMHC, 2007. www.cmhc-schl.gc.ca/en/inpr/su/eqho/index.cfm.

CMHC, 1998. *Tap the Sun: Passive Solar Techniques and Home Designs*. CMHC, Canada, 117 pp.

Christensen, C., R. Anderson, S. Horowitz, A. Courtney, J. Spencer, 2006. *BEopt™ Software for Building Energy Optimisation: Features and Capabilities*. NREL Technical Report, NREL/TP-550-39929, 21 pp.

Christensen, C., S. Horowitz, G. Barker, 2004. A Sequential Search Technique for Identifying Optimal Building Designs on the Path to Zero Energy Buildings. *ASES Annual Meeting*, Portland, Ore.

Christensen, C., S. Horowitz, T. Givler, G. Barker, 2005. BEopt: Software for Identifying Optimal Building Designs on the Path to Zero Net Energy, *ISES Solar World Congress 2005*, Orlando, FLA, 6 pp.

Christenson, M., H. Manz, D. Gyalistras, 2006. Climate warming impact on degree-days and building energy demand in Switzerland. *Energy Conversion and Management* **47,** 671–686.

Coley D., 2005. www.centres.ex.ac.uk/cee/ga/.

Coley D., S. Schukat, 2002. Low-energy design: combining computer-based optimisation and human judgement. *Building and Environment* **37**, 1241-1247.

Conserval Engineering, 2005. www.solarwall.com/roof/roofHow.html.

Crawley D., J. Hand, M. Kummert, G. Griffith, 2005. *Contrasting the capabilities of building energy performance simulation programs*. Version 1.0, United-States Department of Energy, University of Strathclyde, and University of Wisconsin, www.eere.energy.gov/buildings/tools_directory/.

Dasgupta D, DR McGregor, 1993. sGA : a structured genetic algorithm. Technical Report, IKBS-11-93, Dept. of Computer Science, University of Strathclyde, UK.

Dennis M., 2003. Optimising Energy Balance For Systems With Storage. *ISES Solar World Congress 2003*, Gothenburg, Sweden, 8 pp.

Dumont, R., 2000. The Best Insulated House in the World?, *Home Energy*, May/June 2000, 41-45.

Drück H., E. Hahne, 1998. Test and Comparison of Hot Water Stores for Solar Combisystems, *EuroSun98,* Portoroz, Slovenia.

Earth Energy Society, 2007, www.earthenergy.ca/saving.html.

Ellehauge K., 2002. *A report on combisystems modelled in Task 26: Appendix 1: Generic System # 2 A Solar Combisystem Based on a Heat Exchanger Between the Collector Loop and Space Heating Loop,* IEA SHC, report on Subtask C.

EnerGuide, 2005. *EnerGuide Appliances Directory 2005,* http://oee.nrcan.gc.ca/Publications/infosource/Pub/appliances/.

Energy Star, 2005. www.energystar.gov.

EnergyPlus, 2005. www.eere.energy.gov/buildings/energyplus/weatherdata/.

Environment Canada, 2007. www.climate.weatheroffice.ec.gc.ca.

e-tankless, 2006. www.e-tankless.com.

Farhanieh, B., S. Sattari, 2006. Development of an integrated model for airflow in building spaces. *Renewable Energy* **31**, 401–416.

Feustel, H., 1999. COMIS—an international multizone air-flow and contaminant transport model. *Energy and Buildings* **30,** 3–18.

Fonseca, CM, PJ Flemming, 1998. Multiobjective optimisation and multiple constraint handling with evolutionary algorithms-part 1: a unified formulation. IEEE Transactions on Systems, Man and Cybernetics, Part A; **28**(1):26–37.

Frei U., 2003. Solar Thermal Collectors, State Of The Art And Further Development. *ISES Solar World Congress 2003*, Gothenburg, Sweden, 8 pp.

Furbo S., et al., 2003. Smart Solar Tanks For Small Solar Domestic Hot Water Systems. *ISES Solar World Congress 2003*, Gothenburg, Sweden, 8 pp.

Fung A., et al., 2003. Standby power requirements of household appliances in Canada, *Energy and Building* **35**, 217-228.

Goldberg, D. E., J. Richardson, 1987. Genetic Algorithms with Sharing for Multimodal Function Optimisation, *Genetic Algorithms and their Applications: Proceedings of the Second International Conference on Genetic Algorithms*, pp. 41-49.

Grierson D.E., S. Khajehpour, 2002. Method for Conceptual Design Applied to Office Buildings. *Journal of Computing in Civil Engineering* **16**, 83-103.

Guler, B., A. Fung, I. Ugursal, 1999. *Home Entertainment and Home Office Related Appliances Energy Consumption in Canada*, Canadian Residential Energy End-use Data and Analysis Centre, Report: CREEDAC-1999-04-04.

Haas, A., A. Weber, V. Dorer, W. Keilholz, R. Pelletret, 2002. COMIS v3.1 simulation environment for multizone air flow and pollutant transport modelling. *Energy and Buildings* **34**, 873–882

Hamada, Y., et al., 2003. Development of a database of low energy homes around the world and analyses of their trends, *Renewable Energy* **28**, 321-328.

Herring, H., 1995. Electricity Use in Minor Appliances in the UK, *Energy* **20**, 705-710.

Hoffmann, W., 2006. PV solar electricity industry: Market growth and perspective, *Solar Energy Materials & Solar Cells* **90**, 3285–3311.

Hoiting H., G. Donze, L. Verhoef, 2003. 10 Different Zero Energy Projects In The Netherlands. *ISES Solar World Congress*, 2 pp.

IEA PVPS, 2005. *Trends In Photovoltaic Applications: Survey report of selected IEA countries between 1992 and 2004*. Report IEA-PVPS T1-14:2005, 31 pp.

IEA PVPS, 2006. *Trends In Photovoltaic Applications: Survey report of selected IEA countries between 1992 and 2005*. Report IEA-PVPS T1-15:2006, 34 pp.

IEA SHC, 2004. www.iea-shc.org/task28/index.html.

IEA SHC Task 26, 2005. www.iea-shc.org/task26/.

Imrani A., H. Abidine, M. Limouri, A. Essaîd, 1999. Multimodal optimisation of thermal histories, *Earth and Planetary Science* **329** (8), 573-577.

JATS Alternative Power Company, 2005. www.jatsgreenpower.com.

Jin X., H. Ren, X. Xiao, 2005. Prediction-based online optimal control of outdoor air of multi-zone VAV air conditioning systems. *Energy and Buildings* 37, 939–944.

Kalogirou S., 2004. Optimisation of solar systems using artificial neural-networks and genetic algorithms. *Applied Energy* **77**, 383-405.

Karlsson B., Wilson G., 1999. MaReCo - A Large Asymmetric CPC for High Latitudes. *ISES Solar World Congress 1999,* Jerusalem, Israel.

Kelly, N.J., 1998. *Towards a Design Environment for Building-Integrated Energy Systems: The Integration of Electrical Power Flow Modelling with Building Simulation*, PhD Thesis, University of Strathclyde, Glasgow UK.

Klein, S.A., et al., 2000. *TRNSYS: A Transient System Simulation Program – Volume 1 Reference Manual.* Solar Energy Laboratory, University of Wisconsin, Madison, WI.

Kurtz, M., 1995. *Calculations for Engineering Economic Analysis*. McGraw Hill, US.

Kuznik, F., G. Rusaouen, R. Hohota, 2006. Experimental and numerical study of a mechanically ventilated enclosure with thermal effects. *Energy and Buildings* **38,** 931–938.

Lee, A., J.W. Jones, 1997. Analytical Model of a Residential Desuperheater. *Applied Energy* **57**, No. 4, 271-285.

Loomans, M., H. Visser, 2002. Application of the Genetic Algorithm for Optimisation of Large Solar Hot Water Systems, *Solar Energy* **72** (5), 427–439.

Lucas I., et al., 2001. Behavioural Factors Study Of Residential Users Which Influence The Energy Consumption, *Renewable Energy* **24**, 521-527.

M. Conde Engineering, 2005. *Thermophysical Properties of Brines,* www.mrc-eng.com/Downloads/Brine%20Properties.pdf.

Marks W., 1997. Multicriteria Optimisation of Shape of Energy-Saving Buildings. *Building and Environment* **32**, 331-339.

Mattsson, B., 2006. The influence of wind speed, terrain and ventilation system on the air change rate of a single-family house. *Energy* **31**, 719-731.

McLean, D.J., 1982. *The Simulation of Solar Energy Systems*, PhD Thesis, University of Strathclyde, Glasgow UK.

McQuiston, F., J. Parker, J. Spitler, 2005. *Heating, Ventilating, and Air Conditioning: Analysis and Design*, 6th ed., John Wiley & Sons, Hoboken, US.

Meier A., W. Huber, K. Rosen, 1998. *Reducing leaking electricity to 1 Watt, ACEEE Summer Study on Energy Efficiency in Buildings*, Lawrence Berkeley National Laboratory, Pacific Grove, CA, Report LBNL-42108, http://standby.lbl.gov/articles.html, article viewed 2006.

MIT, 2007. http://designadvisor.mit.edu/design/.

Mitchell, M. 1998. *An Introduction to Genetic Algorithms.* The MIT Press, Cambridge, Massachusetts, 208 pp.

Nakamura Y, 2004. Diffusion of PV System Mounted Houses Aiming at 'Zero-Utility-Cost' in Japan, *European Photovoltaic Solar Energy Conference*, Paris.

NextEnergy, 2006. NextEnergy Geothermal Solutions, www.nextenergysolutions.com.

Noguchi M., 2005. Japanese manufacturers' 'cost-performance' marketing strategy for the delivery of solar photovoltaic homes, *ISES Solar World Congress 2005*, Orlando, FLA.

NRCan, 1993. Technical Requirements for Advanced Houses, CANMET, www.buildingsgroup.nrcan.gc.ca/docs/pdf/publications, viewed 2005.

NRCan, 2002. *Residential Earth Energy Systems: A Buyer's Guide*, www.canren.gc.ca/default_en.asp, viewed 2005.

NRCan, 2005a. *Advanced Houses Documentation*, www.buildingsgroup.nrcan.gc.ca/projects/adv_houses_e.html.

NRCan, 2005b. *Energy Use Data Handbook: 1990 and 1996 to 2003*, Energy Publication Office of the Office of Energy Efficiency, http://oee.nrcan.gc.ca.

NRCan, 2005c. *R-2000 Documentation,* http://oee.nrcan.gc.ca/r-2000/, viewed 2005.

NRCan, 2005d. *EnerGuide Appliance Directory 2005*, http://oee.nrcan.gc.ca/Publications/infosource/Pub/appliances/.

NRCan, 2006. *Technical Requirements for Energy Using Products: Part 2, Household Appliances.* http://www.oee.nrcan.gc.ca/regulations/html/EERGuide_Part2_1.cfm.

NRCan, 2007a. https://glfc.cfsnet.nfis.org/mapserver/pv/index.php.

NRCan, 2007b. www.sbc.nrcan.gc.ca/home_e.asp.

NZEHC, 2005, www.netzeroenergyhome.ca.

OPA, 2007. www.powerauthority.on.ca/sop/.

Orgill, J.F., K.G.T. Hollands, 1977. WATSUN, a Solar Heating Simulation and Economic Evaluation Program: Version 3.0: User's Manual, University of Waterloo, Waterloo Canada.

Passive House, 2004. www.passivehouse.com.

Patio Concepts, 2006, www.patioconcepts.ca/awnings_aluminum_window_arms.htm.

Peippo K., P.D. Lund, E. Vartiainen, 1999. Multivariate optimisation of design trade-offs for solar low energy buildings. *Energy and Buildings* **29,** 189-205.

Pratsch L., 2004. Moving Toward Zero Energy Homes. *Solar Power 2*004, San Francisco, CA.

Prowskiw, G., 1992. *Incremental Costs of Residential Energy Conservation Components and Systems.* CANMET Energy Technology Centre Report, 171 pp.

Radiant Floor Company, 2007. http://www.radiantcompany.com/system/open.shtml

RETScreen International, 2007. www.retscreen.net.

Rowlands, I., 2005. Envisaging feed-in tariffs for solar photovoltaic electricity: European lessons for Canada. *Renewable and Sustainable Energy Reviews* **9,** 51–68.

RReDC, 2007. http://rredc.nrel.gov/solar/.

RS Means, 2005a. *Means Building Construction Cost Data,* R.S. Means Company Ltd., Kingston, MA, 63rd edition, 704 pp.

RS Means, 2005b. *Means Assemblies Cost Data,* R.S. Means Company Ltd., Kingston, MA, 30th edition, 590 pp.

RS Means, 2005c. *Means Mechanical Equipment Cost Data,* R.S. Means Company Ltd., Kingston, MA, 28th edition.

RS Means, 2005d. *Means Electrical Equipment Cost Data,* R.S. Means Company Ltd., Kingston, MA, 28th edition, 512 pp.

SBIC, 2007. www.sbicouncil.org/store/e10.php.

Solar Decathlon, 2005. www.solardecathlon.org.

Solar House, 2005. www.solarhouse.com.

Solvis, 2005. www.solvis.de.

Sowell, E.F., D.C. Hittle, 1995. Evolution of Building Energy Simulation Methodology, *ASHRAE Trans.*, 95-9-2.

Tanaka Y., 2003. Japan Photovoltaic Technology Status and Prospects, *IEA PVPS Japan's 2003 Annual Report*, www.iea-pvps.org.

TESS, 2006. Thermal Energy System Specialists, www.tess-inc.com.

Thermo-Dynamics, 2006. www.thermo-dynamics.com/pdfiles/technical/G_Series_tech.pdf.

ThermoMax, 2006. www.thermomax-group.com/PRODUCTS/SOLAR/productsS.htm.

Thevenard, D, S. Dixon, K. Rueb, M. Chandrashekar, 1992. The current-voltage model for PV modules in the WATSUN-PV simulation software. *Proc. 18th Annual Conf. SESCI*, July 4-8, Edmonton, Alberta, Canada, 39-42.

Trane, 2006. www.trane.com/Commercial/

Turner G., 2002. *The Little Book of Real Estate Wisdom*, Key Porter Books Limited, Toronto, 128 pp.

UCLA, 2007. www2.aud.ucla.edu/heed/.

Ulrike, J., V. Klaus, 2001. *Realistic Domestic Hot-Water Profiles in Different Time Scales,* V.2.0, Universität Marburg.

US DOE, 2000. Zero Net Energy Buildings Outreach and Action Plan, www.eere.energy.gov/buildings/info/documents/pdfs/zne.pdf, viewed October 1, 2004.

US DOE, 2007a. EnergyPlus Energy Simulation Software, www.eere.energy.gov/buildings/energyplus/.

US DOE, 2007b. Building Energy Software Tools Directory. www.eere.energy.gov/buildings/tools_directory/.

Usowicza, B., J. Lipieca, W. Marczewskib, A. Ferreroc, 2006. Thermal conductivity modelling of terrestrial soil media—A comparative study. *Planetary and Space Science* **54,** 1086–1095.

Victorino I.R.S., J.P. Maia, E.R. Morais, M.R. Wolf Maciel, R. Maciel Filho, 2007. Optimization for large-scale process based on evolutionary algorithms: Genetic algorithms. *Chemical Engineering Journal* **132**, 1–8.

Wang S., X. Xu, 2006. Parameter estimation of internal thermal mass of building dynamic models using genetic algorithm. *Energy Conversion and Management* **47,** 1927–1941.

Wang W., H. Rivard, R. Zmeureanu, 2005. An object-oriented framework for simulation-based green building design optimisation with genetic algorithms. *Advanced Engineering Informatics* **19**, 5–23.

Wang W., H. Rivard, R. Zmeureanu, 2006. Floor shape optimisation for green building design. *Advanced Engineering Informatics* **20**, 363–378.

Washington Post, 2005. www.washingtonpost.com/wp-srv/weather.

Wassmer M., C. Warner, 2005. Building-energy and monitoring research activities for solar decathlon houses. *IEEE PVSC Conference*, Orlando, FLA.

Weiss W., 2003. Solar Heating Systems - Status And Recent Developments. *ISES Solar World Congress 2003*, Gothenburg, Sweden, 11 pp.

Weiss W., JM Suter, T. Letz, 2003. Comparison Of System Designs Of Solar Combisystems. *ISES Solar World Congress 2003*, Gothenburg, Sweden, 5pp.

Welfonder, T., M. Hiller, S. Holst, A. Knirsch, 2003. Improvements on the Capabilities of TRNSYS 15, *Proceedings of Building Simulation '03*, 1377-1384, International Building Performance Simulation Association, Eindhoven Netherlands.

Wetter M., Wright J., 2004. A comparison of deterministic and probilistic optimisation algorithms for nonsmooth simulation-based optimisation. *Building and Environment* **39**, 989-999.

Wood G., M. Newborough, 2003. Dynamic Energy-Consumption Indicators For Domestic Appliances: Environment, Behaviour And Design, *Energy and Buildings* **35**, 821-841.

Wright J., A. Alajmi, 2005. The Robustness of Genetic Algorithms in Solving Unconstrained Building Optimisation Problems, *Proceedings of Building Simulation '05,* Montreal, Canada, 1361-1368.

Wright J., H. Loosemore, R. Farmani, 2002. Optimisation of building thermal design and control by mutli-criterion genetic algorithm. *Energy and Buildings* **34**, 959-972.

York, 2006. www.yorkupg.com/homeowners/index.asp.

Appendix A: Type 19 Equation Derivation Example

In order to demonstrate how the Type 19 equations were derived, we will take an example where we have two surfaces and an air node. The first surface (surface 1) is a standard surface represented by transfer functions, whereas the second (surface 2) would be a induction inputs surface such as the underfloor heating used in the low energy home model developed for the GA Optimisation Tool. For this example, we will assume that the surfaces do not self radiate. To show that the equations work, we will work backwards by demonstrating that the following matrix multiplication will lead to the typical energy balance equations:

$$Z \cdot T_s = X \qquad \text{(A1)}.$$

For surface 1, we have the following equations for interior surfaces:

$$Z_{i,j} = \frac{h_{r,i,j}}{h_{c,i}} \cdot \left(\frac{c_{o,i}}{h_{c,i}} - 1 \right) \qquad i \neq j \qquad \text{(A2a)},$$

$$Z_{i,i} = 1 - \frac{1}{h_{c,i}} \cdot \left(\frac{c_{o,i}}{h_{c,i}} - 1 \right) \cdot \sum_{j=1}^{N} h_{r,i,j} \qquad \text{(A2b)},$$

$$Z_{i,N+1} = \frac{c_{o,i}}{h_{c,i}} - 1 \qquad \text{(A2c)},$$

$$X_i = \sum_{h=0} \frac{b_{h,i}}{h_{c,i}} \cdot T_{sa,i,h} - \sum_{h=1} \left(\frac{c_{h,i}}{h_{c,i}} - d_h \right) \cdot T_{eq,i,h} - \sum_{h=1} d_{h,i} \cdot T_{s,i,h} - \frac{s_i}{h_{c,i}} \cdot \left(\frac{c_{o,i}}{h_{c,i}} - 1 \right) \qquad \text{(A2d)}.$$

Placing the A2 equations into Eqn. A1 and multiplying both sides by the surface convective heat transfer equation leads to the following energy balance equation:

$$h_{c,1}\cdot(T_1-T_Z)+h_{r1,2}\cdot\left(\frac{c_{0,1}}{h_{c,1}}-1\right)\cdot(T_2-T_1)$$
$$=\sum_{h=0}b_{h,1}\cdot T_{sa,1,h}-\sum_{h=1}(c_{h,1}-d_h)\cdot T_{eq,1,h}-h_{c,1}\cdot\sum_{h=1}d_{h,1}\cdot T_{s,1,h}-s_1\cdot\left(\frac{c_{0,1}}{h_{c,1}}-1\right) \quad \text{(A3).}$$

For the floor-heating surface, the equations change to:

$$Z_{i,j}=\frac{-h_{r,i,j}}{h_{c,i}} \qquad i\neq j \quad \text{(A4a),}$$

$$Z_{i,i}=1+\frac{\sum h_{r,i,j}}{h_{c,i}} \quad \text{(A4b),}$$

$$Z_{i,N+1}=-1 \quad \text{(A4c),}$$

$$X_i=\frac{\dot{Q}_i/A_i+s_i}{h_{c,i}} \quad \text{(A4d).}$$

Putting the A4 equations into A1 and multiplying by the convective heat transfer leads to:

$$h_{r,2,1}\cdot(T_2-T_1)+h_{c,2}\cdot(T_2-T_{zone})=\frac{\dot{Q}_2}{A_2}+s_2 \quad \text{(A5),}$$

which is what the energy balance on the floor node would give.

Finally zone air node equations are:

$$Z_{N+1,j}=h_{c,j}\cdot A_j \quad \text{(A6a),}$$

$$Z_{N+1,N+1}=-\sum_{j=1}^{N}h_{c,j}\cdot A_j-\frac{2\cdot Cap}{\Delta t} \quad \text{(A6b),}$$

$$X_{N+1}=-\dot{Q}_z-\dot{Q}_v-\dot{Q}_{infil}-\dot{Q}_{int}-0.3\cdot\dot{Q}_{s,people}-\frac{2\cdot Cap}{\Delta t}\cdot T_{ZI} \quad \text{(A6c),}$$

which result in the following equation when they are input into Eqn. A1:

$$h_{c,1} \cdot A_1 \cdot (T_1 - T_{zone}) + h_{c,2} \cdot A_2 \cdot (T_2 - T_{zone}) - \frac{2 \cdot Cap}{\Delta t} \cdot T_{zone} =$$
$$-\dot{Q}_z - \dot{Q}_v - \dot{Q}_{infil} - \dot{Q}_{int} - 0.3 \cdot \dot{Q}_{s,people} - \frac{2 \cdot Cap}{\Delta t} \cdot T_{ZI} \qquad \text{A7.}$$

To get the capacitance terms together, we must first substitute the zone temperature by the zone temperature at the end of the time step using the following linear approximation:

$$T_{ZF} = T_{zone} + (T_{zone} - T_{ZI}) \qquad \text{A8.}$$

Using the expression in A8 in A7 leads to the expected energy balance equation:

$$h_{c,1} \cdot A_1 \cdot (T_1 - T_{zone}) + h_{c,2} \cdot A_2 \cdot (T_2 - T_{zone})$$
$$+ \dot{Q}_z + \dot{Q}_v + \dot{Q}_{infil} + \dot{Q}_{int} + 0.3 \cdot \dot{Q}_{s,people} = \frac{Cap}{\Delta t} \cdot (T_{ZF} - T_{ZI}) \qquad \text{A9.}$$

Appendix B: Product Technical Data Sheets and Input Files

Presented in order of appearance from thesis:

1. G-Series flat plate solar collector technical specifications from Thermo Dynamics Ltd. (Thermo-Dynamics, 2006)
2. Mazdon evacuated tube solar collector technical specifications from Thermomax Ltd. (ThermoMax, 2006)
3. Input files for York Affinity R-410a, 2 Ton, SEER 15, Split-System Air Conditioner (York, 2006)
4. Technical Specifications for Model 240 electric tankless water heater from e-Tankless Water Heaters (e-tankless, 2006)
5. Input Files for York Affinity R-410a, 2 Ton, SEER 15, Split-System Heat Pump (York, 2006)
6. Input files for Tranquility 27 TT Series, 2 Ton, Geothermal heating and cooling system from NextEnergy Geothermal Solutions (NextEnergy, 2006)
7. Input files for High Efficiency Water-to-Water, 2 Ton, Water-Source Comfort System from Trane (Trane, 2006)
8. Technical specifications for SQ160-PC PV panel from Shell Solar (JATS Alternative Power Company, 2005)

G-Series Flat Plate Solar Collector (Thermo-Dynamics, 2006)

G SERIES Solar Collectors

Glazed Liquid Flat Plate Collectors
Technical Specifications

J. Collector Efficiency

1.0 General Description

1.1 Test Method:
Tested in accordance with SRCC (Solar Rating and Certification Corporation) Standard OG100-81 with reference ANSI/ ASHRAE Standard 93-86. Thermal efficiency is calculated as recommended in ASHRAE 93-86.

1.2 Testing Information:
Agency: National Solar Test Facility
Location: Ontario, Canada
Lat. 43.53 °N
Long. 79.66 °W
Elevation: 160 m (525 ft)
Date: September 14, 1990

1.3 Details of Tested collector:
Model: G32
Glazing: low-iron tempered Solite
Absorber material: aluminum fin and tube
Absorber coating: Anodic–Cobalt™
Insulation: fiberglass
Gross area: 2.96 m² (31.9 ft²)
Aperture area: 2.78 m² (30.0 ft²)
Absorber area: 2.87 m² (30.9 ft²)

1.4 Comments:
The time constant and thermal efficiency test were determined in the solar simulator. Incident angle modifier was determined from outdoor testing.

2.0 Test Conditions

2.1 Collector Tilt and Orientation:
Normal to the direction of irradiation.

2.2 Heat Transfer Fluid:
Water

2.3 Liquid Flow Rate:
0.0667 kg/s (0.1467 lb/s)

2.4 Range of Ambient Air Temperature:
19.9°C to 20.7°C (67.8°F to 69.3°F)

2.5 Wind Velocity:
3.5 m/sec (11.5 ft/sec)

2.6 Range of insolation:
996 to 1007 W/m²
316 to 319 Btu/ft² h

3.0 Time Constant:
90 sec± 5 sec at 0.0667 kg/s (0.1467 lb/s)

4.0 Efficiency:
Efficiency curve is based on gross collector area, and was determined using the indoor solar simulator.

First order efficiency equation:
$\eta = 0.738 - 5.247(Ti - Ta)/G$

5.0 Incident Angle Modifier:
$K_{\tau\alpha} = 1 - 0.154(1/\cos\theta - 1)$

6.0 FSEC Standard Day Tests:
The following standard day tests were performed by The Florida Solar Energy Center, (FSEC). Standard day: 5045 W•hr/m².

Energy collected per collector per day:
Clear day: 35.3 MJ/d (33.5 MBtu/d)
Mildly Cloudy: 27.7 MJ/d (26.3 MBtu/d)
Cloudy Day: 9.12 MJ/d (8.65 MBtu/d)

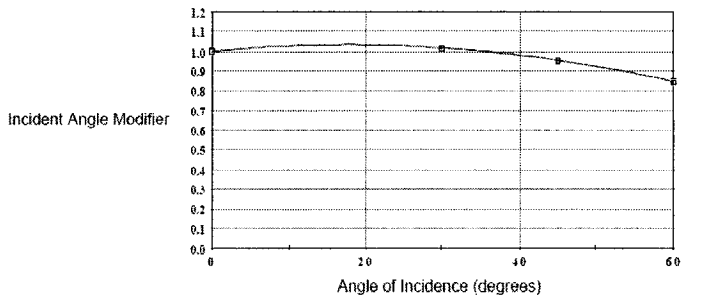

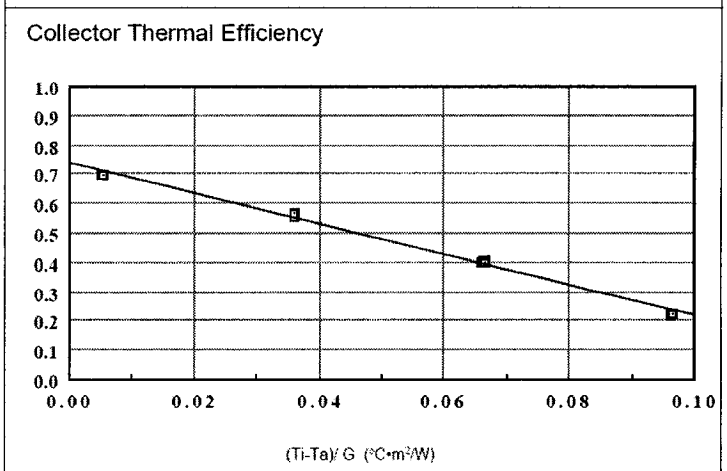

Mazdon Evacuated Tube Collector (ThermoMax, 2006)

2. Collector description

Contact	Thermomax Ltd., GB- Bangor BT19 7UP Tel. +44 (02891) 270411, Fax +44 (02891) 270572
Distributed in *	CH,DE,AT
Type	Evacuated tube collector, water heat pipe, wet connection
Assembly	Heat pipe with temperature limitation.
Installation *	Installation on sloping roof, Flat roof with support
Rated flowrate *	120 l/h
Absorber coating *	Black chrome on nickel on copper "mti"
Dimensions (absorber, aperture, gross)	1.975 m², 2.154 m², 2.762 m²

Collector Test No. C264

SPF Solartechnik Prüfung Forschung

4. Thermal performance (flowrate at test: 114 l/h)

4.1 Efficiency caracteristic curve

Measurement with wind (acc. to ISO, DIN, prEN)

Bezugsfläche:	Absorber	Apertur	Brutto
η_0 (-)			
a_1 (W/m²K)			
a_2 (W/m²K²)			

$\eta(T^*_m) = \eta_0 - a_1 \cdot T^*_m - a_2 \cdot G \cdot T^{*2}_m$ $[T^*_m = (t_m - t_a)/G]$

t_m: avg. fluid temp, t_a: ambient temperature, G: irradiance

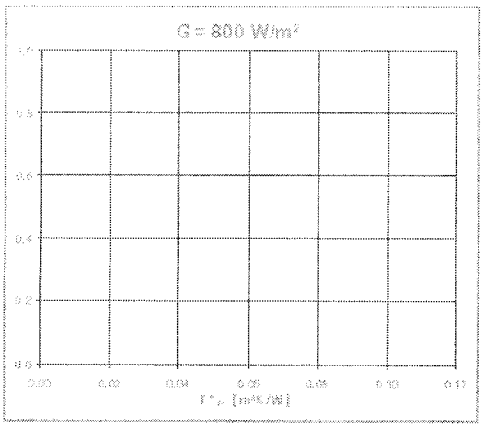

Measurement without wind (acc. to SPF)

Reference area	Absorber	Aperture	Gross
c_0 (-)	0.840	0.770	0.601
c_1 (W/m²K)	2.02	1.85	1.44
c_2 (W/m²K²)	0.0046	0.0042	0.0033

$\eta(x) = c_0 - c_1 \cdot x - c_2 \cdot G \cdot x^2$ $[x = (t_m - t_a)/G]$

t_m: avg. fluid temp, t_a: ambient temperature, G: irradiance

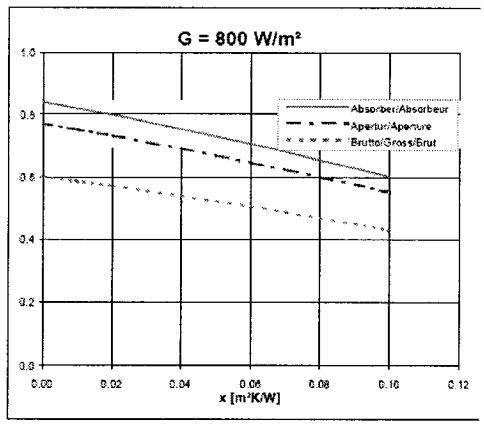

4.2 Characteristic efficiency values (normal incidence, G = 800 W/m²)

Bezugsfläche:	Absorber	Apertur	Brutto
η (T^*_m = 0.00)			
η (T^*_m = 0.05)			
η (T^*_m = 0.10)			

Reference area	Absorber	Aperture	Gross
η (x = 0.00)	0.84	0.77	0.60
η (x = 0.05)	0.73	0.67	0.52
η (x = 0.10)	0.60	0.55	0.43

4.3 Power output (power in watts per collector, normal incidence, beam irradiation)

	400 W/m²	700 W/m²	1000 W/m²
$t_m - t_a$ = 10 K			
$t_m - t_a$ = 30 K			
$t_m - t_a$ = 50 K			

Irradiation	400 W/m²	700 W/m²	1000 W/m²
$t_m - t_a$ = 10 K	623	1'120	1'618
$t_m - t_a$ = 30 K	536	1'033	1'531
$t_m - t_a$ = 50 K	441	939	1'437

4.4 Incidence angle modifier (IAM)

	0°	10°	20°	30°	40°	**50°**	60°	70°	80°	90°
$K(\Theta)_{,long}$	1.0					**0.91**				0.0
$K(\Theta)_{,trans}$	1.0					**0.96**				0.0

York Affinity R-410a, 2 Ton, SEER 15, Split-System Air Conditioner (York, 2006)

259.6 283.2 306.8 330.4 377.6 424.8 !air flow rates in l/s
18.3 23.9 29.4 35 40.6 46.1 51.7 !outdoor dry bulb T (°C)
13.9 16.7 19.4 22.2 !indoor wet bulb T (°C)
26.7 !indoor dry bulb T (°C)
4.8 5.0 0.8 !total capacity (kW), sensible capacity (kW) and power (kW) at 259.6, 18.3, 13.9, 26.7

5.0 4.8 0.7 !total capacity (kW), sensible capacity (kW) and power (kW) at 259.6, 18.3, 16.7, 26.7

4.5 3.5 0.5 !total capacity (kW), sensible capacity (kW) and power (kW) at 259.6, 18.3, 19.4, 26.7

5.6 3.2 0.7 !total capacity (kW), sensible capacity (kW) and power (kW) at 259.6, 18.3, 22.2, 26.7

4.6 4.7 0.9 !total capacity (kW), sensible capacity (kW) and power (kW) at 259.6, 23.9, 13.9, 26.7

4.7 4.6 0.9 !total capacity (kW), sensible capacity (kW) and power (kW) at 259.6, 23.9, 16.7, 26.7

5.0 3.9 0.9 !total capacity (kW), sensible capacity (kW) and power (kW) at 259.6, 23.9, 19.4, 26.7

5.4 3.1 0.8 !total capacity (kW), sensible capacity (kW) and power (kW) at 259.6, 23.9, 22.2, 26.7

4.4	4.5	1.0	!etc...	3.6	3.6	1.7	4.4	4.5	1.1
4.5	4.5	1.0		3.3	3.5	1.8	4.3	4.5	1.1
5.6	4.4	1.0		4.9	4.2	1.8	5.4	4.4	1.2
5.1	3.0	1.0		3.9	2.6	1.7	4.9	3.0	1.2
4.2	4.3	1.2		5.0	5.1	0.7	4.1	4.2	1.3
4.2	4.3	1.2		5.0	5.0	0.7	4.0	4.2	1.3
6.1	4.8	1.2		5.0	4.0	0.6	5.0	4.2	1.3
4.8	2.9	1.1		5.7	3.3	0.7	4.5	2.8	1.3
4.0	4.1	1.4		4.8	4.9	0.8	3.9	4.0	1.5
3.9	4.0	1.4		4.8	4.8	0.8	3.8	4.0	1.5
5.7	4.6	1.4		5.2	4.1	0.9	4.7	4.0	1.5
4.5	2.8	1.3		5.5	3.2	0.9	4.2	2.8	1.5
3.8	3.8	1.6		4.6	4.7	1.0	3.7	3.8	1.7
3.6	3.8	1.6		4.6	4.7	1.0	3.5	3.7	1.7
5.3	4.4	1.6		5.3	4.2	1.1	4.3	3.9	1.7
4.2	2.7	1.5		5.2	3.1	1.0	3.8	2.6	1.7

5.2	5.2	0.6
5.1	5.3	0.7
5.6	4.5	0.7
5.9	3.4	0.7
5.0	5.0	0.8
4.9	5.1	0.8
5.3	4.3	0.9
5.5	3.3	0.9
4.7	4.8	0.9
4.7	4.9	0.9
5.0	4.1	1.0
5.2	3.1	1.0
4.5	4.6	1.1
4.4	4.7	1.1
4.7	3.9	1.2
4.9	3.0	1.2
4.3	4.3	1.3
4.2	4.4	1.3
4.4	3.8	1.4
4.5	2.9	1.4
4.0	4.1	1.5
3.9	4.1	1.5
4.1	3.7	1.6
4.1	2.8	1.6
3.8	3.9	1.7
3.7	3.8	1.7
3.8	3.5	1.7
3.8	2.7	1.7
7.2	7.2	1.3
7.4	7.0	1.3
7.9	5.8	1.4
8.4	4.6	1.4
6.9	6.9	1.5
7.1	6.8	1.5
7.6	5.6	1.5
8.1	4.5	1.6
6.7	6.7	1.7
6.7	6.5	1.7
7.3	5.5	1.7
7.6	4.3	1.8
6.5	6.5	1.9
6.4	6.3	1.8
7.0	5.4	1.9
7.3	4.1	2.0
6.2	6.2	2.2
6.0	6.0	2.1
6.5	5.1	2.2
6.7	4.0	2.3
5.9	5.9	2.5
5.6	5.7	2.4
6.0	4.9	2.5
6.2	3.8	2.6
5.5	5.5	2.8
5.3	5.5	2.7
5.6	4.7	2.8
5.7	3.6	2.8
7.4	7.4	1.3
7.5	7.2	1.3
8.0	5.9	1.4
8.5	4.7	1.4
7.2	7.1	1.5
7.2	7.0	1.5
7.7	5.8	1.5
8.1	4.6	1.6
6.9	6.9	1.7
6.9	6.8	1.7
7.4	5.7	1.7
7.7	4.4	1.8
6.7	6.6	1.9
6.6	6.6	1.9
7.0	5.6	1.9
7.3	4.3	2.0
6.3	6.3	2.2
6.2	6.2	2.2
6.6	5.3	2.2
6.8	4.1	2.3
6.0	5.9	2.5
5.8	5.9	2.5
6.1	5.1	2.5
6.3	3.9	2.5
5.7	5.6	2.8
5.4	5.5	2.7
5.7	4.8	2.8
5.8	3.7	2.8
7.6	7.6	1.3
7.6	7.5	1.3
8.1	6.2	1.4
8.6	4.8	1.4
7.4	7.3	1.5
7.4	7.3	1.5
7.8	6.0	1.5
8.2	4.7	1.6
7.1	7.0	1.7
7.1	7.1	1.7
7.4	5.9	1.7
7.8	4.5	1.8
6.8	6.7	1.9
6.8	6.9	1.9
7.1	5.7	1.9
7.4	4.4	2.0
6.5	6.4	2.2
6.4	6.4	2.2
6.7	5.5	2.2
6.9	4.2	2.3
6.1	6.1	2.5
5.9	6.0	2.5
6.2	5.2	2.5
6.4	4.0	2.5
5.8	5.7	2.8
5.5	5.7	2.8
5.7	5.0	2.8
5.9	3.8	2.8

Model 240 electric tankless water heater (e-tankless, 2006)

Models/Pricing	Model 240	Model 220	Model 180	Model 165	Model 145	Model 110
Dimensions	17"x16"x3"	17"x16"x3"	16"x13.5"x3"	16"x13.5"x3"	16"x13.5"x3"	9"x12"x3"
Weight	12 lbs	12 lbs.	12 lbs.	12 lbs.	12 lbs.	9lbs.
Materials	Copper Exchanger / Aluminum Casing					
Pipe Fittings	3/4" Standard Pipe / ASTM B-88					1/2"
Voltage	208 - 240 volts single phase					
Max.Amps	98.6 @ 240V	93.6A @ 240 V	79A @ 240V	68.5A@240V	58A @ 240V	45.8A @240V
Minimum AMPs to Home	200	200	150	100	100	75
Breakers Required	1X120 AMP	1X120 AMP	1X80 AMP	1X80 AMP	1X70 AMP	1X 50 AMP
Recommended Max Flow	3GPM	3GPM	3GPM	3 GPM	2.5 GPM	2 GPM
KW	24 KW	22 KW	18 KW	16.5 KW	14.5 KW	11 KW
Elements	3	3	2	2	2	2
Energy Efficiency	98.50%					
Activation Flow Rate	.25 GPM					
Frequency	50 - 60 Hz					
Operating Range	5 - 150 PSI (40+PSI Recommended)					
Protection	Thermal / Automatic Reset					
Warranty	Lifetime 100% Parts Replacement					
Certifications	UL and ULC Listed					
BTU Equivalent	81,888	75,064	61,416	54,592	47,768	37,532
Price (US$)	**$ 748.00**	**$ 748.00**	**$ 728.00**	**$ 708.00**	**$ 688.00**	**$ 449.00**
Price (CDN$)	**$ 949.00**	**$ 949.00**	**$ 999.00**	**$ 949.00**	**$ 899.00**	**$ 549.00**

Flow Rate - GPM	Model 240	Model 220	Model 180	Model 165	Model 145	Model 110
0.5	326.5	299.4	244.8	224.4	197.2	149.6
1	163.3	149.7	122.4	112.2	98.6	74.8
1.5	108.8	99.8	81.6	74.8	65.7	49.9
2	81.5	74.9	61.2	56.1	49.3	37.4
2.5	65.3	59.9	49.1	44.9	39.4	29.9
3	54.4	49.9	40.8	37.4	32.9	24.9
3.5	46.6	42.8	35.1	32.1	28.2	21.4
4	40.8	37.4	30.6	28.1	24.7	18.7

York Affinity R410a, 2 Ton, Air-to-Air Heat Pump - Cooling Data

259.6 283.2 306.8 330.4 377.6 424.8 !air flow rates in l/s
13.9 16.7 19.4 22.2 !Return air wet bulb T (°C)
23.9 26.7 !Return air dry bulb T (°C)
23.9 29.4 35 40.6 46.1 51.7 !Outdoor dry bulb T (°C)
5.22 4.13 1.20 !Total capacity (kW), sensible capacity (kW) and power (kW) at 259.6, 13.9, 23.9, 23.9

4.98 3.93 1.40 !total capacity (kW), sensible capacity (kW) and power (kW) at 259.6, 13.9, 23.9, 29.4

4.78 3.69 1.50 !total capacity (kW), sensible capacity (kW) and power (kW) at 259.6, 13.9, 23.9, 35

4.48 3.49 1.90 !total capacity (kW), sensible capacity (kW) and power (kW) at 259.6, 13.9, 23.9, 40.6

4.22 3.25 2.00 !total capacity (kW), sensible capacity (kW) and power (kW) at 259.6, 13.9, 23.9, 46.1

3.99 3.05 2.20 !total capacity (kW), sensible capacity (kW) and power (kW) at 259.6, 13.9, 23.9, 51.7

5.45 5.01 1.20 !total capacity (kW), sensible capacity (kW) and power (kW) at 259.6, 13.9, 26.7, 23.9

5.19	4.75	1.40 !etc...	5.19	3.02	1.50	5.45	2.90	1.70
4.95	4.48	1.50	4.78	2.87	1.80	5.04	2.75	2.00
4.72	4.28	1.80	4.37	2.75	2.00	4.63	2.64	2.20
4.51	4.04	2.00	3.99	2.61	2.20	5.45	4.31	1.20
4.31	3.84	2.20	6.10	4.13	1.20	5.25	4.07	1.30
5.39	4.02	1.20	5.74	3.99	1.30	4.95	3.87	1.50
5.10	3.87	1.30	5.36	3.81	1.50	4.66	3.63	1.70
4.81	3.69	1.50	5.01	3.66	1.70	4.40	3.46	2.00
4.45	3.55	1.80	4.66	3.55	2.00	4.13	3.22	2.20
4.10	3.40	2.00	4.31	3.40	2.20	5.71	5.25	1.20
3.75	3.22	2.20	6.39	2.37	1.20	5.42	4.95	1.30
5.63	4.89	1.20	6.04	2.32	1.30	5.16	4.69	1.50
5.30	4.69	1.30	5.69	2.23	1.50	4.92	4.45	1.70
4.98	4.48	1.50	5.22	2.11	1.80	4.69	4.22	2.00
4.69	4.34	1.70	4.75	1.96	2.00	4.48	3.99	2.20
4.40	4.19	2.00	4.31	1.85	2.20	5.51	4.25	1.20
4.07	4.02	2.20	6.62	3.25	1.20	5.25	4.07	1.30
5.86	3.25	1.20	6.24	3.14	1.30	4.89	3.90	1.50
5.54	3.17	1.30	5.86	3.02	1.50	4.54	3.72	1.70

4.19	3.58	2.00	5.01	4.10	1.50	6.74	5.19	1.60
3.84	3.40	2.20	4.66	3.93	1.70	6.51	5.10	1.70
5.77	5.19	1.20	4.31	3.75	2.00	6.30	5.01	1.90
5.42	4.95	1.30	3.93	3.58	2.20	5.86	4.81	2.20
5.10	4.72	1.50	5.95	5.45	1.20	5.48	4.57	2.50
4.81	4.54	1.70	5.57	5.22	1.30	5.07	4.37	2.80
4.48	4.34	2.00	5.25	4.98	1.50	7.06	6.30	1.60
4.19	4.16	2.20	4.92	4.75	1.70	6.80	6.21	1.80
5.95	3.40	1.10	4.60	4.51	2.00	6.56	6.13	1.90
5.66	3.25	1.30	4.28	4.28	2.20	6.18	5.86	2.20
5.25	3.17	1.50	5.98	3.55	1.10	5.83	5.60	2.50
4.84	3.02	1.70	5.74	3.37	1.20	5.51	5.33	2.80
4.43	2.93	2.00	5.30	3.28	1.50	7.33	4.25	1.60
4.02	2.81	2.20	4.89	3.19	1.70	7.03	4.10	1.70
6.21	4.34	1.10	4.51	3.11	2.00	6.74	3.96	2.00
5.83	4.13	1.30	4.07	3.02	2.20	6.27	3.87	2.30
5.45	3.99	1.50	6.30	4.54	1.10	5.86	3.75	2.50
5.10	3.84	1.70	5.92	4.31	1.20	5.36	3.66	2.80
4.72	3.69	2.00	5.54	4.16	1.50	7.65	5.36	1.60
4.37	3.58	2.20	5.16	4.02	1.70	7.33	5.22	1.80
6.54	2.49	1.10	4.81	3.87	2.00	7.00	5.07	2.00
6.15	2.43	1.30	4.43	3.72	2.20	6.59	4.92	2.30
5.74	2.34	1.50	6.62	2.64	1.10	6.21	4.78	2.50
5.25	2.20	1.70	6.27	2.52	1.20	5.80	4.63	2.80
4.81	2.11	1.90	5.77	2.43	1.50	7.88	3.08	1.60
4.34	1.99	2.20	5.30	2.32	1.70	7.59	2.99	1.70
6.80	3.43	1.10	4.86	2.23	1.90	7.30	2.87	2.00
6.33	3.31	1.30	4.40	2.14	2.20	6.74	2.81	2.30
5.95	3.17	1.50	6.95	3.63	1.10	6.24	2.70	2.60
5.51	3.02	1.70	6.45	3.46	1.20	5.69	2.64	2.80
5.10	2.87	1.90	6.01	3.31	1.50	8.21	4.19	1.60
4.69	2.75	2.20	5.57	3.14	1.70	7.88	4.10	1.80
5.63	4.45	1.20	5.16	2.99	1.90	7.56	3.99	2.00
5.48	4.22	1.30	4.75	2.84	2.20	7.06	3.87	2.30
5.16	4.02	1.50	6.54	5.36	1.60	6.59	3.72	2.60
4.86	3.81	1.70	6.42	5.22	1.60	6.13	3.60	2.80
4.60	3.60	2.00	6.30	5.10	1.90	6.86	5.69	1.60
4.28	3.43	2.20	5.92	4.86	2.20	6.68	5.54	1.60
5.95	5.45	1.20	5.60	4.60	2.50	6.54	5.30	1.80
5.66	5.16	1.30	5.22	4.37	2.80	6.13	5.10	2.20
5.39	4.89	1.50	6.86	6.48	1.60	5.77	4.92	2.50
5.13	4.63	1.70	6.71	6.33	1.70	5.39	4.69	2.80
4.89	4.37	2.00	6.56	6.21	1.90	7.21	6.80	1.60
4.63	4.13	2.20	6.24	5.92	2.20	7.06	6.65	1.70
5.63	4.45	1.20	5.95	5.63	2.50	6.89	6.48	1.90
5.39	4.28	1.30	5.66	5.33	2.80	6.56	6.15	2.20

6.24	5.83	2.50	7.21	6.74	2.00
5.92	5.51	2.80	6.86	6.39	2.20
6.95	5.60	1.60	6.51	6.04	2.50
6.68	5.51	1.70	6.15	5.69	2.80
6.45	5.39	1.90	7.15	6.01	1.60
6.01	5.16	2.20	6.89	5.89	1.70
5.63	4.95	2.50	6.59	5.77	1.90
5.22	4.72	2.80	6.15	5.54	2.20
7.30	6.71	1.60	5.74	5.30	2.50
7.06	6.62	1.80	5.33	5.07	2.80
6.80	6.56	2.00	7.56	7.12	1.60
6.45	6.21	2.20	7.30	7.06	1.80
6.10	5.86	2.50	7.03	6.98	2.00
5.74	5.54	2.80	6.68	6.54	2.30
7.53	4.66	1.60	6.33	6.13	2.50
7.15	4.51	1.70	5.98	5.69	2.80
6.86	4.28	1.90	7.68	5.04	1.60
6.36	4.25	2.30	7.33	4.84	1.70
5.89	4.25	2.50	6.98	4.63	1.90
5.42	4.19	2.80	6.45	4.69	2.20
7.88	5.77	1.60	5.95	4.72	2.50
7.53	5.63	1.80	5.45	4.78	2.80
7.21	5.45	2.00	8.09	6.15	1.60
6.80	5.30	2.30	7.74	6.01	1.80
6.36	5.16	2.50	7.41	5.83	2.00
5.95	5.01	2.80	6.98	5.69	2.30
8.09	3.40	1.60	6.54	5.54	2.50
7.71	3.28	1.70	6.10	5.39	2.80
7.39	3.14	1.90	8.26	3.72	1.60
6.80	3.08	2.30	7.88	3.55	1.70
6.27	3.08	2.60	7.50	3.40	1.90
5.71	3.02	2.80	6.89	3.43	2.20
8.44	4.51	1.60	6.30	3.43	2.60
8.09	4.40	1.80	5.71	3.49	2.80
7.74	4.31	2.00	8.67	4.84	1.60
7.24	4.13	2.30	8.29	4.72	1.80
6.74	3.99	2.60	7.94	4.60	2.00
6.24	3.84	2.80	7.41	4.43	2.30
7.18	6.01	1.60	6.89	4.25	2.60
6.98	5.74	1.70	6.36	4.10	2.80
6.77	5.54	1.90			
6.33	5.39	2.10			
5.92	5.22	2.50			
5.51	5.07	2.80			
7.59	7.12	1.60			
7.39	6.92	1.80			

York Affinity R410a, 2 Ton, Air-to-Air Heat Pump - Heating Data

```
259.6  283.2  306.8  330.4  377.6  424.8        !air flow rates in l/s
15.56  21.11  26.67                            !Indoor dry bulb (°C)
-12.22 -8.33  -1.11  4.44   8.33   15.56        !Outdoor dry bulb (°C)
3.08   1.40                                     !Heat capcity (kW) and power (kW) at
259.6/15.56/-12.22

3.60   1.40                                     !Heat capcity (kW) and power (kW) at
259.6/15.56/-8.33

4.51   1.30                                     !Heat capcity (kW) and power (kW) at
259.6/15.56/-1.11

4.92   1.40                                     !Heat capcity (kW) and power (kW) at
259.6/15.56/4.44

5.71   1.50                                     !Heat capcity (kW) and power (kW) at
259.6/15.56/8.33

6.86   1.60                                     !Heat capcity (kW) and power (kW) at
259.6/15.56/15.56

2.75   1.50                                     !Heat capcity (kW) and power (kW) at
259.6/21.11/-12.22

3.14   1.60                                     !Heat capcity (kW) and power (kW) at
259.6/21.11/-8.33

4.22   1.50                                     !Heat capcity (kW) and power (kW) at
259.6/21.11/-1.11

4.60   1.60 !etc...   6.89   1.50     3.63   1.40     4.63   1.70
5.51   1.70           2.81   1.50     4.54   1.30     5.39   1.90
6.36   1.80           3.19   1.60     4.89   1.30     6.27   1.90
2.43   1.60           4.22   1.50     5.74   1.40     3.99   1.70
2.70   1.80           4.69   1.60     6.95   1.50     4.95   1.80
3.90   1.60           5.54   1.70     2.87   1.50     5.98   1.90
4.28   1.80           6.48   1.70     3.25   1.60     6.80   2.00
5.30   2.00           2.49   1.60     4.25   1.40     7.36   2.00
5.89   2.00           2.78   1.80     4.75   1.50     9.73   2.10
3.14   1.40           3.93   1.60     5.57   1.60     3.90   2.10
3.60   1.40           4.45   1.80     6.59   1.70     4.57   2.00
4.51   1.30           5.36   1.90     2.58   1.60     6.33   2.30
4.89   1.30           6.07   1.90     2.87   1.80     6.33   2.40
5.71   1.40           3.17   1.30     3.96   1.60     7.09   2.30
```

9.35	2.30
3.84	2.40
4.19	2.10
6.71	2.70
5.86	2.80
6.83	2.50
8.97	2.60
3.93	1.70
4.86	1.80
6.04	1.80
6.83	1.90
7.56	1.90
9.73	2.00
3.90	2.00
4.57	1.90
6.39	2.20
6.27	2.20
7.33	2.20
9.38	2.20
3.87	2.30
4.28	2.10
6.71	2.60
5.69	2.50
7.09	2.40
9.03	2.50
3.90	1.70
4.78	1.70
6.10	1.80
6.86	1.80
7.74	1.80
9.73	1.90
3.90	2.00
4.57	1.90
6.42	2.10
6.18	2.00
7.56	2.10
9.41	2.10
3.93	2.20
4.40	2.10
6.74	2.40
5.51	2.20
7.39	2.40
9.09	2.30

Tranquility 27 TT Series – 2 ton GSHP – cooling

344.5 401.2 !Values of airflow in (l/s)
0.2524 0.3785 .5047 !Values of liquid flow rate in (l/s)
-1.11 4.44 10.00 15.56 21.11 26.67 32.22 37.78 43.33 48.84 !Values of entering liquid temperature (°C)
8.88 5.28 0.97 !Total cooling (kW), sensible cooling (kW) and power (kW) at 344.5 / 0.2524 / -1.11
8.79 5.39 1.07 !Total cooling (kW), sensible cooling (kW) and power (kW) at 344.5 / 0.2524 / 4.44
8.56 5.42 1.18 !Total cooling (kW), sensible cooling (kW) and power (kW) at 344.5 / 0.2524 / 10.00
8.24 5.28 1.30 !Total cooling (kW), sensible cooling (kW) and power (kW) at 344.5 / 0.2524 / 15.56
7.80 5.13 1.44 !Total cooling (kW), sensible cooling (kW) and power (kW) at 344.5 / 0.2524 / 21.11
7.33 4.92 1.59 !Total cooling (kW), sensible cooling (kW) and power (kW) at 344.5 / 0.2524 / 26.67
6.86 4.69 1.77 !Total cooling (kW), sensible cooling (kW) and power (kW) at 344.5 / 0.2524 / 32.22
6.39 4.51 1.97 !Total cooling (kW), sensible cooling (kW) and power (kW) at 344.5 / 0.2524 / 37.78
5.92 4.31 2.20 !Total cooling (kW), sensible cooling (kW) and power (kW) at 344.5 / 0.2524 / 43.33
5.51 4.16 2.46 !Total cooling (kW), sensible cooling (kW) and power (kW) at 344.5 / 0.2524 / 48.84
8.94 5.28 0.93 !Total cooling (kW), sensible cooling (kW) and power (kW) at 344.5 / 0.3785 / -1.11
8.88 5.42 1.01 !Total cooling (kW), sensible cooling (kW) and power (kW) at 344.5 / 0.3785 / 4.44
8.70 5.42 1.12 !Total cooling (kW), sensible cooling (kW) and power (kW) at 344.5 / 0.3785 / 10.00
8.44 5.36 1.23 !Total cooling (kW), sensible cooling (kW) and power (kW) at 344.5 / 0.3785 / 15.56
8.03 5.22 1.36 !Total cooling (kW), sensible cooling (kW) and power (kW) at 344.5 / 0.3785 / 21.11
7.59 5.04 1.51 !Total cooling (kW), sensible cooling (kW) and power (kW) at 344.5 / 0.3785 / 26.67
7.09 4.81 1.68 !Total cooling (kW), sensible cooling (kW) and power (kW) at 344.5 / 0.3785 / 32.22
6.62 4.60 1.87 !Total cooling (kW), sensible cooling (kW) and power (kW) at 344.5 / 0.3785 / 37.78
6.13 4.40 2.08 !Total cooling (kW), sensible cooling (kW) and power (kW) at 344.5 / 0.3785 / 43.33
5.69 4.22 2.33 !Total cooling (kW), sensible cooling (kW) and power (kW) at 344.5 / 0.3785 / 48.84

8.97 5.28 0.91 !Total cooling (kW), sensible cooling (kW) and power (kW) at 344.5 / 0.5047 / -1.11
8.91 5.42 0.99 !Total cooling (kW), sensible cooling (kW) and power (kW) at 344.5 / 0.5047 / 4.44
8.79 5.42 1.09 !Total cooling (kW), sensible cooling (kW) and power (kW) at 344.5 / 0.5047 / 10.00
8.53 5.39 1.19 !Total cooling (kW), sensible cooling (kW) and power (kW) at 344.5 / 0.5047 / 15.56
8.15 5.25 1.32 !Total cooling (kW), sensible cooling (kW) and power (kW) at 344.5 / 0.5047 / 21.11
7.71 5.07 1.46 !Total cooling (kW), sensible cooling (kW) and power (kW) at 344.5 / 0.5047 / 26.67
7.21 4.86 1.63 !Total cooling (kW), sensible cooling (kW) and power (kW) at 344.5 / 0.5047 / 32.22
6.74 4.66 1.82 !Total cooling (kW), sensible cooling (kW) and power (kW) at 344.5 / 0.5047 / 37.78
6.24 4.43 2.03 !Total cooling (kW), sensible cooling (kW) and power (kW) at 344.5 / 0.5047 / 43.33
5.80 4.25 2.27 !Total cooling (kW), sensible cooling (kW) and power (kW) at 344.5 / 0.5047 / 48.84
9.06 5.74 1.01 !Total cooling (kW), sensible cooling (kW) and power (kW) at 401.2 / 0.2524 / -1.11
8.97 5.86 1.11 !Total cooling (kW), sensible cooling (kW) and power (kW) at 401.2 / 0.2524 / 4.44
8.73 5.89 1.22 !Total cooling (kW), sensible cooling (kW) and power (kW) at 401.2 / 0.2524 / 10.00
8.41 5.74 1.35 !Total cooling (kW), sensible cooling (kW) and power (kW) at 401.2 / 0.2524 / 15.56
7.97 5.57 1.49 !Total cooling (kW), sensible cooling (kW) and power (kW) at 401.2 / 0.2524 / 21.11
7.50 5.36 1.65 !Total cooling (kW), sensible cooling (kW) and power (kW) at 401.2 / 0.2524 / 26.67
6.98 5.10 1.85 !Total cooling (kW), sensible cooling (kW) and power (kW) at 401.2 / 0.2524 / 32.22
6.51 4.89 2.06 !Total cooling (kW), sensible cooling (kW) and power (kW) at 401.2 / 0.2524 / 37.78
6.04 4.66 2.29 !Total cooling (kW), sensible cooling (kW) and power (kW) at 401.2 / 0.2524 / 43.33
5.63 4.54 2.56 !Total cooling (kW), sensible cooling (kW) and power (kW) at 401.2 / 0.2524 / 48.84
9.11 5.74 0.97 !Total cooling (kW), sensible cooling (kW) and power (kW) at 401.2 / 0.3785 / -1.11
9.06 5.89 1.05 !Total cooling (kW), sensible cooling (kW) and power (kW) at 401.2 / 0.3785 / 4.44
8.88 5.92 1.16 !Total cooling (kW), sensible cooling (kW) and power (kW) at 401.2 / 0.3785 / 10.00

8.62 5.83 1.28 !Total cooling (kW), sensible cooling (kW) and power (kW) at 401.2 / 0.3785 / 15.56
8.21 5.66 1.41 !Total cooling (kW), sensible cooling (kW) and power (kW) at 401.2 / 0.3785 / 21.11
7.77 5.48 1.57 !Total cooling (kW), sensible cooling (kW) and power (kW) at 401.2 / 0.3785 / 26.67
7.24 5.22 1.75 !Total cooling (kW), sensible cooling (kW) and power (kW) at 401.2 / 0.3785 / 32.22
6.74 5.01 1.95 !Total cooling (kW), sensible cooling (kW) and power (kW) at 401.2 / 0.3785 / 37.78
6.24 4.78 2.17 !Total cooling (kW), sensible cooling (kW) and power (kW) at 401.2 / 0.3785 / 43.33
5.80 4.60 2.43 !Total cooling (kW), sensible cooling (kW) and power (kW) at 401.2 / 0.3785 / 48.84
9.14 5.74 0.94 !Total cooling (kW), sensible cooling (kW) and power (kW) at 401.2 / 0.5047 / -1.11
9.09 5.89 1.03 !Total cooling (kW), sensible cooling (kW) and power (kW) at 401.2 / 0.5047 / 4.44
8.97 5.92 1.13 !Total cooling (kW), sensible cooling (kW) and power (kW) at 401.2 / 0.5047 / 10.00
8.70 5.86 1.24 !Total cooling (kW), sensible cooling (kW) and power (kW) at 401.2 / 0.5047 / 15.56
8.32 5.71 1.37 !Total cooling (kW), sensible cooling (kW) and power (kW) at 401.2 / 0.5047 / 21.11
7.88 5.54 1.52 !Total cooling (kW), sensible cooling (kW) and power (kW) at 401.2 / 0.5047 / 26.67
7.36 5.30 1.70 !Total cooling (kW), sensible cooling (kW) and power (kW) at 401.2 / 0.5047 / 32.22
6.86 5.07 1.90 !Total cooling (kW), sensible cooling (kW) and power (kW) at 401.2 / 0.5047 / 37.78
6.36 4.81 2.12 !Total cooling (kW), sensible cooling (kW) and power (kW) at 401.2 / 0.5047 / 43.33
5.92 4.63 2.37 !Total cooling (kW), sensible cooling (kW) and power (kW) at 401.2 / 0.5047 / 48.84

Tranquility 27 TT Series – 2 ton GSHP – cooling correction

15.56 18.33 21.11 23.89 26.67 29.44 32.22 35.00 37.78 !Values of entering dry bulb temperature (°C)
7.22 10.00 12.78 15.56 18.33 19.00 19.44 21.11 23.89 !Values of entering air wet bulb temperature (°C)
0.832 1.346 0.946 !Multiplier for total capacity, sensible capacity and power at 15.56 / 7.22
0.850 1.004 0.953 !Multiplier for total capacity, sensible capacity and power at 15.56 / 10.00
0.880 0.694 0.964 !Multiplier for total capacity, sensible capacity and power at 15.56 / 12.78
0.922 0.362 0.977 !Multiplier for total capacity, sensible capacity and power at 15.56 / 15.56

0.975 0.037 0.993 !etc.
0.990 0.000 0.997
1.000 0.000 1.000
1.040 0.000 1.011
1.117 0.000 1.033
0.832 1.461 0.946
0.850 1.174 0.953
0.880 0.902 0.964
0.922 0.646 0.977
0.975 0.368 0.993
0.990 0.303 0.997
1.000 0.260 1.000
1.040 0.096 1.011
1.117 0.000 1.033
0.832 1.603 0.946
0.850 1.357 0.953
0.880 1.115 0.964
0.922 0.875 0.977
0.975 0.639 0.993
0.990 0.582 0.997
1.000 0.545 1.000
1.040 0.399 1.011
1.117 0.159 1.033
0.832 1.700 0.946
0.850 1.700 0.953
0.880 1.331 0.964

0.922 1.103 0.977
0.975 0.869 0.993
0.990 0.812 0.997
1.000 0.774 1.000
1.040 0.630 1.011
1.117 0.392 1.033
0.832 1.700 0.946
0.850 1.700 0.953
0.880 1.700 0.964
0.922 1.329 0.977
0.975 1.096 0.993
0.990 1.039 0.997
1.000 1.000 1.000
1.040 0.853 1.011
1.117 0.600 1.033
0.832 1.700 0.946
0.850 1.700 0.953
0.880 1.700 0.964
0.922 1.700 0.977
0.975 1.320 0.993
0.990 1.262 0.997
1.000 1.223 1.000
1.040 1.075 1.011
1.117 0.821 1.033
0.832 1.700 0.946
0.850 1.700 0.953

0.880 1.700 0.964
0.922 1.700 0.977
0.975 1.700 0.993
0.990 1.482 0.997
1.000 1.444 1.000
1.040 1.297 1.011
1.117 1.046 1.033
0.832 1.700 0.946
0.850 1.700 0.953
0.880 1.700 0.964
0.922 1.700 0.977
0.975 1.700 0.993
0.990 1.700 0.997
1.000 1.700 1.000
1.040 1.517 1.011
1.117 1.275 1.033
0.832 1.700 0.946
0.850 1.700 0.953
0.880 1.700 0.964
0.922 1.700 0.977
0.975 1.700 0.993
0.990 1.700 0.997
1.000 1.700 1.000
1.040 1.700 1.011
1.117 1.510 1.033

Tranquility 27 TT Series – 2 ton GSHP – heating

```
387.0  448.4                    !Values of airflow in (l/s)
0.2524  0.3785  0.5047          !Values of liquid flow rate in (l/s)
-1.11  4.44  10.00  15.56  21.11  26.67  32.22  !Values of liquid entering T (°C)
5.2     1.5     !Total heating (kW) and power (kW) at 387.0 / 0.2524 / -1.11
6.2     1.6     !Total heating (kW) and power (kW) at 387.0 / 0.2524 / 4.44
7.2     1.7     !Total heating (kW) and power (kW) at 387.0 / 0.2524 / 10.0
8.0     1.8     !Total heating (kW) and power (kW) at 387.0 / 0.2524 / 15.56
8.8     1.8     !Total heating (kW) and power (kW) at 387.0 / 0.2524 / 21.11
9.5     1.9     !Total heating (kW) and power (kW) at 387.0 / 0.2524 / 26.67
10.2    2.0     !Total heating (kW) and power (kW) at 387.0 / 0.2524 / 32.22
5.5     1.5     !Total heating (kW) and power (kW) at 387.0 / 0.3785 / -1.11
6.5     1.6     !Total heating (kW) and power (kW) at 387.0 / 0.3785 / 4.44
7.5     1.7     !Total heating (kW) and power (kW) at 387.0 / 0.3785 / 10.0
8.3     1.8     !Total heating (kW) and power (kW) at 387.0 / 0.3785 / 15.56
9.1     1.9     !Total heating (kW) and power (kW) at 387.0 / 0.3785 / 21.11
9.8     1.9     !Total heating (kW) and power (kW) at 387.0 / 0.3785 / 26.67
10.5    2.0     !Total heating (kW) and power (kW) at 387.0 / 0.3785 / 32.22
5.6     1.5     !Total heating (kW) and power (kW) at 387.0 / 0.5047 / -1.11
6.7     1.6     !Total heating (kW) and power (kW) at 387.0 / 0.5047 / 4.44
7.6     1.7     !Total heating (kW) and power (kW) at 387.0 / 0.5047 / 10.0
8.5     1.8     !Total heating (kW) and power (kW) at 387.0 / 0.5047 / 15.56
9.3     1.9     !Total heating (kW) and power (kW) at 387.0 / 0.5047 / 21.11
10.0    2.0     !Total heating (kW) and power (kW) at 387.0 / 0.5047 / 26.67
10.7    2.1     !Total heating (kW) and power (kW) at 387.0 / 0.5047 / 32.22
5.3     1.5     !Total heating (kW) and power (kW) at 448.4 / 0.2524 / -1.11
6.3     1.5     !Total heating (kW) and power (kW) at 448.4 / 0.2524 / 4.44
7.3     1.6     !Total heating (kW) and power (kW) at 448.4 / 0.2524 / 10.0
8.1     1.7     !Total heating (kW) and power (kW) at 448.4 / 0.2524 / 15.56
8.9     1.8     !Total heating (kW) and power (kW) at 448.4 / 0.2524 / 21.11
9.7     1.8     !Total heating (kW) and power (kW) at 448.4 / 0.2524 / 26.67
10.4    1.9     !Total heating (kW) and power (kW) at 448.4 / 0.2524 / 32.22
5.6     1.5     !Total heating (kW) and power (kW) at 448.4 / 0.3785 / -1.11
6.6     1.6     !Total heating (kW) and power (kW) at 448.4 / 0.3785 / 4.44
7.6     1.6     !Total heating (kW) and power (kW) at 448.4 / 0.3785 / 10.0
8.5     1.7     !Total heating (kW) and power (kW) at 448.4 / 0.3785 / 15.56
9.3     1.8     !Total heating (kW) and power (kW) at 448.4 / 0.3785 / 21.11
10.0    1.9     !Total heating (kW) and power (kW) at 448.4 / 0.3785 / 26.67
10.7    2.0     !Total heating (kW) and power (kW) at 448.4 / 0.3785 / 32.22
5.7     1.5     !Total heating (kW) and power (kW) at 448.4 / 0.5047 / -1.11
6.8     1.6     !Total heating (kW) and power (kW) at 448.4 / 0.5047 / 4.44
7.7     1.7     !Total heating (kW) and power (kW) at 448.4 / 0.5047 / 10.0
8.6     1.7     !Total heating (kW) and power (kW) at 448.4 / 0.5047 / 15.56
9.4     1.8     !Total heating (kW) and power (kW) at 448.4 / 0.5047 / 21.11
10.2    1.9     !Total heating (kW) and power (kW) at 448.4 / 0.5047 / 26.67
10.9    2.0     !Total heating (kW) and power (kW) at 448.4 / 0.5047 / 32.22
```

Tranquility 27 TT Series – 2 ton GSHP – heating correction

4.44 7.22 10.00 12.78 15.56 18.33 20.00 21.11 23.89 26.67 !Values of entering air dry bulb temperature (°C)

1.052 0.779	!Multipliers for heating capacity and power at 4.44
1.043 0.808	!Multipliers for heating capacity and power at 7.22
1.035 0.841	!Multipliers for heating capacity and power at 10.0
1.027 0.877	!Multipliers for heating capacity and power at 12.78
1.019 0.915	!Multipliers for heating capacity and power at 15.56
1.010 0.957	!Multipliers for heating capacity and power at 18.33
1.004 0.982	!Multipliers for heating capacity and power at 20.0
1.000 1.000	!Multipliers for heating capacity and power at 21.11
0.989 1.045	!Multipliers for heating capacity and power at 23.89
0.976 1.093	!Multipliers for heating capacity and power at 26.67

Trane High Efficiency, 2 Ton, Water-to-Water Heat Pump - Cooling

```
7.22  12.0  18.3  23.89          !entering load temperature
10.0  15.56  21.11  26.67  32.22  37.78  43.33  48.89   !Entering source temperature
5.63    0.86                    !Cooling load (kW) and power (kW) at 7.22 / 10.0
5.33    0.99                    !Cooling load (kW) and power (kW) at 7.22 / 15.56
5.16    1.12                    !Cooling load (kW) and power (kW) at 7.22 / 21.11
5.01    1.27                    !Cooling load (kW) and power (kW) at 7.22 / 26.67
4.92    1.45                    !Cooling load (kW) and power (kW) at 7.22 / 32.22
4.84    1.65                    !Cooling load (kW) and power (kW) at 7.22 / 37.78
4.78    1.87                    !Cooling load (kW) and power (kW) at 7.22 / 43.33
4.72    2.12                    !Cooling load (kW) and power (kW) at 7.22 / 48.89
6.15    0.89                    !Cooling load (kW) and power (kW) at 12 / 10.0
5.89    1.00                    !Cooling load (kW) and power (kW) at 12 / 15.56
5.69    1.13                    !Cooling load (kW) and power (kW) at 12 / 21.11
5.57    1.29                    !Cooling load (kW) and power (kW) at 12 / 26.67
5.45    1.47                    !Cooling load (kW) and power (kW) at 12 / 32.22
5.39    1.67                    !Cooling load (kW) and power (kW) at 12 / 37.78
5.30    1.89                    !Cooling load (kW) and power (kW) at 12 / 43.33
5.28    2.13                    !Cooling load (kW) and power (kW) at 12 / 48.89
6.89    0.91                    !Cooling load (kW) and power (kW) at 18.3 / 10.0
6.59    1.02                    !Cooling load (kW) and power (kW) at 18.3 / 15.56
6.42    1.15                    !Cooling load (kW) and power (kW) at 18.3 / 21.11
6.27    1.30                    !Cooling load (kW) and power (kW) at 18.3 / 26.67
6.18    1.48                    !Cooling load (kW) and power (kW) at 18.3 / 32.22
6.10    1.68                    !Cooling load (kW) and power (kW) at 18.3 / 37.78
6.04    1.90                    !Cooling load (kW) and power (kW) at 18.3 / 43.33
5.98    2.15                    !Cooling load (kW) and power (kW) at 18.3 / 48.89
7.50    0.92                    !Cooling load (kW) and power (kW) at 23.89 / 10.0
7.24    1.03                    !Cooling load (kW) and power (kW) at 23.89 / 15.56
7.06    1.16                    !Cooling load (kW) and power (kW) at 23.89 / 21.11
6.92    1.32                    !Cooling load (kW) and power (kW) at 23.89 / 26.67
6.80    1.49                    !Cooling load (kW) and power (kW) at 23.89 / 32.22
6.74    1.69                    !Cooling load (kW) and power (kW) at 23.89 / 37.78
6.62    1.92                    !Cooling load (kW) and power (kW) at 23.89 / 43.33
6.62    2.16                    !Cooling load (kW) and power (kW) at 23.89 / 48.89
```

Trane High Efficiency, 2 Ton, Water-to-Water Heat Pump - Heating

```
15.56  26.67  37.78  48.89              !Values of entering load temperatures
-1.11  4.44  10.0  15.56  21.11  26.67        !Values of entering source temperatures
7.18    1.15                    !Heating capacity (kW) and power (kW) at 15.55 / -1.11
7.74    1.18                    !Heating capacity (kW) and power (kW) at 15.55 / 4.44
8.35    1.21                    !Heating capacity (kW) and power (kW) at 15.55 / 10.0
9.03    1.23                    !Heating capacity (kW) and power (kW) at 15.55 / 15.56
9.76    1.25                    !Heating capacity (kW) and power (kW) at 15.55 / 21.11
10.52   1.27                    !Heating capacity (kW) and power (kW) at 15.55 / 26.67
6.83    1.62                    !Heating capacity (kW) and power (kW) at 26.67 / -1.11
7.39    1.67                    !etc.
7.97    1.71
8.62    1.74
9.29    1.77
10.05   1.80
6.59    2.12
7.12    2.19
7.71    2.24
8.32    2.28
8.97    2.32
9.70    2.35
6.39    2.64
6.92    2.72
7.47    2.79
8.06    2.84
8.70    2.89
9.41    2.93
```

Shell SQ160-PC
Photovoltaic Solar Module

Mechanical Specifications Module

A torsion and corrosion-resistant anodized aluminium frame ensures dependable performance, even under harsh weather conditions. Pre-drilled mounting holes are provided for ease of installation.

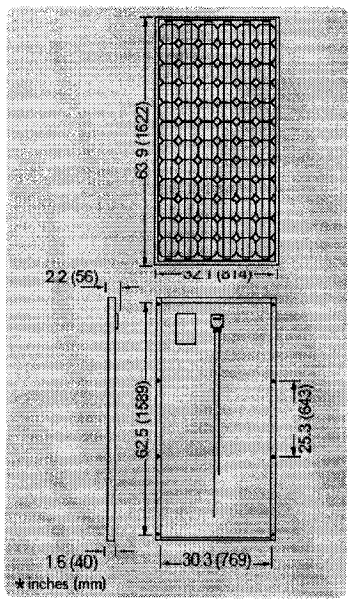

Outside dimensions (in)		63.9 x 32.1
Thickness (inc. junction box) (in)		2.2
Thickness (exc. junction box) (in)		1.6
Weight (lbs)		38
Cable length	- male (in)	51
Cable length	+ female (in)	39

For installation instructions, please refer to the **Installation Manual** which is available from Shell Solar.

Electrical Characteristics

Data at Standard Test Conditions (STC)

STC: irradiance level 1000W/m², spectrum AM 1.5 and cell temperature 25°C

Rated power	P_r	160W
Peak power*	P_{mpp}*	160W
Peak power voltage	V_{mpp}	35V
Peak power current	I_{mpp}	4.58A
Open circuit voltage	V_{oc}	43.5V
Short circuit current	I_{sc}	4.9A
Series fuse rating		15A
Minimum peak power	$P_{mpp\ min}$	152W
*Tolerance on Peak Power		±5%

The abbreviation 'mpp' stands for Maximum Power Point.

Typical data at Nominal Operating Cell Temperature (NOCT) conditions

NOCT: 800W/m² irradiance level, AM 1.5 spectrum, wind velocity 1m/s, T_{amb} 20°C

Temperature	T_{NOCT}	46°C
Mpp power	P_{mpp}	115W
Mpp voltage	V_{mpp}	32V
Open circuit voltage	V_{oc}	40V
Short circuit current	I_{sc}	3.95A

Typical data at low irradiance

The relative reduction of module efficiency at an irradiance of 200W/m² in relation to 1000W/m² both at 25°C cell temperature and AM 1.5 spectrum is 8%.

Temperature coefficients

αP_{mpp}	-0.52%/°C
αV_{mpp}	-167mV/°C
αI_{sc}	1.4mA/°C
αV_{oc}	-161mV/°C

Maximum system voltage: 600 Vdc (UL) and 715 Vdc (TÜV Safety Class II)

Typical I/V Characteristics

The I/V graph below shows the typical performance of the solar module at various levels of irradiance.

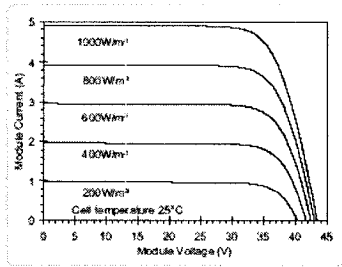

The I/V graph below shows the typical performance of the solar module at various cell temperatures.

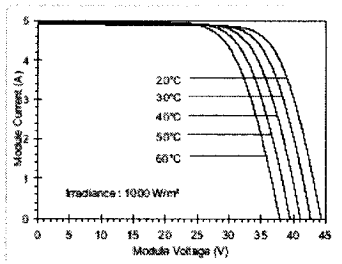

References in this Product Information Sheet to 'Shell Solar' are to companies and other organizational entities within the Royal Dutch/Shell Group of Companies that are engaged in the photovoltaic solar energy business. Shell Solar has its principal office in Amsterdam, the Netherlands.

For further information on all Shell Solar products contact:

Shell Solar
4650 Adohr Lane, Camarillo CA 93012
805-482-6800 Fax 805-388-6395
Web www.shell.com/solar

V2/SQ160-PC/07/03/US

Appendix C: Lighting Consumption Pattern Details

Rooms	# of Lights	0-1	1-2	2-3	3-4	4-5	5-6	6-7	7-8	8-9	9-10	10-11	11-12	12-13	13-14	14-15	15-16	16-17	17-18	18-19	19-20	20-21	21-22	22-23	23-0	Daily kWh	Yearly kWh
Kitchen	3	0	0	0	0	0	0	0.5	0.5	0.5	0	0	0	1	0	0	0	0.5	1	1	0	0	0.25	0	0	0.205	74.7
Dining Room	2	0	0	0	0	0	0	0	0.5	0.5	0	0	0	0.5	0	0	0	0	0.5	0.5	0	0	0	0	0	0.065	23.7
Bdrm 1	2	0	0	0	0	0	0	0	0.25	0.25	0	0	0	0	0	0	0	0.5	0	0	0	0	0.5	0	0	0.039	14.2
Bdrm 2	2	0	0	0	0	0	0	0	0.25	0.25	0	0	0	0	0	0	0	0.5	0	0	0	0	0	0.5	0	0.039	14.2
Bdrm 3	3	0	0	0	0	0	0	0.083	0.5	0.25	0	0	0	0	0	0	0	0	0	0	0	0	0.5	0.5	0.167	0.078	28.5
WR 1	2	0	0	0	0	0	0	0.5	1	0.5	0	0	0	0	0	0	0	0.25	0	0	0.25	0.5	0.5	0.5	0.25	0.111	40.3
1/2 WR	1	0	0	0	0	0	0	0	0.25	0.25	0	0	0	0.25	0	0	0	0	0.25	0	0	0	0.25	0.5	0.25	0.026	9.5
Living Room	2	0	0	0	0	0	0	0.5	1	0.5	0	0	0	0	0	0	0	0	0.5	0.75	1	1	1	1	0.5	0.202	73.5
Den/ Office	2	0	0	0	0	0	0	0	0	1	0.5	0.5	0.5	0.5	0.5	0.5	0.5	0.5	0	0.75	0.75	0.75	0.75	0	0	0.208	75.9
Outside	2	0.5	0.5	0.5	0.5	0.5	0.5	0.25	0	0	0	0	0	0	0	0	0	0	0	0	0	0	0	1	0.5	0.124	45.1
TOTAL	21	0.5	0.5	0.5	0.5	0.5	0.5	1.833	4.25	4	0.5	0.5	0.5	2.25	0.5	0.5	0.5	2.25	2.25	3	2	2.25	3.75	4	1.667	1.1	400
Total (light-hrs)		1	1	1	1	1	1	4.25	9.25	8.5	1	1	1	5.25	1	1	1	5	5.25	7	4	4.5	8	8	3.25		
TOTAL (Wh)	n/a	13	13	13	13	13	13	55	120	111	13	13	13	68	13	13	13	65	68	91	52	59	104	104	042		
Lights Radiative (W)		8.71	8.71	8.71	8.71	8.71	8.71	37.02	80.57	74.04	8.71	8.71	8.71	45.73	8.71	8.71	8.71	43.55	45.73	60.97	34.84	39.2	69.68	69.68	28.31		
Lights Conv. (W)		4.29	4.29	4.29	4.29	4.29	4.29	18.23	39.68	36.47	4.29	4.29	4.29	22.52	4.29	4.29	4.29	21.45	22.52	30.03	17.16	19.31	34.32	34.32	13.94		

Appendix D: Occupancy Pattern Details

	0-1	1-2	2-3	3-4	4-5	5-6	6-7	7-8	8-9	9-10	10-11	11-12	12-13	13-14	14-15	15-16	16-17	17-18	18-19	19-20	20-21	21-22	22-23	23-0
Activity Level	1	1	1	1	1	1	1	4	4	4	4	4	4	4	4	4	4	4	4	1	1	4	4	1
Father	1	1	1	1	1	1	1	1	0	0	0	0	0	0	0	0	0	1	1	1	1	1	1	1
Mother	1	1	1	1	1	1	1	1	1	1	1	1	1	1	1	1	1	1	1	0	0.5	1	1	1
Child 1	1	1	1	1	1	1	1	1	0.5	0	0	0	0	0	0	0	1	1	1	0	0.5	1	1	1
Child 2	1	1	1	1	1	1	1	1	0.5	0	0	0	0	0	0	0	0	1	1	1	1	1	1	1
Total Occ	4	4	4	4	4	4	4	4	2	1	1	1	1	1	1	1	2	4	4	2	3	4	4	4

Activity Level 1:Seated at rest (100W)
Activity Level 4: Seated, light work (120 W)

Appendix E: Appliance Consumption Pattern Details

	kWh/yr	kWh/day	0-1h	1-2h	2-3h	3-4h	4-5h	5-6h	6-7h	7-8h	8-9h	9-10h	10-11h	11-12h	12-13h	13-14h	14-15h	15-16h	16-17h	17-18h	18-19h	19-20h	20-21h	21-22h	22-23h	23-0h
Refrigerator	391.0	1.071	0.045	0.045	0.045	0.045	0.045	0.045	0.045	0.045	0.045	0.045	0.045	0.045	0.045	0.045	0.045	0.045	0.045	0.045	0.045	0.045	0.045	0.045	0.045	0.045
Freezer	354.0	0.970	0.040	0.040	0.040	0.040	0.040	0.040	0.040	0.040	0.040	0.040	0.040	0.040	0.040	0.040	0.040	0.040	0.040	0.040	0.040	0.040	0.040	0.040	0.040	0.040
Dishwasher	103.0	0.282	0.000	0.000	0.000	0.000	0.000	0.000	0.000	0.035	0.035	0.000	0.000	0.035	0.035	0.000	0.000	0.000	0.047	0.047	0.047	0.000	0.000	0.000	0.000	0.000
Clothes washer	13.7	0.038	0.000	0.000	0.000	0.000	0.000	0.000	0.000	0.005	0.005	0.000	0.000	0.000	0.000	0.000	0.000	0.000	0.000	0.009	0.009	0.009	0.000	0.000	0.000	0.000
Clothes dryer	629.0	1.723	0.000	0.000	0.000	0.000	0.000	0.000	0.000	0.215	0.215	0.000	0.000	0.000	0.000	0.000	0.000	0.000	0.000	0.431	0.431	0.431	0.000	0.000	0.000	0.000
Range	449.0	1.230	0.000	0.000	0.000	0.000	0.000	0.000	0.000	0.154	0.154	0.000	0.000	0.154	0.154	0.000	0.000	0.000	0.205	0.205	0.205	0.000	0.000	0.000	0.000	0.000
Total:	1939.7	5.314	0.085	0.085	0.085	0.085	0.085	0.085	0.085	0.494	0.494	0.085	0.085	0.274	0.274	0.085	0.085	0.085	0.337	0.777	0.777	0.525	0.085	0.085	0.085	0.085
kWh Radiation	983.5	2.695	0.060	0.060	0.060	0.060	0.060	0.060	0.060	0.218	0.218	0.060	0.060	0.192	0.192	0.060	0.060	0.060	0.236	0.288	0.288	0.111	0.060	0.060	0.060	0.060
kWh Convection	421.5	1.155	0.026	0.026	0.026	0.026	0.026	0.026	0.026	0.093	0.093	0.026	0.026	0.082	0.082	0.026	0.026	0.026	0.101	0.123	0.123	0.048	0.026	0.026	0.026	0.026
Total:	1405.1	3.849	0.085	0.085	0.085	0.085	0.085	0.085	0.085	0.311	0.311	0.085	0.085	0.274	0.274	0.085	0.085	0.085	0.337	0.411	0.411	0.159	0.085	0.085	0.085	0.085

Top consumption includes total dryer load, bottom removed 85% of load assumed to be lost through the dryer exhaust.

Appendix F: HOT2000 Simulation Results from Advanced House

HOT2000
Natural Resources CANADA
Version 9.34b

GENERAL HOUSE CHARACTERISTICS

House type:	Single Detached		
Number of storeys:	Two storeys		
Plan shape:	Rectangular		
Front orientation:	North		
Year House Built:	1992		
Wall colour:	Default	**Absorptivity:**	0.40
Roof colour:	Medium brown	**Absorptivity:**	0.84
Soil Condition:	Normal conductivity (dry sand, loam, clay)		
Water Table Level:	Normal (7-10m/23-33ft)		

House Thermal Mass Level: (A) Light, wood frame

Effective mass fraction 1.000

Occupants : 2 Adults for 50.0% of the time
1 Children for 50.0% of the time
0 Infants for 0.0% of the time

Sensible Internal Heat Gain From Occupants: 2.00 kWh/day

HOUSE TEMPERATURES

Heating Temperatures

Main Floor:	20.0 °C
Basement:	15.0 °C
TEMP. Rise from 20.0 °C:	2.8 °C

Basement is- Heated: YES **Cooled:** NO **Separate T/S:** YES
Fraction of internal gains released in basement : 0.150

Indoor design temperatures for equipment sizing

Heating: 22.0 °C
Cooling: 24.0 °C

WINDOW CHARACTERISTICS

Label	Location	#	Overhang Width (m)	Header Height (m)	Tilt deg	Curtain Factor	Shutter (RSI)
South							
BsmWdws	Foundation - 1	2	0.00	0.00	90.0	1.00	0.00
DiningRoom	SouthWall	1	0.61	0.24	90.0	1.00	0.00
FamilyRoom	SouthWall	1	0.61	0.24	90.0	1.00	0.00
Kitchen	SouthWall	1	0.61	0.24	90.0	1.00	0.00
TopFloor Large	SouthWall	2	0.61	0.24	90.0	1.00	0.00
TopFlr_Small	SouthWall	2	0.61	0.24	90.0	1.00	0.00
East							
East0001	East_Wall	1	0.00	0.00	90.0	1.00	0.00
WestWdw	West_Wall	1	0.00	0.00	90.0	1.00	0.00
North							
2nd_Floor	NorthWall	4	0.61	0.24	90.0	1.00	0.00
Main_1	NorthWall	1	0.00	0.00	90.0	1.00	0.00
Main_2	NorthWall	1	0.00	0.00	90.0	1.00	0.00

Label	Type	#	Window Width (m)	Window Height (m)	Total Area (m^2)	Window RSI	SHGC
South							
BsmWdws	Trip	2	1.42	1.02	2.90	1.026	0.4027
DiningRoom	Trip	1	1.82	1.52	2.77	1.078	0.4213
FamilyRoom	Trip	1	2.42	1.52	3.68	1.093	0.4266
Kitchen	Trip	1	1.02	1.02	1.04	1.001	0.3923
TopFloor Large	Trip	2	1.42	1.02	2.90	1.026	0.4027
TopFlr_Small	Trip	2	1.02	1.02	2.08	1.001	0.3923
East							
East0001	DumontWdws	1	0.61	1.22	0.74	0.955	0.3731
WestWdw	DumontWdws	1	0.61	1.22	0.74	0.955	0.3731
North							
2nd_Floor	Trip	4	0.72	1.02	2.94	0.965	0.3769
Main_1	Trip	1	2.13	1.52	3.24	1.087	0.4244
Main_2	Trip	1	1.42	1.52	2.16	1.060	0.4152

WINDOW CODE SCHEDULE

Name	Internal Code	Description (Glazings, Coatings, Fill, Spacer, Type, Frame)
Trip	423206	TG with 2 coatings, Low-E .10 (soft), 13 mm Argon, Insulating, Picture, Fibreglass, ER* = 6.96, Eff. RSI= 0.71

* Window Standard Energy Rating estimated for assumed dimensions, and Air tightness type: CSA - A1; Leakage rate = 2.790 $m^3/hr/m$

BUILDING PARAMETER DETAILS

CEILING COMPONENTS

	Construction Type	Code Type	Roof Slope	Heel Ht.(m)	Section Area (m^2)	R. Value (RSI)
Ceiling01	Attic/gable	User specified	4.0/12	0.01	112.53	14.09

MAIN WALL COMPONENTS

Label	Lintel Type	Fac. Dir	Number of Corn.	Number of Inter.	Height (m)	Perim. (m)	Area (m^2)	R. Value (RSI)
East_Wall Type: User specified	100	East	1	1	5.41	9.14	49.45	10.56
NorthWall Type: User specified	100	North	1	1	5.41	13.41	72.55	10.57
SouthWall Type: User specified	100	South	1	1	5.41	13.41	72.55	10.57
West_Wall Type: User specified	100	West	1	1	5.41	9.14	49.45	10.56

DOORS

Label	Type	Height (m)	Width (m)	Gross Area (m^2)	R. Value (RSI)
N_Door Loc: NorthWall	Fibreglass polyurethane core	2.07	0.90	1.86	0.98
S_Door Loc: SouthWall	Fibreglass polyurethane core	2.07	0.90	1.86	0.98

FOUNDATIONS

Foundation Name: Foundation - 1
Foundation Type: Basement
Data Type: Library

Volume: 302.7 m^3
Opening to Main Floor: 0.00 m^2

Total Wall Height: 2.47 m
Depth Below Grade: 1.58 m

Rectangular
Floor Length: 13.41 m

		Floor Width:	9.14 m
Interior wall type:	User specified	**R-value:**	10.57 RSI
Exterior wall type:	User specified	**R-Value:**	0.00 RSI
Number of corners :	4		
Lintel type:	LL1		
Added to slab type :	User specified	**R-Value:**	5.64 RSI
Floors Above Found.:	User specified	**R-Value:**	0.95 RSI

Exposed areas for: Foundation - 1
Exposed Perimeter: 45.10 m

Configuration: BWIA_2
- interior surface of wall insulated over full-height
- any first storey construction type
- wood walls and wood floor
- top of slab fully insulated

FOUNDATION CODE SCHEDULE

Lintel Code Schedule

Name	Code	Description (Type, Material, Insulation)
~ & ~	100	Double, Wood, None
~ & ~	101	Double, Wood, Same as wall framing cavity
LL1	101	Double, Wood, Same as wall framing cavity

ROOF CAVITY INPUTS

Gable Ends		**Total Area:**	12.50 m^2
Sheathing Material	Plywood/Part. bd 9.5 mm (3/8 in)		0.08 RSI
Exterior Material:	Hollow metal/vinyl cladding		0.11 RSI
Sloped Roof		**Total Area:**	118.60 m^2
Sheathing Material	Plywood/Part. bd 12.7 mm (1/2 in)		0.11 RSI
Exterior Material:	Asphalt shingles		0.08 RSI
Total Cavity Volume:	81.1 m^3	**Ventilation Rate:**	0.50 ACH/hr

BUILDING PARAMETERS SUMMARY

ZONE 1 : Above Grade

Component	Area m^2 Gross	Area m^2 Net	Effective (RSI)	Heat Loss MJ	% Annual Heat Loss
Ceiling	112.53	112.53	14.09	3611.44	5.15
Main Walls	243.99	217.98	10.57	11169.73	15.92
Doors	3.73	3.73	0.98	2202.55	3.14
South Windows	12.46	12.46	1.05	6877.81	9.81
East Windows	1.49	1.49	0.96	902.45	1.29
North Windows	8.33	8.33	1.03	4668.19	6.66
		ZONE 1 Totals:		**29432.18**	**41.96**

INTER-ZONE Heat Transfer : Floors Above Basement

	Area m^2 Gross	Area m^2 Net	Effective (RSI)	Heat Loss MJ
	122.57	122.57	0.950	6459.08

ZONE 2 : Basement

Component	Area m^2 Gross	Area m^2 Net	Effective (RSI)	Heat Loss MJ	% Annual Heat Loss
Walls above grade	40.14	37.24	-	2081.55	2.97
South windows	2.90	2.90	1.03	1489.64	2.12
Below grade foundation	193.83	193.83	-	6801.24	9.70
		ZONE 2 Totals:		**10372.43**	**14.79**

Ventilation

House Volume	Air Change	Heat Loss MJ	% Annual Heat Loss
815.00 m^3	0.192 ACH	30335.518	43.25

AIR LEAKAGE AND VENTILATION

Building Envelope Surface Area: 590.49 m^2

Air Leakage Test Results at 50 Pa.(0.2 in H_2O) = 0.47 ACH
Equivalent Leakage Area @ 10 Pa = 143.10 cm2

Terrain Description	**Height**	**m**
@ Weather Station : Open flat terrain, grass	Anemometer	10.0
@ Building site : Suburban, forest	Bldg. Eaves	6.3

Local Shielding: **Walls:** Heavy
Flue : Light

Leakage Fractions-	**Ceiling:** 0.200	**Walls:** 0.650	**Floors:** 0.150

Normalized Leakage Area @ 10 Pa: 0.2423 cm^2/m^2

Estimated Airflow to cause a 5 Pa Pressure Difference: 23 L/s

Estimated Airflow to cause a 10 Pa Pressure Difference: 36 L/s

---

F326 VENTILATION REQUIREMENTS

Kitchen, Living Room, Dining Room	3 rooms @ 5.0 L/s: 15.0 L/s
Utility Room	1 rooms @ 5.0 L/s: 5.0 L/s
Bedroom	1 rooms @ 10.0 L/s: 10.0 L/s
Bedroom	2 rooms @ 5.0 L/s: 10.0 L/s
Bathroom	2 rooms @ 5.0 L/s: 10.0 L/s
Other	2 rooms @ 5.0 L/s: 10.0 L/s
Basement Rooms	: 0.0 L/s

AIR LEAKAGE AND VENTILATION SUMMARY

F326 Required continous ventilation:	60.000 L/s (0.27 ACH)
Other Continuous Supply Flow Rates:	0.000 L/s (ACH)
Other Continuous Exhaust Flow Rates:	0.000 L/s (0.18 ACH)
Total house ventilation is Balanced	
Gross Air Leakage and Ventilation Energy Load:	27678.992 MJ
Seasonal Heat Recovery Ventilator Efficiency:	0.000 %
Estimated Ventilation Electrical Load: Heating Hours:	0.000 MJ
Estimated Ventilation Electrical Load: Non-Heating Hours:	0.000 MJ
Net Air Leakage and Ventilation Load:	30335.518 MJ

SPACE HEATING SYSTEM

Primary Heating Fuel:	Electricity
Equipment:	Baseboard/Hydronic/Plenum(duct) htrs.
Manufacturer:	SPHMan
Model:	SPHMod
Specified Output Capacity:	9.00 kW

Insufficient capacity specified: 9.00 kW (Required = 9.50 kW)

Steady State Efficiency: 100.00 %

DOMESTIC WATER HEATING SYSTEM

Primary Water Heating Fuel:	Solar
Water Heating Equipment:	Solar collector system
Manufactuer:	DHW man
Model:	DHW mod
CSIA Solar Collector Rating:	12000.00 MJ/Year
Secondary Water Heating Fuel:	Solar
Water Heating Equipment:	B-Medium, Wood frame
Manufactuer:	DHW man
Model:	DHW mod
CSIA Solar Collector Rating:	MJ/Year

ANNUAL SPACE HEATING SUMMARY

Design Heat Loss at -35.00 °C (10.25 Watts / m3):	8356.90 Watts
Gross Space Heat Loss:	70140.13 MJ
Gross Space Heating Load:	68598.79 MJ
Usable Internal Gains:	13935.02 MJ
Usable Internal Gains Fraction:	19.87 %
Usable Solar Gains:	20170.56 MJ
Usable Solar Gains Fraction:	28.76 %
Auxilary Energy Required:	34493.21 MJ
Space Heating System Load:	34493.21 MJ
Furnace/Boiler Seasonal efficiency:	100.00 %
Furnace/Boiler Annual Energy Consumption:	34493.21 MJ

ANNUAL DOMESTIC WATER HEATING SUMMARY

Daily Hot Water Consumption:	230.00 Litres
Hot Water Temperature:	55.00 °C
Estimated Domestic Water Heating Load:	17515.40 MJ
Solar Domestic Water Heating System Contribution:	10760.01 MJ
Domestic Water Heating Energy Consumption:	7138.80 MJ
System Seasonal Efficiency:	Secondary 94.63

BASE LOADS SUMMARY

	kwh/day	Annual kWh
Interior Lighting	1.00	365.00
Appliances	9.60	3504.00
Other	0.40	146.00
Exterior Use	4.00	1460.00
Total Average Electrical Load	15.02	5483.76

ENERGY CONSUMPTION SUMMARY REPORT

Estimated Annual Space Heating Energy Consumption	= 34493.21 MJ	= 9581.45 kWh
Ventilator Electrical Consumption: Heating Hours	= 0.00 MJ	= 0.00 kWh
Estimated Annual DHW Heating Energy Consumption	= 7138.80 MJ	= 1983.00 kWh
ESTIMATED ANNUAL SPACE + DHW ENERGY CONSUMPTION	= 41632.01 MJ	= 11564.45 kWh

Estimated Greenhouse Gas Emissions 9.24 tonnes/year

ESTIMATED ANNUAL FUEL CONSUMPTION SUMMARY

Fuel	Space Heating	Space Cooling	DHW Heating	Appliance	Total
Electricity (kWh)	9587.36	0.00	1983.00	5477.85	17048.20

MONTHLY ENERGY PROFILE

Month	Energy Load (MJ)	Internal Gains (MJ)	Solar Gains (MJ)	Aux. Energy (MJ)	HRV Eff. %
Jan	12351.176	1329.803	2521.449	8499.924	0.000
Feb	9900.185	1197.096	2850.052	5853.037	0.000
Mar	9026.890	1328.971	3261.180	4436.739	0.000
Apr	5397.719	1296.424	2003.548	2097.747	0.000
May	3012.405	1354.283	1384.712	273.410	0.000
Jun	1134.662	907.515	227.147	0.000	0.000
Jul	443.037	433.116	9.921	0.000	0.000
Aug	812.925	731.036	81.889	0.000	0.000
Sep	2940.709	1335.458	1425.374	179.877	0.000
Oct	4965.536	1369.402	2127.784	1468.350	0.000
Nov	7900.479	1311.348	2148.791	4440.340	0.000

Dec	10713.066	1340.565	2128.714	7243.787	0.000
Ann	68598.789	13935.018	20170.563	34493.211	0.000

FOUNDATION TEMPERATURES & VENTILATION PROFILE

	Temperature (Deg °C)			Air Change Rate		Heat Loss
Month	**Crawl Space**	**Basement**	**Walkout**	**Natural**	**Total**	**(MJ**
Jan	0.000	16.566	0.000	0.019	0.201	5584.115
Feb	0.000	17.052	0.000	0.016	0.198	4416.843
Mar	0.000	17.643	0.000	0.014	0.196	3969.063
Apr	0.000	18.233	0.000	0.010	0.192	2259.998
May	0.000	18.951	0.000	0.007	0.189	1173.407
Jun	0.000	19.653	0.000	0.005	0.187	556.992
Jul	0.000	20.611	0.000	0.004	0.186	289.265
Aug	0.000	20.799	0.000	0.004	0.186	486.777
Sep	0.000	19.738	0.000	0.007	0.189	1200.171
Oct	0.000	19.039	0.000	0.009	0.191	2109.378
Nov	0.000	17.935	0.000	0.013	0.195	3483.770
Dec	0.000	17.031	0.000	0.016	0.198	4805.740
Ann	0.000	18.614	0.000	0.010	0.192	30335.518

SPACE HEATING SYSTEM PERFORMANCE

Month	**Space Heating Load (MJ)**	**Furnace Input (MJ)**	**Pilot Light (MJ)**	**Indoor Fans (MJ)**	**Heat Pump Input (MJ)**	**Total Input (MJ)**	**System Cop**
Jan	8499.922	8499.922	0.000	0.000	0.000	8499.922	1.000
Feb	5853.039	5853.039	0.000	0.000	0.000	5853.039	1.000
Mar	4436.740	4436.740	0.000	0.000	0.000	4436.740	1.000
Apr	2097.747	2097.747	0.000	0.000	0.000	2097.747	1.000
May	273.410	273.410	0.000	0.000	0.000	273.410	1.000
Jun	0.000	0.000	0.000	0.000	0.000	0.000	0.000
Jul	0.000	0.000	0.000	0.000	0.000	0.000	0.000
Aug	0.000	0.000	0.000	0.000	0.000	0.000	0.000
Sep	179.877	179.877	0.000	0.000	0.000	179.877	1.000
Oct	1468.350	1468.350	0.000	0.000	0.000	1468.350	1.000
Nov	4440.340	4440.340	0.000	0.000	0.000	4440.340	1.000
Dec	7243.787	7243.788	0.000	0.000	0.000	7243.788	1.000
Ann	34493.211	34493.215	0.000	0.000	0.000	34493.215	1.000

MONTHLY ESTIMATED ENERGY CONSUMPTION BY DEVICE (MJ)

	Space Heating		DHW Heating		Lights &	HRV &	Air
Month	Primary	Secondary	Primary	Secondary	Appliances	FANS	Conditioner
Jan	8499.9	0.0	0.0	1298.8	1674.0	2.7	0.0
Feb	5853.0	0.0	0.0	885.8	1512.0	2.4	0.0
Mar	4436.7	0.0	0.0	654.6	1674.0	2.7	0.0
Apr	2097.7	0.0	0.0	318.8	1620.0	2.6	0.0
May	273.4	0.0	0.0	35.8	1674.0	2.7	0.0
Jun	0.0	0.0	0.0	33.6	1620.0	2.6	0.0
Jul	0.0	0.0	0.0	34.7	1674.0	2.7	0.0
Aug	0.0	0.0	0.0	44.9	1674.0	2.7	0.0
Sep	179.9	0.0	0.0	448.9	1620.0	2.6	0.0
Oct	1468.4	0.0	0.0	892.5	1674.0	2.7	0.0
Nov	4440.3	0.0	0.0	1154.8	1620.0	2.6	0.0
Dec	7243.8	0.0	0.0	1335.5	1674.0	2.7	0.0
Ann	34493.2	0.0	0.0	7138.8	19710.0	31.5	0.0

MONTHLY ESTIMATED SOLAR DHW CONTRIBUTION (MJ)

	DHW Heating
Month	Primary
Jan	308.3
Feb	577.3
Mar	951.4
Apr	1199.8
May	1483.3
Jun	1392.3
Jul	1402.6
Aug	1379.2
Sep	937.6
Oct	577.1
Nov	316.3
Dec	234.9
Ann	10760.0

Appendix G: GA Optimisation Tool Results Summary

Case #	Run #	Generation of best individual	Electricity Consumption (kWh)	EE_Costs ($)	Yearly PV Revenue	1st Gen. Avg. CF $/mth	Best GA CF $/mth	% Best Manual CF
1	1	140	4,948	494.75	89,708	1,028.01	411.31	1.0074
1	2	155	5,153	515.30	93,392	1,317.42	428.21	1.0488
1	3	150	4,948	494.77	89,565	1,342.05	410.66	1.0059
1	4	129	4,987	498.73	90,921	1,311.22	416.88	1.0211
1	5	64	4,994	499.40	89,961	1,106.20	412.48	1.0103
1	**AVG.**	**127.6**	**5,006**	**500.59**	**90,709**	**1,220.98**	**415.91**	**1.0187**
2	1	23	5,418	541.78	61,327	821.40	281.19	1.0901
2	2	45	5,836	583.59	61,391	850.54	281.48	1.0912
2	3	76	5,356	535.63	56,879	903.63	260.79	1.0110
2	4	74	5,390	538.96	58,951	953.37	270.30	1.0479
2	5	57	5,078	507.84	57,263	606.19	263.72	1.0224
2	**AVG.**	**55.0**	**5,416**	**541.56**	**59,162**	**827.03**	**271.50**	**1.0525**
3	1	245	5,484	548.44	111,243	1,247.22	510.06	1.0024
3	2	237	5,422	542.25	111,306	1,555.49	510.35	1.0030
3	3	230	5,446	544.60	111,052	1,494.69	509.18	1.0007
3	**AVG.**	**237.3**	**5,451**	**545.10**	**111,201**	**1,432.47**	**509.86**	**1.0020**
4	1	174	7,749	774.92	143,817	2,718.25	700.81	1.0128
4	2	215	7,660	766.02	143,689	2,989.45	692.09	1.0002
4	3	241	7,713	771.34	143,195	2,936.06	694.69	1.0040
4	**AVG.**	**210.0**	**7,708**	**770.76**	**143,567**	**2,881.25**	**695.86**	**1.0057**
5	1	216	5,105	510.47	87,659	845.85	401.92	1.0046
5	2	196	5,105	510.47	87,659	993.53	401.16	1.0027
5	3	199	4,932	493.15	87,492	952.89	402.78	1.0068
5	**AVG.**	**203.7**	**5,047**	**504.69**	**87,603**	**930.76**	**401.95**	**1.0047**
6	1	187	4,498	449.76	62,876	893.94	288.29	1.0209
6	2	206	4,573	457.34	61,918	621.21	283.90	1.0053
6	3	231	4,548	454.84	61,844	566.01	283.56	1.0041
6	**AVG.**	**208.0**	**4,540**	**453.98**	**62,213**	**492.39**	**285.25**	**1.0101**
7	1	235	5,465	546.47	101,327	885.68	464.59	1.0032
7	2	230	5,590	558.99	101,375	1,219.58	464.81	1.0036
7	3	245	5,530	552.97	101,298	1,149.04	464.46	1.0029
7	**AVG.**	**236.7**	**5,528**	**552.81**	**101,333**	**1,084.80**	**464.62**	**1.0032**
8	1	171	5,617	561.69	100,648	1,445.72	461.48	1.0001
8	2	221	6,006	600.63	101,993	1,774.00	467.65	1.0135
8	3	219	5,499	549.95	103,581	1,847.03	474.92	1.0292
8	**AVG.**	**203.7**	**5,708**	**570.76**	**102,074**	**1,688.92**	**468.02**	**1.0143**

Case #	Run #	Generation of best individual	Electricity Consumption (kWh)	EE_Costs ($)	Yearly PV Revenue	1st Gen. Avg. CF $/mth	Best GA CF $/mth	% Best Manual CF
9	1	215	5,107	510.69	92,076	725.75	422.17	1.0130
9	2	206	5,136	513.58	92,403	1,180.15	423.68	1.0166
9	3	249	5,265	526.54	91,175	1,028.31	418.04	1.0031
9	**AVG.**	**223.3**	**5,169**	**516.94**	**91,885**	**978.07**	**421.30**	**1.0109**
10	1	184	5,109	310.94	63,670	800.95	308.60	1.0297
10	2	225	5,195	319.45	62,190	1,167.71	301.81	1.0070
10	3	189	4,979	297.92	62,896	1,113.54	305.05	1.0178
10	**AVG.**	**199.3**	**5,094**	**309.44**	**62,919**	**1,027.40**	**305.15**	**1.0182**
11	1	171	5,003	100.26	36,433	550.31	200.38	1.0209
11	2	227	5,086	108.58	35,863	962.73	197.77	1.0076
11	3	232	5,086	108.58	35,863	908.63	197.77	1.0076
11	**AVG.**	**210.0**	**5,058**	**105.81**	**36,053**	**807.22**	**198.64**	**1.0120**
12	1	208	6,009	0.90	15,781	355.56	122.36	1.0305
12	2	248	5,866	0.00	15,396	723.35	119.48	1.0063
12	3	152	6,009	0.90	15,055	732.55	119.03	1.0025
12	**AVG.**	**202.7**	**5,961**	**0.60**	**15,411**	**603.82**	**120.29**	**1.0131**
13	1	234	7,325	0.00	9,659	239.70	105.33	1.0219
13	2	149	7,552	0.00	8,756	506.30	103.08	1.0000
13	3	189	7,615	0.00	8,880	647.38	104.17	1.0106
13	**AVG.**	**224.0**	**7,497**	**0.00**	**9,099**	**464.46**	**104.19**	**1.0108**
14	1	134	7,552	0.00	8,756	192.44	103.08	1.0000
14	2	215	7,513	0.00	10,128	366.71	109.05	1.0579
14	3	217	7,341	0.00	9,489	575.13	104.68	1.0155
14	**AVG.**	**188.7**	**7,469**	**0.00**	**9,457**	**378.09**	**105.60**	**1.0245**
15	1	241	7,557	0.00	8,773	180.73	103.20	1.0005
15	2	194	8,290	0.00	8,014	218.65	105.83	1.0260
15	3	244	7,058	0.00	9,746	457.74	103.51	1.0035
15	**AVG.**	**226.3**	**7,635**	**0.00**	**8,844**	**285.71**	**104.18**	**1.0100**
16	1	101	5,028	502.85	93,406	1,343.64	428.27	1.0320
16	2	232	5,034	503.37	90,506	1,123.21	414.98	1.0000
16	3	241	4,924	492.39	93,090	1,077.08	426.83	1.0286
16	**AVG.**	**191.3**	**4,995**	**499.54**	**92,334**	**1,181.31**	**423.36**	**1.0202**
17	1	140	5,773	577.28	114,733	1,484.20	526.06	1.0200
17	2	243	5,529	552.87	113,693	1,304.50	521.29	1.0107
17	3	247	5,378	537.81	112,489	1,227.47	515.77	1.0000
17	**AVG.**	**210.0**	**5,560**	**555.99**	**113,638**	**1,338.72**	**521.04**	**1.0102**

Case #	Run #	Generation of best individual	Electricity Consumption (kWh)	EE_Costs ($)	Yearly PV Revenue	1st Gen. Avg. CF $/mth	Best GA CF $/mth	% Best Manual CF
18	1	231	5,312	531.15	99,013	1,335.54	453.98	1.0080
18	2	236	5,226	522.64	98,247	1,161.75	450.47	1.0002
18	3	243	5,271	527.11	99,568	1,122.76	456.52	1.0137
18	**AVG.**	**236.7**	**5,270**	**526.97**	**98,943**	**1,206.68**	**453.66**	**1.0073**
19	1	143	5,324	532.43	93,608	1,351.39	429.20	1.0161
19	2	232	5,034	503.37	92,123	1,131.01	422.39	1.0000
19	3	35	5,150	515.01	98,967	1,083.78	453.77	1.0743
19	**AVG.**	**136.7**	**5,169**	**516.93**	**94,899**	**1,188.73**	**435.12**	**1.0301**
20	1	101	5,028	502.85	91,572	1,335.44	419.86	1.0300
20	2	196	5,057	505.73	88,951	1,114.76	407.84	1.0006
20	3	221	4,903	490.34	91,364	1,070.21	418.91	1.0277
20	**AVG.**	**172.7**	**4,996**	**499.64**	**90,629**	**1,173.47**	**415.54**	**1.0194**
21	1	121	4,987	498.67	105,854	1,364.97	485.35	1.0117
21	2	145	4,917	491.70	105,320	1,159.27	482.90	1.0066
21	3	175	5,134	513.44	106,231	1,113.32	487.08	1.0153
21	**AVG.**	**147.0**	**5,013**	**501.27**	**105,802**	**1,212.52**	**485.11**	**1.0112**
22	1	226	4,917	491.72	102,253	945.19	468.84	1.0065
22	2	218	5,583	558.29	101,592	824.29	465.81	1.0000
22	3	132	4,890	488.97	102,624	932.74	470.54	1.0102
22	**AVG.**	**192.0**	**5,130**	**512.99**	**102,156**	**900.74**	**468.39**	**1.0056**
23	1	183	8,001	0.06	13,090	628.92	126.69	1.0000
23	2	61	7,731	0.00	21,817	474.81	164.46	1.2982
23	3	155	7,266	0.00	22,974	418.57	165.88	1.3094
23	**AVG.**	**133.0**	**7,666**	**0.02**	**19,294**	**507.43**	**152.34**	**1.2025**
24	1	101	5,028	750.98	93,406	1,298.38	413.81	1.0330
24	2	139	5,057	755.21	90,547	1,082.40	400.85	1.0006
24	3	224	5,054	754.85	94,021	1,044.45	416.11	1.0387
24	**AVG.**	**154.7**	**5,047**	**753.68**	**92,658**	**1,141.74**	**410.26**	**1.0241**
25	1	426	5,034	1502.50	90,506	1,148.93	382.63	1.0000
25	2	109	4,906	1464.51	92,972	1,031.38	394.69	1.0315
25	3	239	5,101	1522.66	93,852	1,003.67	397.61	1.0391
25	**AVG.**	**258.0**	**5,013**	**1496.56**	**92,443**	**1,061.33**	**391.64**	**1.0236**
26	1	235	5,010	2243.02	93,338	1,185.22	378.20	1.0371
26	2	150	4,991	2234.55	93,483	980.35	378.06	1.0368
26	3	81	5,179	2318.79	94,770	962.89	382.27	1.0483
26	**AVG.**	**155.3**	**5,060**	**2265.45**	**93,864**	**1,042.82**	**379.51**	**1.0407**

Case #	Run #	Generation of best individual	Electricity Consumption (kWh)	EE_Costs ($)	Yearly PV Revenue	1st Gen. Avg. CF $/mth	Best GA CF $/mth	% Best Manual CF
27	1	193	4,980	1245.07	96,262	1,248.03	400.58	1.0718
27	2	181	5,034	1258.42	90,506	1,033.88	373.75	1.0000
27	3	192	5,061	1265.27	91,453	1,001.31	377.87	1.0110
27	**AVG.**	**188.7**	**5,025**	**1256.25**	**92,740**	**1,094.41**	**384.07**	**1.0276**
28	1	171	5,328	2664.03	94,507	1,055.33	301.66	1.0425
28	2	209	5,322	2661.14	91,811	852.14	289.44	1.0003
28	3	171	5,482	2741.13	94,103	848.46	299.88	1.0364
28	**AVG.**	**183.7**	**5,378**	**2688.77**	**93,474**	**918.64**	**296.99**	**1.0264**
29	1	191	5,765	4323.86	95,746	862.24	201.29	1.0002
29	2	224	6,181	4635.98	101,161	670.89	208.95	1.0383
29	3	229	5,467	4100.51	92,725	695.61	202.39	1.0057
29	**AVG.**	**214.7**	**5,805**	**4353.45**	**96,544**	**742.91**	**204.21**	**1.0147**
30	1	101	5,028	502.85	93,406	1,295.96	404.66	1.0320
30	2	228	5,034	503.37	90,506	1,080.21	392.09	1.0000
30	3	224	5,054	505.43	94,021	1,040.39	407.32	1.0388
30	**AVG.**	**184.3**	**5,039**	**503.88**	**92,644**	**1,138.85**	**401.36**	**1.0236**
31	1	230	4,838	483.81	93,817	2,411.90	872.85	1.0033
31	2	183	4,831	483.08	93,257	2,126.95	880.71	1.0123
31	3	211	4,719	471.94	99,303	1,923.59	887.13	1.0197
31	**AVG.**	**208.0**	**4,796**	**479.61**	**95,459**	**2,154.15**	**880.23**	**1.0118**
32	1	211	5,615	561.52	99,747	1,704.12	457.35	1.0032
32	2	129	5,424	542.38	102,632	1,629.95	470.57	1.0322
32	3	47	5,565	556.53	99,432	1,380.08	455.90	1.0000
32	**AVG.**	**129.0**	**5,535**	**553.48**	**100,603**	**1,571.38**	**461.27**	**1.0118**
33	1	35	5,008	500.76	93,979	1,365.41	430.90	1.0349
33	2	67	4,992	499.18	96,421	1,443.33	442.09	1.0618
33	3	61	5,429	542.87	96,375	1,215.65	441.89	1.0613
33	**AVG.**	**54.3**	**5,143**	**514.27**	**95,591**	**1,341.46**	**438.29**	**1.0527**
34	1	224	5,055	505.51	79,348	1,214.77	363.82	1.0008
34	2	98	5,048	504.77	79,438	1,009.14	364.23	1.0019
34	3	207	5,057	505.74	79,818	980.83	365.97	1.0067
34	**AVG.**	**176.3**	**5,053**	**505.34**	**79,535**	**1,068.25**	**364.67**	**1.0032**
35	1	220	4,101	410.07	78,681	1,277.36	360.76	1.0137
35	2	123	4,104	410.44	79,375	1,052.76	363.94	1.0226
35	3	186	3,963	396.26	79,512	985.40	364.57	1.0244
35	**AVG.**	**176.3**	**4,056**	**405.59**	**79,189**	**1,105.17**	**363.09**	**1.0202**

Case #	Run #	Generation of best individual	Electricity Consumption (kWh)	EE_Costs ($)	Yearly PV Revenue	1st Gen. Avg. CF $/mth	Best GA CF $/mth	% Best Manual CF
36	1	190	5,805	580.47	108,508	1,515.33	497.52	1.0202
36	2	151	5,986	598.58	108,470	1,187.66	497.34	1.0199
36	3	237	5,806	580.56	108,247	1,170.33	496.32	1.0178
36	**AVG.**	**192.7**	**5,865**	**586.54**	**108,408**	**1,291.11**	**497.06**	**1.0193**
37	1	159	4,998	499.84	91,798	864.58	420.90	1.0276
37	2	138	4,976	497.61	90,666	779.81	415.71	1.0149
37	3	238	5,098	509.77	89,331	665.36	409.59	1.0000
37	**AVG.**	**178.3**	**5,024**	**502.40**	**90,598**	**769.92**	**415.40**	**1.0142**
38	1	234	5,168	516.78	97,701	1,563.77	447.97	1.0500
38	2	140	5,415	541.52	93,045	1,355.76	426.62	1.0000
38	3	162	5,422	542.18	97,678	1,280.44	447.86	1.0498
38	**AVG.**	**178.7**	**5,335**	**533.49**	**96,141**	**1,399.99**	**440.81**	**1.0333**
39	1	218	5,496	549.58	99,894	1,539.07	458.02	1.0077
39	2	104	5,487	548.71	99,512	1,342.74	456.27	1.0039
39	3	95	5,312	531.16	102,315	1,202.55	469.12	1.0322
39	**AVG.**	**139.0**	**5,431**	**543.15**	**100,574**	**1,361.45**	**461.14**	**1.0146**
40	1	217	4,591	459.12	105,428	11,675.0	4591.2	1.0126
40	2	182	4,534	453.41	105,484	10,970.0	4534.1	1.0000
40	3	200	4,540	453.96	105,900	9,252.0	4539.6	1.0012
40	**AVG.**	**199.7**	**4,555**	**455.50**	**105,604**	**10,632.3**	**4555.0**	**1.0046**